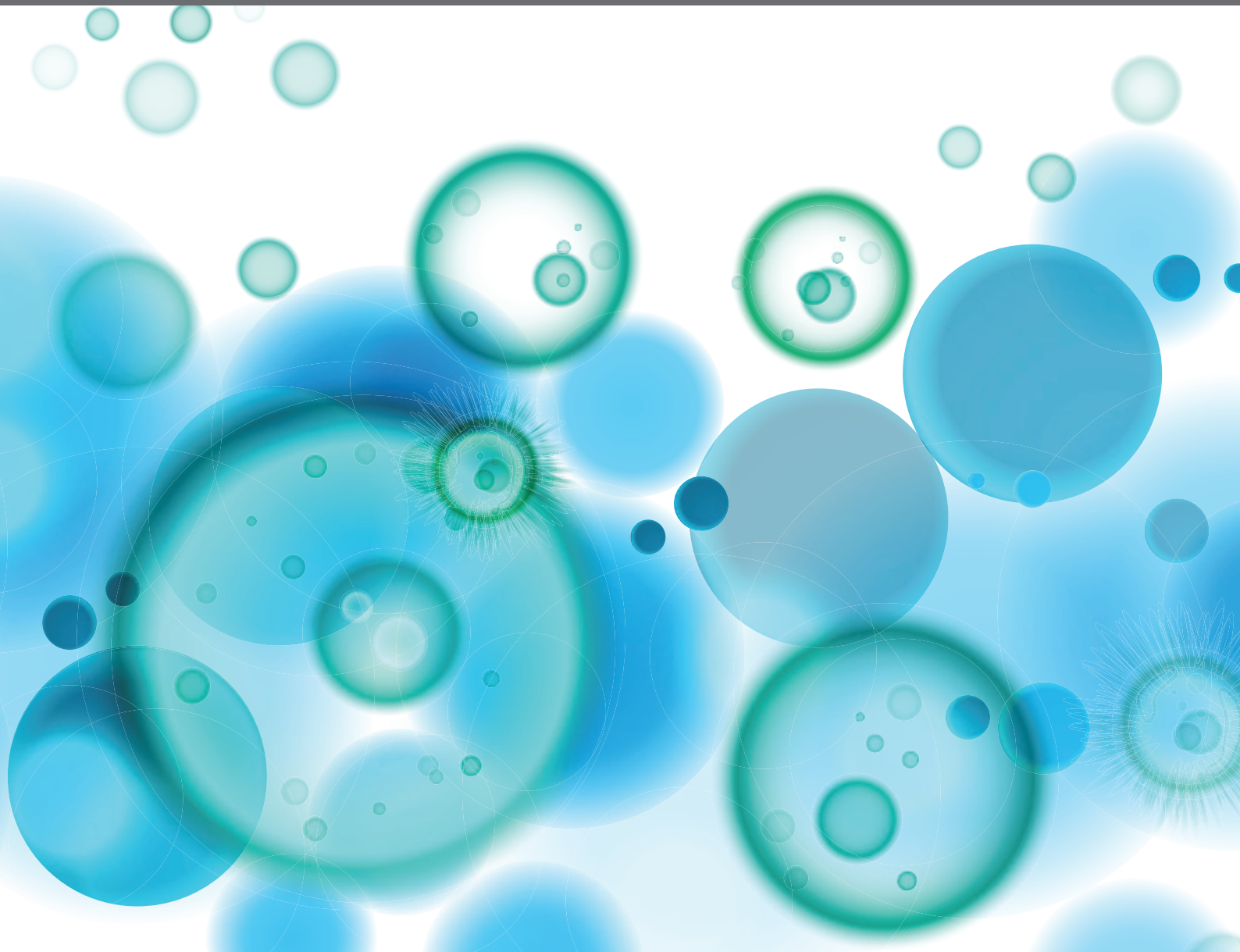


ANTIBODY Fc ENGINEERING: TOWARDS BETTER THERAPEUTICS

EDITED BY: Tianlei Ying and Rui Gong
PUBLISHED IN: Frontiers in Immunology





Frontiers Copyright Statement

© Copyright 2007-2018 Frontiers Media SA. All rights reserved.

All content included on this site, such as text, graphics, logos, button icons, images, video/audio clips, downloads, data compilations and software, is the property of or is licensed to Frontiers Media SA ("Frontiers") or its licensees and/or subcontractors. The copyright in the text of individual articles is the property of their respective authors, subject to a license granted to Frontiers.

The compilation of articles constituting this e-book, wherever published, as well as the compilation of all other content on this site, is the exclusive property of Frontiers. For the conditions for downloading and copying of e-books from Frontiers' website, please see the Terms for Website Use. If purchasing Frontiers e-books from other websites or sources, the conditions of the website concerned apply.

Images and graphics not forming part of user-contributed materials may not be downloaded or copied without permission.

Individual articles may be downloaded and reproduced in accordance with the principles of the CC-BY licence subject to any copyright or other notices. They may not be re-sold as an e-book.

As author or other contributor you grant a CC-BY licence to others to reproduce your articles, including any graphics and third-party materials supplied by you, in accordance with the Conditions for Website Use and subject to any copyright notices which you include in connection with your articles and materials.

All copyright, and all rights therein, are protected by national and international copyright laws.

The above represents a summary only. For the full conditions see the Conditions for Authors and the Conditions for Website Use.

ISSN 1664-8714
ISBN 978-2-88945-678-9
DOI 10.3389/978-2-88945-678-9

About Frontiers

Frontiers is more than just an open-access publisher of scholarly articles: it is a pioneering approach to the world of academia, radically improving the way scholarly research is managed. The grand vision of Frontiers is a world where all people have an equal opportunity to seek, share and generate knowledge. Frontiers provides immediate and permanent online open access to all its publications, but this alone is not enough to realize our grand goals.

Frontiers Journal Series

The Frontiers Journal Series is a multi-tier and interdisciplinary set of open-access, online journals, promising a paradigm shift from the current review, selection and dissemination processes in academic publishing. All Frontiers journals are driven by researchers for researchers; therefore, they constitute a service to the scholarly community. At the same time, the Frontiers Journal Series operates on a revolutionary invention, the tiered publishing system, initially addressing specific communities of scholars, and gradually climbing up to broader public understanding, thus serving the interests of the lay society, too.

Dedication to Quality

Each Frontiers article is a landmark of the highest quality, thanks to genuinely collaborative interactions between authors and review editors, who include some of the world's best academicians. Research must be certified by peers before entering a stream of knowledge that may eventually reach the public - and shape society; therefore, Frontiers only applies the most rigorous and unbiased reviews.

Frontiers revolutionizes research publishing by freely delivering the most outstanding research, evaluated with no bias from both the academic and social point of view. By applying the most advanced information technologies, Frontiers is catapulting scholarly publishing into a new generation.

What are Frontiers Research Topics?

Frontiers Research Topics are very popular trademarks of the Frontiers Journals Series: they are collections of at least ten articles, all centered on a particular subject. With their unique mix of varied contributions from Original Research to Review Articles, Frontiers Research Topics unify the most influential researchers, the latest key findings and historical advances in a hot research area! Find out more on how to host your own Frontiers Research Topic or contribute to one as an author by contacting the Frontiers Editorial Office: researchtopics@frontiersin.org

ANTIBODY Fc ENGINEERING: TOWARDS BETTER THERAPEUTICS

Topic Editors:

Tianlei Ying, Fudan University, China

Rui Gong, Chinese Academy of Sciences, China

Citation: Ying, T., Gong, R., eds (2018). Antibody Fc Engineering: Towards Better Therapeutics. Lausanne: Frontiers Media. doi: 10.3389/978-2-88945-678-9

Table of Contents

- 04 Editorial: Antibody Fc Engineering: Towards Better Therapeutics**
Cheng Lei, Rui Gong and Tianlei Ying
- 06 Crystallizable Fragment Glycoengineering for Therapeutic Antibodies Development**
Wei Li, Zhongyu Zhu, Weizao Chen, Yang Feng and Dimiter S. Dimitrov
- 21 Advances in Therapeutic Fc Engineering – Modulation of IgG-Associated Effector Functions and Serum Half-life**
Abhishek Saxena and Donghui Wu
- 32 Fc Engineering for Developing Therapeutic Bispecific Antibodies and Novel Scaffolds**
Hongyan Liu, Abhishek Saxena, Sachdev S. Sidhu and Donghui Wu
- 47 Engineering of Fc Fragments With Optimized Physicochemical Properties Implying Improvement of Clinical Potentials for Fc-Based Therapeutics**
Chunpeng Yang, Xinyu Gao and Rui Gong
- 61 Immunoglobulin Fc Heterodimer Platform Technology: From Design to Applications in Therapeutic Antibodies and Proteins**
Ji-Hee Ha, Jung-Eun Kim and Yong-Sung Kim
- 77 Corrigendum: Immunoglobulin Fc Heterodimer Platform Technology: From Design to Applications in Therapeutic Antibodies and Proteins**
Ji-Hee Ha, Jung-Eun Kim and Yong-Sung Kim
- 78 Engineered Soluble Monomeric IgG1 Fc With Significantly Decreased Non-Specific Binding**
Chunyu Wang, Yanling Wu, Lili Wang, Binbin Hong, Yujia Jin, Dan Hu, Gang Chen, Yu Kong, Ailing Huang, Guoqiang Hua and Tianlei Ying
- 86 Antibody-Dependent Cell-Mediated Cytotoxicity Epitopes on the Hemagglutinin Head Region of Pandemic H1N1 Influenza Virus Play Detrimental Roles in H1N1-Infected Mice**
Zi-Wei Ye, Shuofeng Yuan, Kwok-Man Poon, Lei Wen, Dong Yang, Zehua Sun, Cun Li, Meng Hu, Huiping Shuai, Jie Zhou, Mei-Yun Zhang, Bo-Jian Zheng, Hin Chu and Kwok-Yung Yuen
- 97 Immunoglobulin Transporting Receptors are Potential Targets for the Immunity Enhancement and Generation of Mammary Gland Bioreactor**
Xuemei Jiang, Jianjun Hu, Diraviyam Thirumalai and Xiaoying Zhang
- 105 Anti-Bovine Programmed Death-1 Rat–Bovine Chimeric Antibody for Immunotherapy of Bovine Leukemia Virus Infection in Cattle**
Tomohiro Okagawa, Satoru Konnai, Asami Nishimori, Naoya Maekawa, Ryoyo Ikebuchi, Shinya Goto, Chie Nakajima, Junko Kohara, Satoshi Ogasawara, Yukinari Kato, Yasuhiko Suzuki, Shiro Murata and Kazuhiko Ohashi



Editorial: Antibody Fc Engineering: Towards Better Therapeutics

Cheng Lei¹, Rui Gong² and Tianlei Ying^{1*}

¹ Key Laboratory of Medical Molecular Virology of Ministries of Education and Health, School of Basic Medical Sciences, Fudan University, Shanghai, China, ² CAS Key Laboratory of Special Pathogens and Biosafety, Wuhan Institute of Virology, Chinese Academy of Sciences, Wuhan, China

Keywords: antibody Fc, antibody engineering, therapeutic antibody, Fc receptor, effector function

Editorial on the Research Topic

Antibody Fc Engineering: Towards Better Therapeutics

OPEN ACCESS

Edited by:

Abdul Qader Abbady,
Atomic Energy Commission of Syria,
Syria

Reviewed by:

Serge Muyldermans,
Vrije Universiteit Brussel, Belgium

***Correspondence:**

Tianlei Ying
tlying@fudan.edu.cn

Specialty section:

This article was submitted to
Vaccines and Molecular Therapeutics,
a section of the journal
Frontiers in Immunology

Received: 27 August 2018

Accepted: 04 October 2018

Published: 24 October 2018

Citation:

Lei C, Gong R and Ying T (2018)
Editorial: Antibody Fc Engineering:
Towards Better Therapeutics.
Front. Immunol. 9:2450.
doi: 10.3389/fimmu.2018.02450

Efficacy of monoclonal antibodies (mAbs) attributes to both the antigen-binding fragment (Fab) and crystallizable fragment (Fc). Fc, which naturally exists in mAbs but also functions as skeleton in Fc-fusion proteins, can be engineered to possess unique properties and various applications. This collection combines six reviews (Li et al.; Saxena and Wu; Liu et al.; Yang et al.; Ha et al.; Jiang et al.) with three original research articles (Wang et al.; Ye et al.; Okagawa et al.) together to provide substantial knowledge of Fc engineering approaches to regulate effector functions, to extend serum half-life by modification of neonatal Fc receptor (FcRn) binding, to heterodimerize of Fc for design of new Fc formats and to monomerize Fc for improved druggability and novel applications.

Two reviews thoroughly offer an extensive perspective on traditional Fc engineering methods, namely glycoengineering and site mutagenesis (Li et al.; Saxena and Wu). These two methods affect mAbs effector functions by modulating the Fc-FcγRs and FcRn interactions. To affect these interactions, glycoengineering and site mutagenesis both alter either Fc conformations or interfaces of interaction. Li et al. give a detailed review of the biology of IgG-Fc N-glycans (their structures, biosynthesis, and efficacy on mAbs effector functions), the strategies to re-model glycosylation (host cell engineering and chemo-enzymatic glycosylation remodeling), and the discussion of two novel mAbs formats (aglycosylated mAbs and Fc glycan specific antibody-drug conjugates). In the other review, Saxena et al. discuss the modulation of mAbs effector functions and serum half-life (Saxena and Wu). To begin with, a detailed description is given to present differences among Fc receptors. Then Saxena et al. summarize the strategy of modulation of mAbs effector function and pharmacokinetics by Fc engineering. At the end of their article, recent Fc engineering-based mAbs under clinical trials are extensively reviewed.

Currently, apart from Fc engineering at certain amino acids, novel Fc variants are designed to meet the requirements of new antibody scaffolds. The novel variants could derive from recent technologies, such as display-based strategies. Two reviews and one original research article highlight the intense interest in the development of monomeric and heterodimeric Fc (Liu et al.; Ha et al.; Wang et al.). There are two side effects that hinder the application of Fc-fusion proteins. The first side effect is the homodimeric nature of IgG1 Fc; the other is non-specific binding of Fc variants.

In order to solve the two problems above, heterodimeric and monomeric Fc are designed. Heterodimeric Fc is designed to address the heavy chain mispairing issue of bispecific antibodies (bsAb) while retaining biophysical and biological properties of the wild-type Fc. Ha et al. firstly focus on the literature of the design and application of heterodimeric Fc (Ha et al.). There are four approaches to design the heterodimeric Fc, namely (i) symmetric-to-asymmetric steric complementarity design (e.g., KiH, knobs-in-holes), (ii) charge-to-charge swap (e.g., DD-KK), (iii) charge-to-steric complementarity swap plus additional long-range electrostatic interactions (e.g., EW-RVT), and (iv) isotype strand swap [e.g., strand-exchange engineered domain (SEED)]. Noteworthily, the pioneering KiH approach's patent is expired and, as a result, widely implemented in current clinical trials. Two different antigen binders could attach to heterodimeric Fc at the N- and/or C-terminus of each Fc chain. This contributes to the creation of various heterodimeric Fc-based antibodies with divergences in specificity, binding valency and binding geometry. Ha et al. then describe a promising scaffold for the next generation of Fc-fusion proteins and cytokines. The authors specified that, in tumor-targeting IgG-based immune-cytokines, in comparison with homodimeric Fc-fused cytokines, the heterodimeric Fc-fused cytokines could reduce the associations with immune cells, which substantially lead to tumor tissue accumulation. This process minimizes systemic toxicity, and further facilitates their development as therapeutics.

Wang et al. report monomeric Fc with half size of IgG1 Fc, significantly lower non-specific binding while retaining FcRn binding (Wang et al.). The phage display library-based technology was utilized to combine rational with random scanning mutagenesis of Fc residues which have been previously identified to impact the Fc dimerization or FcRn binding by the same group. In addition to their latest effort to acquire monomeric Fc, Protein G magnetic beads were introduced to exclude the non-specific binders among the Fc variants. Therefore, this approach could simultaneously identify the monomeric Fc variants (mFc) with low non-specific binding. Moreover, Wang et al. describe the decisive roles of T366R and L368H mutations in creating monomeric status. Importantly, the size of mFc is only half compared with the wild-type Fc while retaining FcRn binding. Consequently, the efficacy of mFc-based fusion proteins and antigen binders could benefit from enhanced tissue penetration and wider range of potential targets.

Recently, some small antibody fragments (e.g., nanobody, human single-domain Ab, scFv, Fab, BITE) and bsAb fragments are designed that have the ability to penetrate better into tissues compared to IgG. However, their small size leads to

shorter serum half-life. Besides, these novel formats, derived from IgG, suffer from low solubility and aggregation. Thus, Fc engineering could provide a platform to solve the druggability issues of novel antibody fragments. For instance, the engineered monomeric Fc could be a potential solution based on the minimized non-specific binding, high solubility, high yield, high thermostability, and long *in vivo* half-life. Liu et al. also review recent advances in the therapeutic potential of bispecific molecules and small novel Ab fragments (Liu et al.). The authors then summarize two key approaches to optimize bsAb, namely structural and physicochemical optimization. In another article reviewed by Yang et al. the authors provide the overview on strategies applied on engineering physicochemical properties of Fc.

Regarding to Fc engineering, only a considerably small portion of Fc-fusion proteins have been approved by FDA to date. Fewer Fc-based antigen binders are in clinical studies. However, according to our collection, Fc engineering have become critical tools in both traditional and novel scaffolds of mAbs, and more regulatory approval of Fc engineering-based therapeutics would be expected shortly.

AUTHOR CONTRIBUTIONS

TY, RG, and CL wrote the manuscript and approved it for publication.

FUNDING

This work was supported by the National Natural Science Foundation of China (31570936, 81822027, 81630090, 81561128006, 81601761), and the 1000 Young Talents Program of China.

ACKNOWLEDGMENTS

The editors would like to thank all contributors for the many excellent submissions to this Research Topic, as well as the reviewers and the *Frontiers in Immunology* editorial office for their kind help and support.

Conflict of Interest Statement: The authors declare that the research was conducted in the absence of any commercial or financial relationships that could be construed as a potential conflict of interest.

Copyright © 2018 Lei, Gong and Ying. This is an open-access article distributed under the terms of the Creative Commons Attribution License (CC BY). The use, distribution or reproduction in other forums is permitted, provided the original author(s) and the copyright owner(s) are credited and that the original publication in this journal is cited, in accordance with accepted academic practice. No use, distribution or reproduction is permitted which does not comply with these terms.



Crystallizable Fragment Glycoengineering for Therapeutic Antibodies Development

Wei Li*, Zhongyu Zhu, Weizao Chen, Yang Feng and Dimiter S. Dimitrov*

Protein Interactions Section, Cancer and Inflammation Program, Center for Cancer Research, National Cancer Institute, National Institutes of Health, Frederick, MD, United States

OPEN ACCESS

Edited by:

Tianlei Ying,
Fudan University, China

Reviewed by:

Johannes S. Gach,
University of California, Irvine,
United States
Yong-Sung Kim,
Ajou University, South Korea
Serge Muyldermans,
Vrije Universiteit Brussel, Belgium

***Correspondence:**

Wei Li
wei.li3@nih.gov;
Dimiter S. Dimitrov
dimitrdi@mail.nih.gov

Specialty section:

This article was submitted to
Vaccines and Molecular
Therapeutics,
a section of the journal
Frontiers in Immunology

Received: 19 September 2017

Accepted: 31 October 2017

Published: 13 November 2017

Citation:

Li W, Zhu Z, Chen W, Feng Y and
Dimitrov DS (2017) Crystallizable
Fragment Glycoengineering for
Therapeutic Antibodies Development.
Front. Immunol. 8:1554.
doi: 10.3389/fimmu.2017.01554

Monoclonal antibody (mAb)-based therapeutics are the fastest growing class of human pharmaceuticals. They are typically IgG1 molecules with N-glycans attached to the N297 residue on crystallizable fragment (Fc). Different Fc glycoforms impact their effector function, pharmacokinetics, stability, aggregation, safety, and immunogenicity. Fc glycoforms affect mAbs effector functions including antibody-dependent cell-mediated cytotoxicity (ADCC) and complement-dependent cytotoxicity (CDC) by modulating the Fc–FcγRs and Fc–C1q interactions. While the terminal galactose enhances CDC activity, the fucose significantly decreases ADCC. Defucosylated immunoglobulin Gs (IgGs) are thus highly pursued as next-generation therapeutic mAbs with potent ADCC at reduced doses. A plethora of cell glycoengineering and chemoenzymatic glycoengineering strategies is emerging to produce IgGs with homogenous glycoforms especially without core fucose. The chemoenzymatic glycosylation remodeling also offers useful avenues for site-specific conjugations of small molecule drugs onto mAbs. Herein, we review the current progress of IgG-Fc glycoengineering. We begin with the discussion of the structures of IgG N-glycans and biosynthesis followed by reviewing the impact of IgG glycoforms on antibody effector functions and the current Fc glycoengineering strategies with emphasis on Fc defucosylation. Furthermore, we briefly discuss two novel therapeutic mAbs formats: aglycosylated mAbs and Fc glycan specific antibody–drug conjugates (ADCs). The advances in the understanding of Fc glycobiology and development of novel glycoengineering technologies have facilitated the generation of therapeutic mAbs with homogenous glycoforms and improved therapeutic efficacy.

Keywords: monoclonal antibodies, crystallizable fragment glycosylation, homogenous glycoforms, effector function, crystallizable fragment glycoengineering, chemoenzymatic glycosylation remodeling, aglycosylated monoclonal antibodies, antibody–drug conjugate

INTRODUCTION

Monoclonal antibody (mAb)-based therapeutics have been the fastest growing class of human pharmaceuticals with applications in various clinical indications such as oncology, inflammatory diseases, organ transplantation, and bacteria and virus infection (1). Currently, more than 60 mAbs and derivatives are approved in USA and Europe for human use with some of them being blockbusters in the biopharmaceutical markets (2, 3). Under the vigorous engine of modern translational

biotechnology, mAbs and derivatives are estimated to be >30% of the new licensed drugs (4). Most recombinant therapeutic mAbs are glycosylated immunoglobulin G (IgG) molecules with glycans attached to the amide nitrogen atom of asparagine 297 (N297) in the crystallizable fragment (Fc) region (**Figure 1A**) (5). It is well accepted that the N297-attached oligosaccharide is structurally integral to the IgG-Fc with multiple non-covalent interactions with the protein surface of the C_H2 domain (6). The extensive carbohydrate–polypeptide interactions as well as carbohydrate–carbohydrate interactions modulate the conformations of the IgG molecules, which would ultimately impact the biological functions of mAbs (7).

During the last several decades, substantial knowledge has been acquired regarding the impact of Fc glycosylation on mAbs efficacy, pharmacokinetics (PK), stability, aggregation, safety, and immunogenicity (8–10). Many mAbs exhibit biological functions through immune effector functions including antibody-dependent cell-mediated cytotoxicity (ADCC), antibody-dependent cell-mediated phagocytosis (ADCP), and complement-dependent cytotoxicity (CDC) mediated by Fc–FcγR and Fc–C1q interactions (11). Alterations of glycoforms impact effector functions through modulating these Fc-ligand interactions (12–14). The effector functions of aglycosylated or deglycosylated IgGs are significantly damped or eliminated due to the much lower binding to FcγRI or no binding to FcγRII and FcγRIII (15). Fc N-glycans impact stability of therapeutic antibodies in terms of shelf storage, thermal and chemical stability (such as pH and urea), aggregation propensity, susceptibility to proteolysis, *in vivo* clearance rate, and PK properties. The biophysical properties of therapeutic antibodies including the size, mass, charge, solubility, and colloidal stability are affected by N-glycans. Thus, different

glycoforms could endow antibodies with distinct physicochemical and storage stabilities. Structurally, the glycans hold together with Fc C_H2 domain with extensive non-covalent interactions, which not only protect the aggregation prone region (Phe241, Phe243, Pro244, Val262, Val264, Val303, and Val305) of C_H2 from solvent exposure but also contribute to reduce the dynamics of C_H2 and aid in C_H2 folding (16, 17). These structural features could explain the decreased thermal, chemical stability, and increased aggregation propensity of aglycosylated IgGs compared with the glycosylated counterparts (16, 18, 19). In addition, the fact that the large complex type N-glycans with terminal galactose support an “open” Fc conformation compared with the “closed” Fc sustained by small glycans indicates N-glycans can also influence the folding of the Fc part (20). On the other hand, N-glycans impact the PK of IgG *via* modulating IgG sensitivity to serum protease cleavage. Due to the glycans protection, glycosylated IgGs are more resistant to trypsin, chymotrypsin, and pepsin than the aglycosylated IgGs (21). Glycoforms with distinct length, branching, and charge of sugar residues relate to the different susceptibilities of IgGs to proteolysis. While the terminal GlcNAc and sialic acid residues improve the resistance to proteolysis and hence enhance *in vivo* stability of IgG, terminal galactose residue confers higher sensitivity to proteases (22–24). The other way of selective clearance of glycosylated IgGs is executed by the C-type lectins mediated endocytosis. N-glycans with high mannose or terminated with GlcNAc could bind to the mannose receptors on macrophages/dendritic cells leading to the accelerated clearance of IgGs (25, 26). IgG with terminal galactose residue could be bound and cleared by the asialoglycoprotein receptor expressed in the hepatocytes (27). Besides, mAbs glycosylation also correlates with their immunogenicity and safety in humans.

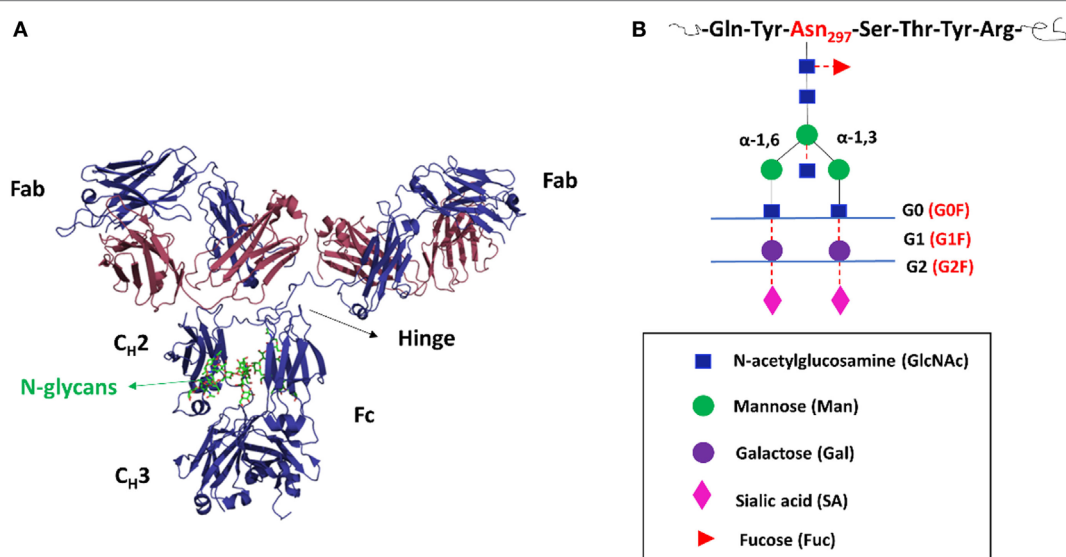


FIGURE 1 | The structures of immunoglobulin G (IgG) and N-glycans. **(A)** Cartoon representations of a full-length IgG showing the functional domains. An IgG consists of two heavy chains (blue) and two light chains (red). The N-glycans are presented by the green color. Crystallizable fragment (Fc) is a dimer of C_H2, C_H3, and glycans. Antigen-binding fragment (Fab) is composed of variable heavy and light domains, as well as two constant domains (CH1 and CL). **(B)** The schematic structures of the possible biantennary oligosaccharides attached to human IgG-Fc at N297. The core heptasaccharide (G0) is linked in black lines; the outer arm sugar residues are attached to the core by the red dash line.

Therapeutic mAbs heterologously produced in CHO and murine myeloma cells (Sp2/0 and NS0 cells) possess non-natural sugars compared with human IgG, such as *N*-glycolylneuraminic acid (NGNA) residues and terminal α -1,3-linked galactose, which could induce potential immunogenicity in humans (28, 29).

Given its importance, glycosylation is considered a critical quality attribute for mAb therapeutics (30). The regulatory authorities require developers to keep glycoforms humanized and consistent with limited heterogeneity. Hence, developers need to strictly control the glycosylation profile during the development and production of mAbs. However, mAbs glycosylation is intrinsically heterogeneous since glycans biosynthesis is not directly template driven. It is the product of sets of biochemical reactions involving a complex network of metabolic enzymes, which depends on the availability of sugar-nucleotide substrates, the enzyme distribution in the host cell, orchestrated process in endoplasmic reticulum (ER) and Golgi bodies and environmental factors (31, 32). Consequently, it is very challenging to achieve a highly homogenous glycoform independent of fermentation batches when expressing mAbs in eukaryotic cells. In the past decade, with significant advances in molecular and cell biology, protein and antibody engineering and gene editing, researchers have demonstrated individual glycoforms of antibodies could provide optimal efficacy for selected indications (Table 1) (33, 34). The pharmaceutical industry is increasingly pursuing the next-generation mAbs with tailored therapeutic effects. Herein, we review the current progress of mAbs Fc glycoengineering. We first present structures and biosynthesis of Fc N-glycans, followed by the discussion of impact of mAbs glycosylation on effector functions and the current glycoengineering strategies with emphasis on Fc defucosylation. Furthermore, we briefly discuss two novel therapeutic mAbs formats involving Fc glycans: aglycosylated mAbs and N-glycans targeted site-specific antibody-drug conjugates (ADCs).

IgG-Fc N-GLYCANS STRUCTURES AND BIOSYNTHESIS

The IgG-Fc N-glycan is usually of limited size with no more than three antennae (33). Typically, oligosaccharides of normal

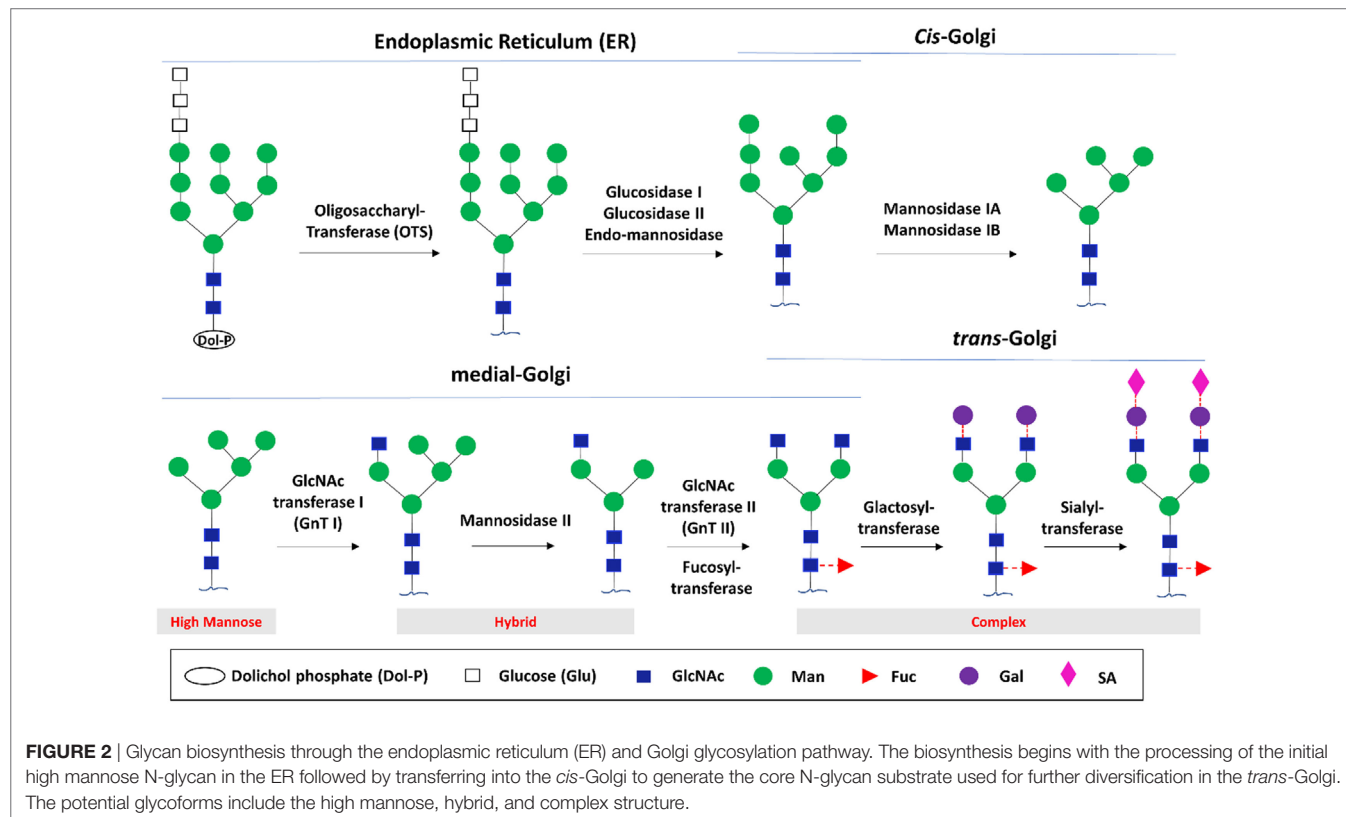
human IgGs are biantennary complex structures with a core heptasaccharide and an outer arm of sugar residues (6) (Figure 1B). The core oligosaccharide (GlcNAc2Man3GlcNAc2, designated as G0) is composed of two inner GlcNAc, three mannoses, and two GlcNAc β -1,2 linked to α -3 and α -6 mannose forming two antennae (α -3 arm and α -6 arm). One major feature of IgG-Fc glycans is the microheterogeneity, which not only stems from the linkage of sugar isomers and glycosylation site occupancy but also results from the outer arm sugar addition depending on the expression system and glycosylation enzymatic machinery (31, 64). Such additions include fucose (Fuc, G0F), galactose (Gal, G1, and G2), bisecting GlcNAc (linked to the core GlcNAc-associated mannose, which is catalyzed by GlcNAc transferases III), and sialic acid including *N*-acetylneuraminic acid (NANA) or *N*-glycolylneuraminic acid (NGNA) residues (9). In addition, structural studies have shown that the two N-glycans from every heavy chain are asymmetrically oriented (65, 66), which further diversifies IgG-Fc glycoforms. Consequently, Fc N-glycans possess more than 400 glycoforms considering random pairing of two different heavy chain glycans (67). Human serum IgG-Fc glycans typically contain ~30% G0F, ~35% G1F, ~16% G2F, and ~15% bisecting GlcNAc (68). Low levels of sialylation are observed in human IgG-Fc glycans with monosialylated and disialylated glycoforms accounting for approximately 5–10 and 1%, respectively (69). Interestingly, mAbs produced in recombinant expression systems share similar N-glycans structures with IgGs from human serum (13). Mabs produced in CHO, NS0, and Sp2/0 cell lines have predominant glycoforms of G0F, G1F, G2F, a paucity of sialylated glycans and do not contain bisecting GlcNAc (34, 70).

Like other glycoproteins, glycosylation of IgG occurs through the conserved ER and Golgi glycosylation pathway (32). N-glycosylation begins with the addition of a pyrophosphate-dolichol precursor (Dol-P, Glc3Man9GlcNAc2) to the consensus N-glycosylation sequon (Asn-X-Ser/Thr, where X is any amino acid except Pro) of a nascent polypeptide by a transmembrane oligosaccharyltransferase (Figure 2) (71). Thereafter, the N-glycans are subjected to series of sequential modifications by sets of glycosidases and glycosyltransferases. In the lumen of the ER, polypeptide associated Glc3Man9GlcNAc2 is sequentially trimmed by glucosidases I and II and endo-mannosidase to yield

TABLE 1 | Selected glycosylation engineering of therapeutic antibodies for targeted diseases.

mAbs name	Target	Indication	Glycol modification	Development status	Reference
Otelixizumab	CD3	Type I diabetes, rheumatoid arthritis	Aglycosylated	Phase I (completed)	(35)
MTRX-1011A	CD4	Rheumatoid arthritis, cutaneous lupus	Aglycosylated	Phase I (completed)	(36)
Mogamulizumab	CCR4	ATLL, CTCL	Afucosylated	Approved	(37, 38)
MDX-1342	CD19	Relapsed or refractory CLL	Afucosylated	Phase I	(39)
Obinutuzumab	CD20	CLL, follicular lymphoma	Low fucose	Approved	(40)
DI-B4	CD19	CD19-positive indolent B-cell lymphoma	Low fucose	Phase I	(41)
RG7160	EGFR	EGFR-positive solid tumors	Bisected; non-fucosylated	Phase II	(42)
GTMAB2.5GEX	Mucin 1	A-MUC1-positive ovarian cancer	Glycooptimized	Phase II	(43)
Rituximab	CD20	CLL and NHL	Galactosylated	NA	(44)
Intravenous immunoglobulin	NA	Autoantibody-driven inflammation	Sialylated	NA	(13)

CCR4, C-C chemokine receptor type 4; EGFR, epidermal growth factor receptor; ATLL, adult T-cell leukemia/lymphoma; CTCL, cutaneous T-cell lymphomas; CLL, chronic lymphocytic leukemia; NHL, non-Hodgkin's lymphoma; NA, not applicable; mAb, monoclonal antibody.



Man₈GlcNAc₂ (72). This process is under protein folding quality control mediated by calnexin–calreticulin complex. In the *cis*-Golgi, the Man₈GlcNAc₂ is sequentially processed by two class I α -mannosidases that act specifically on α -1,2-Man residues to give rise to the core Man₅GlcNAc₂ glycan for further diversification in the medial and *trans*-Golgi, which include stepwise addition of the outer arm monosaccharide residues, catalyzed by GlcNAc transferases I, II, and III (GnT I, II, and III), fucosyltransferases, galactosyltransferases (GalT), and sialyltransferases (SiaT).

IMPACT OF Fc GLYCOSYLATION ON IgG EFFECTOR FUNCTIONS

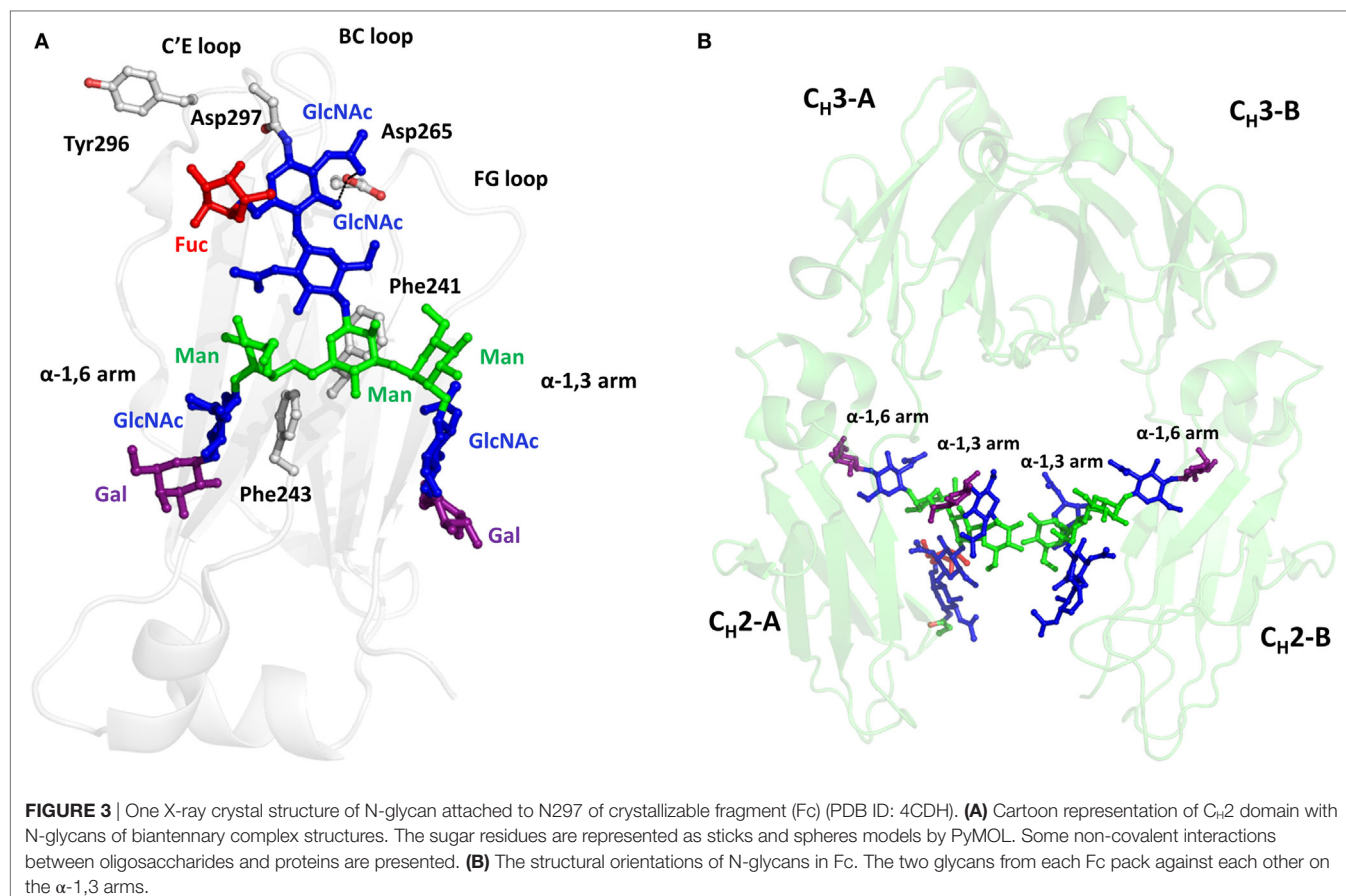
Crystallizable fragment glycoforms affect the effector function of antibodies by modulating the fine structure of Fc and thus altering Fc–ligands interactions. In recent years, structural insights into how antibody Fc glycoforms impact effector functions have been acquired by X-ray crystallography, nuclear magnetic resonance spectroscopy, and thermodynamics studies. Due to the stabilization effect of protein–sugar interaction, the core structures of GlcNAc₂Man₃ on the 1,3 arm and 1,6 arm are usually visible in the crystal structures. These two arms adopt distinct orientations—the 1,6 arm hangs over the hydrophobic face of C_{H2} domain while the 1,3 arm is orientated toward the internal space within the C_{H2} dimer (73). The oligosaccharide is well conserved and spans over 500 Å² of the surface of each C_{H2} domains (20) (Figure 3A). Oligosaccharides make multiple hydrophobic and polar non-covalent interactions with the inner face of the C_{H2}

domain (74). Impressive interactions include D265 hydrogen bonding to the inner GlcNAc and the α -1,6 arm forming strong CH–π packing with Phe241 and 243, which restricts the mobility of the glycans (75). Reciprocally, these intramolecular interactions restrain the C_{H2} conformation by stabilizing the C'E loop where the Asn297 locates, through which N-glycans pre-organize the ligands (FcγRs and C1q) binding interface on Fc (15). Besides, carbohydrate–carbohydrate interactions also contribute to maintain Fc conformation. The reciprocal mannoses from the two heavy chains make *sp-sp* contacts with each other (Figure 3B), which is necessary to establish a proper Fc conformation for ligand binding (14).

Multifaced impacts of terminal sugars on the antibody effector function have been elucidated. While high mannose, low fucose, and bisecting GlcNAc increase ADCC due to enhanced FcγRIIIa binding, terminal sialic acid decrease ADCC of IgG (14). For CDC, terminal galactose increases CDC by improving C1q binding, whereas terminal GlcNAc and sialic acid decrease CDC (12). Among these effects, reduction in fucose and terminal galactose, which improves ADCC and CDC, is highly desirable in antibody glycoengineering (76). Regulating α -2,6-linked terminal sialic acid is also an attractive strategy due to the anti-inflammatory role of these terminal sialic acid (77).

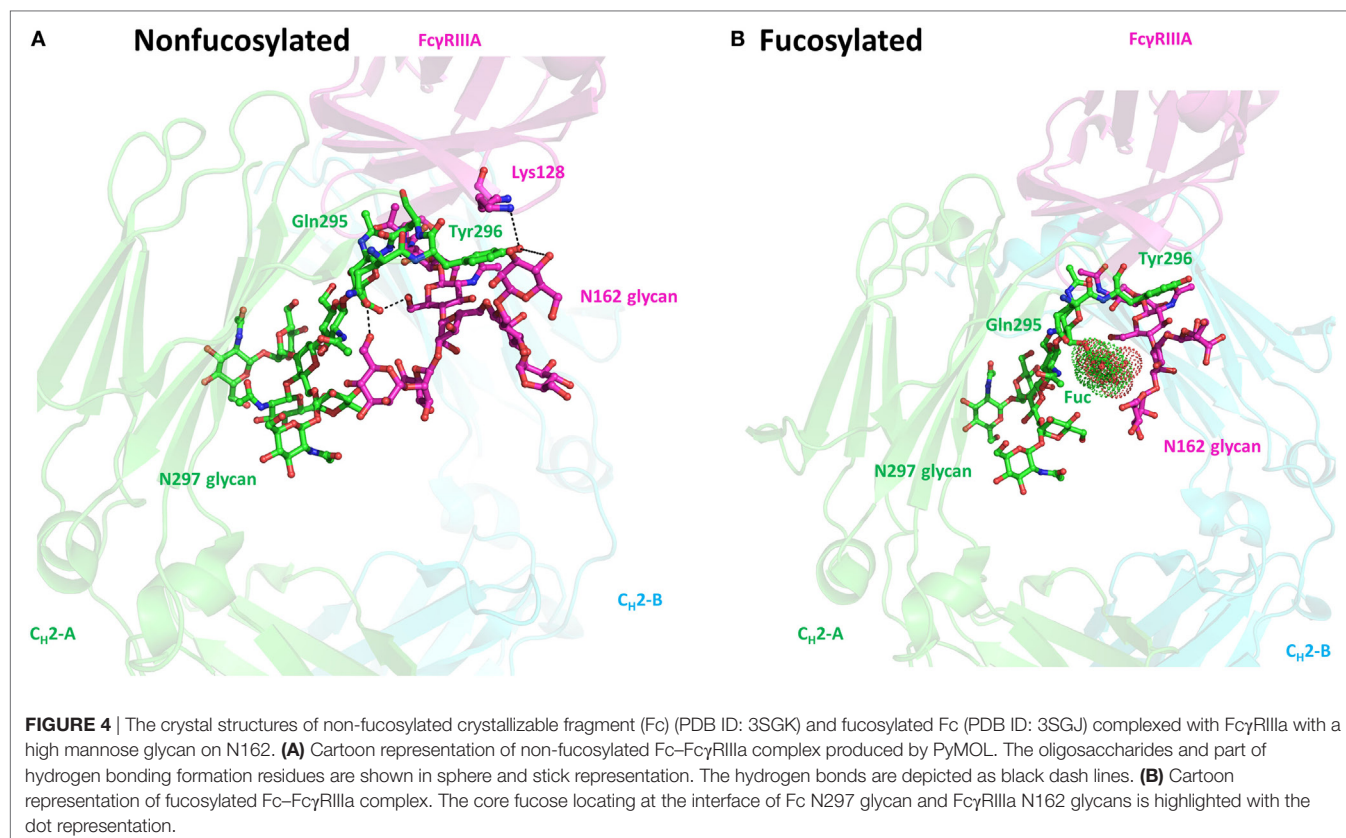
Absence of Core Fucose Results in Improved ADCC Activity of IgG

Addition of a fucose to the innermost GlcNAc (the core fucose) is catalyzed by the α -1,6-fucosyltransferase in the medial-Golgi.



More than 80% of the human IgG and >90% of the recombinant IgG produced by CHO cells contain the core fucose (13). However, the absence of core Fuc residue in the N-glycans significantly improves ADCC activity of IgG due to the substantially enhanced binding affinity to Fc γ RIIIa (31, 75). For example, afucosylated anti-HER2 IgG exhibits a ~100-fold greater ADCC effect compared with the fucosylated counterpart (51). The defucosylated antibody is also more potent than the fucosylated counterpart in the clinic (37, 78). The resolved complex crystal structures of Fc–Fc γ RIIIa have provided molecular rationales underlying the enhanced binding to Fc γ RIIIa for defucosylated IgGs. The crystal structure of sFc γ RIIIa with high mannose-type glycans in Asn162 complexed with the defucosylated Fc show that the lower hinge regions of C_{H2} dimer dock onto the D2 domain of Fc γ RIIIa (79). Both the carbohydrate–carbohydrate and carbohydrate–protein interactions exist at the interface. The chitobiose core of Asn162 glycans hydrogen bond to the innermost GlcNAc of Fc. The 1,3-arm mannose of Fc γ RIIIa forms a hydrogen bond to the Gln295 of Fc. The branching β -mannose and Lys128 of Fc γ RIIIa make contacts with Tyr296 residue of Fc (Figure 4). However, these non-covalent interactions were unfavorable or disrupted due to the steric hindrances imposed by the presence of fucose in the fucosylated Fc. Besides, the conformation of Tyr296 is more constrained in the fucosylated Fc, which prevents Tyr296 from adapting a favorable conformation for binding to Fc γ RIIIa (80). Thus, the fucose

moiety exerts allosterically inhibitory effects on the Fc–Fc γ RIIIa interaction, although it does not contact directly with Fc γ RIIIa. The enhanced binding affinity to Fc γ RIIIa endows defucosylated IgG several therapeutic merits. First, the high affinity could make the exogenous defucosylated IgG outcompete the endogenous serum IgG, thus avoiding the inhibitory effects of high concentration of serum IgGs on therapeutic IgG efficacies. For example, the inhibitory effect of endogenous IgG on ADCC was alleviated by defucosylated anti-CD20 antibodies (81, 82). Second, defucosylated antibodies have enhanced binding to the low affinity allotype of Fc γ RIIIa-158F and reduce the differences of ADCC efficacies of antibodies among the Fc γ RIIIa-158V and Fc γ RIIIa-158F allelic patients. Defucosylated IgGs have broader applications for all patients independent of the Fc γ RIIIa polymorphisms (83, 84). Finally, in addition to enhanced activation of Fc γ RIIIa-expressing killer cells (NK cells, monocytes, and macrophages) to mediate ADCC, the defucosylated antibody has also been reported to evoke ADCP effect through engaging Fc γ RIIb on neutrophils, which in turn facilitates antigen presentation and recruitment of adaptive immunity, as evidenced by the defucosylated anti-CD20 IgG mediating upregulation of MHC class II molecules on neutrophil cell surface (85). Collectively, Fc fucosylation represents the most important influencer in modulating IgG effector function. Since ADCC is the main mode of action for mAbs in clinical oncology, defucosylated IgGs are highly desirable as the next-generation



therapeutic antibodies. The high demand in defucosylated mAbs is driving the development of multiple glycoengineering strategies to produce low fucose antibodies (see below Table 2).

High Galactose Enhances CDC Activity of IgG

Both human serum IgG and recombinant IgG contain predominantly terminal galactose residues in their antennae (31). CHO cells-derived IgGs usually have lower levels of galactosylation compared with IgGs produced in mouse myeloma cells (32). Although the terminal galactose does not affect ADCC activity of IgG, it plays an important role in modulating the CDC activity (86). For example, the galactosylated rituximab exhibited higher CDC than the degalactosylated glycoform due to the higher affinity to C1q (44). Structurally, the extensive hydrophobic and hydrophilic interactions between terminal Gal residue and protein could impact the conformation of the C H_2 domain, resulting in altered C1q binding (20). More hydrogen bonds between sugar residues and amino acids are found in the G2 glycoform compared with the G0 form of IgG1 (Figure 5) (14, 87, 88). Consequently, the stretch from residue 244 to 247 of C H_2 domain is destabilized in the G0 glycoform, which was also supported by the comparative differential scanning microcalorimetry showing that G0 form associates with a lower enthalpy than the G2 form (89). These studies suggest that the non-covalent interactions between galactose and amino acid residues may account for the increased binding affinity between galactosylated Fc and C1q. Although the role of terminal galactose is not completely elucidated and in

some cases the effect of terminal galactose has been reported to be antibody dependent, a proper control of galactosylation during manufacturing is still warranted.

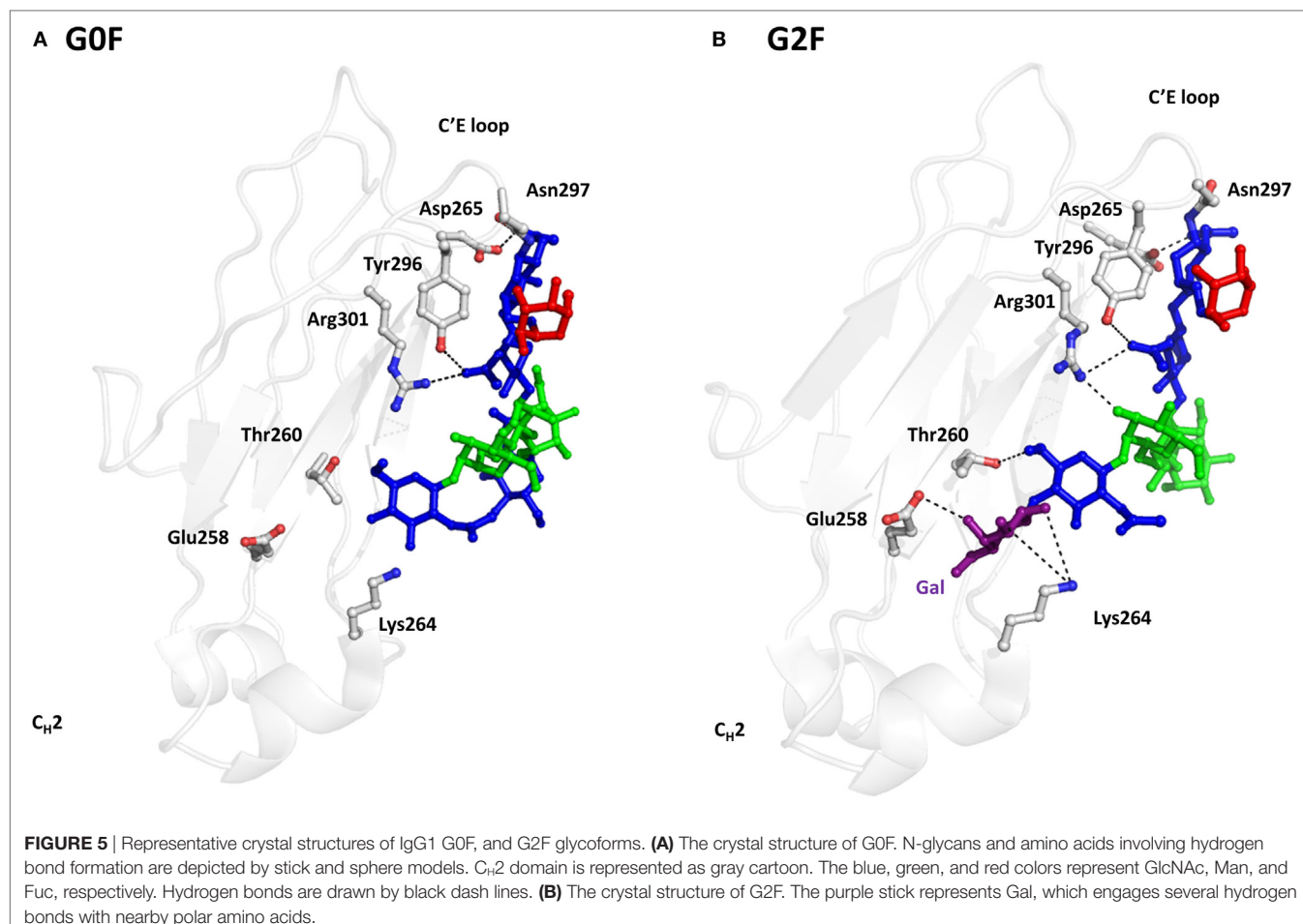
Impact of Terminal Sialylation on IgG Functions

The terminal sialic acid residue prolongs IgG half-life in the serum by shielding “galactose” residues from exposure to galactose-specific receptors in hepatocytes (32). On the other hand, sialylation may be undesirable because it renders IgGs more sensitive to protease compared with asialylated antibodies, probably due to the bulkier sialic acid leading to structural perturbations of C H_2 domains (22, 90). The crystal structure has shown that the 1,6-arm sialic acid poses away from the protein-associated galactose residue and is entirely exposed to the solvent (91). The α -2,3-sialylation negatively impacts the canonical galactose-protein interactions and potentially destabilizes the C H_2 domain (92). In addition, sialylation has negative effect on the ADCC activity of mAb (93), which may either stem from the decreased hinge flexibility upon sialylation causing reduced Fc γ RIIIa binding, or from the reduced bivalent antigen binding due to the lack of hinge flexibility (94). Antibody sialylation is desired due to its anti-inflammatory effects with potential applications in autoimmune and inflammatory diseases (95). The effect of sialylation was first discovered from human intravenous immunoglobulin but can also be recapitulated by the α -2,6-sialylation in recombinant IgG (96). Although not fully understood, this anti-inflammatory effect is triggered by the

TABLE 2 | Summary of the cell glycoengineering strategies to produce defucosylated antibodies.

Cell type		Glycoengineering modification	Company and technology platform	Antibody name	Targets	Development status	Reference
Non-mammalian cells	Yeasts	och or alg3 KO	NA GS4.0	Rituximab	Anti-CD20	NA	(45–47)
	Plants	RNAi of β -1,2-XyIT and α -1,3-FucT	MAPP Biopharmaceutical	ZMAPP	Anti-Ebola	Phase 2/3	(48, 49)
Mammalian cells	YB2/0	Intrinsic low core fucose content YB2/0 (FUT8 low); Lec13 (GMD low)	LFB Biotechnologies EMABling Technology	Ublituximab; roledumab	Anti-CD20; anti-RhD	Phase 2/3	(50)
	CHO cells	Lec13 cells	Biowa	Hu4D5	Anti-HER2	NA	(51)
Genetically modified CHO	WT CHO	Addition of sugar analog into culture medium (process engineering)	Seattle Genetics SEA Technology	SEA-CD40	Anti-CD40	Phase 1	(52)
	GMD KO	GMD knockout CHO/DG44	Rituximab	Anti-CD20	NA	(53)	
	RMD overexpression	ProBioGen, GlymaxX Technology	Trastuzumab	Anti-HER2	NA	(54)	
	GFT KO	CRISPR-Cas9 KO GFT CHO-F6	LSEVh-LS-F	Anti-HIV-1 Env	Pre-clinic	(55, 56)	
	GnT III overexpression	Roche GlycoMab Technology	Obinutuzumab RG7116	Anti-CD20 Anti-HER3	Approved Phase 1	(57) (58)	
	RNAi of FUT8 and/or GMD	FG16	KM2160	Anti-CCR4	NA	(59, 60)	
	FUT8 KO	Kyowa Hakko Kirin Potelligent Technology	Mogamulizumab Benralizumab, ecromeximab, MEDI-551, BIW-8962, KHK2804, 2823, 2898, 4083	Anti-CCR4 Anti-IL-5R α , GD3, CD19, GM2, CD123, CD98	Approved In clinical trials	(61) (31)	
		FUT8 knockout CHO/DG44	NA	Anti-CD20	NA	(62)	
	293 FreeStyle cells	α -Mannosidase inhibitors kifunensine	NA	4Dm2m-F	Anti-HIV-1 Env	NA	(63)

NA, not applied; RhD, rhesus D antigen; GFT, GDP-fucose transporter; GM2, ganglioside mono-sialic acid 2; GD3, ganglioside di-sialic acid 3; GMD, GDP-mannose 4,6-dehydratase; GnT III, GlcNAc transferase III.



sialylated IgG interacting with the murine C-type lectin-like receptor-specific intracellular adhesion molecule-grabbing non-integrin R1 (SIGN-RI) on macrophage and dendritic cells (human ortholog, DCSIGN), which leads to increased Fc γ RIIb expression and expansion of Treg cell populations suppressing of inflammatory response (97, 98). Collectively, terminal sialic acid residues have both positive and negative effects on antibodies biological functions. It is necessary to strictly control sialylation in recombinant IgGs.

IgG-Fc GLYCOENGINEERING

Since different glycoforms have distinct impacts on antibody effector function, it is necessary to control antibody glycoforms. With advanced knowledge of glycobiology, it is feasible to produce homogeneously glycosylated antibodies with tailored effector function. Strategies include host cell based glycoengineering involving manipulations of biosynthetic pathways and *in vitro* chemoenzymatic glycosylation remodeling.

Cell Glycoengineering

Host cell glycoengineering has been highly pursued in recent years to produce recombinant IgG with desired glycoforms. As mentioned above, antibody glycoforms resulting from sets of

enzymatic reactions pathways are a combined function of host cells, enzyme kinetical parameters, nucleotide sugar substrates, and the external factors. Following this lead, we classify cell glycoengineering strategies into the following four types.

Selection of Cell Type, Environmental Factors, and Cell Culture Conditions

Antibody glycosylation is largely influenced by the host cells from which they are manufactured. mAbs produced by CHO cells are somewhat under-sialylation due to the lack of α -2, 6-sialyltransferase in these cells (31). Host cells with intrinsically low α -1,6 fucosyltransferase activity could be used to produce IgGs with low core fucose (99). For example, the rat hybridoma cell line YB2/0 with low FUT8 activity, a type of α -1,6 fucosyltransferase responsible for adding the core fucose, is used for the productions of defucosylated IgG (50). Another example is the Lec13 cell line, a derivative of CHO cells with deficiency in GDP-mannose 4,6-dehydratase (GMD) function leading to low fucosylation (51). On the other hand, the cell culture environment could be manipulated during the fermentation process to alter and optimize antibody glycoforms (process glycoengineering) (32). For example, addition of uridine, manganese chloride, and galactose could increase terminal Gal to enhance CDC activity of IgG (76, 100). Addition of UDP-GlcNAc and using

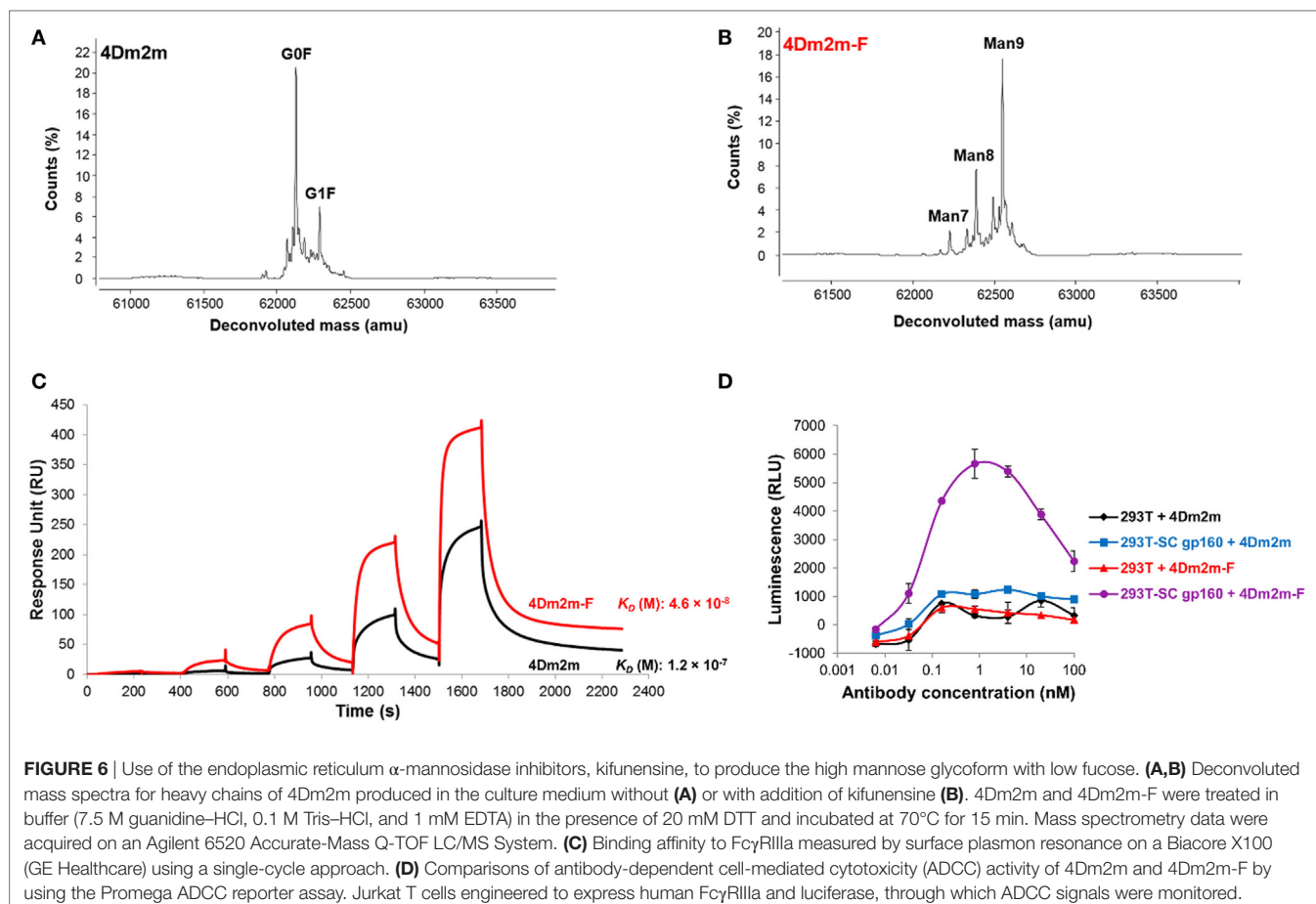
serum-free culture increased sialylation of IgG1 (101). Addition of modified sugars such as 2-fluorofucose to the culture medium inhibits core fucose incorporation (102).

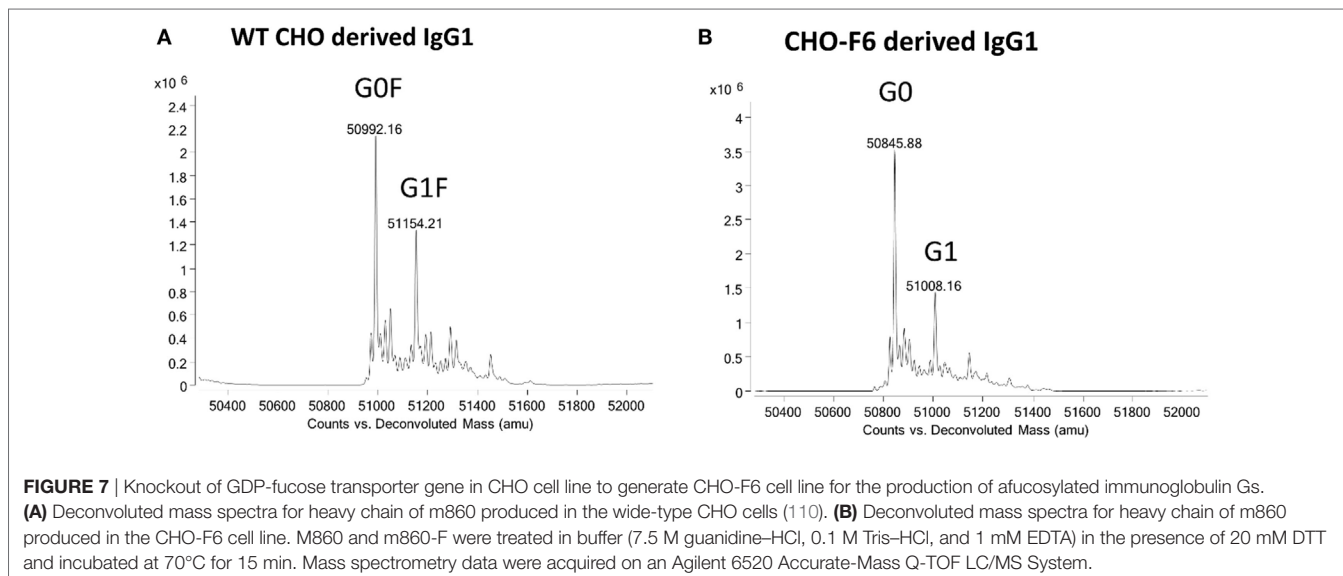
Using Enzyme Inhibitors to Intervene Host Biosynthesis Pathway

Inhibitors able to modulate mAbs glycosylation have been reported. Antibody glycosylation is the result of multiple stepwise events. Enzyme inhibitors arresting mAbs in the intermediate glycoforms could prevent the additions of outer arm sugar residues including fucose (13). Such examples include the ER glucosidases I and II inhibitors, deoxynojirimycin and castanospermine producing Glc3Man9GlcNAc2 glycoform; the ER α -mannosidase inhibitors, deoxymannojirimycin and kifunensine producing the high mannose (Man9GlcNAc2) glycoform; and Golgi α -mannosidase II inhibitor swainsonine producing hybrid glycoforms such as GlcNAcMan5GlcNAc2Fuc (103). The authors' group has used kifunensine to produce a defucosylated IgG-like bispecific and multivalent anti-HIV-1 molecule, 4Dm2m-F (63). 4Dm2m-F exhibits approximately threefolds higher binding affinity to Fc γ RIIIa than fucosylated 4Dm2m (**Figure 6**). The ADCC activity of 4Dm2m-F is also significantly improved based on the Promega ADCC reporter assay.

Genetic Modifications of the Host Biosynthesis Pathway

Antibody glycoforms can be altered by modulating host N-glycosylation pathway. The substrate availability can be changed by inactivation or overexpression of the corresponding nucleotide sugar transporters. For example, knockout of the mammalian *GMD* gene decreases the synthesis of the fucose donor, GDP-fucose, leading to production of defucosylated IgG (104). A similar method involves the overexpression of the GDP-6-deoxy-d-lyxo-4-hexulose reductase (RMD) (ProBioGen, GlymaxX technology) (105). In another example, co-transfection of cytidine monophosphate-sialic acid synthase, cytidine monophosphate-sialic acid transporter, and α -2,3-SiaT in CHO cell lines significantly has increased the intracellular CMP-SA level and improved the SA content of the recombinant protein (106). Recently, the gene editing technology is also used to engineer defucosylated antibodies. ZFNs and TALENs were used to inactivate GDP-fucose transporter (GFT) gene (*Slc35c1*) in CHO cells for production of fucose-free antibodies (107). Our group recently has used CRISPR-Cas9 to knockout GFT gene in CHO cell line (termed as CHO-F6) for the production of various afucosylated mAbs and Fc-fusion proteins (**Figure 7**) (55). Alternatively, the unwanted glycan pathways could be outcompeted by desired ones. For example, Roche's GlycArt





technology overexpresses β -1,4-GlcNAc transferase III (GnT III) to inhibit the downstream α -1,6-fucosyltransferase processing leading to the bisecting GlcNAc glycoforms rather than fucosylation (108). This technology has been used to produce the FDA approved anti-CD20 obinutuzumab (Gazyva[®]) (57). Co-overexpression of GnT III and α -mannosidase II leads to further lower fucose content by introducing non-fucosylated hybrid-type glycans (109). Another approach to control the desired or unwanted glycoforms is either genetically inactivating or increasing glycosyltransferases activity directly responsible for transferring of single monosaccharides to glycan structures. For sialylation, overexpression of α -2,3-sialyltransferase and β -1,4-galactosyltransferase elevates IgG sialylation and galactosylation (32). For fucosylation, genetically dampening FUT8 expression encoding α -1,6-fucosyltransferase significantly decreases or completely abolishes the terminal fucose (99). Small interfering RNA (siRNA) technique has been used to reduce α -1,6-fucosyltransferase activity for production of partially defucosylated IgGs (59). Furthermore, double siRNA knockdown of FUT8 and GMD gene achieves completely afucosylated IgG (60). Alternatively, knockout of FUT8 gene by the disruption of the genomic locus via homologous recombination could result in 100% afucosylated IgGs (62). One such afucosylation platform is the Potelligent Technology from Kyowa Hakko Kirin company utilizing FUT8 KO CHO cell line to develop the anti-CCR4 mogamulizumab (**Table 1**, the first approved glycoengineered antibody) (61).

“Humanization” of N-Glycosylation Pathway of Non-Mammalian Cells

Some non-mammalian cell lines have been used to produce therapeutic antibodies due to the cost-effectiveness and/or decreased fucosylation (31). Glycoengineering of non-mammalian cells aims to humanize the immunogenic glycoforms by eliminating enzymes responsible for adding non-mammalian glycans and subsequently introducing the mammalian glycan processing enzymes. For example, knockout of the *och* or *alg3* genes in yeasts

and knockout of plant-specific β -1,2-xylosyltransferase (β -1,2-XylT) and α -1,3-fucosyltransferase (α -1,3-FucT) genes achieve the elimination of the high mannose glycoforms and β 1,2-xylose and core α 1,3-fucose. The mammalian glycan processing enzymes such as mannosidases I and II, GnT I and II, β -1,4-GalT, and α -2,6-SiaT are then used to introduce human IgG-like glycoforms (13). Examples include the production of the rituximab in *Pichia pastoris* (45), the anti-HIV mAb 2G12 in *Nicotiana benthamiana* (111), and the anti-Ebola ZMAPP antibody cocktail (lack of core fucose) in plant (48).

Chemoenzymatic Glycoengineering

Despite much progress in cell glycoengineering, it is still very challenging to produce IgGs with highly homogenous glycoforms in host cells. Consequently, the *in vitro* chemoenzymatic glycosylation remodeling provides an attractive alternative for the production of therapeutic mAbs with predefined and homogeneous glycoforms (34, 112). This method usually contains three steps: deglycosylation of IgG by an endo- β -N-acetylglucosaminidase (ENGase, such as endoglycosidase S, EndoS), simultaneously leaving the innermost GlcNAc at N297; preparation of oxazoline derivatives of customized N-linked glycan structures as sugars donors by chemical methods; transglycosylation of the glycan oxazoline donor to the innermost GlcNAc acceptor (113). The transglycosylation usually proceeds stereo-specifically under the catalysis of an ENGase, which was engineered to abolish the hydrolytic activity and improve substrate specificities (e.g., EndoS D233Q, EndoA N171A, EndoA E173Q, EndoMN175A, and EndoM N175Q) (114, 115). This chemoenzymatic approach has been successfully used to produce homogenous Fc glycoforms including non-fucosylated, fully sialylated and bisecting GlcNAc (116, 117). For example, rituximab was engineered from G0F, G1F, and G2F glycoforms to G2 and G2S2F glycoforms by EndoS-D233A and D233Q (114). Recently, the chemoenzymatic glycosylation remodeling was also elegantly used for site-specific conjugation of drugs onto antibodies (see below).

AGLYCOSYLATED FULL-LENGTH IgG AS A NOVEL THERAPEUTIC FORMAT

In recent years, aglycosylated full-length IgGs have gained substantial attentions due to their novel features (43, 118). Although the absence of N-glycans leads to the “closed” conformation of Fc and destabilization of C’E loop, the overall structures of aglycosylated IgG are similar to the glycosylated counterparts (119, 120). Thus, aglycosylated IgGs have almost identical antigen-binding affinity and pH-dependent FcRn binding and hence PK to glycosylated IgGs (121), which endows aglycosylated mAbs applications in the cases not requiring or avoiding undesired effector functions such as receptor blocking, targeted delivery, and anti-inflammation (122). Aglycosylated mAbs can be either produced in prokaryotic hosts (*E. coli*) or in eukaryotic hosts by introducing mutations at the Fc N297 or by the chemoenzymatic methods such as EndoS and PNGase-F enzyme treatment (120). Compared with the glycosylated IgG, aglycosylated IgG is devoid of glycan heterogeneity, hence significantly simplifies the biomanufacturing process leading to faster development timelines and lower developmental cost. Besides, aglycosylated IgG may be more susceptible to engineering due to the higher flexibility of the Fc conferred by the lack of N-glycans (118). Aglycosylated Fc could be engineered to restore or even improve its binding to FcγRs compared with glycosylated counterparts, which potentially extends the applications of aglycosylated IgGs into the cases effector functions are needed. For example, aglycosylated IgG-Fc could be engineered to bind to FcγRIIa and FcγRIIb comparably with glycosylated IgG-Fc by introducing double mutations S298G/T299A (123). More importantly, the higher flexibility renders the aglycosylated Fc being relatively easily engineered to exhibit unique FcγR specificity and novel effector functions. Jung et al. have used high-throughput library screening to develop an aglycosylated trastuzumab variant with five mutations (S298G/T299A/N390D/E382V/M428L) in Fc exhibiting >160-fold enhanced binding to FcγRIIa-R131 and 25-fold increased selectivity to FcγRIIa-R131 over FcRIIyb compared with the wide-type trastuzumab (124). Aglycosylated IgGs have established a new way for immunotherapy. Currently, several aglycosylated antibodies are under clinical investigation for efficacy and safety (120).

Fc N-GLYCAN SPECIFIC ADC

Antibody-drug conjugates are IgGs conjugated with cytotoxic small molecules through chemical linkers. By specifically targeting cancer cells and selective delivery of highly cytotoxic drugs, ADCs fundamentally revolutionized the way of cancer immunotherapy and chemotherapy (125). Currently, four ADCs (Adcetris®, Kadlecia®, Besponsa®, and Mylotarg®) have been approved by FDA with more than 80 ADCs under clinical evaluations (126). The mode of action of ADCs involves antigen-mediated endocytosis, followed by the release of drugs by either lysosomal degradation or hydrolytic/proteolytic cleavage (127). The methods for conjugating the small molecule drugs onto IgG represent one of the key technologies in ADC development. The

conventional conjugation approaches involve random addition of drugs onto Lys or reduced Cys residues by amide coupling and maleimide alkylation chemistry, which leads to highly heterogeneous mixtures with different drug–antibody ratios and inconsistent yield (128). This heterogeneity negatively impacts the *in vivo* efficacy, stability, PK of ADCs (129). Thus, site-specific conjugation methods are highly pursued (130). Conjugation through IgG-Fc N-glycans represents one of the most widely used site-specific conjugation methods (131). Glycosite-specific conjugation proceeds with the introduction of a chemically active moiety onto the Fc N-glycans followed by reacting with payloads carrying another chemically active group. In this method, native IgG with heterogeneous N-glycans is deglycosylated by a wild-type endoglycosidase followed by the transglycosylation of a chemical group capped homogenous N-glycan substrate. The transglycosylation is catalyzed by an endoglycosynthase (a mutant of endoglycosidase) that lacks hydrolytic activity but possesses transglycosylation activity (132). Subsequently, the drug payload can be conjugated by biocompatible chemical reactions such as click chemistry and oximation. Boons et al. have reported the utilization of a sialyltransferase to attach an azido-tagged sialic acid moiety onto the galactosylated IgG N-glycan and conjugate the payload, doxorubicin on the azido group *via* the “click chemistry” (133). van Geel et al. reported a different method to produce ADC, which involved the endoglycosidase-mediated deglycosylation to obtain the Fuc- α -1,6-GlcNAc disaccharide glycoform of IgG, followed by the addition of azido-capped UDP-galactose catalyzed by a mutant galactosyltransferase (134). Our group has exploited a galactosyltransferase mutant (β -1,4-Gal-T1-Y289L) to achieve glycosite-specific conjugation by transferring the keto-tagged or azido-tagged galactose onto the degalactosylated GOF glycoform of IgG. The final ADC products, m860-AF (Auristatin F) ADC and m276-PBD (pyrrolobenzodiazepine) ADC, were obtained through the keto oximation-mediated addition of AF and the “click chemistry”-mediated addition of PBD dimer onto m860 IgG1 and m276 IgG1, respectively (110, 135). The glycosite-specific conjugation strategies provide novel routes for the preparations of ADCs with better homogeneity and drug to antibody ratios.

CONCLUSION AND PERSPECTIVES

Unlike DNA and protein synthesis, antibody glycosylation synthesis is not directly template driven but is rather a result of networks of enzymatic reactions. Both host cells and the culture environment impact antibody glycosylation. Recombinant mAbs produced in host cells carry heterogeneous Fc glycosylation, presumably with more than 400 possible glycoforms. Different glycoforms affect the *in vivo* efficacy, effector function, PK, stability, aggregation, safety, and immunogenicity of IgG. Among these, the impacts of Fc N-glycans on antibody effector function including ADCC and CDC are widely studied. IgG N-glycans affect their ADCC and CDC activity by altering Fc conformations and modulating the non-covalent interactions between oligosaccharides and C_H2 domains. While the terminal Gal enhances CDC activity, the core fucose significantly inhibits

ADCC by sterically hindering the interactions between IgG-Fc and Fc γ RIIIa. Thus, the regulatory authorities require developers to keep glycoforms of mAbs consistent with limited heterogeneity, which has driven the development of multiple cell glycoengineering strategies to produce mAbs with desired glycoforms, especially without fucose. Although progress has been made, it is still challenging to consistently produce fully homogenously glycosylated antibodies by glycoengineered cell lines. The chemoenzymatic glycosylation remodeling offers revolutionized avenues to IgG with homogenous glycoforms. However, most current chemoenzymatic glycoengineering is still under lab-scale explorations, which is very challenging to scale up for industrial development. The chemoenzymatic glycoengineering approaches also provide novel routes for the productions of ADCs. On the other hand, the glyco-heterogeneity of mAbs could be bypassed by aglycosylated full-length IgGs. However, it remains to be seen for the outcomes of the clinical trials of aglycosylated antibodies in terms of the *in vivo* stability and immunogenicity. In the future, “omics” technologies and systems biology modeling hold promises to aid the glycoengineering for

developing next-generation mAbs with homogenous glycoforms and improved therapeutic efficacy.

AUTHOR CONTRIBUTIONS

DD conceived the topic; WL wrote the manuscript; ZZ, YF, and WC revised the manuscript.

FUNDING

The authors thank the Intramural AIDS Targeted Antiviral Program (IATAP) of the National Institutes of Health (NIH), the Intramural Research Program of the NIH, National Cancer Institute (NCI), Center for Cancer Research, the U.S.–China Program for Biomedical Research Cooperation, and the U.S.–China Program for Research toward a Cure for HIV/AIDS. The content of this publication does not necessarily reflect the views or policies of the Department of Health and Human Services nor does the mention of trade names, commercial products, or organizations imply endorsement by the U.S. Government.

REFERENCES

- Elvin JG, Coustou RG, van der Walle CF. Therapeutic antibodies: market considerations, disease targets and bioprocessing. *Int J Pharm* (2013) 440:83–98. doi:10.1016/j.ijpharm.2011.12.039
- Reichert JM. Antibodies to watch in 2017. *MABs* (2017) 9:167–81. doi:10.1080/19420862.2016.1269580
- Niwa R, Satoh M. The current status and prospects of antibody engineering for therapeutic use: focus on glycoengineering technology. *J Pharm Sci* (2015) 104:930–41. doi:10.1002/jps.24316
- Walsh G. Biopharmaceutical benchmarks 2014. *Nat Biotechnol* (2014) 32:992–1000. doi:10.1038/nbt.3040
- Beck A, Wagner-Rousset E, Bussat MC, Lokteff M, Klinguer-Hamour C, Haeuw JF, et al. Trends in glycosylation, glycan analysis and glycoengineering of therapeutic antibodies and Fc-fusion proteins. *Curr Pharm Biotechnol* (2008) 9:482–501. doi:10.2174/138920108786786411
- Jeffery R. Glycosylation of recombinant antibody therapeutics. *Biotechnol Prog* (2005) 21:11–6. doi:10.1021/bp040016j
- Jeffery R. Glycosylation as a strategy to improve antibody-based therapeutics. *Nat Rev Drug Discov* (2009) 8:226–34. doi:10.1038/nrd2804
- Liu L. Pharmacokinetics of monoclonal antibodies and Fc-fusion proteins. *Protein cell* (2017). doi:10.1007/s13238-017-0408-4
- Liu L. Antibody glycosylation and its impact on the pharmacokinetics and pharmacodynamics of monoclonal antibodies and Fc-fusion proteins. *J Pharm Sci* (2015) 104:1866–84. doi:10.1002/jps.24444
- Liu H, Nowak C, Andrien B, Shao M, Ponniah G, Neill A. Impact of IgG Fc-oligosaccharides on recombinant monoclonal antibody structure, stability, safety, and efficacy. *Biotechnol Prog* (2017) 33(5):1173–81. doi:10.1002/btpr.2498
- Bournazos S, Wang TT, Dahan R, Maamary J, Ravetch JV. Signaling by antibodies: recent progress. *Annu Rev Immunol* (2017) 35:285–311. doi:10.1146/annurev-immunol-051116-052433
- Quast I, Peschke B, Lunemann JD. Regulation of antibody effector functions through IgG Fc N-glycosylation. *Cell Mol Life Sci* (2017) 74:837–47. doi:10.1007/s00018-016-2366-z
- Le NP, Bowden TA, Struwe WB, Crispin M. Immune recruitment or suppression by glycan engineering of endogenous and therapeutic antibodies. *Biochim Biophys Acta* (2016) 1860:1655–68. doi:10.1016/j.bbagen.2016.04.016
- Raju TS. Terminal sugars of Fc glycans influence antibody effector functions of IgGs. *Curr Opin Immunol* (2008) 20:471–8. doi:10.1016/j.co.2008.06.007
- Subedi GP, Barb AW. The structural role of antibody N-glycosylation in receptor interactions. *Structure* (2015) 23:1573–83. doi:10.1016/j.str.2015.06.015
- Brader ML, Estey T, Bai S, Alston RW, Lucas KK, Lantz S, et al. Examination of thermal unfolding and aggregation profiles of a series of developable therapeutic monoclonal antibodies. *Mol Pharm* (2015) 12:1005–17. doi:10.1021/mp400666b
- Mimura Y, Church S, Ghirlando R, Ashton PR, Dong S, Goodall M, et al. The influence of glycosylation on the thermal stability and effector function expression of human IgG1-Fc: properties of a series of truncated glycoforms. *Mol Immunol* (2000) 37:697–706. doi:10.1016/S0161-5890(00)00105-X
- Feige MJ, Walter S, Buchner J. Folding mechanism of the CH2 antibody domain. *J Mol Biol* (2004) 344:107–18. doi:10.1016/j.jmb.2004.09.033
- Zheng K, Bantog C, Bayer R. The impact of glycosylation on monoclonal antibody conformation and stability. *MABs* (2011) 3:568–76. doi:10.4161/mabs.3.6.17922
- Krapp S, Mimura Y, Jefferis R, Huber R, Sondermann P. Structural analysis of human IgG-Fc glycoforms reveals a correlation between glycosylation and structural integrity. *J Mol Biol* (2003) 325:979–89. doi:10.1016/S0022-2836(02)01250-0
- Tao MH, Morrison SL. Studies of aglycosylated chimeric mouse-human IgG. Role of carbohydrate in the structure and effector functions mediated by the human IgG constant region. *J Immunol* (1989) 143:2595–601.
- Raju TS, Scallion B. Fc glycans terminated with N-acetylglucosamine residues increase antibody resistance to papain. *Biotechnol Prog* (2007) 23:964–71. doi:10.1021/bp070118k
- Raju TS, Scallion BJ. Glycosylation in the Fc domain of IgG increases resistance to proteolytic cleavage by papain. *Biochem Biophys Res Commun* (2006) 341:797–803. doi:10.1016/j.bbrc.2006.01.030
- Raju TS, Briggs JB, Chamow SM, Winkler ME, Jones AJ. Glycoengineering of therapeutic glycoproteins: *in vitro* galactosylation and sialylation of glycoproteins with terminal N-acetylglucosamine and galactose residues. *Biochemistry* (2001) 40:8868–76. doi:10.1021/bi010475i
- Jones AJ, Papac DI, Chin EH, Keck R, Baughman SA, Lin YS, et al. Selective clearance of glycoforms of a complex glycoprotein pharmaceutical caused by terminal N-acetylglucosamine is similar in humans and cynomolgus monkeys. *Glycobiology* (2007) 17:529–40. doi:10.1093/glycob/cwm017
- Goetze AM, Liu YD, Zhang Z, Shah B, Lee E, Bondarenko PV, et al. High-mannose glycans on the Fc region of therapeutic IgG antibodies increase serum clearance in humans. *Glycobiology* (2011) 21:949–59. doi:10.1093/glycob/cwr027
- Wright A, Sato Y, Okada T, Chang K, Endo T, Morrison S. *In vivo* trafficking and catabolism of IgG1 antibodies with Fc associated carbohydrates of differing structure. *Glycobiology* (2000) 10:1347–55. doi:10.1093/glycob/10.12.1347

28. Ghaderi D, Taylor RE, Padler-Karavani V, Diaz S, Varki A. Implications of the presence of N-glycolylneuraminic acid in recombinant therapeutic glycoproteins. *Nat Biotechnol* (2010) 28:863–7. doi:10.1038/nbt.1651
29. Chung CH, Mirakhur B, Chan E, Le QT, Berlin J, Morse M, et al. Cetuximab-induced anaphylaxis and IgE specific for galactose-alpha-1,3-galactose. *N Engl J Med* (2008) 358:1109–17. doi:10.1056/NEJMoa074943
30. Reusch D, Tejada ML. Fc glycans of therapeutic antibodies as critical quality attributes. *Glycobiology* (2015) 25:1325–34. doi:10.1093/glycob/cwv065
31. Dicker M, Strasser R. Using glyco-engineering to produce therapeutic proteins. *Expert Opin Biol Ther* (2015) 15:1501–16. doi:10.1517/14712598.2015.1069271
32. Costa AR, Rodrigues ME, Henriques M, Oliveira R, Azeredo J. Glycosylation: impact, control and improvement during therapeutic protein production. *Crit Rev Biotechnol* (2014) 34:281–99. doi:10.3109/07388551.2013.793649
33. Jefferis R. Isotype and glycoform selection for antibody therapeutics. *Arch Biochem Biophys* (2012) 526:159–66. doi:10.1016/j.abb.2012.03.021
34. Mimura Y, Katoh T, Saldova R, O’Flaherty R, Izumi T, Mimura-Kimura Y, et al. Glycosylation engineering of therapeutic IgG antibodies: challenges for the safety, functionality and efficacy. *Protein Cell* (2017). doi:10.1007/s13238-017-0433-3
35. Hale G, Rebello P, Al Bakir I, Bolam E, Wiczling P, Jusko WJ, et al. Pharmacokinetics and antibody responses to the CD3 antibody otelixizumab used in the treatment of type 1 diabetes. *J Clin Pharmacol* (2010) 50:1238–48. doi:10.1177/0091270009356299
36. Ng CM, Stefanich E, Anand BS, Fielder PJ, Vaickus L. Pharmacokinetics/pharmacodynamics of nondepleting anti-CD4 monoclonal antibody (TRX1) in healthy human volunteers. *Pharm Res* (2006) 23:95–103. doi:10.1007/s11095-005-8814-3
37. Ishida T, Joh T, Uike N, Yamamoto K, Utsunomiya A, Yoshida S, et al. Defucosylated anti-CCR4 monoclonal antibody (KW-0761) for relapsed adult T-cell leukemia-lymphoma: a multicenter phase II study. *J Clin Oncol* (2012) 30:837–42. doi:10.1200/JCO.2011.37.3472
38. Duvic M, Pinter-Brown L, Foss FM, Sokol L, Jorgensen J, Spitalny GL, et al. Results of a phase 1/2 study for KW-0761, a monoclonal antibody directed against CC chemokine receptor type 4 (CCR4), in CTCL patients. *Blood* (2010) 116:962–962.
39. Camacho LH, Joyce R, Brown JR, Chanan-Khan A, Amrein PC, Assad A, et al. A phase 1, open-label, multi-center, multiple-dose, dose-escalation study of MDX-1342 in patients with CD19-positive refractory/relapsed chronic lymphocytic leukemia. *Blood* (2009) 114:3425–3425.
40. Goede V, Fischer K, Busch R, Engelke A, Eichhorst B, Wendtner CM, et al. Obinutuzumab plus chlorambucil in patients with CLL and coexisting conditions. *N Engl J Med* (2014) 370:1101–10. doi:10.1056/NEJMoa1313984
41. Yu X, Marshall MJE, Cragg MS, Crispin M. Improving antibody-based cancer therapeutics through glycan engineering. *BioDrugs* (2017) 31:151–66. doi:10.1007/s40259-017-0223-8
42. Paz-Ares LG, Gomez-Roca C, Delord JP, Cervantes A, Markman B, Corral J, et al. Phase I pharmacokinetic and pharmacodynamic dose-escalation study of RG7160 (GA201), the first glycoengineered monoclonal antibody against the epidermal growth factor receptor, in patients with advanced solid tumors. *J Clin Oncol* (2011) 29:3783–90. doi:10.1200/JCO.2011.34.8888
43. Hristodorov D, Fischer R, Linden L. With or without sugar? (A)glycosylation of therapeutic antibodies. *Mol Biotechnol* (2013) 54:1056–68. doi:10.1007/s12033-012-9612-x
44. Peschke B, Keller CW, Weber P, Quast I, Lunemann JD. Fc-galactosylation of human immunoglobulin gamma isotypes improves C1q binding and enhances complement-dependent cytotoxicity. *Front Immunol* (2017) 8:646. doi:10.3389/fimmu.2017.00646
45. Li H, Sethuraman N, Stadheim TA, Zha D, Prinz B, Ballew N, et al. Optimization of humanized IgGs in glycoengineered *Pichia pastoris*. *Nat Biotechnol* (2006) 24:210–5. doi:10.1038/nbt1178
46. Liu B, Gong X, Chang S, Yang Y, Song M, Duan D, et al. Disruption of the OCH1 and MNN1 genes decrease N-glycosylation on glycoprotein expressed in *Kluyveromyces lactis*. *J Biotechnol* (2009) 143:95–102. doi:10.1016/j.biote.2009.06.016
47. Davidson RC, Nett JH, Renfer E, Li H, Stadheim TA, Miller BJ, et al. Functional analysis of the ALG3 gene encoding the Dol-P-Man: Man5GlcNAc2-PP-Dol mannosyltransferase enzyme of *P. pastoris*. *Glycobiology* (2004) 14:399–407. doi:10.1093/glycob/cwh023
48. Castilho A, Bohorova N, Grass J, Bohorov O, Zeitlin L, Whaley K, et al. Rapid high yield production of different glycoforms of Ebola virus monoclonal antibody. *PLoS One* (2011) 6:e26040. doi:10.1371/journal.pone.0026040
49. Davey RT Jr, Dodd L, Proschak MA, Neaton J, Neuhaus Nordwall J, Koopmeiners JS, et al. A randomized, controlled trial of ZMapp for Ebola virus infection. *N Engl J Med* (2016) 375:1448–56. doi:10.1056/NEJMoa1604330
50. Urbain R, Teillaud JL, Prost JF. [EMABling antibodies: from feto-maternal allo-immunisation prophylaxis to chronic lymphocytic leukaemia therapy]. *Med Sci (Paris)* (2009) 25:1141–4. doi:10.1051/medsci/200925121141
51. Shields RL, Lai J, Keck R, O’Connell LY, Hong K, Meng YG, et al. Lack of fucose on human IgG1 N-linked oligosaccharide improves binding to human Fc_{gamma}RIII and antibody-dependent cellular toxicity. *J Biol Chem* (2002) 277:26733–40. doi:10.1074/jbc.M202069200
52. Gardai SJ, Epp A, Linares G, Westendorf L, Sutherland MK, Neff-LaFord H, et al. A sugar engineered non-fucosylated anti-CD40 antibody, SEA-CD40, with enhanced immune stimulatory activity alone and in combination with immune checkpoint inhibitors. *J Clin Oncol* (2015) 33:3074–3074. doi:10.1200/jco.2015.33.15_suppl.3074
53. Kanda Y, Imai-Nishiya H, Kuni-Kamochi R, Mori K, Inoue M, Kitajima-Miyama K, et al. Establishment of a GDP-mannose 4,6-dehydratase (GMD) knockout host cell line: a new strategy for generating completely non-fucosylated recombinant therapeutics. *J Biotechnol* (2007) 130:300–10. doi:10.1016/j.jbiotec.2007.04.025
54. von Horsten HH, Ogorek C, Blanchard V, Demmler C, Giese C, Winkler K, et al. Production of non-fucosylated antibodies by co-expression of heterologous GDP-6-deoxy-D-lyxo-4-hexulose reductase. *Glycobiology* (2010) 20:1607–18. doi:10.1093/glycob/cwq109
55. Bardhi A, Wu Y, Chen W, Zhu Z, Zheng JH, Wong H, et al. Potent in vivo NK cell-mediated elimination of HIV-1-infected cells mobilized by a gp120-bispecific and hexavalent broadly neutralizing fusion protein. *J Virol* (2017) 91(20):e937–917. doi:10.1128/JVI.00937-17
56. Chen W, Bardhi A, Feng Y, Wang Y, Qi Q, Li W, et al. Improving the CH1-CK heterodimerization and pharmacokinetics of 4Dm2m, a novel potent CD4-antibody fusion protein against HIV-1. *MAbs* (2016) 8:761–74. doi:10.1080/19420862.2016.1160180
57. Robak T, Robak E. New anti-CD20 monoclonal antibodies for the treatment of B-cell lymphoid malignancies. *BioDrugs* (2011) 25:13–25. doi:10.2165/11539590-00000000-00000
58. Mirschberger C, Schiller CB, Schraml M, Dimoudis N, Friess T, Gerdes CA, et al. RG7116, a therapeutic antibody that binds the inactive HER3 receptor and is optimized for immune effector activation. *Cancer Res* (2013) 73:5183–94. doi:10.1158/0008-5472.CAN-13-0099
59. Mori K, Kuni-Kamochi R, Yamane-Ohnuki N, Wakitani M, Yamano K, Imai H, et al. Engineering Chinese hamster ovary cells to maximize effector function of produced antibodies using FUT8 siRNA. *Biotechnol Bioeng* (2004) 88:901–8. doi:10.1002/bit.20326
60. Imai-Nishiya H, Mori K, Inoue M, Wakitani M, Iida S, Shitara K, et al. Double knockdown of alpha1,6-fucosyltransferase (FUT8) and GDP-mannose 4,6-dehydratase (GMD) in antibody-producing cells: a new strategy for generating fully non-fucosylated therapeutic antibodies with enhanced ADCC. *BMC Biotechnol* (2007) 7:84. doi:10.1186/1472-6750-7-84
61. Matsushita T. Engineered therapeutic antibodies with enhanced effector functions: clinical application of the Potelligent(R) Technology. *Korean J Hematol* (2011) 46:148–50. doi:10.5045/kjh.2011.46.3.148
62. Yamane-Ohnuki N, Kinoshita S, Inoue-Urakubo M, Kusunoki M, Iida S, Nakano R, et al. Establishment of FUT8 knockout Chinese hamster ovary cells: an ideal host cell line for producing completely defucosylated antibodies with enhanced antibody-dependent cellular cytotoxicity. *Biotechnol Bioeng* (2004) 87:614–22. doi:10.1002/bit.20151
63. Chen W, Feng Y, Prabakaran P, Ying T, Wang Y, Sun J, et al. Exceptionally potent and broadly cross-reactive, bispecific multivalent HIV-1 inhibitors based on single human CD4 and antibody domains. *J Virol* (2014) 88: 1125–39. doi:10.1128/JVI.02566-13
64. Zhang P, Woen S, Wang T, Liu B, Zhao S, Chen C, et al. Challenges of glycosylation analysis and control: an integrated approach to producing optimal and consistent therapeutic drugs. *Drug Discov Today* (2016) 21:740–65. doi:10.1016/j.drudis.2016.01.006
65. Nagae M, Yamaguchi Y. Function and 3D structure of the N-glycans on glycoproteins. *Int J Mol Sci* (2012) 13:8398–429. doi:10.3390/ijms13078398

66. Wormald MR, Rudd PM, Harvey DJ, Chang SC, Scragg IG, Dwek RA. Variations in oligosaccharide-protein interactions in immunoglobulin G determine the site-specific glycosylation profiles and modulate the dynamic motion of the Fc oligosaccharides. *Biochemistry* (1997) 36:1370–80. doi:10.1021/bi9621472
67. Jefferis R. Recombinant antibody therapeutics: the impact of glycosylation on mechanisms of action. *Trends Pharmacol Sci* (2009) 30:356–62. doi:10.1016/j.tips.2009.04.007
68. Zauner G, Selman MHJ, Bondt A, Rombouts Y, Blank D, Deelder AM, et al. Glycoproteomic analysis of antibodies. *Mol Cell Proteomics* (2013) 12:856–65. doi:10.1074/mcp.R112.026005
69. Wuhrer M, Stam JC, van de Geijn FE, Koeleman CA, Verrips CT, Dolhain RJ, et al. Glycosylation profiling of immunoglobulin G (IgG) subclasses from human serum. *Proteomics* (2007) 7:4070–81. doi:10.1002/pmic.200700289
70. Raju TS, Briggs JB, Borge SM, Jones AJ. Species-specific variation in glycosylation of IgG: evidence for the species-specific sialylation and branch-specific galactosylation and importance for engineering recombinant glycoprotein therapeutics. *Glycobiology* (2000) 10:477–86. doi:10.1093/glycob/10.5.477
71. Butters TD. Control in the N-linked glycoprotein biosynthesis pathway. *Chem Biol* (2002) 9:1266–8. doi:10.1016/S1074-5521(02)00290-9
72. Brooks SA. Appropriate glycosylation of recombinant proteins for human use: implications of choice of expression system. *Mol Biotechnol* (2004) 28:241–55. doi:10.1385/MB:28:3:241
73. Girardi E, Holdom MD, Davies AM, Sutton BJ, Beavil AJ. The crystal structure of rabbit IgG-Fc. *Biochem J* (2009) 417:77–83. doi:10.1042/BJ20081355
74. Matsumiya S, Yamaguchi Y, Saito J, Nagano M, Sasakawa H, Otaki S, et al. Structural comparison of fucosylated and nonfucosylated Fc fragments of human immunoglobulin G1. *J Mol Biol* (2007) 368:767–79. doi:10.1016/j.jmb.2007.02.034
75. Kiyoshi M, Tsumoto K, Ishii-Watabe A, Caaveiro JMM. Glycosylation of IgG-Fc: a molecular perspective. *Int Immunol* (2017) 29(7):311–7. doi:10.1093/intimm/dxx038
76. Chiang AW, Li S, Spahn PN, Richelle A, Kuo CC, Samoudi M, et al. Modulating carbohydrate-protein interactions through glycoengineering of monoclonal antibodies to impact cancer physiology. *Curr Opin Struct Biol* (2016) 40:104–11. doi:10.1016/j.sbi.2016.08.008
77. Raju TS, Lang SE. Diversity in structure and functions of antibody sialylation in the Fc. *Curr Opin Biotechnol* (2014) 30:147–52. doi:10.1016/j.copbio.2014.06.014
78. Bologna L, Gotti E, Manganini M, Rambaldi A, Intermesoli T, Introna M, et al. Mechanism of action of type II, glycoengineered, anti-CD20 monoclonal antibody GA101 in B-chronic lymphocytic leukemia whole blood assays in comparison with rituximab and alemtuzumab. *J Immunol* (2011) 186:3762–9. doi:10.4049/jimmunol.1000303
79. Ferrara C, Grau S, Jager C, Sondermann P, Brunker P, Waldhauer I, et al. Unique carbohydrate-carbohydrate interactions are required for high affinity binding between Fc γ RIII and antibodies lacking core fucose. *Proc Natl Acad Sci U S A* (2011) 108:12669–74. doi:10.1073/pnas.1108455108
80. Mizushima T, Yagi H, Takemoto E, Shibata-Koyama M, Isoda Y, Iida S, et al. Structural basis for improved efficacy of therapeutic antibodies on defucosylation of their Fc glycans. *Genes Cells* (2011) 16:1071–80. doi:10.1111/j.1365-2443.2011.01552.x
81. Iida S, Misaka H, Inoue M, Shibata M, Nakano R, Yamane-Ohnuki N, et al. Nonfucosylated therapeutic IgG1 antibody can evade the inhibitory effect of serum immunoglobulin G on antibody-dependent cellular cytotoxicity through its high binding to Fc γ RIIIa. *Clin Cancer Res* (2006) 12:2879–87. doi:10.1158/1078-0432.CCR-05-2619
82. Iida S, Kuni-Kamochi R, Mori K, Misaka H, Inoue M, Okazaki A, et al. Two mechanisms of the enhanced antibody-dependent cellular cytotoxicity (ADCC) efficacy of non-fucosylated therapeutic antibodies in human blood. *BMC Cancer* (2009) 9:58. doi:10.1186/1471-2407-9-58
83. Niwa R, Hatanaka S, Shoji-Hosaka E, Sakurada M, Kobayashi Y, Uehara A, et al. Enhancement of the antibody-dependent cellular cytotoxicity of low-fucose IgG1 is independent of Fc γ RIIIa functional polymorphism. *Clin Cancer Res* (2004) 10:6248–55. doi:10.1158/1078-0432.CCR-04-0850
84. Weng W-K, Levy R. Two immunoglobulin G fragment C receptor polymorphisms independently predict response to rituximab in patients with follicular lymphoma. *J Clin Oncol* (2003) 21:3940–7. doi:10.1200/JCO.2003.05.013
85. Shibata-Koyama M, Iida S, Misaka H, Mori K, Yano K, Shitara K, et al. Nonfucosylated rituximab potentiates human neutrophil phagocytosis through its high binding for Fc γ RIIIb and MHC class II expression on the phagocytic neutrophils. *Exp Hematol* (2009) 37:309–21. doi:10.1016/j.exphem.2008.11.006
86. Hodoniczky J, Zheng YZ, James DC. Control of recombinant monoclonal antibody effector functions by Fc N-glycan remodeling in vitro. *Biotechnol Prog* (2005) 21:1644–52. doi:10.1021/bp050228w
87. Starovasnik MA, Braisted AC, Wells JA. Structural mimicry of a native protein by a minimized binding domain. *Proc Natl Acad Sci U S A* (1997) 94:10080–5. doi:10.1073/pnas.94.19.10080
88. Sauer-Eriksson AE, Kleywegt GJ, Uhlen M, Jones TA. Crystal structure of the C2 fragment of streptococcal protein G in complex with the Fc domain of human IgG. *Structure* (1995) 3:265–78. doi:10.1016/S0969-2126(01)00157-5
89. Ghirlando R, Lund J, Goodall M, Jefferis R. Glycosylation of human IgG-Fc: influences on structure revealed by differential scanning micro-calorimetry. *Immunol Lett* (1999) 68:47–52. doi:10.1016/S0165-2478(99)00029-2
90. Raju TS, Davidson EA. Role of sialic acid on the viscosity of canine tracheal mucin glycoprotein. *Biochem Biophys Res Commun* (1994) 205:402–9. doi:10.1006/bbrc.1994.2679
91. Crispin M, Yu X, Bowden TA. Crystal structure of sialylated IgG Fc: implications for the mechanism of intravenous immunoglobulin therapy. *Proc Natl Acad Sci U S A* (2013) 110:E3544–6. doi:10.1073/pnas.1310657110
92. Fang J, Richardson J, Du Z, Zhang Z. Effect of Fc-Glycan structure on the conformational stability of IgG revealed by hydrogen/deuterium exchange and limited proteolysis. *Biochemistry* (2016) 55:860–8. doi:10.1021/acs.biochem.5b01323
93. Scallon BJ, Tam SH, McCarthy SG, Cai AN, Raju TS. Higher levels of sialylated Fc glycans in immunoglobulin G molecules can adversely impact functionality. *Mol Immunol* (2007) 44:1524–34. doi:10.1016/j.molimm.2006.09.005
94. Sondermann P, Kaiser J, Jacob U. Molecular basis for immune complex recognition: a comparison of Fc-receptor structures. *J Mol Biol* (2001) 309:737–49. doi:10.1006/jmbi.2001.4670
95. Kaneko Y, Nimmerjahn F, Ravetch JV. Anti-inflammatory activity of immunoglobulin G resulting from Fc sialylation. *Science* (2006) 313:670–3. doi:10.1126/science.1129594
96. Anthony RM, Nimmerjahn F, Ashline DJ, Reinhold VN, Paulson JC, Ravetch JV. Recapitulation of IVIG anti-inflammatory activity with a recombinant IgG Fc. *Science* (2008) 320:373–6. doi:10.1126/science.1154315
97. Anthony RM, Ravetch JV. A novel role for the IgG Fc glycan: the anti-inflammatory activity of sialylated IgG Fcs. *J Clin Immunol* (2010) 30 (Suppl 1):S9–14. doi:10.1007/s10875-010-9405-6
98. Anthony RM, Kobayashi T, Wermeling F, Ravetch JV. Intravenous gamma-globulin suppresses inflammation through a novel T(H)2 pathway. *Nature* (2011) 475:110–3. doi:10.1038/nature10134
99. Yamane-Ohnuki N, Satoh M. Production of therapeutic antibodies with controlled fucosylation. *MABS* (2009) 1:230–6. doi:10.4161/mabs.1.3.8328
100. Crowell CK, Gramp GE, Rogers GN, Miller J, Scheinman RI. Amino acid and manganese supplementation modulates the glycosylation state of erythropoietin in a CHO culture system. *Biotechnol Bioeng* (2007) 96:538–49. doi:10.1002/bit.21141
101. Patel TP, Parekh RB, Moellering BJ, Prior CP. Different culture methods lead to differences in glycosylation of a murine IgG monoclonal antibody. *Biochem J* (1992) 285(Pt 3):839–45. doi:10.1042/bj2850839
102. Okeley NM, Alley SC, Anderson ME, Boursalian TE, Burke PJ, Emmerton KM, et al. Development of orally active inhibitors of protein and cellular fucosylation. *Proc Natl Acad Sci U S A* (2013) 110:5404–9. doi:10.1073/pnas.1222263110
103. Powell LD. Inhibition of N-linked glycosylation. *Curr Protoc Immunol*. (2001) 9:8.14–1–9. doi:10.1002/0471142735.im0814s09
104. Sullivan FX, Kumar R, Kriz R, Stahl M, Xu GY, Rouse J, et al. Molecular cloning of human GDP-mannose 4,6-dehydratase and reconstitution of GDP-fucose biosynthesis in vitro. *J Biol Chem* (1998) 273:8193–202. doi:10.1074/jbc.273.14.8193
105. King JD, Poon KK, Webb NA, Anderson EM, McNally DJ, Brisson JR, et al. The structural basis for catalytic function of GMD and RMD, two closely

- related enzymes from the GDP-D-rhamnose biosynthesis pathway. *FEBS J* (2009) 276:2686–700. doi:10.1111/j.1742-4658.2009.06993.x
106. Son YD, Jeong YT, Park SY, Kim JH. Enhanced sialylation of recombinant human erythropoietin in Chinese hamster ovary cells by combinatorial engineering of selected genes. *Glycobiology* (2011) 21:1019–28. doi:10.1093/glycob/cwr034
107. Chan KF, Shahreel W, Wan C, Teo G, Hayati N, Tay SJ, et al. Inactivation of GDP-fucose transporter gene (*Slc35c1*) in CHO cells by ZFNs, TALENs and CRISPR-Cas9 for production of fucose-free antibodies. *Biotechnol J* (2016) 11:399–414. doi:10.1002/biot.201500331
108. Evans JB, Syed BA. From the analyst's couch: next-generation antibodies. *Nat Rev Drug Discov* (2014) 13:413–4. doi:10.1038/nrd4255
109. Ferrara C, Bruncker P, Suter T, Moser S, Puntener U, Umana P. Modulation of therapeutic antibody effector functions by glycosylation engineering: influence of Golgi enzyme localization domain and co-expression of heterologous beta1, 4-N-acetylglucosaminyltransferase III and Golgi alpha-mannosidase II. *Biotechnol Bioeng* (2006) 93:851–61. doi:10.1002/bit.20777
110. Zhu Z, Ramakrishnan B, Li J, Wang Y, Feng Y, Prabakaran P, et al. Site-specific antibody-drug conjugation through an engineered glycotransferase and a chemically reactive sugar. *MABs* (2014) 6:1190–200. doi:10.4161/mabs.29889
111. Strasser R, Stadlmann J, Schahs M, Steigler G, Quendler H, Mach L, et al. Generation of glyco-engineered *Nicotiana benthamiana* for the production of monoclonal antibodies with a homogeneous human-like N-glycan structure. *Plant Biotechnol J* (2008) 6:392–402. doi:10.1111/j.1467-7652.2008.00330.x
112. Rich JR, Withers SG. Emerging methods for the production of homogeneous human glycoproteins. *Nat Chem Biol* (2009) 5:206–15. doi:10.1038/nchembio.148
113. Wang LX, Lomino JV. Emerging technologies for making glycan-defined glycoproteins. *ACS Chem Biol* (2012) 7:110–22. doi:10.1021/cb200429n
114. Huang W, Giddens J, Fan SQ, Toonstra C, Wang LX. Chemoenzymatic glycoengineering of intact IgG antibodies for gain of functions. *J Am Chem Soc* (2012) 134:12308–18. doi:10.1021/ja3051266
115. Umekawa M, Huang W, Li B, Fujita K, Ashida H, Wang LX, et al. Mutants of *Mucor hiemalis* endo-beta-N-acetylglucosaminidase show enhanced transglycosylation and glycosynthase-like activities. *J Biol Chem* (2008) 283:4469–79. doi:10.1074/jbc.M707137200
116. Parsons TB, Struwe WB, Gault J, Yamamoto K, Taylor TA, Raj R, et al. Optimal synthetic glycosylation of a therapeutic antibody. *Angew Chem Int Ed Engl* (2016) 55:2361–7. doi:10.1002/anie.201508723
117. Huang W, Li C, Li B, Umekawa M, Yamamoto K, Zhang X, et al. Glycosynthases enable a highly efficient chemoenzymatic synthesis of N-glycoproteins carrying intact natural N-glycans. *J Am Chem Soc* (2009) 131:2214–23. doi:10.1021/ja8074677
118. Jung ST, Kang TH, Kelton W, Georgiou G. Bypassing glycosylation: engineering aglycosylated full-length IgG antibodies for human therapy. *Curr Opin Biotechnol* (2011) 22:858–67. doi:10.1016/j.copbio.2011.03.002
119. Borrok MJ, Jung ST, Kang TH, Monzingo AF, Georgiou G. Revisiting the role of glycosylation in the structure of human IgG Fc. *ACS Chem Biol* (2012) 7:1596–602. doi:10.1021/cb300130k
120. Ju MS, Jung ST. Aglycosylated full-length IgG antibodies: steps toward next-generation immunotherapeutics. *Curr Opin Biotechnol* (2014) 30:128–39. doi:10.1016/j.copbio.2014.06.013
121. Jung ST, Reddy ST, Kang TH, Borrok MJ, Sandlie I, Tucker PW, et al. Aglycosylated IgG variants expressed in bacteria that selectively bind Fc_{gamma}RI potentiate tumor cell killing by monocyte-dendritic cells. *Proc Natl Acad Sci U S A* (2010) 107:604–9. doi:10.1073/pnas.0908590107
122. Labrijn AF, Aalberse RC, Schuurman J. When binding is enough: nonactivating antibody formats. *Curr Opin Immunol* (2008) 20:479–85. doi:10.1016/j.coim.2008.05.010
123. Sazinsky SL, Ott RG, Silver NW, Tidor B, Ravetch JV, Wittrup KD. Aglycosylated immunoglobulin G1 variants productively engage activating Fc receptors. *Proc Natl Acad Sci U S A* (2008) 105:20167–72. doi:10.1073/pnas.0809257105
124. Jung ST, Kelton W, Kang TH, Ng DT, Andersen JT, Sandlie I, et al. Effective phagocytosis of low Her2 tumor cell lines with engineered, aglycosylated IgG displaying high Fc_{gamma}RIIa affinity and selectivity. *ACS Chem Biol* (2013) 8:368–75. doi:10.1021/cb300455f
125. Thomas A, Teicher BA, Hassan R. Antibody-drug conjugates for cancer therapy. *Lancet Oncol* (2016) 17:e254–62. doi:10.1016/S1470-2045(16)30030-4
126. Tsuchikama K, An Z. Antibody-drug conjugates: recent advances in conjugation and linker chemistries. *Protein Cell* (2016). doi:10.1007/s13238-016-0323-0
127. Teicher BA. Antibody drug conjugates. *Curr Opin Oncol* (2014) 26:476–83. doi:10.1097/CCO.0000000000000108
128. Feng Y, Zhu Z, Chen W, Prabakaran P, Lin K, Dimitrov DS. Conjugates of small molecule drugs with antibodies and other proteins. *Biomedicines* (2014) 2:1–13. doi:10.3390/biomedicines2010001
129. Li W, Prabakaran P, Chen W, Zhu Z, Feng Y, Dimitrov DS. Antibody aggregation: insights from sequence and structure. *Antibodies* (2016) 5:19. doi:10.3390/antib5030019
130. Panowski S, Bhakta S, Raab H, Polakis P, Junutula JR. Site-specific antibody drug conjugates for cancer therapy. *MABs* (2014) 6:34–45. doi:10.4161/mabs.27022
131. Vogel CW. Preparation of immunoconjugates using antibody oligosaccharide moieties. *Methods Mol Biol* (2004) 283:87–108. doi:10.1385/1-59259-813-7:087
132. Tang F, Wang L-X, Huang W. Chemoenzymatic synthesis of glycoengineered IgG antibodies and glycosite-specific antibody-drug conjugates. *Nat Protoc* (2017) 12:1702–21. doi:10.1038/nprot.2017.058
133. Li X, Fang T, Boons GJ. Preparation of well-defined antibody-drug conjugates through glycan remodeling and strain-promoted azide-alkyne cycloadditions. *Angew Chem Int Ed Engl* (2014) 53:7179–82. doi:10.1002/anie.201402606
134. van Geel R, Wijdeven MA, Heesbeen R, Verkade JMM, Wasieł AA, van Berkel SS, et al. Chemoenzymatic conjugation of toxic payloads to the globally conserved N-glycan of native mAbs provides homogeneous and highly efficacious antibody-drug conjugates. *Bioconjug Chem* (2015) 26:2233–42. doi:10.1021/acs.bioconjchem.5b00224
135. Seaman S, Zhu Z, Saha S, Zhang XM, Yang MY, Hilton MB, et al. Eradication of tumors through simultaneous ablation of CD276/B7-H3-positive tumor cells and tumor vasculature. *Cancer Cell* (2017) 31:501–515.e8. doi:10.1016/j.ccr.2017.03.005

Conflict of Interest Statement: The authors declare that the research was conducted in the absence of any commercial or financial relationships that could be construed as a potential conflict of interest.

Copyright © 2017 Li, Zhu, Chen, Feng and Dimitrov. This is an open-access article distributed under the terms of the Creative Commons Attribution License (CC BY). The use, distribution or reproduction in other forums is permitted, provided the original author(s) or licensor are credited and that the original publication in this journal is cited, in accordance with accepted academic practice. No use, distribution or reproduction is permitted which does not comply with these terms.



Advances in Therapeutic Fc Engineering – Modulation of IgG-Associated Effector Functions and Serum Half-life

Abhishek Saxena and Donghui Wu*

Laboratory of Antibody Engineering, Shanghai Institute for Advanced Immunochemical Studies, ShanghaiTech University, Shanghai, China

OPEN ACCESS

Edited by:

Tianlei Ying,
Fudan University, China

Reviewed by:

Pierre Guermonprez,
King's College London, UK

Estrella Mariel Levy,
National Scientific and Technical
Research Council, Argentina
Shane Miersch,
University of Toronto, Canada

*Correspondence:

Donghui Wu
wudh@shanghaitech.edu.cn

Specialty section:

This article was submitted to
Immunotherapies and Vaccines,
a section of the journal
Frontiers in Immunology

Received: 12 July 2016

Accepted: 24 November 2016

Published: 12 December 2016

Citation:

Saxena A and Wu D (2016) Advances in Therapeutic Fc Engineering – Modulation of IgG-Associated Effector Functions and Serum Half-life. *Front. Immunol.* 7:580.
doi: 10.3389/fimmu.2016.00580

Today, monoclonal immunoglobulin gamma (IgG) antibodies have become a major option in cancer therapy especially for the patients with advanced or metastatic cancers. Efficacy of monoclonal antibodies (mAbs) is achieved through both its antigen-binding fragment (Fab) and crystallizable fragment (Fc). Fab can specifically recognize tumor-associated antigen (TAA) and thus modulate TAA-linked downstream signaling pathways that may lead to the inhibition of tumor growth, induction of tumor apoptosis, and differentiation. The Fc region can further improve mAbs' efficacy by mediating effector functions such as antibody-dependent cellular cytotoxicity, complement-dependent cytotoxicity, and antibody-dependent cell-mediated phagocytosis. Moreover, Fc is the region interacting with the neonatal Fc receptor in a pH-dependent manner that can slow down IgG's degradation and extend its serum half-life. Loss of the antibody Fc region dramatically shortens its serum half-life and weakens its anticancer effects. Given the essential roles that the Fc region plays in the modulation of the efficacy of mAb in cancer treatment, Fc engineering has been extensively studied in the past years. This review focuses on the recent advances in therapeutic Fc engineering that modulates its related effector functions and serum half-life. We also discuss the progress made in aglycosylated mAb development that may substantially reduce the cost of manufacture but maintain similar efficacies as conventional glycosylated mAb. Finally, we highlight several Fc engineering-based mAbs under clinical trials.

Keywords: antibody Fc region, ADCC, CDC, ADCP, serum half-life, aglycosylated antibody, FcRn, cancer therapy

INTRODUCTION

Monoclonal antibodies (mAbs) can target tumors through specific recognition of tumor-associated antigens and subsequent recruitment of effector elements including macrophages, dendritic cells, natural killer (NK) cells, T-cells, and the complement pathway components (1). Such recruitments are achieved by interactions among the immunoglobulin gamma (IgG)-crystallizable fragment (Fc) and the immune cell receptors like Fcγ receptors (FcγRs) and the complement protein C1q of the complement system (2–4). These interactions lead to the activation of immune cells for enhanced antibody-dependent cellular cytotoxicity (ADCC)/antibody-dependent cell-mediated phagocytosis (ADCP), formation of the membrane attack complex, and more efficient presentation of antigen

to the dendritic cells (1). Through a recycling mechanism, the neonatal Fc receptor (FcRn) prolongs the half-life of mAbs in a pH-dependent interaction with the Fc region (5). The schematic of overall IgG structure and its binding regions with FcγRs, C1q, and FcRn is depicted in **Figure 1**.

The FcγRs, consisting of FcγRI (CD64), FcγRII (CD32), and FcγRIII (CD16) classes, are heterogeneous in terms of their cellular expression and Fc binding affinities (1, 6). FcγRI binds to the Fc region with $K_D \sim 10^{-8}\text{--}10^{-9}$ M and is expressed on mononuclear phagocytes, dendritic cells, and IFN- γ -activated neutrophils (1, 7, 8). FcγRII binds to the Fc region with relatively lower affinity ($K_D \sim 10^{-7}$ M) and exists in five isoforms; among them, activating (FcγRIIa, harboring an immunoreceptor tyrosine-based activation motif on neutrophils) or inhibitory (FcγRIIb, harboring an immunoreceptor tyrosine-based inhibitory motif predominantly on B-lymphocytes) are critical for immune regulation (1, 7). FcγRIII, expressed in two isoforms, binds the Fc region with the lowest affinities ($K_D \sim 10^{-5}$ M) (1, 7). Among these, FcγRIIIa has a moderate Fc binding allele (V158) and a low binding allele (F158), and is expressed on NK cells, macrophages, and T-cell subsets and activates NK and T cell-mediated ADCC response (1, 6, 7); FcγRIIIb is exclusively present on neutrophils and lacks signal generation capacity (1, 7).

Crystal structures of Fc in complex with FcγRI (9) (**Figure 2A**), Fc in complex with FcγRII (10) (**Figure 2B**), and Fc in complex with FcγRIII (11) (**Figure 2C**) reveal that the FcγRs' interaction sites on Fc are all located within the lower hinge-upper heavy chain constant domain 2 (CH2). Furthermore, the binding affinity of Fc region to FcγRs also varies with the IgG subclasses (12).

The C1q is a multisubunit protein of the complement system (3). It uses one of its six heads to establish a low-affinity ($\sim 10^{-6}$ M) interaction with the lower hinge-upper CH2 domain of the Fc region (3). Crystal structure of the human C1q head revealed that it is assembled with a heterotrimer globular architecture (14). Though the molecular basis of how the C1q head recognizes the Fc region is not known at the atomic resolution, Schneider and Zacharias (15) proposed a working model of C1q in complex with Fc based on known experimental data, docking, and molecular dynamics simulation. According to this model, upon initial weak interaction between the C1q head and the Fc region, IgGs can aggregate while recognizing “multiple epitopes” on the antigen surface and thus give many C1q molecules an opportunity to bind to their Fc regions, which enhance the “cumulative affinity” to $\sim 10^{-9}$ M (3, 15). This leads to the deposition of complement component 3 (C3b) on the target cell and ultimate formation of the membrane attack complex that disrupts the lipid bilayer of the target cell, promotes cytolysis, and completes complement dependent cytotoxicity (CDC) (16, 17).

The pharmacokinetic profiles of antibodies vary among subclasses and are related to the structural features of the Fc region (18, 19). It is known that the serum half-life of IgG subclasses (IgG1, IgG2, and IgG4) is ~ 23 days as compared to 2–6 days for IgG3 and other Ig classes (18, 19). The Fc region spanning the interface of CH2 and CH3 domains interacts with the FcRn in the placenta, liver, mammary glands, and adult intestine to regulate IgG homeostasis and deliver maternal IgG across the placenta to the fetus (5). This interaction is favored by an acidic environment of the endosome after IgG is pinocytosed

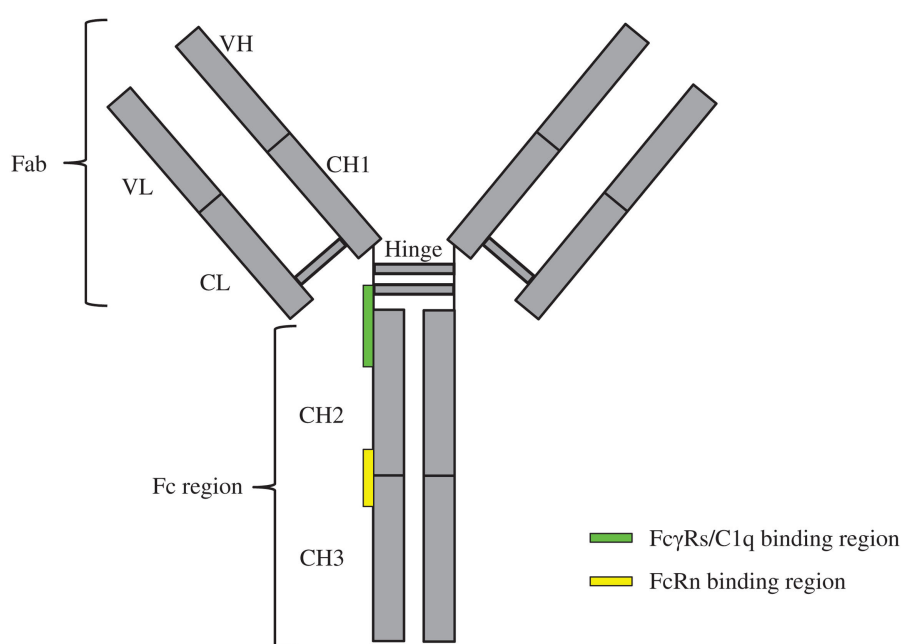


FIGURE 1 | Schematics of immunoglobulin gamma overall structure and its binding regions with FcγRs, C1q, and FcRn. The constituent heavy [VH, CH1, hinge, CH2, and CH3 (gray)] and light chains [VL and CL (gray)] linked by inter-chain disulfide bonds are shown. The site at which FcγRs/C1q interacts with the crystallizable fragment (Fc) region is located in the lower hinge-upper CH2 (green rectangle); the site at which FcRn interacts with the Fc region is located in the interface of CH2-CH3 (yellow rectangle).

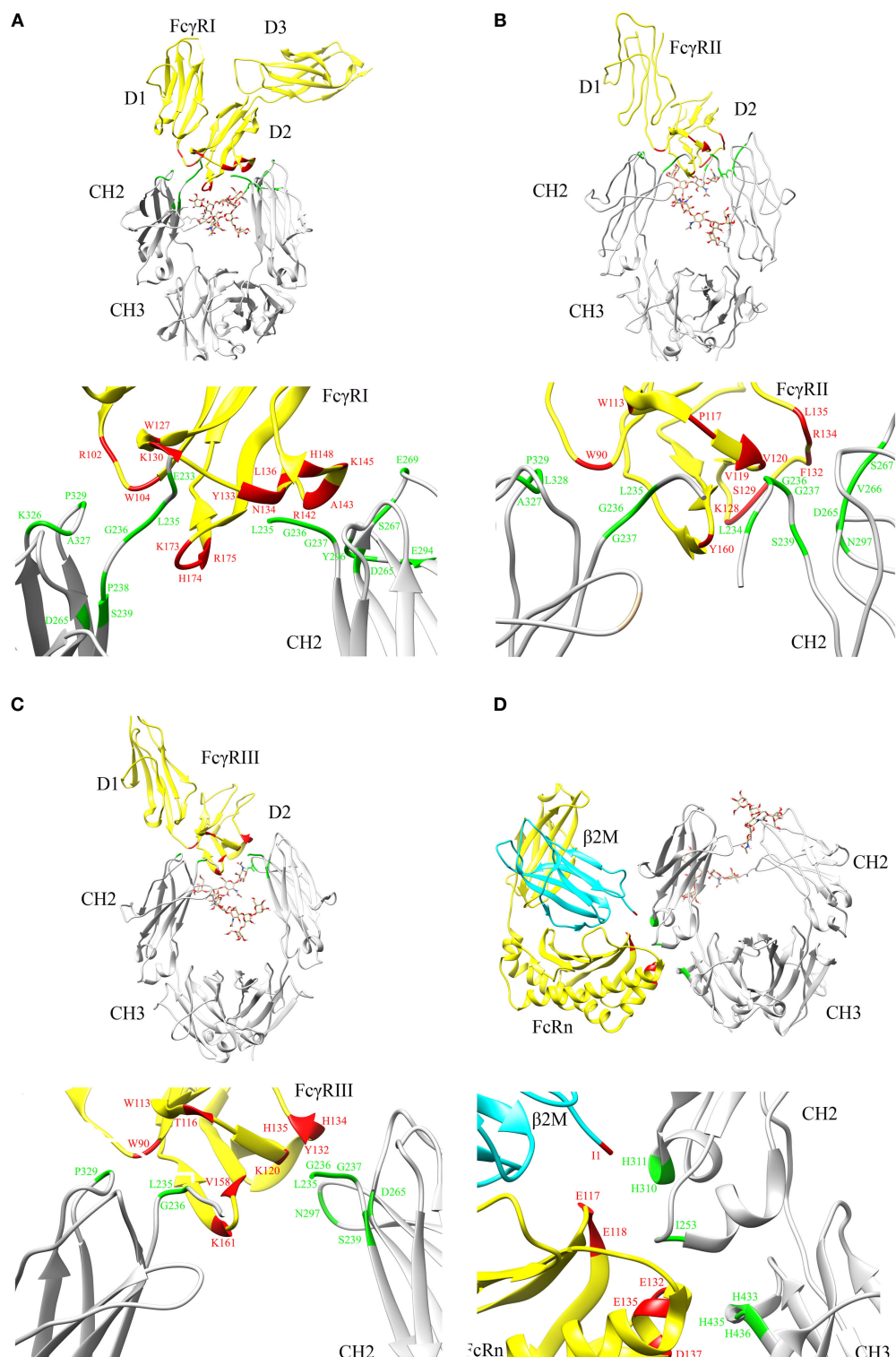


FIGURE 2 | Crystal structures illustrating crystallizable fragment (Fc) interactions with Fc γ Rs and FcRn. Representative structures are shown for (A) Fc–Fc γ RI cocrystals [PDB: 4W4O (9)], (B) Fc–Fc γ RII cocrystals [PDB: 3RY6 (10)], (C) Fc–Fc γ RIII cocrystals [PDB: 1T89 (11)], and (D) Fc–FcRn cocrystals [PDB: 111A (13)] with β 2 microglobulin (β 2M) domain shown in cyan. The Fc region and Fc γ Rs are represented by gray and yellow color, respectively (A–D). N297 glycans within the CH2 domain are shown in stick model. The critical binding regions are highlighted in the upper part of each panel; region from the Fc fragment in green, region from the Fc γ Rs, FcRn, and β 2M in red. The lower part of each panel shows the detailed residues, which are involved in the interactions between Fc and its binding partners.

and thus IgG is protected from lysosomal degradation (20). The endocytosed IgG is then recycled to the cell surface and released into the blood stream at an alkaline pH, thereby maintaining the sufficient IgG serum half-life for proper immune functions and desired therapeutic efficacies (20). Recently, the endothelial and hematopoietic cells are identified as the major sites associated with FcRn expression and their critical role in IgG homeostasis (20–23).

Based on site-directed mutagenesis of Fc region and design of a hybrid Fc heterodimer harboring one half of Fc wild type (WT) and one half of Fc mutant, Kim and coworkers identified the key Fc residues involved in the FcRn interaction and proposed a preliminary model that one Fc hinge homodimer bound with two FcRn molecules (24, 25). Shortly thereafter, Burmeister and coworkers reported high resolution crystal structure of FcRn alone at 2.2 Å and low resolution crystal structure of Fc in complex with FcRn at 6.5 Å (26, 27). Structural analysis and biophysical data confirmed that one Fc homodimer binds with two FcRn molecules (26–29). Later, Martin and coworkers reported a high resolution crystal structure of Fc in complex with FcRn at 2.8 Å (13). This structure clearly shows the key residues involved in Fc and FcRn interactions and reveals the pH-dependent binding mechanism (13) (**Figure 2D**).

Evidence demonstrates the presence of oligosaccharides, attached to the N297 residue within the CH2 domain Asn-X-Ser/Thr glycosylation motif of Fc region, is essential in maintaining the Fc conformation and mediating its interactions with FcγRs (FcγRI, FcγRIIa, FcγRIIb, and FcγRIIIa) and C1q, but not FcRn (30–41). The glycan moiety is formed by two N-linked biantennary oligosaccharide chains consisting of a core heptasaccharide [N-acetylglucosamine (GlcNAc) and mannose (Man)] but occurrence of other residues like terminal N-acetylneurameric acid, galactose (Gal), bisecting N-acetylglucosamine (GlcNAc), and fucose (Fuc) have also been reported (1, 42, 43). Additionally,

5–17 and 2–7% of IgG structures could be monosialylated and disialylated, respectively (1, 44). This imparts a significant complexity and heterogeneity to therapeutic IgG molecules when expressed in mammalian cells, which can affect the therapeutic profile of IgG (30). On the other hand, the presence of bisected N-acetylglucosamine structures in rituximab, a purer glycoform with lesser heterogeneity, leads to an efficient engagement of FcγRIII and increases ADCC activity against CD20⁺ cells by up to 20-fold (30, 45). Similarly, non-fucosylated glycoform of Herceptin produced in engineered Chinese hamster ovary (CHO) cell line (LEC13) can enhance ADCC via FcγRIII engagement by up to 50-fold (30, 46).

However, mAb-associated glycan heterogeneity poses several key challenges (30, 33, 45–51) including (1) difficulties in developing therapeutic mAbs with glycan composition similar to naturally occurring human IgG1, (2) difficulties in controlling glycan heterogeneity, (3) lengthier development time to construct cell lines producing glycan homogeneity, (4) lengthier IgG production time and higher manufacturing cost in mammalian cells as compared to that in *E. coli* or yeast-based expression systems, (5) dominance of particular glycoforms that can affect effector functions of IgG molecules, and (6) difficulties in separating various glycoforms generated from mammalian cells. Alternatively, development of aglycosylated mAbs with similar efficacy as glycosylated counterpart but lower manufacturing cost has attracted great efforts in the past decade.

In this review, we focus on the recent progress in therapeutic Fc engineering-associated effector functions (ADCC, ADCP, and CDC) and pharmacokinetics. The mutations known to induce profound effects on Fc interaction with FcγRs, C1q, and FcRn are summarized (see **Table 1**). We also briefly describe the advances in aglycosylated mAb development. Finally, we highlight clinical trials of several mAbs developed from relevant Fc engineering.

TABLE 1 | Tabulation of the Fc mutations known to mediate a profound effect on antibody effector functions and immunoglobulin gamma homeostasis.

Fc type	Mutation	Target	Functional	Reference
Hu-IgG2-Glyco	K326W/E333S	C1q	Yes	(52)
Mu-IgG2b-Glyco	E235L	FcγRI	Yes	(2)
Hu-IgG3-Glyco	E235Y	FcγRI	Yes	(35)
Hu-IgG1-Glyco	S239D, I332E, S239D/I332E, and S239D/I332E/A330L	FcγRIIIa	Yes	(6, 53–55)
Hu-IgG1-Glyco	G236A, G236A/I332E, S239D/I332E, and G236A/S239D/I332E	FcγRIIIa > FcγRIIIa > FcγRI	Yes	(56)
Hu-IgG1-Glyco	L235V/F243L/R292P/Y300L/P396L	FcγRIIIa	Yes	(57, 58)
Hu-IgG1-Glyco	P238D/L328E	FcγRIIb	NA	(59)
Hu-IgG1/IgA-Glyco	IgGA (many motifs)	FcγRs + FcαRI	Yes	(60)
Hu-IgG1-Glyco	F243L/R292P/Y300L and F243L/R292P/Y300L/P396L	FcγRIIIa/FcγRIIa	Yes	(29)
Hu-IgG1-Aglyco	S298G/T299A	FcγRIIIa	NA	(61)
Hu-IgG1-(Fuc)	F234L	FcγRIIIa	Yes	(62)
Hu-IgG1-Aglyco	E382V/M428I	FcγRI	Yes	(63)
Hu-IgG1-Aglyco	Q295R/L328W/A330V/P331V/I332Y	FcγRI	Yes	(64)
Hu-IgG1-Glyco	M428L/N434S	FcRn	Yes	(65)
Hu-IgG1-Glyco	M252Y/S254T/T256E and H433K/N434F/Y436H	FcRn	Yes	(66, 67)
Hu-IgG1-Glyco	N343A/E380A	FcRn	Yes	(68)
Hu-IgG1-Glyco	M252Y/S254T/T256E	FcRn	Yes	(69)
Hu-IgG1-Glyco	T250R/M428L	FcRn	Yes	(70)
Hu-IgG1-Aglyco	Q295R/L328W/A330V/P331V/I332Y	FcRn	Yes	(64)

Hu, Human; *Mu*, Murine; *Glyco*, Glycosylated; *Aglyco*, Aglycosylated; *Fuc*, Fucose; *NA*, not available.

MODULATION OF EFFECTOR FUNCTIONS BY Fc ENGINEERING

To develop more effective antibodies with desired ADCC, ADCP, and CDC activities, various strategies including site-directed mutagenesis, alanine scanning, structure-based computational design, and directed evolution technologies are employed.

The Fc amino acid residues that confer improved binding to FcγRs/C1q and enhanced immune response were initially characterized by site-directed mutagenesis studies. The earliest described mutations were discovered by scanning residues to isolate non-binders while focusing on the conserved residues. Fc residues (E318, K320, and L322) in the mouse IgG2b-Fc region were identified as the C1q binding site (3). However, the relevance of E318 and K320 was challenged in human Fc-C1q interaction (71). Novel residues (D270, K322, P329, and P331) were proposed for normal C1q binding on human Fc (71). This finding underscores the interspecies differences in such molecular interactions that may show a different effect in preclinical models. Furthermore, an IgG1 isotype of rituximab carrying K326W/E333S mutations was shown to have fivefold more binding to C1q (52) and the same motif, when transferred to the IgG2 isotype (poor complement activator) of rituximab, increased the cell lysis by fivefold (52). Next, a single mutation from E to L at position 235 of the mouse IgG2b-Fc region proposed it to be the “major determinant” for FcγRI binding (with ~100-fold increased affinity to human monocyte FcγRI) (2). Additionally, using a mouse-human chimeric antibody, amino acids at position 234 and 237 were shown to mainly influence the interaction with FcγRII. Based on these observations, FcγRI and FcγRII were proposed to recognize an overlapping but non-identical site on the Fc region (35).

Alanine scanning mutagenesis of selected Fc residues resulted in many variants with altered binding to specific FcγRs, which was also reflected in their ability to promote ADCC. Activating FcγRIIIa mutations improved ADCC by 100% (68). Furthermore, mutants based on the activating or suppressing effect on FcγRs were categorized into different classes. Among these, IgG1 mutations A327Q/P329A (interact with FcγRI), D265A/S267A/H268A/D270A/K326A/S337A (interact with FcγRIIa), and T256A/K290A/S298A/E333A/K334A (interact with FcγRIIIa) promoted high-affinity interactions (68).

Computational optimization of the Fc region by creating a single (S239D or I332E), double (S239D/I332E), and triple mutations (S239D/I332E/A330L) improved the affinity against human FcγRIIIa^{V158/F158} allele by up to 169-fold (6). The mutations favoring Fc binding to activating (FcγRIIIa) receptor over the inhibitory (FcγRIIb) receptor are important to develop IgGs with better activating to inhibitory capacity (IIIa:IIb ratio), which was monitored using surface plasmon resonance. These mutations showed up to ninefold improvement in IIIa:IIb ratio and contributed to more than twofold enhancement in ADCC/ADCP activity, and the S239D/I332E double mutant significantly depleted CD20⁺ B cells *in vivo* compared to WT IgG (6). The same Fc mutations also enhanced *in vitro* ADCC/ADCP activity against lymphoma cell lines and directly translated into a more effective treatment of lymphoproliferative diseases when

incorporated into anti-CD19/CD40 mAbs (53, 54). Furthermore, it was shown that a change from glycine to alanine at residue 236 can shift the immune balance toward activating FcγRIIa relative to inhibitory FcγRIIb (56). The coupling of G236A to either I332E or S239D/I332E had dual beneficial effect as these mutants not only improve FcγRIIa:FcγRIIb ratio but also enhance binding to FcγRIIIa by ~6- to 31-fold (56). These mutants had significantly improved NK cell-mediated ADCC and macrophage-mediated ADCP activity (56).

In addition, “shuffled variants” of anti-CD20/CD57 antibody were constructed by grafting the CH1/hinge and CH3 carboxyl-terminal of IgG1 into the Fc of IgG3 to retain both the ADCC activity from IgG1 and the CDC activity from IgG3 (72). It is known that IgG1 is the most potent ADCC activator, while IgG3 has highest potency to recruit complement system (72). Therefore, IgG1 and IgG3 Fc regions can complement one another to maximize the immune effector response. These variants with chimeric CH regions showed ~25–60% increase in ADCC and CDC activity compared to WT of IgG1 and IgG3 molecules (72). Furthermore, the CDC activity of humanized anti-CD20 IgG1 (ocrelizumab) was increased by ~23-fold while retaining normal IgG1 ADCC by combining a triple mutant (S267E/H268F/S324T) with earlier reported G236A/I332E in the CH2 domain (73).

Multiple mutations (L235V/F243L/R292P/Y300L/P396L) in the trastuzumab Fc region (MGAH22) increased the potency against low Her2-expressing cells *via* low-affinity FcγRIIIa^{F158} engagement (57). The same Fc motif was applied to the MGA271 mAb (anti-CD276), which targets B7-H3⁺ tumor cells and resulted in an increased binding to FcγRIIIa, enhanced ADCC, and potent antitumor activity in a renal cell carcinoma/bladder cancer xenograft mouse model (58). Recently, the immune activating potential of IgA *via* FcαRI engagement was exploited by developing IgG and IgA hybrid molecules “IgGA” through substituting α1 loop residues of CH_{γ1}2/3 region with CH_{α1}2/3 (60). The “IgGA” hybrid trastuzumab mediated an enhanced ADCC/ADCP activity against Her2 overexpressing cells and destroyed up to 50% SkBr3 breast cancer cells (*via* ADCC) and MDA-MB-453 cells (*via* ADCP) (60). Similarly, “IgGA” hybrid rituximab lysed ~70% of the CD20⁺ calcein-AM-loaded Raji tumor cells when compared to the WT counterparts (60).

A negative selection strategy was applied using yeast surface display to enrich Fc mutants exhibiting selective high affinity to FcγRIIIa (29). Among these isolates, F243L was predicted to make a direct contact with the carbohydrate portion, which can “influence sialylation and affect the quaternary structure” of the Fc domain (29). Additionally, R292P partially reduced the binding to FcγRIIa, while Y300L, in combination with other mutations (F243L/R292P/V305I/P396L), showed an ~10-fold less K_D , 100-fold enhanced ADCC activity, and potency in a xenograft mouse model of ovarian and breast cancer (29). Furthermore, an Fc variant with three changes (F243L/R292P/Y300L) was also effective in increasing the rate of cytosis by ~100-fold (29). In another report, human IgG1 Fc variants were generated by an error-prone PCR and ribosome display to select high-affinity glycosylated binders to human FcγRIIIa using a solution phase method (62). The isolated Fc mutant (F243L) lacked Fuc residues in most oligosaccharide chains and exhibited an improved FcγRIIIa^{V158/}

^{F158} binding and enhanced ADCC as compared to WT Fc (62). Recently, an anti-EGFR antibody (S239D/I332E) was noted to elicit mononuclear cell-mediated ADCC *via* Fc γ RIIa engagement and at the same time showed impaired polymorphonuclear cell (PMN)-mediated ADCC due to the engagement of Fc γ RIIb, a highly homologous isoform to Fc γ RIIa (55). The inability of Fc γ RIIb to activate immune signaling in such a scenario can be overcome by imparting high-affinity binding to Fc γ RIIa, which can enhance both NK cell- and PMN mediated ADCC (55). These observations highlight that Fc engineering toward related Fc γ Rs needs to be tailored specifically to achieve desirable immune effects.

MODULATION OF ANTIBODY PHARMACOKINETICS BY Fc ENGINEERING

Along with the efforts to engineer Fc regions for enhanced effector functions, attempts have been made to improve antibody pharmacokinetics. Clearly, enhanced Fc-FcRn interaction at acidic pH can extend IgG's serum half-life and positively regulate its homeostasis, which may benefit patients by greater therapeutic efficacy, less frequent dosing, and lower cost burden. Alanine scanning and display/directed evolution are commonly used techniques to identify favorable Fc mutants that can strengthen Fc-FcRn pH-dependent interactions.

A human Fc variant (N434A), isolated by alanine scanning of all solvent-exposed residues, showed fourfold increased binding to FcRn at pH 6.0 (68), which later, when studied in cynomolgus monkeys, showed a twofold extension of IgG serum half-life confirming the modulation of pharmacokinetics (74). Such an interaction at pH 6.0 prolongs IgG availability in serum, which correlates with the therapeutic effectiveness as demonstrated by the improved antitumor activity of IgG-Fc mutant (M428L/N434S from the CH3 domain) in a human FcRn transgenic mouse model (65).

A phage displayed antibody library approach was employed with the aim of isolating high-affinity binders against FcRn at pH 6.0. Random mutations were created at residues T252, T254, and T256, which are proximal to the IgG-FcRn interaction site, and binders were selected in a solution phase against FcRn at pH 6.0 and eluted by PBS at pH 7.4 (66). The Fc mutants generated in this manner were able to bind both human and rat FcRn with high affinity at pH 6.0; however, these variants (M252Y/S254T/T256E from the CH2 domain and H433K/N434F/Y436H from the CH3 domain) also showed tighter binding to mouse FcRn at pH 7.4 that decreased the serum IgG concentration in a mouse model (67). Yeung and coworkers (74) reported a similar observation that an Fc mutant (N434W), though possessing an ~80-fold enhanced affinity to FcRn at both acidic and neutral pH, did not stabilize serum IgG due to the loss in pH selectivity. These results suggest that high-affinity binding to the receptor at neutral pH can compromise the “beneficiary effect” of increased affinity at pH 6.0. Later, a humanized anti-respiratory syncytial virus antibody (MEDI-524) with a triple mutant Fc (M252Y/S254T/T256E from the CH2 domain) was reported to have a 10-fold increase

in a pH-dependent way toward FcRn and about 4-fold improvement in serum half-life in cynomolgus monkey (69). Similarly, a high-affinity Fc variant (T250R/M428L) bound FcRn selectively at pH 6.0 and accounted for a 2.8-fold lesser degradation of serum IgG2 (70) and IgG1 (75) in rhesus monkey. Accumulating studies highlight that to prolong IgG serum half-life, pH-dependent FcRn affinity has to be maintained.

Of note, Greys and coworkers recently analyzed known IgG-Fc mutants, which show enhanced FcRn pH-dependent affinity and extended serum half-life (M252Y/S254T/T256E from the CH2 domain and M428L/N434S from the CH3 domain), for their effects on ADCC, ADCP, and CDC (65, 69, 76). Surprisingly, they found that both mutants showed reduced effector functions with regards to ADCC, ADCP, and CDC. More interestingly, they found one previously known mutant (H433K/N434F from the CH3 domain), which showed reduced FcRn pH-dependent affinity and shortened serum half-life, displayed enhanced effector functions in ADCP, CDC, and ADCC (76, 77). These findings highlight that, though the interaction region of Fc with Fc γ Rs and C1q (lower hinge region-CH2 domain) is distant from its interaction with FcRn (CH2-CH3 domain interface), it is still possible that these mutants can trigger a long range effect to other part of the Fc region in an unknown mechanism.

AGLYCOSYLATED Fc TO OVERCOME GLYCAN HETEROGENEITY

The demand for therapeutic antibodies is high, and it has been estimated that 8,000 kg of clinical grade mAbs were produced in 2013 (78). Currently, ~50% of the clinical grade biologics are produced in mammalian cells like CHO, mouse myeloma cell lines NSO and SP2/0 (30, 78–80).

However, the inherent glycan heterogeneity of mAbs when expressed in mammalian cell systems can cause high production cost and variations of mAb functions from batch to batch. Recently, great efforts have been invested in developing aglycosylated mAbs as an alternative. Ideally, aglycosylated mAbs would be as efficient as or even better than its glycosylated peers in mediating effector functions for antigen or target cell clearance.

To develop aglycosylated IgGs as alternatives, Sazinsky and coworkers constructed three small subsets of saturation substitutions covering the Asn-X-Ser/Thr glycan motif of the Fc C'/E loop and displayed these libraries on the yeast cell surface (61). After selection against Fc γ RIIa by fluorescence-activated cell sorting (FACS), a double Fc mutant isolate (S298G/T299A) in an aglycosylated form showed threefold stronger binding as compared to the WT and variants with single mutation, which indicates that the glycosylation of N297 is not a strict requirement for the interaction of Fc with Fc γ RIIa (61). In contrast, the indispensable role of asparagine at position 297 was demonstrated in the backdrop of N297Q, N297D, or N297A mutation, which abolished the double mutant (S298G/T299A) binding to Fc γ RIIa (61). Moreover, this dual mutant is functional *in vivo* in that murine platelet clearance is as efficient as that of WT mAb. Based on the modeling of Fc dual mutants in complex with Fc γ RIIa, the N297 residue of an aglycosylated IgG can

make a hydrogen bond with the S126 residue of Fc γ RIIa (61, 81). Furthermore, such interaction may be strengthened by a bridging water molecule present in an unbound Fc γ RII crystal (61, 81). However, this dual mutant showed 10-fold reduced Fc γ RI binding and no binding to both Fc γ RIII and C1q proteins. The inability of aglycosylated mAbs to bind with C1q and thus activate CDC can limit their application in treating hospital acquired microbial infections among cancer patients where complement activity plays an important role (82).

In another major breakthrough, bacterial display and FACS was used to isolate Fc variants displaying increased binding and specificity to Fc γ RI (63). One such aglycosylated variant called “Fc5” (E382V/M428I) was incorporated into trastuzumab. The trastuzumab-Fc5 variant bound selectively to the Fc γ RI with nanomolar range affinity and promoted monocyte-derived dendritic cell-dependent lysis of SkBr3 breast cancer cells that over-express Her2. (63). The three-dimensional structure of human aglycosylated Fc domain suggests a greater “conformational flexibility of the CH2-CH3 domain interface,” as compared to the glycosylated counterpart (83). Additional mutations (Q295R/L328W/A330V/P331V/I332Y) in trastuzumab-Fc5 variant (63) increased the affinity for Fc γ RI by ~120-fold and retained pH-dependent FcRn binding and function (64). Other mutants were also reported with specific binding to Fc γ RI and without compromising the pH-dependent FcRn binding (84).

It is worth mentioning that removal of appended glycans, though does not affect IgG's solubility, binding affinities to Fc γ Rs, and *in vivo* half-life but often compromises IgG related CDC, lowers its thermostability and increases its aggregation at the low pH (85–87).

Fc ENGINEERING-BASED mAbs UNDER CLINICAL TRIALS

A number of mAbs harboring various modifications in the Fc region are being investigated in different clinical trial stages (see Table 2 for Fc engineering-based mAbs being tested in clinics). These molecules broadly fall into three categories (1) with enhanced effector response to treat cancer and infectious diseases, (2) capable of inhibiting immune activation to treat

inflammatory diseases, and (3) new class of aglycosylated mAbs with either inert or active-immune function.

The Fc variants capable of inducing enhanced ADCC are being tested in many antibody candidates. Anti-CD37 antibody (BI836826; Boehringer) against B cell malignancies is currently under phase-1 trial for the treatment of chronic lymphocytic leukemia (CLL) (6, 88, 89). This is a mouse-human chimeric antibody, which targets tetraspanin CD37 and shows high pro-apoptotic activity against malignant B cells *via* enhanced ADCC. Using human CD37 transgenic mice, a single dose of BI836826 was demonstrated to reduce peripheral B cells (88) and efficacious in suppressing tumor growth in Ramos mouse model of human B-cell lymphoma (88). Furthermore, therapeutic efficacy of a surrogate Fc-engineered antibody against macaque CD37 has also been demonstrated in cynomolgus monkey (88). A fully humanized anti-CD123 antibody (JNJ-56022473; Janssen R & D) targeting overexpressed interleukin-3 receptor α -chain is being tested in acute myeloid leukemia patients (89–91). The Fc fragment of JNJ-56022473 has been engineered for enhanced NK cell-mediated ADCC. The molecule efficiently reduced the growth of the patient-derived acute myelogenous leukemia xenografts in bone marrow and peripheral organs and increased the survival in animal models (91). Similarly, a humanized anti-CD30 antibody (XmAb2513; Xencor) with enhanced binding to Fc γ RIIIa is being evaluated in the treatment of CD30 $^{+}$ Hodgkin's lymphoma (HL) patients who had previously received two or more therapies (89, 92, 93). It has been shown to be safely administered and biologically active in relapsed, refractory HL subjects and reduces tumor in a majority of patients (92, 93). Another interesting molecule is an anti-CD19 antibody (XmAb5774; Xencor), which induces potent NK cell-mediated ADCC/ADCP response against CLL (89, 96). The antibody is known to get internalized in primary CLL cells and induces a modest toxicity (96).

Antibodies harboring Fc mutations that can suppress the immune response are being tested for the treatment of inflammatory diseases. The immunosuppressive version of anti-CD19 antibody (XmAb5871; Xencor) binds inhibitory Fc γ RIIb with ~430-fold enhanced affinity and efficiently depletes CD19 $^{+}$ B-cells in systemic lupus erythematosus (SLE) patients (90, 94). The depletion of CD19 $^{+}$ B-cells correlates with the strong inhibition

TABLE 2 | Fc-engineered antibody candidates under clinical evaluation.

Antibody	Target	Fc modification	Disease	Clinical development	Company	Reference
BI836826	CD37	NA	CLL	Phase-1	Boehringer	(6, 88, 89)
JNJ56022473	CD123	NA	AML	Phase-2	Janssen R & D	(89–91)
XmAb2513	CD30	NA	Hodgkin/large cell lymphoma	Phase-1	Xencor, Inc.	(89, 92, 93)
XmAb5871	CD19	S267E/L328F	SLE	Phase-1	Xencor, Inc.	(90, 94)
XmAb7195	IgE	S267E/L328F	Allergic diseases	Phase-1	Xencor, Inc.	(95)
XmAb5774	CD19	S239D/I332E	CLL	Phase-1	Xencor, Inc.	(89, 96)
TRX4	CD3	N297A	Type-1 diabetes mellitus (autoimmune)	Phase-3	GSK/Tolerx	(48, 49, 97)
Onartuzumab	MET	N297A	NSCLC/gastroesophageal cancer	Phase-3	Roche	(48, 98, 99)
ALD518	IL-6	N297A	RA/NSCLC/oral mucositis	Phase-2	Alder	(48, 49, 100)
TRX518	GITR	N297A	Malignant melanoma	Phase-1	Tolerx	(48, 49, 101)

CLL, chronic lymphocytic leukemia; AML, acute myeloid leukemia; SLE, systemic lupus erythematosus; NSCLC, non-small cell lung cancer; RA, rheumatoid arthritis; NA, not available.

Source: <https://clinicaltrials.gov/>.

of B-cell receptor-induced calcium mobilization among healthy volunteers and SLE patients (94). The same Fc fragment has been engineered into a humanized anti-IgE antibody (XmAb7195; Xencor) for the treatment of allergies (95). This antibody prevents the binding of IgE to its high-affinity IgE receptor (FcεRI) that is present on basophils and mast cells and is useful in the treatment of allergic asthma (95). The XmAb7195 has 5- and ~430-fold higher affinity for human IgE and FcγRIIb, respectively, and therefore is effective in inhibiting IgE production and plasma cell differentiation (95).

Finally, aglycosylated IgG molecules have recently been shown to have therapeutic properties (48, 49, 61, 63), and a few of them are undergoing clinical testing. An anti-CD3 antibody (TRX4; Tolerx) incorporating the N297A mutation suppresses pathogenic T-cells in type-1 diabetes (T1D) patients (48, 49, 97) and is being evaluated in phase-3 trials. The antibody downregulates pathogenic T-cells while restoring the normal activity of T-regulatory cells and thereby inhibits autoimmune mediated T1D (97).

It is widely accepted that hepatocyte growth factor (HGF) binding to receptor tyrosine kinase MET aggravates malignancy in a variety of cancers (98). Therefore, an aglycosylated anti-MET antibody (Onartuzumab; Roche) is being evaluated in phase-3 trials to inhibit the binding of HGF for treating lung and gastroesophageal cancers (49, 98, 99). This is an *E. coli*-derived humanized, affinity-matured antibody, which engages MET, thereby inhibiting HGF binding and receptor phosphorylation in HGF-dependent tumor models (98). Similarly, an aglycosylated mAb (ALD518; Alder) targeting IL-6 is being tested in phase-2 for a variety of diseases including rheumatoid arthritis, non-small cell lung cancer (NSCLC), and oral mucositis (48, 49, 100). The antibody was developed to inhibit proinflammatory cytokine IL-6 in oncogenic niches, which can otherwise lead to a cancer. The mAb ALD518 is reported to be well tolerated in phase-1 and -2 studies and ameliorated NSCLC-related anemia and cachexia (100). Another aglycosylated mAb (TRX518; Tolerx) is currently in phase-1 trials to treat malignant myeloma (48, 49, 101). TRX518 mAb recognizes the glucocorticoid-induced tumor necrosis factor receptor on regulatory and effector T-cells, B-cells, NK cells, and antigen-presenting cells to enhance effector T-cell response and inhibits T-regulatory cell-mediated suppression (101). Furthermore, the efficacy of TRX518 mAb in reducing tumor burden and increased survival rates has been demonstrated in mouse and non-human primate models (101).

REFERENCES

1. Jefferis R, Lund J, Pound JD. IgG-Fc-mediated effector functions: molecular definition of interaction sites for effector ligands and the role of glycosylation. *Immunol Rev* (1998) 163:59–76. doi:10.1111/j.1600-065X.1998.tb01188.x
2. Duncan AR, Woof JM, Partridge LJ, Burton DR, Winter G. Localization of the binding site for the human high-affinity Fc receptor on IgG. *Nature* (1988) 332:563–4. doi:10.1038/332563a0
3. Duncan AR, Winter G. The binding site for C1q on IgG. *Nature* (1988) 332:738–40. doi:10.1038/332738a0
4. Rayner LE, Hui GK, Gor J, Heenan RK, Dalby PA, Perkins SJ. The solution structures of two human IgG1 antibodies show conformational stability

These studies highlight that Fc engineering has played important roles in developing antibodies with desirable properties and functions, and the ongoing clinical studies can give valuable information on the efficacy of the Fc-engineered mAbs, as compared to their existing peers.

FINAL REMARKS

Crystallizable fragment engineering has made substantial progress in the identification of new mutant(s) that can enhance effector functions and improve pharmacokinetics of mAbs for cancer treatment. Two major notions have emerged during the past decades' efforts. First, the ratio of human activating FcγRs (FcγRI, FcγRIIa, and FcγRIIIa) and inhibitory FcγR (FcγRIIb) has to be taken into account during Fc engineering design. Beneficial effect can be achieved when Fc mutant(s) show higher selectivity and binding affinity toward activating FcγRs, as compared to the inhibitory FcγR. Second, the synergistic effects of improved ADCC, ADCP, and CDC of Fc region could increase the potency in cancer treatment.

Excitingly, aglycosylated mAb, expressed in bacteria and yeast, have been found to possess similar properties as glycosylated mAb with regards to FcγRs binding and serum half-life. However, efforts are still needed to improve its thermostability, solubility, and its binding affinity to C1q and CDC activity before it can really compete with its glycosylated peer for cancer therapy. On the other hand, the inability of aglycosylated mAbs to bind to C1q may have beneficial effects when CDC activity is not required such as for treatment of autoimmune diseases where CDC is chronically and pathologically activated (102). Similarly, aglycosylated mAbs may have advantages over glycosylated counterparts when only selective activation of FcγRs is desired such as activation of FcγRI (63) or FcγRIIa (84) to stimulate tumor cell killing.

AUTHOR CONTRIBUTIONS

DW conceived the topic; AS and DW wrote the manuscript; and DW revised the manuscript.

FUNDING

This work was supported by National Natural Science Foundation of China (Grant No: 81572698) to DW.

- and accommodate their C1q and FcγR ligands. *J Biol Chem* (2015) 290:8420–38. doi:10.1074/jbc.M114.631002
5. Ghettie V, Ward ES. Multiple roles for the major histocompatibility complex class I-related receptor FcRn. *Annu Rev Immunol* (2000) 18:739–66. doi:10.1146/annurev.immunol.18.1.739
 6. Lazar GA, Dang W, Karki S, Vafa O, Peng JS, Hyun L, et al. Engineered antibody Fc variants with enhanced effector function. *Proc Natl Acad Sci U S A* (2006) 103:4005–10. doi:10.1073/pnas.0508123103
 7. Ghirlando R, Keown MB, Mackay GA, Lewis MS, Unkeless JC, Gould HJ. Stoichiometry and thermodynamics of the interaction between the Fc fragment of human IgG1 and its low-affinity receptor FcγRIII. *Biochemistry* (1995) 34:13320–7. doi:10.1021/bi00041a007

8. Ravetch JV, Bolland S. IgG Fc receptors. *Annu Rev Immunol* (2001) 19:275–90. doi:10.1146/annurev.immunol.19.1.275
9. Kiyoshi M, Caaveiro JM, Kawai T, Tashiro S, Ide T, Asaoka Y, et al. Structural basis for binding of human IgG1 to its high-affinity human receptor FcγRI. *Nat Commun* (2015) 6:6866. doi:10.1038/ncomms7866
10. Ramsland PA, Farrugia W, Bradford TM, Sardjono CT, Esparon S, Trist HM, et al. Structural basis for Fc gammaRIIa recognition of human IgG and formation of inflammatory signaling complexes. *J Immunol* (2011) 187:3208–17. doi:10.4049/jimmunol.1101467
11. Radaev S, Motyka S, Fridman WH, Sautes-Fridman C, Sun PD. The structure of a human type III Fcgamma receptor in complex with Fc. *J Biol Chem* (2001) 276:16469–77. doi:10.1074/jbc.M100350200
12. Bruhns P, Iannascoli B, England P, Mancardi DA, Fernandez N, Jorieux S, et al. Specificity and affinity of human Fcgamma receptors and their polymorphic variants for human IgG subclasses. *Blood* (2009) 113:3716–25. doi:10.1182/blood-2008-09-179754
13. Martin WL, West AP, Gan L, Bjorkman PJ. Crystal structure at 2.8 Å of an FcRn/heterodimeric Fc complex. *Mol Cell* (2001) 7:867–77. doi:10.1016/s1097-2765(01)00230-1
14. Gaboriaud C, Juanhuix J, Gruez A, Lacroix M, Darnault C, Pignol D, et al. The crystal structure of the globular head of complement protein C1q provides a basis for its versatile recognition properties. *J Biol Chem* (2003) 278:46974–82. doi:10.1074/jbc.M307764200
15. Schneider S, Zacharias M. Atomic resolution model of the antibody Fc interaction with the complement C1q component. *Mol Immunol* (2012) 51:66–72. doi:10.1016/j.molimm.2012.02.111
16. Sarma JV, Ward PA. The complement system. *Cell Tissue Res* (2011) 343:227–35. doi:10.1007/s00441-010-1034-0
17. Vidarsson G, Dekkers G, Rispens T. IgG subclasses and allotypes: from structure to effector functions. *Front Immunol* (2014) 5:520. doi:10.3389/fimmu.2014.00520
18. Firman M, Bawdon R, Radu C, Ober RJ, Eaken D, Antohe F, et al. The MHC class I-related receptor, FcRn, plays an essential role in the maternofoetal transfer of gamma-globulin in humans. *Int Immunol* (2001) 13:993–1002. doi:10.1093/intimm.13.8.993
19. Medesani C, Matesoi D, Radu C, Ghetie V, Ward ES. Delineation of the amino acid residues involved in transcytosis and catabolism of mouse IgG1. *J Immunol* (1997) 158:2211–7.
20. Pyzik M, Rath T, Lencer WI, Baker K, Blumberg RS. FcRn: the architect behind the immune and nonimmune functions of IgG and albumin. *J Immunol* (2015) 194:4595–603. doi:10.4049/jimmunol.1403014
21. Akilesh S, Christianson GJ, Roopenian DC, Shaw AS. Neonatal FcR expression in bone marrow-derived cells functions to protect serum IgG from catabolism. *J Immunol* (2007) 179:4580–8. doi:10.4049/jimmunol.179.7.4580
22. Montoyo HP, Vaccaro C, Hafner M, Ober RJ, Mueller W, Ward ES. Conditional deletion of the MHC class I-related receptor FcRn reveals the sites of IgG homeostasis in mice. *Proc Natl Acad Sci USA* (2009) 106:2788–93. doi:10.1073/pnas.0810796106
23. Zhu X, Meng G, Dickinson BL, Li X, Mizoguchi E, Miao L, et al. MHC class I-related neonatal Fc receptor for IgG is functionally expressed in monocytes, intestinal macrophages, and dendritic cells. *J Immunol* (2001) 166:3266–76. doi:10.4049/jimmunol.166.5.3266
24. Kim JK, Tsen MF, Ghetie V, Ward ES. Localization of the site of the murine IgG1 molecule that is involved in binding to the murine intestinal Fc receptor. *Eur J Immunol* (1994) 24:2429–34. doi:10.1002/eji.1830241025
25. Kim JK, Tsen MF, Ghetie V, Ward ES. Identifying amino acid residues that influence plasma clearance of murine IgG1 fragments by site-directed mutagenesis. *Eur J Immunol* (1994) 24:542–8. doi:10.1002/eji.1830240308
26. Burmeister WP, Huber AH, Bjorkman PJ. Crystal structure of the complex of rat neonatal Fc receptor with Fc. *Nature* (1994) 372:379–83. doi:10.1038/372379a0
27. Burmeister WP, Gastinel LN, Simister NE, Blum ML, Bjorkman PJ. Crystal structure at 2.2 Å resolution of the MHC-related neonatal Fc receptor. *Nature* (1994) 372:336–43. doi:10.1038/37236a0
28. Huber AH, Kelley RF, Gastinel LN, Bjorkman PJ. Crystallization and stoichiometry of binding of a complex between a rat intestinal Fc receptor and Fc. *J Mol Biol* (1993) 230:1077–83. doi:10.1006/jmbi.1993.1220
29. Stavenhagen JB, Gorlatov S, Tuailon N, Rankin CT, Li H, Burke S, et al. Fc optimization of therapeutic antibodies enhances their ability to kill tumor cells in vitro and controls tumor expansion in vivo via low-affinity activating Fcgamma receptors. *Cancer Res* (2007) 67:8882–90. doi:10.1158/0008-5472.CAN-07-0696
30. Jefferis R. Glycosylation of recombinant antibody therapeutics. *Biotechnol Prog* (2005) 21:11–6. doi:10.1021/bp040016j
31. Wright A, Morrison SL. Effect of glycosylation on antibody function: implications for genetic engineering. *Trends Biotechnol* (1997) 15:26–32. doi:10.1016/S0167-7799(96)10062-7
32. Krapp S, Mimura Y, Jefferis R, Huber R, Sondermann P. Structural analysis of human IgG-Fc glycoforms reveals a correlation between glycosylation and structural integrity. *J Mol Biol* (2003) 325:979–89. doi:10.1016/s0022-2836(02)01250-0
33. Jefferis R. Recombinant antibody therapeutics: the impact of glycosylation on mechanisms of action. *Trends Pharmacol Sci* (2009) 30:356–62. doi:10.1016/j.tips.2009.04.007
34. Jefferis R, Lund J. Interaction sites on human IgG-Fc for FcgammaR: current models. *Immunol Lett* (2002) 82:57–65. doi:10.1016/S0165-2478(02)00019-6
35. Lund J, Winter G, Jones PT, Pound JD, Tanaka T, Walker MR, et al. Human Fc gamma RI and Fc gamma RII interact with distinct but overlapping sites on human IgG. *J Immunol* (1991) 147:2657–62.
36. Lund J, Toshiyuki T, Noriko T, Sarmay G, Yoji A, Jefferis R. A protein structural change in glycosylated IgG3 correlates with loss of huFcγR1 and huFcγR111 binding and/or activation. *Mol Immunol* (1990) 27:1145–53. doi:10.1016/0161-5890(90)90103-7
37. Medesani C, Radu C, Kim JK, Ghetie V, Ward ES. Localization of the site of the IgG molecule that regulates maternofoetal transmission in mice. *Eur J Immunol* (1996) 26:2533–6. doi:10.1002/eji.1830261038
38. Mimura Y, Sondermann P, Ghirlando R, Lund J, Young SP, Goodall M, et al. Role of oligosaccharide residues of IgG1-Fc in Fc gamma RIIb binding. *J Biol Chem* (2001) 276:45539–47. doi:10.1074/jbc.M107478200
39. Radaev S, Sun PD. Recognition of IgG by Fcgamma receptor. The role of Fc glycosylation and the binding of peptide inhibitors. *J Biol Chem* (2001) 276:16478–83. doi:10.1074/jbc.M100351200
40. Roopenian DC, Akilesh S. FcRn: the neonatal Fc receptor comes of age. *Nat Rev Immunol* (2007) 7:715–25. doi:10.1038/nri2155
41. Walker MR, Lund J, Thompson KM, Jefferis R. Aglycosylation of human IgG1 and IgG3 monoclonal antibodies can eliminate recognition by human cells expressing FcγRI and/or FcγRII receptors. *Biochem J* (1989) 259:347–53. doi:10.1042/bj2590347
42. Jefferis R, Lund J, Mizutani H, Nakagawa H, Kawazoe Y, Arata Y, et al. A comparative study of the N-linked oligosaccharide structures of human IgG subclass proteins. *Biochem J* (1990) 268:529–37. doi:10.1042/bj2680529
43. Raju TS. Terminal sugars of Fc glycans influence antibody effector functions of IgGs. *Curr Opin Immunol* (2008) 20:471–8. doi:10.1016/j.coi.2008.06.007
44. Routier FH, Hounsell EF, Rudd PM, Takahashi N, Bond A, Hay FC, et al. Quantitation of the oligosaccharides of human serum IgG from patients with rheumatoid arthritis: a critical evaluation of different methods. *J Immunol Methods* (1998) 213:113–30. doi:10.1016/S0022-1759(98)00032-5
45. Davies J, Jiang L, Pan LZ, LaBarre MJ, Anderson D, Reff M. Expression of GnIII in a recombinant anti-CD20 CHO production cell line: expression of antibodies with altered glycoforms leads to an increase in ADCC through higher affinity for Fc gamma RIII. *Biotechnol Bioeng* (2001) 74:288–94. doi:10.1002/bit.1119.abs
46. Shields RL, Lai J, Keck R, O'Connell LY, Hong K, Meng YG, et al. Lack of fucose on human IgG1 N-linked oligosaccharide improves binding to human Fcgamma RIII and antibody-dependent cellular toxicity. *J Biol Chem* (2002) 277:26733–40. doi:10.1074/jbc.M202069200
47. Jefferis R. Glycosylation as a strategy to improve antibody-based therapeutics. *Nat Rev Drug Discov* (2009) 8:226–34. doi:10.1038/nrd2804
48. Ju MS, Jung ST. Aglycosylated full-length IgG antibodies: steps toward next-generation immunotherapeutics. *Curr Opin Biotechnol* (2014) 30:128–39. doi:10.1016/j.copbio.2014.06.013
49. Jung ST, Kang TH, Kelton W, Georgiou G. Bypassing glycosylation: engineering aglycosylated full-length IgG antibodies for human therapy. *Curr Opin Biotechnol* (2011) 22:858–67. doi:10.1016/j.copbio.2011.03.002

50. Raju TS. Assessing Fc glycan heterogeneity of therapeutic recombinant monoclonal antibodies using NP-HPLC. *Methods Mol Biol* (2013) 988:169–80. doi:10.1007/9781627033275_10
51. Kubota T, Niwa R, Satoh M, Akinaga S, Shitara K, Hanai N. Engineered therapeutic antibodies with improved effector functions. *Cancer Sci* (2009) 100:1566–72. doi:10.1111/j.1349-7006.2009.01222.x
52. Idusogie EE, Wong PY, Presta LG, Gazzano-Santoro H, Totpal K, Ultsch M, et al. Engineered antibodies with increased activity to recruit complement. *J Immunol* (2001) 166:2571–5. doi:10.4049/jimmunol.166.4.2571
53. Horton HM, Bennett MJ, Pong E, Peipp M, Karki S, Chu SY, et al. Potent in vitro and in vivo activity of an Fc-engineered anti-CD19 monoclonal antibody against lymphoma and leukemia. *Cancer Res* (2008) 68:8049–57. doi:10.1158/0008-5472.CAN-08-2268
54. Horton HM, Bennett MJ, Peipp M, Pong E, Karki S, Chu SY, et al. Fc-engineered anti-CD40 antibody enhances multiple effector functions and exhibits potent in vitro and in vivo antitumor activity against hematologic malignancies. *Blood* (2010) 116:3004–12. doi:10.1182/blood-2010-01-265280
55. Derer S, Glorius P, Schlaeth M, Lohse S, Klausz K, Muchhal U, et al. Increasing FcgammaRIIa affinity of an FcgammaRIII-optimized anti-EGFR antibody restores neutrophil-mediated cytotoxicity. *MAbs* (2014) 6:409–21. doi:10.4161/mabs.27457
56. Richards JO, Karki S, Lazar GA, Chen H, Dang W, Desjarlais JR. Optimization of antibody binding to FcgammaRIIa enhances macrophage phagocytosis of tumor cells. *Mol Cancer Ther* (2008) 7:2517–27. doi:10.1158/1535-7163.MCT-08-0201
57. Nordstrom JL, Gorlatov S, Zhang W, Yang Y, Huang L, Burke S, et al. Anti-tumor activity and toxicokinetics analysis of MGAH22, an anti-HER2 monoclonal antibody with enhanced Fcgamma receptor binding properties. *Breast Cancer Res* (2011) 13:R123. doi:10.1186/bcr3069
58. Loo D, Alderson RF, Chen FZ, Huang L, Zhang W, Gorlatov S, et al. Development of an Fc-enhanced anti-B7-H3 monoclonal antibody with potent antitumor activity. *Clin Cancer Res* (2012) 18:3834–45. doi:10.1158/1078-0432.CCR-12-0715
59. Mimoto F, Katada H, Kadono S, Igawa T, Kuramochi T, Muraoka M, et al. Engineered antibody Fc variant with selectively enhanced FcgammaRIIB binding over both FcgammaRIIa(R131) and FcgammaRIIa(H131). *Protein Eng Des Sel* (2013) 26:589–98. doi:10.1093/protein/gzt022
60. Kelton W, Mehta N, Charab W, Lee J, Lee CH, Kojima T, et al. IgGA: a “cross-isotype” engineered human Fc antibody domain that displays both IgG-like and IgA-like effector functions. *Chem Biol* (2014) 21:1603–9. doi:10.1016/j.chembiol.2014.10.017
61. Sazinsky SL, Ott RG, Silver NW, Tidor B, Ravetch JV, Wittrup KD. Aglycosylated immunoglobulin G1 variants productively engage activating Fc receptors. *Proc Natl Acad Sci U S A* (2008) 105:20167–72. doi:10.1073/pnas.0809257105
62. Stewart R, Thom G, Levens M, Guler-Gane G, Holgate R, Rudd PM, et al. A variant human IgG1-Fc mediates improved ADCC. *Protein Eng Des Sel* (2011) 24:671–8. doi:10.1093/protein/gzr015
63. Jung ST, Reddy ST, Kang TH, Borrok MJ, Sandlie I, Tucker PW, et al. Aglycosylated IgG variants expressed in bacteria that selectively bind FcgammaRI potentiate tumor cell killing by monocyte-dendritic cells. *Proc Natl Acad Sci U S A* (2010) 107:604–9. doi:10.1073/pnas.0908590107
64. Jung ST, Kang TH, Kim D-il. Engineering an aglycosylated Fc variant for enhanced FcγRI engagement and pH-dependent human FcRn binding. *Biotechnol Bioprocess Eng* (2014) 19:780–9. doi:10.1007/s12257-013-0432-z
65. Zalevsky J, Chamberlain AK, Horton HM, Karki S, Leung IW, Sproule TJ, et al. Enhanced antibody half-life improves in vivo activity. *Nat Biotechnol* (2010) 28:157–9. doi:10.1038/nbt.1601
66. Ghetie V, Popov S, Borvak J, Radu C, Matesoi D, Medesan C, et al. Increasing the serum persistence of an IgG fragment by random mutagenesis. *Nat Biotechnol* (1997) 15:637–40. doi:10.1038/nbt0797-637
67. Dall'Acqua WF, Woods RM, Ward ES, Palaszynski SR, Patel NK, Brewah YA, et al. Increasing the affinity of a human IgG1 for the neonatal Fc receptor: biological consequences. *J Immunol* (2002) 169:5171–80. doi:10.4049/jimmunol.169.9.5171
68. Shields RL, Namenuk AK, Hong K, Meng YG, Rae J, Briggs J, et al. High resolution mapping of the binding site on human IgG1 for Fc gamma RI, Fc gamma RII, Fc gamma RIII, and FcRn and design of IgG1 variants with improved binding to the Fc gamma R. *J Biol Chem* (2001) 276:6591–604. doi:10.1074/jbc.M009483200
69. Dall'Acqua WF, Kiener PA, Wu H. Properties of human IgG1s engineered for enhanced binding to the neonatal Fc receptor (FcRn). *J Biol Chem* (2006) 281:23514–24. doi:10.1074/jbc.M604292200
70. Hinton PR, Johlfs MG, Xiong JM, Hanestad K, Ong KC, Bullock C, et al. Engineered human IgG antibodies with longer serum half-lives in primates. *J Biol Chem* (2004) 279:6213–6. doi:10.1074/jbc.C300470200
71. Idusogie EE, Presta LG, Gazzano-Santoro H, Totpal K, Wong PY, Ultsch M, et al. Mapping of the C1q binding site on rituxan, a chimeric antibody with a human IgG1 Fc. *J Immunol* (2000) 164:4178–84. doi:10.4049/jimmunol.164.8.4178
72. Natsume A, In M, Takamura H, Nakagawa T, Shimizu Y, Kitajima K, et al. Engineered antibodies of IgG1/IgG3 mixed isotype with enhanced cytotoxic activities. *Cancer Res* (2008) 68:3863–72. doi:10.1158/0008-5472.CAN-07-6297
73. Moore GL, Chen H, Karki S, Lazar GA. Engineered Fc variant antibodies with enhanced ability to recruit complement and mediate effector functions. *MAbs* (2010) 2:181–9. doi:10.4161/mabs.2.2.11158
74. Yeung YA, Leabman MK, Marvin JS, Qiu J, Adams CW, Lien S, et al. Engineering human IgG1 affinity to human neonatal Fc receptor: impact of affinity improvement on pharmacokinetics in primates. *J Immunol* (2009) 182:7663–71. doi:10.4049/jimmunol.0804182
75. Hinton PR, Xiong JM, Johlfs MG, Tang MT, Keller S, Tsurushita N. An engineered human IgG1 antibody with longer serum half-life. *J Immunol* (2006) 176:346–56. doi:10.4049/jimmunol.176.1.346
76. Greys A, Bern M, Foss S, Bratlie DB, Moen A, Gunnarsen KS, et al. Fc engineering of human IgG1 for altered binding to the neonatal Fc receptor affects Fc effector functions. *J Immunol* (2015) 194:5497–508. doi:10.4049/jimmunol.1401218
77. Vaccaro C, Bawdon R, Wanjie S, Ober RJ, Ward ES. Divergent activities of an engineered antibody in murine and human systems have implications for therapeutic antibodies. *Proc Natl Acad Sci U S A* (2006) 103:18709–14. doi:10.1073/pnas.0606304103
78. Ecker DM, Jones SD, Levine HL. The therapeutic monoclonal antibody market. *MAbs* (2015) 7:9–14. doi:10.4161/19420862.2015.989042
79. Naso MF, Tam SH, Scallon BJ, Raju TS. Engineering host cell lines to reduce terminal sialylation of secreted antibodies. *MAbs* (2010) 2:519–27. doi:10.4161/mabs.2.5.13078
80. Chu L, Robinson DK. Industrial choices for protein production by large-scale cell culture. *Curr Opin Biotechnol* (2001) 12:180–7. doi:10.1016/S0958-1669(00)00197-X
81. Maxwell KE, Powell MS, Hulett MD, Barton PA, McKenzie IF, Garrett TP, et al. Crystal structure of the human leukocyte Fc receptor, Fc gammaRIIa. *Nat Struct Biol* (1999) 6:437–42. doi:10.1038/2841
82. Steele RW. Managing infection in cancer patients and other immunocompromised children. *Ochsner J* (2012) 12:202–10.
83. Borrok MJ, Jung ST, Kang TH, Monzingo AF, Georgiou G. Revisiting the role of glycosylation in the structure of human IgG Fc. *ACS Chem Biol* (2012) 7:1596–602. doi:10.1021/cb300130k
84. Jung ST, Kelton W, Kang TH, Ng DT, Andersen JT, Sandlie I, et al. Effective phagocytosis of low Her2 tumor cell lines with engineered, aglycosylated IgG displaying high FcgammaRIIA affinity and selectivity. *ACS Chem Biol* (2013) 8:368–75. doi:10.1021/cb300455f
85. Latypov RF, Hogan S, Lau H, Gadgil H, Liu D. Elucidation of acid-induced unfolding and aggregation of human immunoglobulin IgG1 and IgG2 Fc. *J Biol Chem* (2012) 287:1381–96. doi:10.1074/jbc.M111.297697
86. Alsenaidy MA, Kim JH, Majumdar R, Weis DD, Joshi SB, Tolbert TJ, et al. High-throughput biophysical analysis and data visualization of conformational stability of an IgG1 monoclonal antibody after deglycosylation. *J Pharm Sci* (2013) 102:3942–56. doi:10.1002/jps.23730
87. Hristodorov D, Fischer R, Joerissen H, Muller-Tiemann B, Apeler H, Linden L. Generation and comparative characterization of glycosylated and aglycosylated human IgG1 antibodies. *Mol Biotechnol* (2013) 53:326–35. doi:10.1007/s12033-012-9531-x
88. Heider KH, Kiefer K, Zenz T, Volden M, Stilgenbauer S, Ostermann E, et al. A novel Fc-engineered monoclonal antibody to CD37 with enhanced ADCC

- and high proapoptotic activity for treatment of B-cell malignancies. *Blood* (2011) 118:4159–68. doi:10.1182/blood-2011-04-351932
89. Sondermann P, Szymkowski DE. Harnessing Fc receptor biology in the design of therapeutic antibodies. *Curr Opin Immunol* (2016) 40:78–87. doi:10.1016/j.coim.2016.03.005
 90. Horton HM, Chu SY, Ortiz EC, Pong E, Cemerski S, Leung IW, et al. Antibody-mediated coengagement of FcgammaRIIb and B cell receptor complex suppresses humoral immunity in systemic lupus erythematosus. *J Immunol* (2011) 186:4223–33. doi:10.4049/jimmunol.1003412
 91. Lee EM, Yee D, Busfield SJ, McManus JF, Cummings N, Vairo G, et al. Efficacy of an Fc-modified anti-CD123 antibody (CSL362) combined with chemotherapy in xenograft models of acute myelogenous leukemia in immunodeficient mice. *Haematologica* (2015) 100:914–26. doi:10.3324/haematol.2014.113092
 92. Blum KA, Smith M, Fung H, Zalevsky J, Combs D, Ramies DA, et al. Phase I study of an anti-CD30 Fc engineered humanized monoclonal antibody in Hodgkin lymphoma (HL) or anaplastic large cell lymphoma (ALCL) patients: safety, pharmacokinetics (PK), immunogenicity, and efficacy. *J Clin Oncol* (2009) 27:8531.
 93. Kumar A, Blum KA, Fung HC, Smith MR, Foster PA, Younes A. A phase 1 dose-escalation study of XmAb(R) 2513 in patients with relapsed or refractory Hodgkin lymphoma. *Br J Haematol* (2015) 168:902–4. doi:10.1111/bjh.13152
 94. Chu SY, Vostiar I, Karki S, Moore GL, Lazar GA, Pong E, et al. Inhibition of B cell receptor-mediated activation of primary human B cells by coengagement of CD19 and FcgammaRIIb with Fc-engineered antibodies. *Mol Immunol* (2008) 45:3926–33. doi:10.1016/j.molimm.2008.06.027
 95. Chu SY, Horton HM, Pong E, Leung IW, Chen H, Nguyen DH, et al. Reduction of total IgE by targeted coengagement of IgE B-cell receptor and FcgammaRIIb with Fc-engineered antibody. *J Allergy Clin Immunol* (2012) 129:1102–15. doi:10.1016/j.jaci.2011.11.029
 96. Awan FT, Lapalombella R, Trotta R, Butchar JP, Yu B, Benson DM Jr, et al. CD19 targeting of chronic lymphocytic leukemia with a novel Fc-domain-engineered monoclonal antibody. *Blood* (2010) 115:1204–13. doi:10.1182/blood-2009-06-229039
 97. Aronson R, Gottlieb PA, Christiansen JS, Donner TW, Bosi E, Bode BW, et al. Low-dose otezixizumab anti-CD3 monoclonal antibody DEFEND-1 study: results of the randomized phase III study in recent-onset human type 1 diabetes. *Diabetes Care* (2014) 37:2746–54. doi:10.2337/dc13-0327
 98. Merchant M, Ma X, Maun HR, Zheng Z, Peng J, Romero M, et al. Monovalent antibody design and mechanism of action of onartuzumab, a MET antagonist with anti-tumor activity as a therapeutic agent. *Proc Natl Acad Sci U S A* (2013) 110:E2987–96. doi:10.1073/pnas.1302725110
 99. Park HI, Yoon HW, Jung ST. The highly evolvable antibody Fc domain. *Trends Biotechnol* (2016) 34:895–908. doi:10.1016/j.tibtech.2016.04.005
 100. Bayliss TJ, Smith JT, Schuster M, Dragnev KH, Rigas JR. A humanized anti-IL-6 antibody (ALD518) in non-small cell lung cancer. *Expert Opin Biol Ther* (2011) 11:1663–8. doi:10.1517/14712598.2011.627850
 101. Rosenzweig M, Ponte J, Apostolou I, Doty D, Guild J, Slavonic M, et al. Development of TRX518, an glycosyl humanized monoclonal antibody (Mab) agonist of huGITR. *J Clin Oncol* (2010) 28:e13028.
 102. Melis JP, Strumane K, Ruuls SR, Beurskens FJ, Schuurman J, Parren PW. Complement in therapy and disease: regulating the complement system with antibody-based therapeutics. *Mol Immunol* (2015) 67:117–30. doi:10.1016/j.molimm.2015.01.028

Conflict of Interest Statement: The authors declare that the research was conducted in the absence of any commercial or financial relationships that could be construed as a potential conflict of interest.

Copyright © 2016 Saxena and Wu. This is an open-access article distributed under the terms of the Creative Commons Attribution License (CC BY). The use, distribution or reproduction in other forums is permitted, provided the original author(s) or licensor are credited and that the original publication in this journal is cited, in accordance with accepted academic practice. No use, distribution or reproduction is permitted which does not comply with these terms.



Fc Engineering for Developing Therapeutic Bispecific Antibodies and Novel Scaffolds

Hongyan Liu^{1†}, Abhishek Saxena^{1†}, Sachdev S. Sidhu^{1,2,3*} and Donghui Wu^{1*}

¹Laboratory of Antibody Engineering, Shanghai Institute for Advanced Immunochemical Studies, ShanghaiTech University, Shanghai, China, ²Banting and Best Department of Medical Research, Terrence Donnelly Center for Cellular and Biomolecular Research, University of Toronto, Toronto, ON, Canada, ³Department of Molecular Genetics, Terrence Donnelly Center for Cellular and Biomolecular Research, University of Toronto, Toronto, ON, Canada

OPEN ACCESS

Edited by:

Tianlei Ying,
Fudan University, China

Reviewed by:

Thorsten Demberg,
Immatics Biotechnologies,
Germany

Dimiter S. Dimitrov,
National Institutes of Health (NIH),
USA

***Correspondence:**

Sachdev S. Sidhu
sachdev.sidhu@utoronto.ca;
Donghui Wu
wudh@shanghaitech.edu.cn

[†]These authors have contributed
equally to this work.

Specialty section:

This article was submitted to
Vaccines and Molecular
Therapeutics,
a section of the journal
Frontiers in Immunology

Received: 30 August 2016

Accepted: 10 January 2017

Published: 26 January 2017

Citation:

Liu H, Saxena A, Sidhu SS and
Wu D (2017) Fc Engineering for
Developing Therapeutic Bispecific
Antibodies and Novel Scaffolds.
Front. Immunol. 8:38.
doi: 10.3389/fimmu.2017.00038

Therapeutic monoclonal antibodies have become molecules of choice to treat autoimmune disorders, inflammatory diseases, and cancer. Moreover, bispecific/multispecific antibodies that target more than one antigen or epitope on a target cell or recruit effector cells (T cell, natural killer cell, or macrophage cell) toward target cells have shown great potential to maximize the benefits of antibody therapy. In the past decade, many novel concepts to generate bispecific and multispecific antibodies have evolved successfully into a range of formats from full bispecific immunoglobulin gammas to antibody fragments. Impressively, antibody fragments such as bispecific T-cell engager, bispecific killer cell engager, trispecific killer cell engager, tandem diabody, and dual-affinity-retargeting are showing exciting results in terms of recruiting and activating self-immune effector cells to target and lyse tumor cells. Promisingly, crystallizable fragment (Fc) antigen-binding fragment and monomeric antibody or half antibody may be particularly advantageous to target solid tumors owing to their small size and thus good tissue penetration potential while, on the other hand, keeping Fc-related effector functions such as antibody-dependent cellular cytotoxicity, complement-dependent cytotoxicity, antibody-dependent cell-mediated phagocytosis, and extended serum half-life via interaction with neonatal Fc receptor. This review, therefore, focuses on the progress of Fc engineering in generating bispecific molecules and on the use of small antibody fragment as scaffolds for therapeutic development.

Keywords: mAbs, Fc region, FcRn, bispecific, monovalent, heterodimer, monomeric Fc, Fc antigen-binding

INTRODUCTION

Since approval of the first therapeutic monoclonal antibody (mAb) muromonab-CD3 by the United States Food and Drug Administration for treatment of organ transplant-associated acute rejections in 1992, a total of 62 mAbs have been approved by the USFDA for clinical use as of May 2016 (1, 2). Therefore, the USFDA has approved an average of two to three mAbs each year over the last 25 years. Surprisingly, in 2015, a total of 10 mAbs were approved (2). Clearly, the demand for antibody molecules and global sales have been rising rapidly.

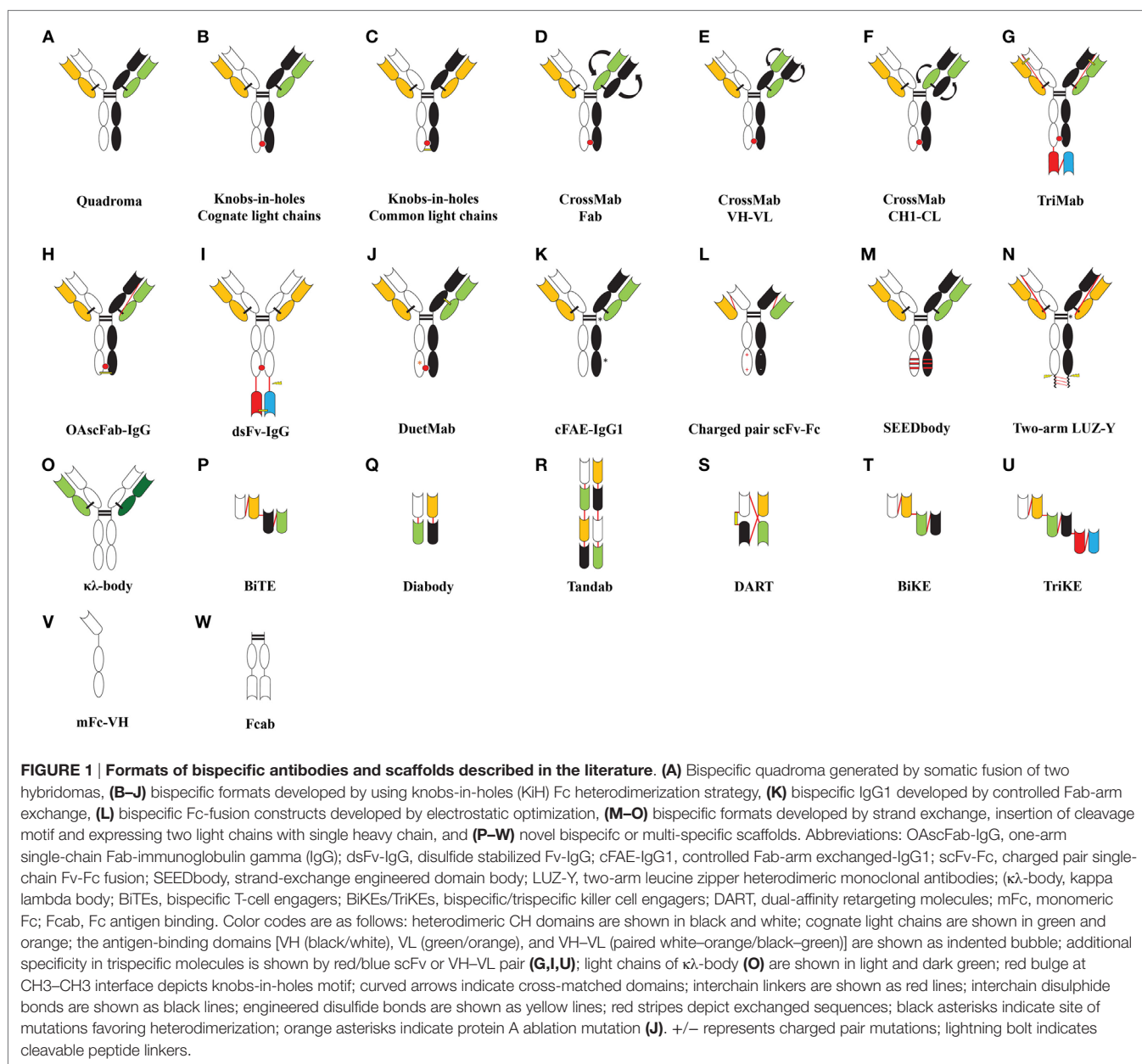
Most therapeutic mAbs are complete immunoglobulin gamma (IgG) molecules which consist of two heavy and two light chains that fold into a complex quaternary Y-shaped structure (1). The

two arms of the Y-shaped molecule form the antigen-binding domains called antigen-binding fragment (Fab) regions, and the stalk forms the crystallizable fragment (Fc) region. Native IgG molecules can be digested by papain protease into separate F(ab)₂ dimers and Fc domains (3). Fab arms are responsible for antigen binding and have been extensively engineered for developing highly specific and synthetic antibodies against numerous targets (4). The Fc region bears recognition motifs for binding innate immune receptors [Fcγ receptors (FcγRs), C1q, and neonatal Fc receptor (FcRn)] on an effector cell and thus is responsible for mediating immune effector functions and *in vivo* IgG stability (5–11). This part has been a prime molecular engineering target for either enhancing or inhibiting the immune response including antibody-dependent cellular cytotoxicity (ADCC), complement-dependent cytotoxicity (CDC), and antibody-dependent cell-mediated phagocytosis (ADCP) (9, 12–14). Besides the Fab

domain, antigen-binding character has also been engineered into the Fc, CH2, and CH3 domains (15, 16). Such novel fragments have demonstrated therapeutic-like profiles in early studies and remain attractive ventures.

Antibody molecules can be made more efficient by engineering additional specificities so that multiple antigens or epitopes present on a cell can be targeted (17, 18). Extensive academic and industrial research in the past decade focused on developing bispecific Abs and Igs (bsAbs and bsIgs) and multispecific antibodies (e.g., TriMabs) (17–20).

Initially, bsAbs were generated by a quadroma technology, which required the somatic fusion of two hybridomas harboring different specificities (21, 22). This led to the foundation of bispecific antibody production for simultaneous targeting of two different antigens or epitopes on a cell (Figure 1A). However, these molecules suffered from low production yields, heterogeneity,



and human anti-mouse antibody (HAMA) response and therefore a decreased efficacy in patients (23). Nevertheless, one such bsAb EpCAM × CD3 (triamab; catumaxomab) was approved by the European Medicines Agency in 2009 for the treatment of patients with epithelial cancer-associated malignant ascites (24). Two additional bsAbs produced using the quadroma method, HER2 × CD3 (triamab; ertumaxomab) and CD20 × CD3 (triamab; FBTA05), are being evaluated in clinical trials for cancer treatment (25, 26).

Later, bsAb construction primarily relied on Fc heterodimerization by creating “knobs-in-holes” (KiH) mutations in the CH3 domain, which is prerequisite to assemble two half antibodies (common Fc heterodimer and unique VH-CH and VL-CL domains) (27–29). However, a major bottleneck in this strategy has been the incorrect pairing of light-heavy chains. Consequently, newer strategies based on KiH and other platforms have been developed to circumvent faulty heavy and light chain pairing.

Small antibody fragments like nanobodies from llama and camel immune systems (30–33), single human domain antibodies (34–37), and single-chain variable fragments (scFvs) (38, 39) can be used to impart bispecificity or multispecificity to antibody molecules (18). Moreover, small non-immunoglobulin fragments like monoclonal lamprey antibodies (lambodies) (40), affibodies (41), and DNA/RNA aptamers (42, 43) can be fused with the antibody Fc fragment (homodimerization or heterodimerization) to have antibody-like properties such as Fc-associated effector functions (ADCC, CDC, and ADCP), extended pharmacokinetics and bispecificity (44, 45).

In this review, we describe recent advances in the therapeutic potential of bispecific molecules and small Ab fragments as novel scaffolds. We summarize the key breakthroughs achieved by employing and optimizing various strategies. Representative design, expression, purification, and purity of final bispecific molecules are summarized (see **Table 1**). Some bispecific antibodies and antibody fragments currently under clinical evaluation are listed (see **Table 2**), and graphical models of bispecific molecules under development are presented (see **Figure 1**).

STRUCTURAL OPTIMIZATION

The KiH (**Figure 1B**) concept was first proposed by Ridgway et al. (29) to develop Fc heterodimers. It allows the generation of complementary interacting interfaces by manipulating key amino acid residues that participate in the Fc dimeric interaction. Amino acids with small side chain are replaced by ones with larger side chains, thereby creating a knob or protrusion in one chain and *vice versa* to create a hole or socket in the partner chain. Traditionally, a T366Y mutation in one CH3 domain has been used to create a knob while an Y407T mutation in the other CH3 domain (hereafter denoted as Y407'T) gives rise to a hole (29). Such mutations establish intermolecular interactions and promote the heterodimer formation due to knob/hole pairing and bring about the association of two different Fab regions to give rise to a monovalent bsIg. It was also found that complementing existing knob/hole mutations with F405A and T394'W on the knob and hole side, respectively, yielded 92% molecules as heterodimers

(29). In an effort to further improve and stabilize the KiH model, a phage-displayed library of CH3 (T366W) knob domain and CH3 (randomized at 366', 368' and 407') hole domain was created by fusing FLAG-tagged CH3-hole to the N-terminal region of the gene-III minor coat protein of M13 bacteriophage (27). The heterodimers were selected by an anti-FLAG antibody and were found to be completely diverse from parent T366W-Y407'A clone. Phage display optimized variants existed preferably as heterodimers and exhibited greater stabilities (27).

The KiH concept suffered from mispairing of heavy and light chains in the heterodimers. Merchant et al. (28) suggested using identical light chains for both Fab domains, which can be further stabilized by engineered disulfide bonds (**Figure 1C**). They employed a scFv phage-displayed library with restricted light chain usage to identify antibodies recognizing c-MPL and HER3 using common light chains and developed a bispecific c-MPL × HER3 antibody with approximately 95% heterodimer recovery (28).

However, it is not always possible to use a common light chain for developing bispecific molecules because antigen recognition can critically rely on the partner light chain (73, 74). To circumvent the existing light chain mispairing in bsIgs, a methodology termed as “CrossMab” (47) was developed and combined with the KiH technology. In principle, “CrossMab” is achieved by the exchange between heavy and light chains of the Fab portion of one partner in order to generate formats of “CrossMab Fab” (**Figure 1D**), “CrossMab VH-VL” (**Figure 1E**), or “CrossMab CH1-CL” (**Figure 1F**) (47). Such bispecific formats clearly reduced the heavy-light chain mispairing, allowed simultaneous recognition of the two antigens (VEGF-A and Ang2), retained the affinity and stability profiles of the parent antibodies and exhibited antiangiogenic and antitumor activity *in vivo* (47).

Similarly, trispecific antibodies “TriMabs” (**Figure 1G**) were developed and combined with the KiH technology using N-terminal single-chain Fab (scFab) and C-terminal scFv fusions of Fc region, which avoids the light chain mispairing. The concept was demonstrated by using four specificities (EGFR, IGF1R, cMET, and HER3) incorporated into three structural formats (19). TriMabs 1 and 2 engage their respective antigen in a monovalent manner while TriMab 3 binds HER3 in a bivalent fashion. These molecules retained their ability to bind individual antigens and shared kinetic properties with their parent molecules. Besides, the TriMabs were also shown to simultaneously recognize their respective antigens when immobilized on a chip or expressed on human pancreatic adenocarcinoma cells (BXPC-3) and inhibited receptor signaling and tumor growth (19).

An scFab heterodimeric bsIg format (OAscFab-IgG) (**Figure 1H**) with anti-IGF1R and anti-EGFR specificities has also been described to prevent faulty chain pairing (48). The light chains in the scFab format were attached to the N-terminus of the heavy chain through a 32-residue linker, and heterodimer formation was achieved by KiH mutations. This strategy allowed the recovery of 99% pure heterodimers, which exhibited comparative antigen-binding affinity to the parent antibodies (48).

Further, a conditional functionality was engineered in a bispecific molecule which relied on proteolytic cleavage to generate functional binders. The VH and VL domains incorporating C44

TABLE 1 | Strategies to promote bispecificity by heterodimer formation.

Strategy/format	Mutation	Target	Bispecificity analysis/yield (%)	Protein expression/purification/yield (g/L)	Remarks	Reference
Quadroma	NA	EpCAM × CD3, HER3 × CD3, CD20 × CD3	Ion-exchange chromatography and SEC/12.5%	Hybridoma/protein A	Associated human anti-mouse antibody response	(26, 46)
Knobs-in-holes	T366W/T366Y (knobs) and T366S/L368A/T394W/F405A/Y407V(T) (holes)	CD3 × CD4, c-MPL × HER3, VEGF-A × Ang2, CD20 × hL243γ1, EGFR × IGF1R, HER3 × cMET, CD3 × EpCAM, CD3 × HER2, EGFR × HER2, CD4 × CD70, MET × EGFR	Electroblotting, SLD, SEC, MS-TOF (73–100%)	HEK293, <i>Escherichia coli</i> , and cell-free expression system/protein A, DEAE, and Mab Select Sure/0.004–1.0 g/L	Faulty light and heavy chain pairing	(19, 27–29, 47–53)
Biochemical optimization	S364H/F405A (CH3A) and Y349T/T394F (CH3B)	CD16 × HER2 and CD3 × HER2	HPLC/SEC (89%)	HEK293F/protein A, nickel affinity chromatography		(54)
Biochemical optimization	L368E/K409R (CH3), R221E/R228E (IgG1-hinge), and R223E/R225E/R228E (IgG2-hinge)	CD3 × CD20, EGFR × ErbB2	Ion-exchange chromatography and LCMS (65–100%)	HEK293/protein A/ <i>in vitro</i> cell-free assembly	Cognate chain pairing	(55)
Biochemical optimization	P228S (IgG1-hinge) and F405L/K409R (CH3)	CD20 × EGFR	ESI-MS (95.7%)	HEK293/protein A/SEC/473.4 g/L	High yield and efficiency	(56)
Biochemical optimization	H435R and Y436F (IgG1-CH3)	CD20 × CD3	SEC (100%)	Stable CHO-K1/protein A/0.2–0.3 g/L	Cognate chain pairing	(57, 58)
Biochemical optimization	S354C (CH3A), Y394C (CH3B), F126C (CH1), S121C (LC), C44 (VH), and C100 (VL)	EGFR × IGF1R, CD20 × hL243γ1, HER3 × cMET	MS-TOF, SEC (73%)	HEK293/protein A/0.004–0.03 g/L	Prevent homodimer formation	(49, 52, 53)
Biochemical optimization	F241R, F243S, F241S, F243R (CH2) and C226S, C229S (hinge)	NA	MS-TOF (90%)	<i>E. coli</i> /protein A	Avoid covalent bonding of heterodimers	(50)
Electrostatic optimization	K409D (CH3A), D399R (CH3B), K409E (CH3A), D399K (CH3B), and K409E (CH3A), D399R (CH3B)	CD3 × TARTK	LC/MS (98%)	HEK293>Select Sure column and SEC	Prevent homodimer formation	(59)
Electrostatic optimization	K409W, K360E, K370E (CH3A) and D399V, F405T, Q347R, E357N, S364B (CH3B)	VEGFR-2 × MET	SEC (80–90%)	HEK293/protein A	Prevent homodimer formation	(60, 61)
Electrostatic optimization	Q39K, Q105K (VH), S183D (CH1), Q38D (VL), S176D (CL), K392D, K409D (CH3A), and E356K, D399K (CH3B)	HER2 × EGFR	SEC (100%)	Stable CHO/protein A/0.2–0.3 g/L	Cognate chain pairing	(57)
Electrostatic optimization	T350V, L351Y, F405A, Y407V (CH3A) and T350V, T366L, K393L, T394W (CH3B)	HER2 × ErbB2	SEC (95%)	CHO/protein A/0.25 g/L	Improved biophysical properties	(62)
κλ-body	NA	CD19 × CD47, CD47 × EpCAM	Isoelectric focusing/41.5%	PEAK cells/protein A, CaptureSelect immunoglobulin gamma (IgG)-CH1, KappaSelect, and LambdaFabSelect affinity chromatography/1.5 g/L	Exploits variable light chains for generating bispecifics	(63)

(Continued)

TABLE 1 | Continued

Strategy/ format	Mutation	Target	Bispecificity analysis/yield (%)	Protein expression/purification/ yield (g/L)	Remarks	Reference
Bispecific T-cell engagers	NA	CD3 × 17-1A, CD3 × CD19	Cytofluorometry ELISA, and SDS-PAGE	CHO/nickel-nitrilotriacetic acid (Ni-NTA) affinity chromatography	Recruitment of T-cells via CD3 ligation	(64, 65)
Diabody	NA	HEL × phOX	FPLC	<i>E. coli</i> /affinity chromatography/0.3–1.0 mg/L	Easy construction and expression in bacteria	(64–66)
Tandem diabody	NA	CD16 × CD80, CD3 × CD19	SEC	<i>E. coli</i> /immobilized-metal chelating chromatography (IMAC)/0.48–0.6 mg/L	Increased valence and stability and activity	(66–68)
Dual-affinity-retargeting	NA	CD16 × CD32B	SEC	HEK293, CHO-S/affinity chromatography	Increased valence and affinity	(67–69)
Bispecific/trispecific killer cell engager	NA	CD16×CD19, CD16×CD19×CD22	SEC	<i>E. coli</i> /ion-exchange chromatography	Natural killer cell activation	(69–72)

CH3A and CH3B mean that these mutations are located on the partner chain.
 Abbreviations: SLD, scanning laser densitometry; SEC, size exclusion chromatography; MS-TOF, time-of-flight mass spectrometry; FPLC, fast protein liquid chromatography; LCMS, liquid chromatography–mass spectrometry; ESI-MS, electrospray ionization mass spectrometry; DEAE, diethylaminoethanol ion-exchange resin; NA, information not available.

or C100 mutations, respectively, were attached to the C-termini of the Fc region in knob and hole mutant, respectively, *via* a flexible linker. The VH C44 and VL C100 generate a disulfide stabilized Fv (**Figure 1I**), bypassing the requirement of a VH–VL linker to promote heterodimer formation in such an arrangement (49). Here, the C-terminal attachment does not affect off-rate and instead relieves steric hindrance after proteolytic cleavage. This methodology can be applied to express toxic products in an inactive state in a cell which can be activated later during the processing steps by proteolytic cleavage (49). This design incorporated a proteolytic motif for Pre-Scission within the peptide linker on one of the partner chains. The recognition motif for other proteolytic systems like furin, matrix metalloproteinase-2/9, or urinary plasminogen activator can also be engineered for varying applications (49).

Next, a structure-guided approach was used to generate bsIg by separately expressing monomeric IgG (harboring KiH mutations) in *Escherichia coli*. Equimolar amounts of two monomeric IgGs, when mixed together at a basic pH, resulted mostly in heterodimeric IgGs (50). These constructs also incorporated mutations in CH2 domain residues (F241R/F243S or F241S/F243R) which remain solvent exposed in glycosylated IgG molecules and the hinge region (C226S/C229S) to avoid covalent association of knob/knob or hole/hole monomers (50).

Recently, Xu et al. (51) utilized a cell-free expression system to generate bsIg based on KiH format. They used anti-CD3, anti-EpCAM, and anti-HER2 antibodies to generate eight bsIgs in four different KiH scaffolds. Among these scaffolds, scFv-KiH and scFv-KiH' (reverse) exhibited superior yields. Moreover, this system allowed optimal heterodimer expression by using equimolar plasmid ratios with an insignificant amount of free chains (51). The Fc fragments with a hole were found to be more stable than Fc-knob, and it was suggested to fuse difficult-to-express proteins to Fc-hole for high-level of expression (51).

Using the KiH platform, Mazor et al. (52) introduced two cysteine pairs in the CH1–CL interface of one of the Fab arm to create disulfide bonds for correct light chain pairing. Almost 100% monovalent bsIg was recovered from variant with CH1 (F126C) and CL (S121C) mutations. These mutations were applied to construct EGFR × HER2 and CD4 × CD70 “DuetMabs” (**Figure 1J**) (52) and were shown to be devoid of any free chains or fragments and had a molecular mass similar to native IgG. The thermal stabilities of EGFR × HER2 ($T_m = 55^\circ\text{C}$) and CD4 × CD70 ($T_m = 58^\circ\text{C}$) antibodies were comparable to the parental antibodies. DuetMabs could simultaneously engage their targets and as a result CD4 × CD70 DuetMab preferentially recognized CD4⁺CD70⁺ T cells over CD4⁺CD70⁻ or CD4⁻CD70⁺ T cells. Similarly, the EGFR × HER2 molecule shared binding kinetics with parental antibodies and also exhibited normal binding to Fc γ Rs, C1q, and FcRn (52).

Based on multistate designs involving molecular modeling, X-ray crystallography validation, and rounds of iteration, Lewis and coworkers (75) identified several favorable mutants across the interface of VH–VL and CH1–CL for formation of an orthogonal Fab interface. In combination with previously reported Fc mutations in favor of the Fc heterodimerization (59), five bsIgs were correctly assembled from six parental mAbs with an average of

TABLE 2 | Bispecific antibody candidates under clinical evaluation.

	Format	Strategy	Target	Clinical development phase	Disease	Company
bsAb/bsAb Fragment						
Catumaxomab	Triomab	Quadroma	EpCAM × CD3	Approved by European Medicines Agency	EpCAM ⁺ tumor; malignant ascites Platinum refractory epithelial ovarian carcinoma Gastric adenocarcinoma Ovarian cancer	Neovii Biotech AGO Study Group AIO-Studien-gGmbH Grupo Espanol de Investigacion en Cancer de Ovario
				Phase-2 (NCT00189345)		
				Phase-2 (NCT01504256) Phase-2 (NCT01246440)		
Ertumaxomab	Triomab	Quadroma	HER2 × CD3	Phase-1/2 (NCT01569412)	Her2/Neu ⁺ advanced solid tumor Advanced metastatic breast cancer	Krankenhaus Nordwest Neovii Biotech
				Phase-2 (NCT00351858)		
				Phase-2 (NCT00452140)		
FBTA05	Triomab	Quadroma	CD20 × CD3	Phase-1/2 (NCT01138579)	CLL	Technische Universitat Munchen
RO695688	Crossmab	Knobs-in-holes (KiH)	CEA × CD3	Phase-1 (NCT02324257)	Advanced metastatic CEA ⁺ solid tumors	Hoffmann-La Roche
RO5520985	Crossmab	KiH	Ang2 × VEGFA	Phase-1 (NCT01688206)	Advanced or metastatic solid tumors	Hoffmann-La Roche
RO5520985	Crossmab	KiH	Ang2 × VEGFA	Phase-2 (NCT01688206) Phase-2 (NCT02484690)	Advanced or metastatic solid tumors AMD	Hoffmann-La Roche Hoffmann-La Roche
RG7813	scFv-IgG	NA	CEA × IL-2	Phase-1 (NCT02004106)	Advanced metastatic CEA ⁺ solid tumors	
MM-141	scFv-IgG	NA	IGF × HER3	Phase-1 (NCT01733004) Phase-2 (NCT02399137)	Advanced solid tumor Metastatic pancreatic cancer	Merrimack Pharmaceuticals Merrimack Pharmaceuticals
MOR209/ES414	scFv-IgG	NA	PSMA × CD3	Phase-1 (NCT02262910)	Metastatic prostate cancer	Aptevo Therapeutics
LY3164530	Ortho-Fab IgG	Structural optimization	MET × EGFR	Phase-1 (NCT02221882)	Metastatic neoplasm	Eli Lilly and Company
ALX-0061	Nanobody	NA	IL-6R × HSA	Phase-2 (NCT01284569)	Rheumatoid arthritis	Ablynx
ATN-103	Nanobody	NA	TNF × HSA	Phase-2 (NCT01063803)	Rheumatoid arthritis	Ablynx
Blinatumomab	Bispecific T-cell engager BiTE	NA	CD3 × CD19	Approved by Food and Drug Administration Phase-1 (NCT00274742) Phase-2 (NCT01207388) Phase-2 (NCT01209286) Phase-1 (NCT02568553) Phase-2 (NCT02143414) Phase-3 (NCT02003222)	ALL Relapsed NHL Residual ALL Relapsed/refractory ALL Relapsed NHL ALL BCR-ABL ^{-/-} B-cell lineage ALL	Amgen GmbH Amgen GmbH Amgen GmbH Amgen GmbH National Cancer Institute National Cancer Institute National Cancer Institute
Solitomab	BiTE	NA	CD3 × EpCAM	Phase-1 (NCT00635596)	Advanced solid tumors	Amgen GmbH
AMG330	BiTE	NA	CD33 × CD3	Phase-1 (NCT02520427)	AML	Amgen GmbH

(Continued)

TABLE 2 | Continued

Format	Strategy	Target	Clinical development phase	Disease	Company
bsAb/bsAb Fragment					
MT112 (BAY2010112)	BITE	NA	PSMA × CD3	Phase-1 (NCT01723475)	Castration resistant prostate cancer
MT111 (MED1-565)	BITE	NA	CEA × CD3	Phase-1 (NCT01284231)	Advanced gastrointestinal adenocarcinoma
AFM11	Tandab diabody (Tandab)	NA	CD19 × CD3	Phase-1 (NCT02106091)	CD19+ B-cell NHL
AFM13	Tandab	NA	CD30 × CD16A	Phase-2 (NCT02321592)	Relapsed/refractory Hodgkin's lymphoma
rM28	Tandab	NA	CD28 × MAPG	Phase-2 (NCT00204594)	Metastatic melanoma
MGD006	Dual-affinity-retargeting (DART)	NA	CD3 × CD123	Phase-1 (NCT02152956)	Relapsed/refractory AML
MGD007	DART	NA	CD3 × gpA33	Phase-1 (NCT02248805)	Metastatic colorectal carcinoma
MGD010	DART	NA	CD32B × CD79B	Phase-1 (NCT02376036)	Healthy subjects

Abbreviations: CLL, chronic lymphocytic leukemia; AML, age-related macular degeneration; CEA, carcinoembryonic antigen; ALL, acute lymphocytic leukemia; NHL, non-Hodgkin's lymphoma; AML, acute myeloid leukemia; NA, information not available.
Source: <https://clinicaltrials.gov/ci2/home>.

93% success rate (75). More recently, Leaver-Fay and coworkers (76) furthered the multistate design strategy by construction of a negative state pool across the CH3 interface *via* protein docking and sequence design. Several novel mutants were discovered to favor the formation of Fc heterodimerization with a purity of more than 90% (76). In combination with the orthogonal Fab interface, four fully bsIgs could be correctly formed with an average success rate of more than 93% in one-step process (76).

CH1–CK heterodimeric scaffold can be used to build bispecific molecules (77, 78). However, it is known that the CH1–CK pair alone is not strong enough to form a stable heterodimer and CH1–CK pair requires cooperation from VH–VL pair for a stable heterodimer assembly (79, 80). To improve the CH1–CK heterodimerization in the absence of VH–VL pair cooperation, Chen et al. employed structure-based design in combination with phage display directed evolution (81). They identified that a S66V mutation in the CH1 domain together with a S69L in the CK domain can stabilize CH1–CK heterodimerization and increase the *in vivo* serum half-life of a previously described CD4-antibody fusion protein (4Dm2m), which targets the CD4-induced (CD4i) coreceptor binding site of the human immunodeficiency virus (HIV) 1 envelope glycoprotein 120 (81–84). It seems that this CH1–CK stabilization may increase the overall stability of 4Dm2m and thus improve its pharmacokinetics. Moreover, the strengthened CH1–CK heterodimerization may pave the way for construction of bispecific molecules based on this scaffold (81).

BIOCHEMICAL OPTIMIZATION

A structure and sequence guided approach identified low energy amino acid pairs in the CH3 domain, which could promote heterodimer formation (54). These mutations were engineered into the design of a new library, which increased the heterodimer yield up to 89%. The strategy was applied to either Fc/single-chain Fv-Fc fusion (scFv-Fc) or scFv-Fc formats utilizing two different CH3 domains favoring heterodimer formation to generate CD16 × HER2 bispecific, which exhibited improved antitumor attributes against the breast cancer cell line SKBr3 in the presence of CD16⁺ natural killer (NK) cells from human peripheral blood mononuclear cells (PBMCs) (54).

In another approach, Strop et al. (55) developed bispecific IgG1 and IgG2 antibodies by oxidation/reduction methodology for chain pairing. They described bispecific mutations (K409 and L368) in the CH3 domain, which allowed the development of bsIg either by coexpressing monomers bearing common light chains or by mixing the purified monomers under mild reducing conditions. Highest bispecificity was achieved by complementing K409/L368 with either IgG1-hinge or IgG2-hinge mutations (55). A CD3 × CD20 bsIg so generated showed *in vitro* cytotoxicity against mouse B-cell lymphoma in the presence of freshly isolated mouse primary T cells. Further, the bsIg mediated a dose-dependent lysis of target cells and also depleted CD20⁺ B cells *in vivo* by T-cell engagement (55).

A similar concept to generate IgG1 bispecific molecules was applied by Labrijn et al. (56). They incorporated a P228S hinge mutation which makes bonds more susceptible to cleavage under reducing conditions and additional mutations in separate human

IgG1-CH3 domains to promote Fab-arm exchange. Two mutated antibodies in IgG1 format (anti-EGFR and anti-CD20) were expressed separately and then mixed together in the presence of reducing agent, which resulted in 96% efficient Fab-arm exchange (**Figure 1K**) (56). The bispecific molecules so generated were stable at 5°C for over a period of 6 months and had comparable pharmacokinetics to their parent antibodies. A dual targeting CD3 × HER2 bispecific IgG1 was also constructed and showed a great enhancement in the T cell-mediated cytotoxicity against breast adenocarcinoma cells (AU565) in comparison to control antibody and *in vivo* tumor growth inhibition in an adoptive transfer xenograft model of gastric carcinoma with freshly prepared human PBMCs (56).

ELECTROSTATIC OPTIMIZATION

Gunasekaran et al. (59) exploited charged pair based attraction/repulsion in different Fc chains in the scFv-Fc format (**Figure 1L**). They identified conserved oppositely charged residues in the CH3-CH3 domain interface (D356-K439', E357-K370', K392-D399', and D399-K409'). Among these, the D399-K409' pair is buried and contributes to CH3-CH3 interaction. Mutations in these key residues (K409D-D399'K, K409D-D399'R, K409E-D399'K, and K409E-D399'R) favored greater than 90% heterodimer formation (59). The strategy was applied to generate a CD3 × TARTK bsAb and shown to kill U87-TARTK⁺ human glioma cell line by CD3 ligation in the presence of human PBMCs (59).

Similarly, Choi et al. (60) substituted conserved and charged amino acids from the core of the CH3 domain with hydrophobic residues to perturb the structural symmetry and designed long-range electrostatic attraction at the edge of the CH3 domain to promote heterodimer formation. A “W-VT” CH3 mutant pair (K409W and D399'V/F405'T) and “ER” CH3 mutant pair (K360E and Q347'R) accounted for 77 and 53% heterodimer species, respectively. This was attributed to the disruption of electrostatic and hydrophobic interactions and increased steric hindrance due to the K409W-F405'T mutations (60). Further, the combination of W-VT and ER mutant increased heterodimer formation up to 91%, enhanced binding to FcRn and imparted parent-like thermal stability. The “ERW-VT” mutant was used to generate MET × VEGFR-2 bispecific scFv (bscFv)-Fc, which bound more strongly to HUVEC cells and inhibited cell growth and VEGF/HGF-mediated ERK/AKT signaling. The MET × VEGFR-2 bsAb induced a twofold greater reduction in tumor volume in MKN45 human gastric cancer xenograft models compared to parent antibodies (60).

Subsequently, Fc heterodimer mutants were isolated based on displayed (CH3A) or secreted (CH3B) yeast libraries from either W-VT mutant or wild-type Fc incorporating K370-E357'/S364' or D399-K392'/K409' interaction pairs. The haploid yeast cells carrying individual libraries upon mating resulted in a diploid cell harboring both Fc variants, which if heterodimerized were displayed on the cell surface (61). In addition, these Fc variants carried C228S/C231S mutations to prevent homodimer formation and N297Q to avoid hypermannosylation in yeast (61).

Further, structure-guided design assisted with the computational algorithm and optimized energy function in between the partner chains were used to improve biophysical properties of bsIg molecules. Identified mutations [ZW1—Chain A (T350V/L351Y/F405A/Y407V) and Chain B (T350V/T366L/K393L/T394W)], which favor pure heterodimer formation (95%) and stability comparable to the wild-type Fc, were applied to create bispecific molecules (62). These mutations greatly improved the stability of the heterodimer when exposed to heat, acid, base, agitation, oxidation, freeze-thaw, and varying pH (62).

Electrostatic interactions were also optimized for the correct pairing of the heavy chain and its cognate light chain when coexpressed in the same cell. To achieve this, structure-guided mutations were made by replacing polar or hydrophobic residues of the CH1-CL and VH-VL interfaces with charged amino acids. These mutations promoted correct pairing of the heavy and light chains due to the maximization of electrostatic interactions over H-bonding and Van der Waals forces. The HER2 × EGFR bsIg induced a greater receptor internalization than achieved by the combination of parental antibodies and, furthermore, exhibited enhanced capability to inhibit BXPC-3, PANC-1, and Calu-3 tumors in xenograft models (57).

CONCEPTUAL ADVANCES

Davis et al. (85) exploited the sequence diversity in CH3 domains of IgG and IgA (~47% diverse in humans) and proposed that if diverse patches of IgG and IgA CH3 domains are mutually replaced then they can be heterodimerized (85). This strategy resulted in a unique complementarity among the CH3-CH3 interface. It was experimentally shown by constructing a strand-exchange engineered domain body (SEEDbody) fusion protein [IgG1-hinge-CH2-(SEED-IgA-CH3)], which preferentially associated into heterodimers (85–95%) (85). Depending on the patched sequence, these molecules were referred to as either AG or GA SEED. Further, novel SEEDbodies (**Figure 1M**) retained normal FcRn and protein A binding due to a specific motif introduced from IgG into the IgA. The major advantage of SEEDbody is to engineer additional specificity *via* scFv fused to the N-terminus of the SEEDbody, which overcomes the faulty light chain pairing (85).

Antibody scaffolds have also been used to develop bispecific pharmacophore fusions “COVX-Bodies” by chemical optimization of bsAbs (86). The principle involved here is to chemically link two pharmacophore peptides *via* branched azetidinone linker followed by an irreversible site-specific covalent fusion to the scaffold antibody. The azetidinone linker interacts with the K94 of Ig heavy chain and establishes an amide bond with the antibody. For example, a humanized IgG1κ aldolase antibody has been used as a scaffold for monovalent display of anti-VEGF and anti-Ang2 peptide pharmacophores to develop a monovalent bispecific COVX-241 (86). The bispecific COVX-241 inhibited VEGF-VEGFR2/Ang2-Tie2 interactions and further exhibited an improved efficacy against colon adenocarcinoma xenograft model as compared to the monospecific COVX-body (86).

Another methodology to develop bsAbs was proposed by Wranik et al. (87), which employed a common light chain and leucine zipper (LUZ-Y) (**Figure 1N**). They demonstrated

heterodimer assembly by creating a point mutation and the addition of a leucine zipper at the heavy chain C-terminus (87). Further, K222A substitution was made in the hinge region to avoid Lys-C endopeptidase-mediated cleavage if used for removing leucine zipper through C-terminal lysine of the CH3 domain. The light chain (VL-CL) was fused to the N-terminus of the heavy chain construct by a non-cleavable linker. However, the leucine zipper did not completely prevent homodimer formation, as an outcome of disproportionate expression in CHO cells most probably due to an incorrect DNA ratio during the transfection (87). Two armed LUZ-Y bispecific molecules hFc ϵ RI α × hFc γ RIIb showed desirable binding to respective targets and inhibited histamine release from hFc ϵ RI α /hFc γ RIIb $^+$ rat basophil leukemia cells when activated by IgE. Similarly, EGFR × HER3 bispecific LUZ-Y inhibited the growth of EGFR/HER3-dependent FaDu cells (87).

Bispecific IgG has also been assembled from a bacterial expression system. Half-IgG (one heavy and one light chain) molecule representing MET (hole mutant) and EGFR (knob mutant) specificities were expressed in bacterial cultures separately. The half-IgGs were purified by protein A affinity chromatography and analyzed to quantify monomeric form by size exclusion chromatography. Two half-IgGs were mixed in the presence of a reducing agent and subsequently oxidized to generate bsAb, which binds to the targets in a monovalent fashion (88). Similarly, a bacterial coculture of two strains expressing individual half-IgGs was shown to be the most rapid and efficient way to produce bsAbs (88). These bsAb molecules also inhibited MET × EGFR driven tumor growth (88).

In another effort, broadly neutralizing anti-HA1 (Ab-002) and HA2 (Ab-005) antibodies against influenza virus A were covalently linked by their C-termini. This methodology involved the fusion of a bacterial sortase recognition motif (LPETGG) via G₄S linker to the C-terminus of the IgG heavy chain. Click chemistry in the form of either cyclooctyne (DIBAC) or azide was used in the presence of sortase to promote covalent association of the two antibody molecules (89). Such covalently linked antibodies remained stable for up to 3 weeks at 37°C and also retained the Fc effector functions. These bispecific covalently linked IgGs contributed to an increased breadth of HA binding and antiviral potency as compared to the monospecific molecules (89).

Further, the light chain pairing was also used to generate bsIg molecules ($\kappa\lambda$ -bodies) (Figure 1O). This was achieved by coexpressing a single heavy chain with two light chains (κ and λ) through a single expression vector (63). It was presumed that 50% yield would be of $\kappa\lambda$ heterodimers. The strategy involved a three-step purification to separate (a) whole IgG fraction by protein A/CH1 resin, (b) κ light chain by kappa select resin, and (c) λ light chain by lambda select resin. Fed-batch culture yielded 1.5 g/L of total IgG with 41% being $\kappa\lambda$ heterodimer (63).

Smith et al. (58) used antibody isotype local chimeras to develop a bsAb that could trigger T cell-mediated B-cell killing. The rationale behind this approach was to exploit the differential protein A binding ability of antibody isotypes. It is known that IgG3 does not bind protein A and harbors a dipeptide Arg-Phe at the CH3 domain that corresponds to IgG1 H435 and Y436, respectively, while IgG1 can bind protein A with high affinity. Moreover, crystal structure of IgG1 in complex with protein A

confirms that H435 is involved in interaction with protein A (90). Fc substitutions (H435R, Y436F) were created in anti-CD3 antibody to develop CD3 × CD20 bsAb using a common light chain. Such isotype local chimeras exhibited asymmetric binding to protein A, which was exploited for separation of heterodimers by a pH gradient (58). The yield of the bispecific CD3 × CD20 IgG1 (REGN2280) was 43%. The IgG4 isotype of CD3 × CD20 (REGN1979) exhibited T cell-mediated cytotoxicity against CD20 $^+$ Raji lymphoma and inhibited the growth of Raji lymphoma cells in NOD SCIDy (NSG) mice when injected along with the human PBMCs (58).

bsAb FRAGMENTS FOR T CELL AND NK CELL ACTIVATION

Besides the different formats of full-length bsAb design, significant effort has also been invested on bsAb fragment designs that lack Fc region or only contain some constant domains. The building blocks of bsAb fragments include nanobodies, human single-domain antibodies, scFvs, and Fabs (18). More than 25 bsAb fragment formats have been documented, and most formats currently under clinical trial for treatment of different tumors involve bridging immune effector T cell (CD3 as the antigen) toward tumor specific antigens (18).

Blinatumomab, the first bsAb fragment and second bispecific molecule approved for therapy, is a bispecific T-cell engager (BiTE) molecule (Figure 1P; Table 2 for clinical status) that is built from two scFvs linked in tandem with a short peptide linker (64, 91). Blinatumomab uses one arm to recognize CD19, which is highly expressed on B-cell acute lymphocytic leukemia (ALL), and the other arm to recruit CD3, which is expressed on T cells, and induces a T-cell–tumor cell contact and potent lysis of tumor cell (64, 91, 92). Interestingly, the BiTE format of CD3 × CD19 bispecific antibody is superior to other formats including diabody (66) (Figure 1Q), tandem diabody (Tandab) (67, 68) (Figure 1R) and quadroma in terms of T cell-mediated tumor cell lysis (93). This finding highlights that the relative orientation and distance between the two scFvs may have significant impacts on how to bridge T cell and tumor cell into close contact so as to trigger T cell-mediated tumor cell lysis. Currently, several bispecific antibody fragments based on BiTE, Tandab, and dual-affinity-retargeting (Figure 1S) (69) formats are under clinical trials involving CD3 and tumor related antigens (18, 94) (Table 2).

Effects of bsAb fragments capable of interacting with NK cells via CD16 have also been investigated. Gleason and coworkers demonstrated the enhanced efficacy of bscFv CD16 × CD19 and trispecific scFv CD16 × CD19 × CD22 constructs in targeting tumor cells by coengaging NK cell effector function (70). These molecules were termed as bispecific and trispecific killer cell engagers (BiKEs and TriKEs) (Figures 1T,U), respectively. Such molecules are constructed by linking specific binders together through a short linker derived from human muscle aldolase. Further, a BiKE construct against CD16 and CD33 has been shown to activate CD16 $^+$ NK cells to lyse CD33 $^+$ HL60 target cells (71). Recently, a TriKE construct with additional specificity against IL-15 induced enhanced NK cell cytotoxicity, degranulation, and cytokine production against CD33 $^+$ HL60 cells via

increased NK cell proliferation and survival (72). Reusch et al. designed a Tandab-based anti-CD16A × CD30 bispecific tetravalent fragment and found that this format is better than normal monoclonal anti-CD30 IgG, optimized monoclonal anti-CD30 IgG for Fc γ R binding, and diabody (bispecific and bivalent anti-CD16A and anti-CD30) formats in triggering NK cell lysis of Hodgkin lymphoma cells (CD30 as the antigen) (95, 96). This format of anti-CD16A × CD30 bispecific fragment (known as AFM13) is under phase-2 clinical trial (**Table 2**) for treatment of refractory or relapsed Hodgkin lymphoma patients (97).

MONOMERIC Ig SCAFFOLDS

Much work in the last 5 years has focused on engineering the IgG constant domains as scaffolds. The IgG-Fc region and isolated CH domains have shown promising virtues in terms of small size, antigen targeting, effector function, and serum half-life.

Soluble monomeric Fc (mFc) was developed by destabilizing the CH3–CH3 domain interface. A phage-displayed library was constructed with random mutations introduced within seven key residues known to be involved in CH3 domain homodimerization and selected against binding of protein G first to enrich well-folded mutants and then against human FcRn (16). The selected clones were diverse in their CH3 domain, and monomer promoting mutations were identified (16). These variants with each containing six to seven mutations had considerably lower melting temperature but exhibited comparable stabilities and pH-dependent FcRn binding profiles to that of dimeric Fc (16). The experimental conceptualization was proved by mFc67.3–m36VH fusion (**Figure 1V**) targeting HIV-1 envelope glycoprotein (ENV) and neutralization of viral isolates (16). Based on the identified mFc mutants, the same group (98) optimized mFc to generate mutants with fewer mutations and improved thermostability while maintaining similar pH-dependent FcRn binding as that of wild-type Fc dimer. Interestingly, the new mFc mutants when expressed either in bacteria or mammalian cells all showed selective binding to only Fc γ RI but not to other receptors including Fc γ RIIa, Fc γ RIIb, Fc γ RIIIa, and C1q (98). This selectivity attractively made the mFc mutant as a potential carrier to treat chronic inflammatory diseases where inflammatory macrophages showed increased expression of Fc γ RI (98–103). In addition, this selectivity also excluded unwanted cytotoxicities such as ADCC from Fc γ RIIIa and CDC from C1q (98).

In another strategy to keep Fc in a monomeric form, asparagine-linked glycan structures were engineered into the CH3–CH3 interface of IgG1 Fc lacking the hinge (104). A mutant incorporating N-glycosylation sites (asparagine at positions 364 and 407) yielded a stable, soluble, and mFc scaffold with wild-type-like FcRn binding activity, which suggests that N-glycosylation promotes functional monomeric state and improves the biophysical characteristics (104).

Smaller scaffolds like CH2 domains also possess interesting properties like a properly folded structure, conformational flexibility, lesser propensity to dimerize, and associated FcRn/C1q binding functions, which can have therapeutic benefits (103, 105). A CH2 domain variant (m01) harboring disulfide bond mutations (L12C and K104C) was found to exist solely as a monomer

and remained thermally more stable than native counterparts (105). Further, 50% of monomeric CH2 unfolded at a urea concentration of 6.8 M as compared to 4.8 M for the wild-type CH2 (105). The biophysical attributes of the CH2 domain (m01) were further optimized by developing a shorter version where the unstructured random coil at the N-terminus was shortened by seven residues (m01s) (106). This strategy increased the melting temperature of CH2 isolate up to 82.6°C, enhanced stability in serum and mediated stronger binding to soluble FcRn (106). Similarly, a structure-guided design allowed the engineering of an IgG1-CH3 FcRn recognition motif into the CH2 scaffold to impart enhanced pH-dependent FcRn binding, prolongation of serum half-life, and epithelial transcytosis in comparison to parent CH2 isolate (m01s) (107).

Antigen recognition activity was engineered in CH2 scaffolds carrying mutations in the BC and FG loops by selecting against the HIV-1 envelope glycoprotein (gp120)–CD4 complex (15), which yielded CH2 fragments bearing the same BC but different FG loops, suggesting the importance of the latter in such interactions. One such isolate (m1a1) specifically recognized a highly conserved CD4i epitope on the HIV-1 gp120 protein and neutralized HIV-1 isolates in a cell based pseudovirus assay (15). In another approach, a randomly selected VH domain targeting the HIV-1 gp41 protein was grafted into the BC/FG loops of “m01s” without affecting the flanking regions to develop antigen targeting CH2 domains (m2a1) (108). This domain bound to sp62 peptide of HIV-1 envelope membrane-proximal external region, neutralized HIV-1 isolates, and showed pH-dependent FcRn interaction (108).

Initial success with the mFc and CH2 domains prompted the development of a monomeric CH3 (mCH3) scaffold (103, 109). The seven contact residues of the CH3 domain from the previously reported mFc molecules (16) were mutated, and a combination of mutations was found to be required for CH3 monomer to exist (109). These mutations were responsible for stronger intermolecular hydrophobic interactions, which resulted in an intact, folded and thermally stable CH3 monomer (109). The mCH3 scaffold exhibited significant binding to FcRn and protein G (109). Furthermore, mCH3 fused to a VH domain of an HIV-1 targeting antibody (m36.4) showed satisfactory stability, viral neutralization, and pH-dependent FcRn binding (109). A comparative analysis between the dimeric and monomeric scaffolds has demonstrated increased solubility, comparable serum stability, and higher pH-dependent FcRn binding by monomers (103). These properties make antibody scaffolds promising potential therapeutic candidates.

Fc ANTIGEN-BINDING FRAGMENT

The Fc has also been developed as an antigen-binding domain “Fcab” (**Figure 1W**) by imparting specificity against antigens through yeast surface display (110). The AB and EF loops of IgG1-CH3 domain were randomly mutagenized, cloned into a yeast surface display vector, and selected against HER2/neu extracellular domain (ECD) for two rounds. The selected binders were again randomized in the AB loop and selected on HER2/neu ECD. One of the isolated Fcab molecules (H10-03-6) showed

specificity for binding to HER2, retained binding to Fc γ RI/protein A, and exhibited an *in vivo* pharmacokinetics profile similar to the native human Fc (110). Post-affinity maturation, Fcab exhibited ~10-fold enhanced binding to the antigen as compared to the parental molecule and elicited NK cell-mediated cytotoxicity *in vitro* against the breast cancer cell line Calu-3, but the potency was ~20-fold weaker than that of Herceptin (110).

Introducing antigen-binding ability into the Fc fragment could compromise stability, and therefore, additional disulfide bonds were engineered within the CH3 domain to provide increased stability (111). Further, these mutations did not affect pH-dependent FcRn binding, which suggests the correct folding of the engineered Fc fragments (111). Similarly, immune modulating activity of Fcab was demonstrated using a HER2 targeting Fcab (HAF3–4), bearing CD16a modulating mutations (111). Both mutants showed binding to the recombinant or cell surface expressed HER2 and had an expected CD16a modulating behavior which correlated with the ADCC potency (111). Later, Woisetschläger and coworkers (112) showed the *in vivo* tumor reduction efficacy of anti-HER2 Fcab (H10-03-6) by simultaneous engagement of the HER2/CD16a and the involvement of ADCC (112).

Since antigen–antibody interaction at an acidic pH can negatively affect drug pharmacokinetics, anti-HER2 Fcab (H10-03-6) variants with weaker binding at pH 6.0 were developed (113). The residues in the AB and EF loops were randomized and selected against HER2-ECD alternately at pH 7.4 and 6.0 using yeast display. The isolated binders exhibited lower affinity at an acidic pH and similarly engaged HER2 $^{+}$ cells in a pH-dependant manner (113). A year later, Leung et al. (114) developed Fcab that could degrade HER2 and induce apoptosis. The AB and EF loop residues of IgG-Fc were randomly mutagenized and selected *via* yeast display for binding to HER2-ECD. After affinity maturation, the candidate Fcab (FS102) exhibited an affinity for HER2-ECD that was equivalent to that of pertuzumab and trastuzumab and an extended serum half-life comparable to the native Fc (114). Further, EC₅₀ values of 1.1 and 3.3 nM were observed against SKBr3 and HCC1954 breast cancer cells, respectively, and a complete tumor regression was shown using HER2 $^{+}$ patient-derived colorectal/gastric cancer xenografts (114). This effect correlated with caspase 3/7 activation in SKBr3 cells in a dose-dependent manner indicating the induction of tumor cell apoptosis (114).

CHALLENGES IN CLINICAL DEVELOPMENT OF bsAbs AND FRAGMENTS

Smaller antibody fragments (nanobody, human single-domain Ab, scFv, or Fab) and bsAb fragments offer a number of advantages over full-length IgG, including ability to penetrate tissue, cost effective and facile manufacturing methods, and high yields (23, 115). However, their small size leads to a shorter serum half-life, lesser tissue retention, and rapid clearance from the blood through kidneys. This is true for blinatumomab, which has a serum half-life of around 2 h while the serum half-life of full-length IgG1 is around 2–3 weeks. Thus, patients need a regimen

of at least 3-cycle treatment with each cycle consisting of continuous infusion for 4 weeks in a cycle of 6 weeks (116). On the other hand, the fast clearance of small size bsAb fragments may be desirable in imaging and radioimmunotherapy (117, 118).

Specific approaches can be used to increase the longevity of small bsAb fragments in blood and tissue by (1) fusion of the Fc region of IgG molecules or human serum albumin to prolong the serum half-life. These fusions not only increase molecular size of bsAb fragments and therefore protect them from being excreted out of the body but also mediate binding to the FcRn expressed on the endothelial cells to enter IgG serum stabilization pathway (25, 119–121); (2) multimerization of antibody fragments to increase the molecular size for stabilizing concentration in blood and enhancing the valency of antigen binding (120, 122). The multimerization approach, however, runs a risk of imparting heterogeneity to the molecule and can also lead to undesirable effects by crosslinking of the target receptor (120); and (3) linking of a hydrophobic molecule like polyethylene glycol, a clinically proven technology for serum half-life extension (120, 123). Besides, other polymers like polysialic acid, N-(2-hydroxypropyl) methacrylamide, and dextran can also provide protection to the small antibody fragments (25, 120).

Currently, there are more than 60 bsAb formats (18). Of note, the success story of blinatumomab in the format of BiTE, but not in other formats including diabody, Tandab, and quadroma indicates that bispecific molecule design has to consider more than one format from the beginning (93). Moreover, expression and purification of these variable formats require tailored procedures based on each design. This may pose a great challenge in developing bispecific molecules. **Table 1** summarizes relevant information from available literatures.

FINAL REMARKS

Considerable progress has been made in the development of bispecific molecules based on different scaffolds in recent years. Much of this understanding has made it possible to enter an era of bispecific clinical development with two such molecules (catumaxomab and blinatumomab) having been approved for clinical use in humans (18). The field of bsAbs has been evolutionary and revolutionary, which is reflected in our ability to obtain 100% pure heterodimers, the complete evasion of heavy and light chain mispairing, fairly standardized production/purification/analytical methods and, importantly, clear ideas of their potential applications.

The full-length mAbs have relatively poor tissue penetration ability. In contrast, smaller antibody fragments like BiTE, BiKE, and TriKE can effectively penetrate tumor tissue and efficiently recruit and activate immune effector cells to lyse tumor cells (23, 70, 93, 115). Besides, the recent success in delivering a bsIg across the blood–brain barrier by targeting transferrin receptor and β -secretase to reduce brain amyloid- β in non-human primate model may open the era of specific antibody brain delivery and treatment of neurodegenerative diseases (124). In another possibility, combining non-antibody small fragments such as lambody, affibody, and aptamer with current antibody scaffolds may expand the treatment arsenal of bispecific molecules.

Moreover, monomeric Ig domain scaffold and Fcab are potent new formats to target difficult to reach sites in the body and to add additional antigen specificity along with enhanced stability, effector function, and extended serum half-life. These properties make them suitable for clinical validation.

In the future, bispecific molecules based on various scaffolds will represent an indispensable class of therapeutic options to treat a variety of clinical indications. However, efforts to improve production and purification on an industrial scale must continue to ensure harvesting of the full benefits of these entities.

REFERENCES

- Ecker DM, Jones SD, Levine HL. The therapeutic monoclonal antibody market. *MAbs* (2015) 7:9–14. doi:10.4161/19420862.2015.989042
- Henry HC. Therapeutic monoclonal antibodies approved by FDA in 2015. *MOJ Immunol* (2016) 3:00087. doi:10.15406/moji.2016.03.00087
- Schroeder HW Jr, Cavacini L. Structure and function of immunoglobulins. *J Allergy Clin Immunol* (2010) 125:S41–52. doi:10.1016/j.jaci.2009.09.046
- Igawa T, Tsunoda H, Kuramochi T, Sampei Z, Ishii S, Hattori K. Engineering the variable region of therapeutic IgG antibodies. *MAbs* (2011) 3:243–52. doi:10.4161/mabs.3.3.15234
- Duncan AR, Winter G. The binding site for C1q on IgG. *Nature* (1988) 332:738–40. doi:10.1038/332738a0
- Ghetie V, Ward ES. Multiple roles for the major histocompatibility complex class I-related receptor FcRn. *Annu Rev Immunol* (2000) 18:739–66. doi:10.1146/annurev.immunol.18.1.739
- Idusogie EE, Presta LG, Gazzano-Santoro H, Totpal K, Wong PY, Ultsch M, et al. Mapping of the C1q binding site on rituxan, a chimeric antibody with a human IgG1 Fc. *J Immunol* (2000) 164:4178–84. doi:10.4049/jimmunol.164.8.4178
- Jefferis R, Lund J, Pound JD. IgG-Fc-mediated effector functions: molecular definition of interaction sites for effector ligands and the role of glycosylation. *Immunol Rev* (1998) 163:59–76. doi:10.1111/j.1600-065X.1998.tb01188.x
- Jung ST, Kang TH, Kelton W, Georgiou G. Bypassing glycosylation: engineering glycosylated full-length IgG antibodies for human therapy. *Curr Opin Biotechnol* (2011) 22:858–67. doi:10.1016/j.copbio.2011.03.002
- Kim JK, Tsen MF, Ghetie V, Ward ES. Localization of the site of the murine IgG1 molecule that is involved in binding to the murine intestinal Fc receptor. *Eur J Immunol* (1994) 24:2429–34. doi:10.1002/eji.1830241025
- Lund J, Winter G, Jones PT, Pound JD, Tanaka T, Walker MR, et al. Human Fc gamma RI and Fc gamma RII interact with distinct but overlapping sites on human IgG. *J Immunol* (1991) 147:2657–62.
- Park HI, Yoon HW, Jung ST. The highly evolvable antibody Fc domain. *Trends Biotechnol* (2016) 16:30024–5. doi:10.1016/j.tibtech.2016.04.005
- Sondermann P, Szymkowski DE. Harnessing Fc receptor biology in the design of therapeutic antibodies. *Curr Opin Immunol* (2016) 40:78–87. doi:10.1016/j.coim.2016.03.005
- Saxena A, Wu D. Advances in therapeutic Fc engineering – modulation of IgG-associated effector functions and serum half-life. *Front Immunol* (2016) 7:580. doi:10.3389/fimmu.2016.00580
- Xiao X, Feng Y, Vu BK, Ishima R, Dimitrov DS. A large library based on a novel (CH2) scaffold: identification of HIV-1 inhibitors. *Biochem Biophys Res Commun* (2009) 387:387–92. doi:10.1016/j.bbrc.2009.07.044
- Ying T, Chen W, Gong R, Feng Y, Dimitrov DS. Soluble monomeric IgG1 Fc. *J Biol Chem* (2012) 287:19399–408. doi:10.1074/jbc.M112.368647
- Kontermann RE, Brinkmann U. Bispecific antibodies. *Drug Discov Today* (2015) 20:838–47. doi:10.1016/j.drudis.2015.02.008
- Spiess C, Zhai Q, Carter PJ. Alternative molecular formats and therapeutic applications for bispecific antibodies. *Mol Immunol* (2015) 67:95–106. doi:10.1016/j.molimm.2015.01.003
- Castoldi R, Jucknische U, Pradel LP, Arnold E, Klein C, Scheiblich S, et al. Molecular characterization of novel trispecific ErbB-cMet-IGF1R antibodies and their antigen-binding properties. *Protein Eng Des Sel* (2012) 25:551–9. doi:10.1093/protein/gzs048
- Nuñez-Prado N, Compte M, Harwood S, Álvarez-Méndez A, Lykkenmark S, Sanz L, et al. The coming of age of engineered multivalent antibodies. *Drug Discov Today* (2015) 20:588–94. doi:10.1016/j.drudis.2015.02.013
- Köhler G, Milstein C. Continuous cultures of fused cells secreting antibody of predefined specificity. *Nature* (1975) 256:495–7. doi:10.1038/256495a0
- Milstein C, Cuello AC. Hybrid hybridomas and their use in immunohistochemistry. *Nature* (1983) 305:537–40. doi:10.1038/305537a0
- Chames P, Van Regenmortel M, Weiss E, Baty D. Therapeutic antibodies: successes, limitations and hopes for the future. *Br J Pharmacol* (2009) 157:220–33. doi:10.1111/j.1476-5381.2009.00190.x
- Heiss MM, Murawa P, Koralewski P, Kutarska E, Kolesnik OO, Ivanchenko VV, et al. The trifunctional antibody catumaxomab for the treatment of malignant ascites due to epithelial cancer: results of a prospective randomized phase II/III trial. *Int J Cancer* (2010) 127:2209–21. doi:10.1002/ijc.25423
- Fan G, Wang Z, Hao M, Li J. Bispecific antibodies and their applications. *J Hematol Oncol* (2015) 8:130. doi:10.1186/s13045-015-0227-0
- Lindhofer H, Mocikat R, Steipe B, Thierfelder S. Preferential species-restricted heavy/light chain pairing in rat/mouse quadromas. Implications for a single-step purification of bispecific antibodies. *J Immunol* (1995) 155:219–25.
- Atwell S, Ridgway JB, Wells JA, Carter P. Stable heterodimers from remodeling the domain interface of a homodimer using a phage display library. *J Mol Biol* (1997) 270:26–35. doi:10.1006/jmbi.1997.1116
- Merchant AM, Zhu Z, Yuan JQ, Goddard A, Adams CW, Presta LG, et al. An efficient route to human bispecific IgG. *Nat Biotechnol* (1998) 16:677–81. doi:10.1038/nbt0798-677
- Ridgway JB, Presta LG, Carter P. ‘Knobs-into-holes’ engineering of antibody CH3 domains for heavy chain heterodimerization. *Protein Eng* (1996) 9:617–21. doi:10.1093/protein/9.7.617
- Hamers-Casterman C, Atarhouch T, Muyldeermans S, Robinson G, Hamers C, Songa EB, et al. Naturally occurring antibodies devoid of light chains. *Nature* (1993) 363:446–8. doi:10.1038/363446a0
- Muyldeermans S. Nanobodies: natural single-domain antibodies. *Annu Rev Biochem* (2013) 82:775–97. doi:10.1146/annurev-biochem-063011-092449
- Wolfson W. Ablynx makes nanobodies from llama bodies. *Chem Biol* (2006) 13:1243–4. doi:10.1016/j.chembiol.2006.12.003
- Coppelters K, Dreier T, Silence K, de Haard H, Lauwereys M, Casteels P, et al. Formatted anti-tumor necrosis factor alpha VHH proteins derived from camelids show superior potency and targeting to inflamed joints in a murine model of collagen-induced arthritis. *Arthritis Rheum* (2006) 54:1856–66. doi:10.1002/art.21827
- Davies J, Riechmann L. Antibody VH domains as small recognition units. *Biotechnology (N Y)* (1995) 13:475–9. doi:10.1038/nbt0595-475
- van den Beucken T, van Neer N, Sablon E, Desmet J, Celis L, Hoogenboom HR, et al. Building novel binding ligands to B7.1 and B7.2 based on human antibody single variable light chain domains. *J Mol Biol* (2001) 310:591–601. doi:10.1006/jmbi.2001.4703
- Barthelemy PA, Raab H, Appleton BA, Bond CJ, Wu P, Wiesmann C, et al. Comprehensive analysis of the factors contributing to the stability and solubility of autonomous human VH domains. *J Biol Chem* (2008) 283:3639–54. doi:10.1074/jbc.M708536200
- De Bernardis F, Liu H, O’Mahony R, La Valle R, Bartollino S, Sandini S, et al. Human domain antibodies against virulence traits of *Candida albicans* inhibit

AUTHOR CONTRIBUTIONS

DW conceived the topic; DW, HL, and AS wrote the manuscript; HL and AS contributed equally in writing the manuscript; DW and SS revised the manuscript.

FUNDING

This work was supported by National Natural Science Foundation of China (Grant No.: 81572698) to DW.

- fungus adherence to vaginal epithelium and protect against experimental vaginal candidiasis. *J Infect Dis* (2007) 195:149–57. doi:10.1086/509891
38. Bird RE, Hardman KD, Jacobson JW, Johnson S, Kaufman BM, Lee SM, et al. Single-chain antigen-binding proteins. *Science* (1988) 242:423–6. doi:10.1126/science.3140379
 39. Huston JS, Levinson D, Mudgett-Hunter M, Tai MS, Novotny J, Margolies MN, et al. Protein engineering of antibody binding sites: recovery of specific activity in an anti-digoxin single-chain Fv analogue produced in *Escherichia coli*. *Proc Natl Acad Sci USA* (1988) 85:5879–83. doi:10.1073/pnas.85.16.5879
 40. Hong X, Ma MZ, Gildersleeve JC, Chowdhury S, Barchi JJ Jr, Mariuzza RA, et al. Sugar binding proteins from fish: selection of high affinity “lambodies” that recognize biomedically relevant glycans. *ACS Chem Biol* (2013) 8:152–60. doi:10.1021/cb300399s
 41. Hansson M, Ringdahl J, Robert A, Power U, Goetsch L, Nguyen TN, et al. An in vitro selected binding protein (affibody) shows conformation-dependent recognition of the respiratory syncytial virus (RSV) G protein. *Immunotechnology* (1999) 4:237–52. doi:10.1016/S1380-2933(98)00026-8
 42. Pestourie C, Tavitian B, Duconge F. Aptamers against extracellular targets for in vivo applications. *Biochimie* (2005) 87:921–30. doi:10.1016/j.biochi.2005.04.013
 43. Nimjee SM, Rusconi CP, Sullenger BA. Aptamers: an emerging class of therapeutics. *Annu Rev Med* (2005) 56:555–83. doi:10.1146/annurev.med.56.062904.144915
 44. Ronnmark J, Hansson M, Nguyen T, Uhlen M, Robert A, Stahl S, et al. Construction and characterization of affibody-Fc chimeras produced in *Escherichia coli*. *J Immunol Methods* (2002) 261:199–211. doi:10.1016/S0022-1759(01)00563-4
 45. Dickgiesser S, Rasche N, Nasu D, Middel S, Horner S, Avrutina O, et al. Self-assembled hybrid aptamer-Fc conjugates for targeted delivery: a modular chemoenzymatic approach. *ACS Chem Biol* (2015) 10:2158–65. doi:10.1021/acscchembio.5b00315
 46. Moldenhauer G. Bispecific antibodies from hybrid hybridoma. In: Kontermann RE, editor. *Bispecific Antibodies*. Berlin, Heidelberg: Springer (2011). p. 29–46.
 47. Schaefer W, Regula JT, Bähner M, Schanzer J, Croasdale R, Dürr H, et al. Immunoglobulin domain crossover as a generic approach for the production of bispecific IgG antibodies. *Proc Natl Acad Sci U S A* (2011) 108:11187–92. doi:10.1073/pnas.1019002108
 48. Schanzer JM, Wartha K, Croasdale R, Moser S, Künkele KP, Ries C, et al. A novel glycoengineered bispecific antibody format for targeted inhibition of epidermal growth factor receptor (EGFR) and insulin-like growth factor receptor type I (IGF-IR) demonstrating unique molecular properties. *J Biol Chem* (2014) 289:18693–706. doi:10.1074/jbc.M113.528109
 49. Metz S, Panke C, Haas AK, Schanzer J, Lau W, Croasdale R, et al. Bispecific antibody derivatives with restricted binding functionalities that are activated by proteolytic processing. *Protein Eng Des Sel* (2012) 25:571–80. doi:10.1093/protein/gzs064
 50. Elliott JM, Ultsch M, Lee J, Tong R, Takeda K, Spiess C, et al. Antiparallel conformation of knob and hole aglycosylated half-antibody homodimers is mediated by a CH2-CH3 hydrophobic interaction. *J Mol Biol* (2014) 426:1947–57. doi:10.1016/j.jmb.2014.02.015
 51. Xu Y, Lee J, Tran C, Heibeck TH, Wang WD, Yang J, et al. Production of bispecific antibodies in “knobs-into-holes” using a cell-free expression system. *MAbs* (2015) 1:231–42. doi:10.4161/19420862.2015.989013
 52. Mazor Y, Oganesyan V, Yang C, Hansen A, Wang J, Liu H, et al. Improving target cell specificity using a novel monovalent bispecific IgG design. *MAbs* (2015) 7:377–89. doi:10.1080/19420862.2015.1007816
 53. Zhao L, Xie F, Tong X, Li H, Chen Y, Qian W, et al. Combating non-Hodgkin lymphoma by targeting both CD20 and HLA-DR through CD20-243 CrossMab. *MAbs* (2014) 3:740–8. doi:10.4161/mabs.28613
 54. Moore GL, Bautista C, Pong E, Nguyen DH, Jacinto J, Eivazi A, et al. A novel bispecific antibody format enables simultaneous bivalent and monovalent co-engagement of distinct target antigens. *MAbs* (2011) 3:546–57. doi:10.4161/mabs.3.6.18123
 55. Strop P, Ho WH, Boustany LM, Abdiche YN, Lindquist KC, Farias SE, et al. Generating bispecific human IgG1 and IgG2 antibodies from any antibody pair. *J Mol Biol* (2012) 420:204–19. doi:10.1016/j.jmb.2012.04.020
 56. Labrijn AF, Meesters JI, de Goeij BE, van den Bremer ET, Neijissen J, van Kampen MD, et al. Efficient generation of stable bispecific IgG1 by controlled Fab-arm exchange. *Proc Natl Acad Sci USA* (2013) 110:5145–50. doi:10.1073/pnas.1220145110
 57. Liu Z, Leng EC, Gunasekaran K, Pentony M, Shen M, Howard M, et al. A novel antibody engineering strategy for making monovalent bispecific heterodimeric IgG antibodies by electrostatic steering mechanism. *J Biol Chem* (2015) 290:7535–62. doi:10.1074/jbc.M114.620260
 58. Smith EJ, Olson K, Haber LJ, Varghese B, Duramad P, Tustian AD, et al. A novel, native-format bispecific antibody triggering T-cell killing of B-cells is robustly active in mouse tumor models and cynomolgus monkeys. *Sci Rep* (2015) 5:17943. doi:10.1038/srep17943
 59. Gunasekaran K, Pentony M, Shen M, Garrett L, Forte C, Woodward A, et al. Enhancing antibody Fc heterodimer formation through electrostatic steering effects: applications to bispecific molecules and monovalent IgG. *J Biol Chem* (2010) 285:19637–46. doi:10.1074/jbc.M110.117382
 60. Choi HJ, Kim YJ, Lee S, Kim YS. A heterodimeric Fc-based bispecific antibody simultaneously targeting VEGFR-2 and Met exhibits potent anti-tumor activity. *Mol Cancer Ther* (2013) 12:2748–59. doi:10.1158/1535-7163.MCT-13-0628
 61. Choi HJ, Kim YJ, Choi DK, Kim YS. Engineering of immunoglobulin Fc heterodimers using yeast surface-displayed combinatorial Fc library screening. *PLoS One* (2015) 10:e0145349. doi:10.1371/journal.pone.0145349
 62. Von Kreudenstein TS, Escobar-Carbrera E, Lario PI, D’Angelo I, Brault K, Kelly J, et al. Improving biophysical properties of a bispecific antibody scaffold to aid developability: quality by molecular design. *MAbs* (2013) 5:646–54. doi:10.4161/mabs.25632
 63. Fischer N, Elson G, Magistrelli G, Dheilly E, Fouque N, Laurendon A, et al. Exploiting light chains for the scalable generation and platform purification of native human bispecific IgG. *Nat Commun* (2015) 6:6113. doi:10.1038/ncomms7113
 64. Löfler A, Kufer P, Lutterbuse R, Zettl F, Daniel PT, Schwenkenbecher JM, et al. A recombinant bispecific single-chain antibody, CD19 x CD3, induces rapid and high lymphoma-directed cytotoxicity by unstimulated T lymphocytes. *Blood* (2000) 95:2098–103.
 65. Mack M, Riethmüller G, Kufer P. A small bispecific antibody construct expressed as a functional single-chain molecule with high tumor cell cytotoxicity. *Proc Natl Acad Sci U S A* (1995) 92:7021–5. doi:10.1073/pnas.92.15.7021
 66. Holliger P, Prospero T, Winter G. “Diabodies”: small bivalent and bispecific antibody fragments. *Proc Natl Acad Sci U S A* (1993) 90:6444–8. doi:10.1073/pnas.90.14.6444
 67. Arndt MA, Krauss J, Kipriyanov SM, Pfreundschuh M, Little M. A bispecific diabody that mediates natural killer cell cytotoxicity against xenotransplanted human Hodgkin’s tumors. *Blood* (1999) 94:2562–8.
 68. Kipriyanov SM, Moldenhauer G, Schuhmacher J, Cochlovius B, Von der Lieth CW, Matys ER, et al. Bispecific tandem diabody for tumor therapy with improved antigen binding and pharmacokinetics. *J Mol Biol* (1999) 293:41–56. doi:10.1006/jmbi.1999.3156
 69. Johnson S, Burke S, Huang L, Gorlatov S, Li H, Wang W, et al. Effector cell recruitment with novel Fv-based dual-affinity re-targeting protein leads to potent tumor cytotoxicity and in vivo B-cell depletion. *J Mol Biol* (2010) 399:436–49. doi:10.1016/j.jmb.2010.04.001
 70. Gleason MK, Verneris MR, Todhunter DA, Zhang B, McCullar V, Zhou SX, et al. Bispecific and trispecific killer cell engagers directly activate human NK cells through CD16 signaling and induce cytotoxicity and cytokine production. *Mol Cancer Ther* (2012) 11:2674–84. doi:10.1158/1535-7163.MCT-12-0692
 71. Wiernik A, Foley B, Zhang B, Verneris MR, Warlick E, Gleason MK, et al. Targeting natural killer cells to acute myeloid leukemia in vitro with a CD16 x 33 bispecific killer cell engager and ADAM17 inhibition. *Clin Cancer Res* (2013) 19:3844–55. doi:10.1158/1078-0432.CCR-13-0505
 72. Valleria DA, Felices M, McElmurry R, McCullar V, Zhou X, Schmohl JU, et al. IL15 trispecific killer engagers (TriKE) make natural killer cells specific to CD33+ targets while also inducing persistence, in vivo expansion, and enhanced function. *Clin Cancer Res* (2016) 22:3440–50. doi:10.1158/1078-0432.CCR-15-2710

73. Song MK, Oh MS, Lee JH, Lee JN, Chung JH, Park SG, et al. Light chain of natural antibody plays a dominant role in protein antigen binding. *Biochem Biophys Res Commun* (2000) 268:390–4. doi:10.1006/bbrc.2000.2134
74. Persson H, Ye W, Wernimont A, Adams JJ, Koide A, Koide S, et al. CDR-H3 diversity is not required for antigen recognition by synthetic antibodies. *J Mol Biol* (2013) 425:803–11. doi:10.1016/j.jmb.2012.11.037
75. Lewis SM, Wu X, Pustilnik A, Sereno A, Huang F, Rick HL, et al. Generation of bispecific IgG antibodies by structure-based design of an orthogonal Fab interface. *Nat Biotechnol* (2014) 32:191–8. doi:10.1038/nbt.2797
76. Leaver-Fay A, Froning KJ, Atwell S, Aldaz H, Pustilnik A, Lu F, et al. Computationally designed bispecific antibodies using negative state repertoires. *Structure* (2016) 24:641–51. doi:10.1016/j.str.2016.02.013
77. Muller KM, Arndt KM, Strittmatter W, Pluckthun A. The first constant domain (C(H)1 and C(L)) of an antibody used as heterodimerization domain for bispecific minibodies. *FEBS Lett* (1998) 422:259–64. doi:10.1016/S0014-5793(98)00021-0
78. Allaway GP, Davis-Bruno KL, Beaudry GA, Garcia EB, Wong EL, Ryder AM, et al. Expression and characterization of CD4-IgG2, a novel heterotetramer that neutralizes primary HIV type 1 isolates. *AIDS Res Hum Retroviruses* (1995) 11:533–9. doi:10.1089/aid.1995.11.533
79. Schoonjans R, Willems A, Schoonooghe S, Fiers W, Grooten J, Mertens N. Fab chains as an efficient heterodimerization scaffold for the production of recombinant bispecific and trispecific antibody derivatives. *J Immunol* (2000) 165:7050–7. doi:10.4049/jimmunol.165.12.7050
80. Rothlisberger D, Homogger A, Pluckthun A. Domain interactions in the Fab fragment: a comparative evaluation of the single-chain Fv and Fab format engineered with variable domains of different stability. *J Mol Biol* (2005) 347:773–89. doi:10.1016/j.jmb.2005.01.053
81. Chen W, Bardhi A, Feng Y, Wang Y, Qi Q, Li W, et al. Improving the CH1-CK heterodimerization and pharmacokinetics of 4Dm2m, a novel potent CD4-antibody fusion protein against HIV-1. *MAbs* (2016) 8:761–74. doi:10.1080/19420862.2016.1160180
82. Chen W, Feng Y, Prabakaran P, Ying T, Wang Y, Sun J, et al. Exceptionally potent and broadly cross-reactive, bispecific multivalent HIV-1 inhibitors based on single human CD4 and antibody domains. *J Virol* (2014) 88:1125–39. doi:10.1128/JVI.02566-13
83. Chen W, Feng Y, Gong R, Zhu Z, Wang Y, Zhao Q, et al. Engineered single human CD4 domains as potent HIV-1 inhibitors and components of vaccine immunogens. *J Virol* (2011) 85:9395–405. doi:10.1128/JVI.05119-11
84. Chen W, Xiao X, Wang Y, Zhu Z, Dimitrov DS. Bifunctional fusion proteins of the human engineered antibody domain m36 with human soluble CD4 are potent inhibitors of diverse HIV-1 isolates. *Antiviral Res* (2010) 88:107–15. doi:10.1016/j.antiviral.2010.08.004
85. Davis JH, Aperlo C, Li Y, Kurosawa E, Lan Y, Lo KM, et al. SEEDbodies: fusion proteins based on strand-exchange engineered domain (SEED) CH3 heterodimers in an Fc analogue platform for asymmetric binders or immuno fusions and bispecific antibodies. *Protein Eng Des Sel* (2010) 23:195–202. doi:10.1093/protein/gzp094
86. Doppalapudi VR, Huang J, Liu D, Jin P, Liu B, Li L, et al. Chemical generation of bispecific antibodies. *Proc Natl Acad Sci U S A* (2010) 107:22611–6. doi:10.1073/pnas.1016478108
87. Wranik BJ, Christensen EL, Schaefer G, Jackman JK, Vendel AC, Eaton D. LUZ-Y, a novel platform for the mammalian cell production of full-length IgG-bispecific antibodies. *J Biol Chem* (2012) 287:43331–9. doi:10.1074/jbc.M112.397869
88. Spiess C, Merchant M, Huang A, Zheng Z, Yang NY, Peng J, et al. Bispecific antibodies with natural architecture produced by co-culture of bacteria expressing two distinct half-antibodies. *Nat Biotechnol* (2013) 31:753–8. doi:10.1038/nbt.2621
89. Wagner K, Kwakkenbos MJ, Claassen YB, Maijor K, Böhne M, van der Sluijs KF, et al. Bispecific antibody generated with sortase and click chemistry has broad antiinfluenza virus activity. *Proc Natl Acad Sci U S A* (2014) 111:16820–5. doi:10.1073/pnas.1408605111
90. Deisenhofer J. Crystallographic refinement and atomic models of a human Fc fragment and its complex with fragment B of protein A from *Staphylococcus aureus* at 2.9- and 2.8-A resolution. *Biochemistry* (1981) 20:2361–70. doi:10.1021/bi00512a001
91. Topp MS, Gökbüget N, Stein AS, Zugmaier G, O'Brien S, Bargou RC, et al. Safety and activity of blinatumomab for adult patients with relapsed or refractory B-precursor acute lymphoblastic leukaemia: a multicentre, single-arm, phase 2 study. *Lancet Oncol* (2015) 16:57–66. doi:10.1016/S1470-2045(14)71170-2
92. Wolf E, Hofmeister R, Kufer P, Schlereth B, Baeuerle PA. BiTEs: bispecific antibody constructs with unique anti-tumor activity. *Drug Discov Today* (2005) 10:1237–44. doi:10.1016/S1359-6446(05)03554-3
93. Mølholm M, Crommer S, Brischwein K, Rau D, Sriskandarajah M, Hoffmann P, et al. CD19-/CD3-bispecific antibody of the BiTE class is far superior to tandem diabody with respect to redirected tumor cell lysis. *Mol Immunol* (2007) 44:1935–43. doi:10.1016/j.molimm.2006.09.032
94. Reusch U, Duell J, Ellwanger K, Herbrecht C, Knackmuss SH, Fucek I, et al. A tetravalent bispecific TandAb (CD19/CD3), AFM11, efficiently recruits T cells for the potent lysis of CD19(+) tumor cells. *MAbs* (2015) 7:584–604. doi:10.1080/19420862.2015.1029216
95. Wu J, Fu J, Zhang M, Liu D. AFM13: a first-in-class tetravalent bispecific anti-CD30/CD16A antibody for NK cell-mediated immunotherapy. *J Hematol Oncol* (2015) 8:96. doi:10.1186/s13045-015-0188-3
96. Reusch U, Burkhardt C, Fucek I, Le Gall F, Le Gall M, Hoffmann K, et al. A novel tetravalent bispecific TandAb (CD30/CD16A) efficiently recruits NK cells for the lysis of CD30+ tumor cells. *MAbs* (2014) 6:728–39. doi:10.4161/mabs.28591
97. Rothe A, Sasse S, Topp MS, Eichenauer DA, Hummel H, Reiners KS, et al. A phase 1 study of the bispecific anti-CD30/CD16A antibody construct AFM13 in patients with relapsed or refractory Hodgkin lymphoma. *Blood* (2015) 125:4024–31. doi:10.1182/blood-2014-12-614636
98. Ying T, Feng Y, Wang Y, Chen W, Dimitrov DS. Monomeric IgG1 Fc molecules displaying unique Fc receptor interactions that are exploitable to treat inflammation-mediated diseases. *MAbs* (2014) 6:1201–10. doi:10.4161/mabs.29835
99. Mancardi DA, Albanesi M, Jönsson F, Iannascoli B, Van Rooijen N, Kang X, et al. The high-affinity human IgG receptor FcgammaRI (CD64) promotes IgG-mediated inflammation, anaphylaxis, and antitumor immunotherapy. *Blood* (2013) 121:1563–73. doi:10.1182/blood-2012-07-44251
100. Thépen T, Huhn M, Melmer G, Tur MK, Barth S. Fcgamma receptor 1 (CD64), a target beyond cancer. *Curr Pharm Des* (2009) 15:2712–8. doi:10.2174/13816120978923967
101. van der Poel CE, Spaapen RM, van de Winkel JG, Leusen JH. Functional characteristics of the high affinity IgG receptor, FcgammaRI. *J Immunol* (2011) 186:2699–704. doi:10.4049/jimmunol.1003526
102. Wynn TA, Chawla A, Pollard JW. Macrophage biology in development, homeostasis and disease. *Nature* (2013) 496:445–55. doi:10.1038/nature12034
103. Ying T, Ju TW, Wang Y, Prabakaran P, Dimitrov DS. Interactions of IgG1 CH2 and CH3 domains with FcRn. *Front Immunol* (2014) 5:146. doi:10.3389/fimmu.2014.00146
104. Ishino T, Wang M, Mosyak L, Tam A, Duan W, Svenson K, et al. Engineering a monomeric Fc domain modality by N-glycosylation for the half-life extension of biotherapeutics. *J Biol Chem* (2013) 288:16529–37. doi:10.1074/jbc.M113.457689
105. Gong R, Vu BK, Feng Y, Prieto DA, Dyba MA, Walsh JD, et al. Engineered human antibody constant domains with increased stability. *J Biol Chem* (2009) 284:14203–10. doi:10.1074/jbc.M900769200
106. Gong R, Wang Y, Feng Y, Zhao Q, Dimitrov DS. Shortened engineered human antibody CH2 domains: increased stability and binding to the human neonatal Fc receptor. *J Biol Chem* (2011) 286:27288–93. doi:10.1074/jbc.M111.254219
107. Ying T, Wang Y, Feng Y, Prabakaran P, Gong R, Wang L, et al. Engineered antibody domains with significantly increased transcytosis and half-life in macaques mediated by FcRn. *MAbs* (2015) 7:922–30. doi:10.1080/19420862.2015.1067353
108. Gong R, Wang Y, Ying T, Dimitrov DS. Bispecific engineered antibody domains (nanoantibodies) that interact noncompetitively with an HIV-1 neutralizing epitope and FcRn. *PLoS One* (2012) 7:e42288. doi:10.1371/journal.pone.0042288
109. Ying T, Chen W, Feng Y, Wang Y, Gong R, Dimitrov DS. Engineered soluble monomeric IgG1 CH3 domain: generation, mechanisms of function, and implications for design of biological therapeutics. *J Biol Chem* (2013) 288:25154–64. doi:10.1074/jbc.M113.484154

110. Wozniak-Knopp G, Bartl S, Bauer A, Mostageer M, Woisetschläger M, Antes B, et al. Introducing antigen-binding sites in structural loops of immunoglobulin constant domains: Fc fragments with engineered HER2/neu-binding sites and antibody properties. *Protein Eng Des Sel* (2010) 23:289–97. doi:10.1093/protein/gzq005
111. Kainer M, Antes B, Wiederkum S, Wozniak-Knopp G, Bauer A, Rüker F, et al. Correlation between CD16a binding and immuno effector functionality of an antigen specific immunoglobulin Fc fragment (Fcab). *Arch Biochem Biophys* (2012) 526:154–8. doi:10.1016/j.abb.2012.05.010
112. Woisetschläger M, Antes B, Borrowdale R, Wiederkum S, Kainer M, Steinkellner H, et al. In vivo and in vitro activity of an immunoglobulin Fc fragment (Fcab) with engineered Her-2/neu binding sites. *Biotechnol J* (2014) 9:844–51. doi:10.1002/biot.201300387
113. Traxlmayr MW, Lobner E, Hasenhindl C, Stadlmayr G, Oostenbrink C, Rüker F, et al. Construction of pH-sensitive Her2-binding IgG1-Fc by directed evolution. *Biotechnol J* (2014) 9:1013–22. doi:10.1002/biot.201300483
114. Leung KM, Batey S, Rowlands R, Isaac SJ, Jones P, Drewett V, et al. A HER2-specific modified Fc fragment (Fcab) induces antitumor effects through degradation of HER2 and apoptosis. *Mol Ther* (2015) 23:1722–33. doi:10.1038/mt.2015.127
115. Holliger P, Hudson PJ. Engineered antibody fragments and the rise of single domains. *Nat Biotechnol* (2005) 23:1126–36. doi:10.1038/nbt1142
116. Hladnik L, Augustin K, DeFrates S. Advancements in therapy for acute lymphoblastic leukemia: blinatumomab. *J Adv Pract Oncol* (2016) 7:76–82. doi:10.6004/jadpro.2016.7.1.6
117. Sharkey RM, Cardillo TM, Rossi EA, Chang CH, Karacay H, McBride WJ, et al. Signal amplification in molecular imaging by pretargeting a multivalent, bispecific antibody. *Nat Med* (2005) 11:1250–5. doi:10.1038/nm1322
118. Sharkey RM, Rossi EA, McBride WJ, Chang CH, Goldenberg DM. Recombinant bispecific monoclonal antibodies prepared by the dock-and-lock strategy for pretargeted radioimmunotherapy. *Semin Nucl Med* (2010) 40:190–203. doi:10.1053/j.semnuclmed.2009.12.002
119. Andersen JT, Sandlie I. The versatile MHC class I-related FcRn protects IgG and albumin from degradation: implications for development of new diagnostics and therapeutics. *Drug Metab Pharmacokinet* (2009) 24:318–32. doi:10.2133/dmpk.24.318
120. Herrington-Symes AP, Farys M, Khalili H, Brocchini S. Antibody fragments: prolonging circulation half-life special issue-antibody research. *Adv Biosci Biotechnol* (2013) 4:689–98. doi:10.4236/abb.2013.45090
121. Müller D, Karle A, Meissburger B, Hofig I, Stork R, Kontermann RE. Improved pharmacokinetics of recombinant bispecific antibody molecules by fusion to human serum albumin. *J Biol Chem* (2007) 282:12650–60. doi:10.1074/jbc.M700820200
122. Plückthun A, Pack P. New protein engineering approaches to multivalent and bispecific antibody fragments. *Immunotechnology* (1997) 3:83–105. doi:10.1016/S1380-2933(97)00067-5
123. Haraldsson B, Nyström J, Deen WM. Properties of the glomerular barrier and mechanisms of proteinuria. *Physiol Rev* (2008) 88:451–87. doi:10.1152/physrev.00055.2006
124. Yu YJ, Atwal JK, Zhang Y, Tong RK, Wildsmith KR, Tan C, et al. Therapeutic bispecific antibodies cross the blood-brain barrier in nonhuman primates. *Sci Transl Med* (2014) 6:261ra154. doi:10.1126/scitranslmed.3009835

Conflict of Interest Statement: The authors declare that the research was conducted in the absence of any commercial or financial relationships that could be construed as a potential conflict of interest.

Copyright © 2017 Liu, Saxena, Sidhu and Wu. This is an open-access article distributed under the terms of the Creative Commons Attribution License (CC BY). The use, distribution or reproduction in other forums is permitted, provided the original author(s) or licensor are credited and that the original publication in this journal is cited, in accordance with accepted academic practice. No use, distribution or reproduction is permitted which does not comply with these terms.



Engineering of Fc Fragments with Optimized Physicochemical Properties Implying Improvement of Clinical Potentials for Fc-Based Therapeutics

Chunpeng Yang^{1,2†}, Xinyu Gao^{1,2†} and Rui Gong^{1*}

¹ CAS Key Laboratory of Special Pathogens and Biosafety, Wuhan Institute of Virology, Chinese Academy of Sciences, Wuhan, China, ² University of Chinese Academy of Sciences, Beijing, China

OPEN ACCESS

Edited by:

Lee Mark Wetzler,
Boston University,
United States

Reviewed by:

Mohey Eldin El Shikh,
Queen Mary University of London,
United Kingdom
Johannes S. Gach,
University of California, Irvine,
United States

*Correspondence:

Rui Gong
gong@wh.iov.cn

[†]These authors have contributed equally to this work.

Specialty section:

This article was submitted to
Vaccines and Molecular
Therapeutics,
a section of the journal
Frontiers in Immunology

Received: 11 September 2017

Accepted: 07 December 2017

Published: 08 January 2018

Citation:

Yang C, Gao X and Gong R (2018)
Engineering of Fc Fragments with
Optimized Physicochemical
Properties Implying Improvement
of Clinical Potentials for
Fc-Based Therapeutics.
Front. Immunol. 8:1860.
doi: 10.3389/fimmu.2017.01860

Therapeutic monoclonal antibodies and Fc-fusion proteins are successfully used in treatment of various diseases mainly including cancer, immune disease, and viral infection, which belong to the Fc-based therapeutics. In recent years, engineered Fc-derived antibody domains have also shown potential for Fc-based therapeutics. To increase the druggability of Fc-based therapeutic candidates, many efforts have been made in optimizing physicochemical properties and functions mediated by Fc fragment. The desired result is that we can simultaneously obtain Fc variants with increased physicochemical properties *in vitro* and capacity of mediating appropriate functions *in vivo*. However, changes of physicochemical properties of Fc may result in alternation of Fc-mediated functions and vice versa, which leads to undesired outcomes for further development of Fc-based therapeutics. Therefore, whether modified Fc fragments are suitable for achievement of expected clinical results or not needs to be seriously considered. Now, this question comes to be noticed and should be figured out to make better translation from the results of laboratory into clinical applications. In this review, we summarize different strategies on engineering physicochemical properties of Fc, and preliminarily elucidate the relationships between modified Fc *in vitro* and the subsequent therapeutic influence *in vivo*.

Keywords: monoclonal antibody, Fc-fusion protein, Fc-based therapeutics, optimization, physicochemical property, stability, aggregation

INTRODUCTION

Since the hybridoma technology for the production of monoclonal antibodies (mAbs) was invented more than 40 years ago, mAbs are widely used as diagnostics and therapeutics. The first commercial therapeutic mAb, muromonab-CD3 (trade name Orthoclone OKT3), was approved by the U.S. Food and Drug Administration (FDA) for prevention of kidney transplant rejection in 1986 (1). Because it is a murine antibody, administration of this antibody in human might lead to the production of human anti-mouse antibody (HAMA) responses. To reduce the immunogenicity, the development of therapeutic mAbs undergoes four generations: murine mAbs, chimeric mAbs, humanized mAbs, and fully human mAbs (2). Nine therapeutic mAbs have been approved by the U.S. FDA

since the start of 2017¹ (3) while the total sales of 70 mAbs for clinical treatment will exceed 100 billion U.S. dollars this year. Among those mAbs, Adalimumab (trade name Humira) the first approved fully human mAb derived from phage display, led the list of top-selling pharmaceutical products with global sales of 16 billion U.S. dollars in 2016 (4).

Fc-fusion proteins are composed of an immunoglobulin (Ig) Fc domain that is directly linked to another peptide, protein, or protein domain. For therapeutic propose, the first description of CD4-Fc fusion protein showed the inhibitory activity against the formation of syncytia during HIV-1 infection in 1989, which showed the proof-of-concept of use of therapeutic Fc-fusion proteins for treatment of HIV-1 infection (5). Subsequently, many modified CD4-Fc fusion proteins were constructed including PRO 542, which was still clinically evaluated (6, 7). Etanercept (trade name Enbrel), a recombinant human tumor necrosis factor (TNF) receptor-Fc fusion protein, was the first TNF- α antagonist approved in the USA for the treatment of rheumatoid arthritis in 1998 (8, 9). The total sale of etanercept is about six billion U.S. dollars in 2016 reported by Amgen (Chairman and CEO Letter and Amgen Inc. 2016 Annual Report²), which demonstrates huge market for therapeutic Fc-fusion proteins.

Fc-derived antibody domains are emerging candidates as Fc-based therapeutics. Since they are part of Fc fragments, they may have complete or partial Fc-mediated functions. Therefore, they could be used as scaffold for selection of functional binders, or as carrier for generation of novel fusion proteins for potential clinical use (10). Several candidates have been selected based on Fc-derived scaffolds while Fc-derived domain-fusion protein were also constructed, which were promisingly functional in the aspect of potential therapeutic significance. However, the gap between current progress and clinical use is still huge.

Although great success has been achieved, there are still many limitations during the development of Fc-based therapeutics from bench to bedside (1, 11). The poor physicochemical properties are considerable factors that lead to failure of potential candidates in clinical trials. For marketed drugs, such drawbacks could increase their adverse effects. Therefore, a new-developed candidate should be well characterized in its physicochemical properties which may need to be optimized for better therapeutic outcomes, while increase of physicochemical properties could also be one strategy to make current biologics better (biobetter). Although a lot of effort has been put into modification of physicochemical properties on Fc fragment, whether modified physicochemical properties can lead to desired efficacy *in vivo* has not be well understood yet. Here, we summarize the methodology in engineering of physicochemical properties of Fc and try to discuss how the improvement of physicochemical properties influences the efficacy for administration *in vivo*.

Fc-BASED THERAPEUTICS

As described above, Fc-based therapeutics are now widely used in therapy and prevention of various diseases. Fc is the

crystallizable fragment derived from Ig which has five classes including IgG, IgA, IgD, IgM, and IgE in human (12). An Ig molecule is composed of antigen-binding fragments (Fab) Fc. Fc plays multiple roles in dimerization for formation of Y-shaped structure of Ig and maintenance of the structure, and Fc-mediated effector functions and extension of serum half-life. There are two domains: second constant domain (CH2) and third constant domain (CH3) in monomeric Fc of IgG. CH2 domain has a single N-linked glycan at N297 (all the antibody residues here are numbered according to EU numbering (13) unless specified). Two CH3 domains interact strongly with each other to form homodimer resulting in dimerization of Fc. These elements contribute to the physicochemical characteristics of Fc. Through the binding of Fc in IgG to its receptor Fc-gamma receptors (Fc γ Rs), immune leukocytes presenting Fc γ Rs on their surface membrane are recruited and activated, which subsequently triggers antibody-dependent cell-mediated cytotoxicity (ADCC) and antibody-dependent cell-mediated phagocytosis to kill and clear target cells (e.g., tumor cells) (14, 15). In addition, Fc can bind to the serum complement molecule (C1q) to initiate the assembly of membrane attack complex formed by complement cascade proteins to destroy target cells, which is termed complement-dependent cytotoxicity (CDC) (16, 17). These effector functions are important for the pharmaceutical efficacies of Fc-based therapeutics. Besides mediation of effector functions, Fc can also bind to neonatal Fc receptor (FcRn) in a pH-dependent manner, which leads to the extension of the serum half-life of IgG (18). In addition, binding of Fc to immune-related molecules such as Fc receptors can regulate immune response *in vivo* (19). Taking together, Fc part in an Fc-based therapeutic protein plays important roles in biological and pharmacological properties including (i) increased stability and aggregation resistance; (ii) acquired multivalent binding to the target; (iii) enhanced Fc-mediated effector functions; (iv) extended serum half-life; and (v) modulated immunogenicity.

Full-Size mAbs

The therapeutic mAbs have been successfully used for the treatment of various diseases including cancer, immune disease, and infection (20–22). They are highly specific and efficient. Currently, most of the U.S. FDA-approved therapeutic mAbs are full-size IgG molecules with a molecular weight of approximately 150 kDa. Within the IgG isotype, there are four subtypes (IgG1–IgG4) with differing properties distinguished by different hinge regions and Fc fragments. Most of the currently marketed therapeutic IgGs are of the IgG1 subtype while no mAb of IgG3 format is approved yet. A typical IgG1 molecule contains two copies of Fab fragments and one Fc fragment. Each Fab fragment contains a heavy chain variable domain (VH), a light chain variable domain (VL), a first heavy chain constant domain (CH1), and a light chain constant domain (CL). The Fc fragment is dimeric which contains two CH2 domains and two CH3 domains. Fab and Fc are connected by flexible hinge region. In total, a full-size mAb has 12 Ig-fold domains, which means the formation of corrected folding is a complicated process in the production of functional IgG1 molecule. Therefore, how to

¹<http://www.antibodysociety.org/tag/approved-antibodies/>.

²<http://investors.amgen.com/phoenix.zhtml?c=61656&p=irol-reportsannual>.

prevent them from unfolding and aggregating is still a big challenge in modern biopharmaceutical industry (23).

Fc-Fusion Proteins

Lots of endogenous proteins in our body and other foreign proteins may have potential to treat various diseases due to the antagonistic or agonistic effects. However, these proteins may have many limitations (e.g., instability and rapid clearance rate from the circulation), which constrains their further application in clinic. To solve this problem, fusion of them to the antibody Fc fragment is an effective strategy. Fc-fusion proteins are molecules in which the Fc fragments are fused to proteins of interests, such as extracellular domains of receptors, soluble cytokines, ligands, enzymes, engineered domains, or peptides (24–27). Therefore, Fc-fusion proteins inherit some antibody-like properties such as relatively good physicochemical characteristics for easy expression, purification, formulation, storage and transportation, bi- or multivalent, long serum half-life, enhanced function, and adjustable immunogenicity, which increases the possibilities for clinic use. However, the similar problems as mentioned in the above paragraph should also be considered during clinical development of Fc-fusion proteins.

Engineered Domains from Fc Fragment as Potential Therapeutics

A major problem for full-size mAbs is their poor penetration into tissues (e.g., solid tumors) and weak or absent binding to sterically restricted regions on the surface of some molecules (e.g., on the viral envelope glycoproteins), which are fully accessible only by molecules with small size (28). Reduction of molecular weight of full-size mAbs such as identification of the minimum binding domain is one of attractive directions to overcome the drawbacks. Therefore, lots of derivates from intact IgGs appeared during last two decades. These derivates include Fab, single chain variable fragment (scFv), heavy chain variable domain (VH) and light chain variable domain (VL) (29). The functional VH from camelidae, specially termed as nanobody, has been clinically developed by Ablynx. However, due to the lack of Fc part, the serum half-lives of these variants are relatively short, which is one of the major obstacles for *in vivo* administration (29). Other Ig domains including CH2 and CH3 derived from Fc and Fc itself have been proposed as new scaffolds for development of novel Fc-based therapeutics (10, 28, 30, 31). They are also smaller than full-size mAbs. Compared with those variants from Fab-based backbone, these scaffolds from Fc-based backbone might offer additional Fc-mediated advantages such as high stability, potential effector functions, and long half-life due to incorporation of full length or truncated Fc fragment (10, 28). Optimization of the Fc-based scaffolds on their folding and aggregation resistance could confer better potentially therapeutic outcomes.

The full-size mAbs, Fc-fusion proteins, and engineered domains from Fc fragment share Fc fragment or portion of Fc fragment as common region. Therefore, engineering of Fc could be benefit for all of them. Here, we focus on the current progress in increase of physicochemical properties of Fc including stability and aggregation resistance toward better clinic consequences.

INCREASE OF PHYSICOCHEMICAL PROPERTIES OF Fc FRAGMENT

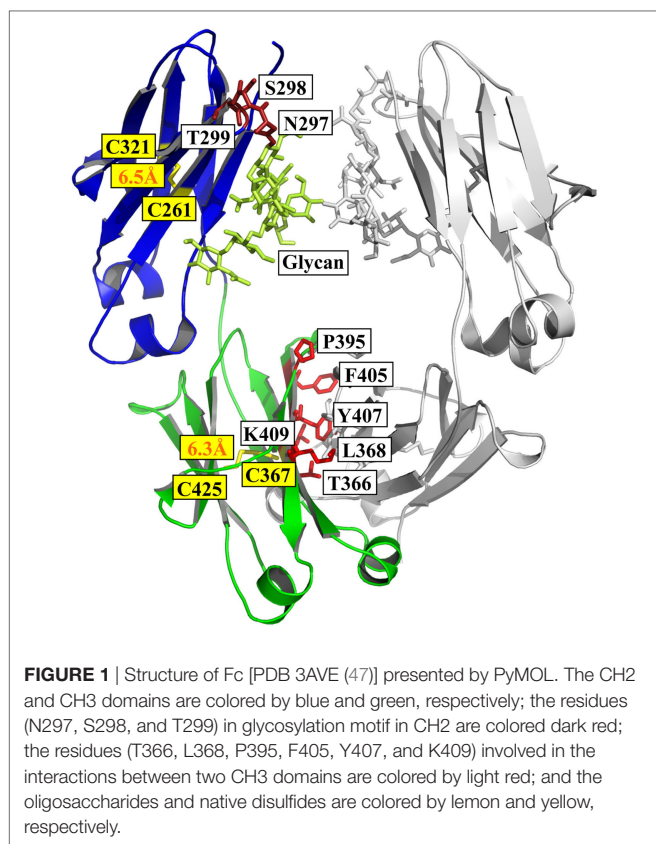
In general, the stability and aggregation resistance of a protein are two major physicochemical properties we most concern. The stability is the ability of a protein which retains its correctly folded conformation under harsh conditions such as high temperature, chemical denaturant, protease, and others, while the aggregation-resistant property is to reduce the formation of soluble oligomers and insoluble precipitates during expression, concentration, storage, and others.

One important restrictive factor in development of Fc-based therapeutics is that these proteins may tend to unfold and aggregate upon exposure to various stresses (32), including agitation (33, 34), high temperature (35, 36), low pH (37, 38), high protein concentration for subcutaneous therapeutic delivery (39), freeze-thaw cycle (40, 41), and transportation and long-term storage (42, 43), which means loss of function and increase of immunogenic risk. For example, aggregation may lead to not only loss of activity but also immune response, and negatively impact on many production processes including expression, purification, and formulation (44). A stable protein typically could be correctly expressed at high level, easily purified with no requirement of specific conditions such as low temperature and additional protease inhibitor, which makes the manufacture process much easier and cheaper. It remains active during long-term storage and after administration *in vivo*, which achieves less frequent usage at a lower dosage. An aggregation-resistant protein could be concentrated to high concentration without formation of inactive oligomer, which reduces the injection volume and makes patient more comfortable. Although stability and aggregation propensity are in different descriptions, the relationships between them are close (45). In many cases, increased stability can also lead to less aggregation propensity. Hence, during the development of recombinant therapeutic proteins, prevention of unfolding and aggregation is essential for ensuring efficacy and safety. The structure of a protein is maintained by covalent and non-covalent interactions (46). The covalent interactions are typically caused by the formation of disulfide bonds between two cysteine residues. The non-covalent interactions include hydrogen bonds, Van der Waals forces, hydrophobic interactions, and salt bridges (ionic bonds). These interactions guide the correct folding of a protein to form secondary structure such as α -helix and β -sheet, then form advanced tertiary structure and quaternary structure. Therefore, optimizing the covalent and non-covalent interactions is major direction to increase the physicochemical properties of Fc fragment.

Role of CH2 and CH3 in Maintaining Fc Structure

The antibody heavy chain constant domain is generally defined as CH1–CH2–CH3 in IgG, IgA, and IgD, with an additional domain (CH4) for IgM and IgE (12). The crystal structure of a fucosylated human IgG1 Fc is used here for presenting (PDB 3AVE) (47) (**Figure 1**).

Structural comparison of fucosylated CH2 in IgG, IgA, and IgD is equal to CH3 in IgM and IgE. The primary sequence of IgG



CH2 has a glycosylation motif N297–S298–T299 that results in N-linked glycosylation (48). The oligosaccharides are important for the stability, aggregation propensity, and effector functions of Fc fragment (49). For example, removal of the oligosaccharides results in reduction of aggregation resistance in IgG1 under acidic conditions (50).

The secondary structure of CH2 consists of two β -sheets forming a barrel as solved crystal structure of glycosylated IgG1 CH2 in an intact IgG1 molecule (51), a fucosylated human IgG1 Fc (47), or isolated aglycosylated CH2 (52) (Figure 1). There are seven β -strands from A to G connected by three loops (loops BC, DE, and FG) and two helices (helix 1 and 2) in CH2 (Figure 1). The native disulfide bond between strand B (C261) and F (C321), buried in the hydrophobic core of the molecule, should be important for the structural stability of CH2 although the direct evidence is still lacking (Figure 1). CH2 is relatively unstable compared with other Ig domains such as CH3 (53, 54). For example, during thermo-induced unfolding, the melting temperature (T_m) of mouse IgG1 CH2 is only 41°C. The T_m of human IgG1 CH2 is 54°C, which is also low but higher than that of mouse IgG1 CH2 (55). In serial comprehensive studies, it was found that (i) different IgG subclasses have different stability and aggregation propensities due to the sequence variation of their CH2 domains, and IgG1 is the best one among all the four subclasses in general (56–59); (ii) Fc aggregation induced by low pH is firstly triggered by CH2 unfolding associated with the protonation of specific acidic residues (54, 60). Therefore, it is one of

the major determinants for the unfolding of Fc-based molecules (61). Engineering of CH2 to increase its stability and aggregation resistance is expected to improve the physicochemical properties of Fc, which could be used to modify Fc-based therapeutics.

CH3 is the Ig domain following CH2. The structure of CH3 is very similar to that of CH2 (Figure 1). It also contains seven β -strands from A to G connected by three loops (loops BC, DE, and FG) and two helices (helix 1 and 2) with a native disulfide bond between strand B (C367) and F (C425) as CH2 although strand D seems to be shorter than that in CH2 according to the crystal structure (Figure 1) (47, 51). Distinguishing from two CH2 domain with in Fc, two CH3 domains can interact with each other very strongly, which leads to the formation of dimeric Fc structure. Probably due to the homo-interaction, dimeric CH3 has much higher stability than monomeric CH2 (62). In the interface of two IgG1 CH3 domains, there are at least six residues (T366, L368, P395, F405, Y407, and K409) involved in the interactions (Figure 1) (63). In detail, residues T366 and Y407 form a hydrogen bond and represent the principal intermolecular and intramolecular contact with each other, while residue K409 forms a hydrogen bond with residue D399 on the partner CH3 domain. Residues L368 and F405 form intermolecular and intramolecular contacts through van der Waals interactions only. These five residues locate on the two internal antiparallel β -strands and form a patch at the center of the interface. P395 contributes to the flexibility of the proline-containing loop constituting the domain–domain interface. Furthermore, the direct evidence showed that the native disulfide bond is not only involved in the folding of single CH3 domain, but also related to the dimerization process of two CH3 domains (64, 65), which is helpful for prevention of aggregation (66). Combination of display technology and high-throughput sequencing discloses a stability landscape of the CH3 domain (67). For example, it has been found that hotspots locate at C- and F-strand (positions 378–383 and 423–428, respectively) which are tolerant and intolerant to substitution due to their different orientations in a β -sheet. The side chains of hydrophobic residues V379, W381, F423, and V427, as well as the disulfide bond forming residue C425, are directed to the hydrophobic core of the CH3 domain and interact with residues of the inner β -sheet. They are highly intolerant to mutation. By contrast, the solvent-exposed side chains of A378, E380, E382, S424, S426, and M428 are more tolerant to mutation. This strongly suggests that the intolerance to mutation of a particular residue is not primarily caused by its localization in a secondary structural element, but by side-chain interactions with other parts of the molecule. The factors are more complicated for those residues in the inner β -sheet because they interact with other residues either in other chains in the same domain or in the same chains in the symmetrical partner CH3 domain.

Interestingly, although the glycan chain does not contact the CH3 domain, the CH3 domain in glycosylated Fc reveals a higher stability than that in aglycosylated Fc, implying an indirect contribution of the glycan chain to maintain the CH3 structure domain possible through stabilization of CH2 domain (68). Although the CH2 domain firstly unfolds during acid-induced unfolding, the colloidal stability of the CH3 homodimer in the fully unfolded state is lower than that of CH2 monomer and aglycosylated Fc,

and the unfolded CH3 homodimer forms much larger aggregates (68, 69). Therefore, it was concluded that (1) the unfolding process of CH2 and CH3 domains is independently from each other in the aglycosylated Fc region; (2) the colloidal stabilities of the CH2 and CH3 domains affect the aggregation process of the unfolded aglycosylated Fc region in a compensatory manner; and (3) the CH3 domain plays the most critical role among different Ig domains in driving intact antibody aggregation under acidic conditions (68, 69).

Although different antibody subclasses and subtypes have different Fc sequences, Fc is the common part of all the full-size antibodies and Fc-fusion proteins. To increase the stability and aggregation resistance of Fc, most previous work has focused on introducing mutations to form covalent interactions such as disulfide bonds or enhance the non-covalent interactions. In addition, change of the glycosylation form may also alter the folding of the Fc-based molecules.

Introduction of Covalent Bond in Fc

Disulfide bonds are main kind of covalent interactions in intra- or inter-Ig domains, formed by the oxidation of two thiol groups within cysteine residues, which fix and stabilize the structure of proteins in an oxidative environment. There are 12 intra-domain disulfide bonds (each domain has one intra-domain disulfide bond located in hydrophobic core) that exist in IgG, while 4, 6, 13, and 4 inter-chain disulfide bonds exist in IgG1, IgG2, IgG3, and IgG4, respectively, due to different length of hinge regions (70). Disruption of the intra-domain disulfide bonds in CL, VH, VL or CH3 results in a significant reduction of the structural stability of those domains, especially the thermodynamic stability (66, 71–77). Similarly, inter-domain disulfide bonds also have an effect on structural stability of IgG (68, 78). The existence of one disulfide bond in hydrophobic core of IgG domain could stabilize the structure. Hence, additional disulfide bond may improve the stability of Ig domain. The IgG1 Fc fragment consisting of two CH2 domains and two CH3 domains has four inherent intra-domain disulfide bonds (one disulfide bond in each domain). Additional disulfide bonds could be engineered in single domain or between two domains.

Engineering of Disulfide Bond in CH2

There is one intrinsic disulfide bond in hydrophobic core of CH2 domain between β -strand B and F (C261 in strand B and C321 in strand F) as mentioned earlier (Figure 1). In our previous research, based on possible distance of forming disulfide bond between two cysteines, five pairs of amino acids were substituted to cysteines among which two of them could be well expressed in bacterial expression system (55). Those two mutants termed m01 and m02, respectively, in which an additional disulfide bond between β -strand A and G was engineered by mutations on L242C and K334C in m01 (Figure 2A) as well as V240C and L334C in m02 (Figure 2B). The Tm of m01 is 73.8°C, which is almost 20°C higher than that of wide-type CH2 (wtCH2). Both of them are also much more stable against urea unfolding compared with wtCH2. Meanwhile, the secondary structure of m01 is not affected by this additional disulfide bond measured by circular dichroism (CD) and nuclear magnetic resonance. The stability of

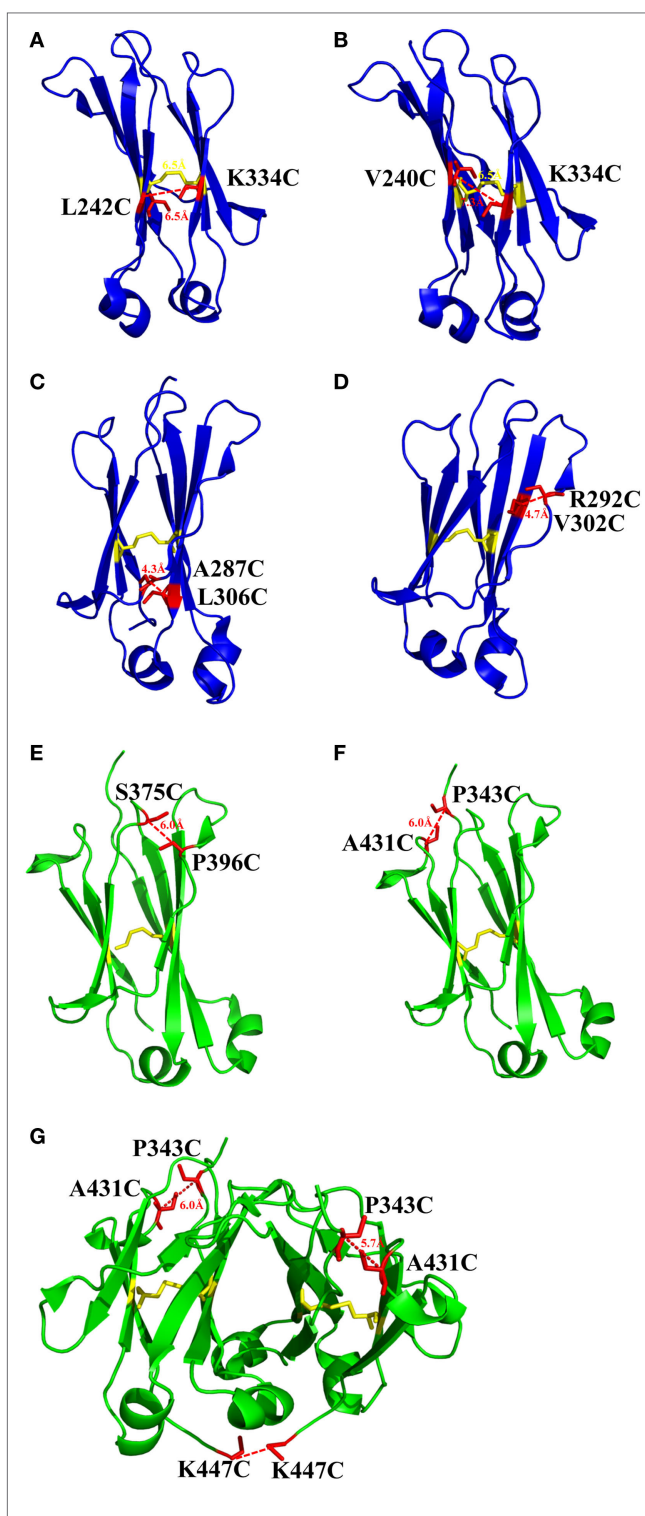


FIGURE 2 | The structures of CH2 and CH3 domains [PDB 3AVE (47)] with different mutations for introduction of additional disulfide bonds presented by PyMOL. **(A)** CH2 mutant L242C/K334C. **(B)** CH2 mutant V240C/K334C. **(C)** CH2 mutant A287C/L306C. **(D)** CH2 mutant R292C/V302C. **(E)** CH3 mutant S375C/P396C. **(F)** CH3 mutant P343C/A431C. **(G)** CH3 mutant P343C/A431C/K447C. The native disulfide bond is colored by yellow, whereas the mutated residues for additional disulfide bonds are colored by red. All the marked distance is the measured between two α -carbon atoms in related two cysteines after mutagenesis by using PyMOL.

m02 is also much better than that of wtCH2, but the aggregation-resistant property is not as good as m01. It has been shown that the Tm of CH2 with mutations in L242C and L334C in IgG1 is 8.7°C higher than that in wtIgG1 (79). In another research (80), to improve the stability of an IgG1 variant with mutation of N297G (mAbW.IgG1, an effector function silenced IgG1), an additional disulfide bond according to the design of m01 was introduced between position L242 and K334 (81). As expected, the stability of this IgG1 variant (mAbW.SEFL2.0) with mutations on L242C/N297G/K334C is improved particular in the thermal stability, but it shows faster clearance in the rat in pharmacokinetics study. Another four IgG1 variants with different additional disulfide bond formation were designed, constructed, and expressed in CHO expression system, among which two variants mAbW.SEFL2.1 with mutations of A287C/N297G/L306C in CH2 domain (**Figure 2C**) and mAbW.SEFL2.2 with mutations of R292C/N297G/V302C in CH2 domain (**Figure 2D**) with improved stability, decreased rate of clearance, and longer half-lives in both the rat and cynomolgus monkey models compared with mAbW.IgG1. Importantly, the Tm values of mAbW.SEFL2.1 and mAbW.SEFL2.2 are about 8°C higher than that of mAbW.IgG1, while mAbW.SEFL2.0 is about 2°C higher than that of mAbW.IgG1, which indicates introduction of disulfide bonds in different positions results in different outcomes.

Addition of Disulfide Bond in CH3

The same as CH2 domain, CH3 domain also has one intrinsic disulfide bond in hydrophobic core (C367 and C425). To investigate the influence of this disulfide bond in CH3, a variant of CH3 reducing disulfide bond was engineered (66). And in the following studies it has been shown that the thermal stability of the reduced form is lower than that of the oxidized form measured by CD and differential scanning calorimetry (DSC) results. In addition, the reversibility after unfolding is also significantly lower. And although most of reduced form retained a stable dimeric structure, aggregation is improved. Similarly to CH2, introduction of additional disulfide bond inside the domain could also improve the stability of CH3. In another study, an additional disulfide bond was engineered into isolated monomeric CH3 by mutation of P343 and A431 to two cysteines, resulting in improved protein expression (up to fivefold) and elevated Tm (from 40.6 to 76.0°C), without affecting FcRn binding ability (82). In a more previous study, two additional disulfide bonds were engineered into CH3 domain, respectively. Hence the Tm value of Fc variant with dual mutations of P343C/A431C and S375C/P396 in CH3 domain (**Figures 2E,F**, respectively) was obviously improved measured by CD and DSC experiment compared with wtFc (83). Since two CH3 domains interact non-covalently with each other, in addition to introduction of intra-domain disulfide bonds, there are some works on engineering of additional inter-domain disulfide bonds between two CH3 domains. The last three amino acids (P445, G446, and K447) at C-terminal of CH3 were replaced by G, E, and C, respectively, derived from CL domain (**Figure 2G**), which could introduce an additional inter-domain disulfide bond between two CH3 domains in Fc or dimeric CH3 (68, 84). And the conformational stability of both the CH2 and CH3 domains could be improved in an Fc variant with this kind

TABLE 1 | Introduction of disulfide bonds and engineering of non-covalent interactions in CH2 and CH3 domains.

Position	Domain ^a	ΔTm (°C)	Description ^b	Reference
Covalent				
L242C/K334C	CH2	18.7	Isolated IgG1 CH2	(55)
V240C/L334C	CH2	11.2	Isolated IgG1 CH2	(55)
L242C/K334C	CH2	8.7	CH2 in IgG1	(79)
L242C/K334C	CH2	2.1	CH2 in aglycosylated IgG1	(81)
A287C/L306C	CH2	7.8	CH2 in aglycosylated IgG1	(81)
R292C/V302C	CH2	8.1	CH2 in aglycosylated IgG1	(81)
P343C/A431C	CH3	35.4	Isolated IgG1 CH3	(82)
P343C/A431C	CH3	10.2	CH3 in IgG1 Fc	(83)
S375C/P396C	CH3	4.7	CH3 in IgG1 Fc	(83)
P343C/A431C	CH3	15.2	CH3 in IgG1 Fc	(83)
S375C/P396C				
P445G/G446E/	CH3	3.5	CH2 in IgG1 Fc	(84)
K447C		9.1	CH3 in IgG1 Fc	(84)
P343C/A431C	CH3	14.5	CH2 in IgG1 Fc	(84)
P445G/G446E/		18.1	CH3 in IgG1 Fc	(84)
K447C				
Non-covalent				
L235K/L309K	CH2	2.7	CH2 in IgG	(45)
L234F/L235Q	CH2	5.7	Compare to IgG1 with Mutation of "TM-YTE"	(99)
K322Q/M252Y				
S254T/T256E				
G197K/S207G/T246L	Bovine CH3	10.0	Compare to bovine wtCH3	(102)
Q295F/Y296A	CH2	3.2	CH2 in IgG1 Fc	(103)
Truncation of N-terminal residues "APELLGG"	CH2	5.1	Isolated IgG1 CH2	(107)

^aAll the domains are from human IgG1 if not specified.

^bAll the isolated domains are expressed in *Escherichia coli*, others are expressed in eukaryotic cells.

of inter-domain disulfide bond (68). In another research, an Fc variant (P343C, A431C P445G, G446E, and K447C) with not only additional intra-domain but also inter-domain disulfide bond could increase the thermostability of CH2 and CH3 (84). The Tm of CH3 in this variant was improved by 18.1°C compared with the wtFc. Furthermore, the properties of pH and aggregation resistance of this variant were also increased when compared with the wtFc. The mutations in CH2 and CH3 domains for introducing disulfide bonds are listed in Table 1.

Optimization on Non-Covalent Interaction in Fc

Although introduction of disulfide bonds can significantly increase the stability of a protein, the risk of increasing aggregation propensity caused by incorrectly paired cysteines might not be neglected. Therefore, optimization of non-covalent interactions is another efficient strategy to improve the stability or aggregation resistance of Fc fragments. The optimization could be performed by site-directed mutations (without forming covalent disulfide bond) under the aid of sequence and structural information, and computation, which could change the local residue-to-residue interactions and influence the whole Fc-based molecule.

Introduction of Intramolecular Non-Covalent Interactions in CH2

The exposure of hydrophobic residues may increase the aggregation propensity due to non-specific hydrophobic interactions, especially when the large hydrophobic clusters form. Therefore, rational disruption of those continuous hydrophobic residues without affecting the molecular structure may be helpful for decreasing the formation of aggregation. A computational technology termed spatial aggregation propensity (SAP) was developed to measure the dynamic exposure of hydrophobic patches and identify the location and size of these aggregation-prone regions based on the atomistic molecular dynamics simulations, which can guide the performance of target mutations for engineering of protein stability and aggregation resistance (45, 85, 86). By this technology, several mutations with different combinations were introduced to generate several IgG variants (45). One variant with combinational mutations of L235K and L309K in the CH2 domain (**Figure 3A**) showed not only increased thermostability but also improved aggregation resistance. Being a hydrophilic amino acid, lysine can discontinue the hydrophobic patch and reduce the non-specific interactions between hydrophobic patches. Furthermore, as mentioned earlier, CH2 domain is typically the least stable domain in the Fc portion, which influences the whole molecular stability and aggregation propensity. Therefore, the physicochemical properties of the antibody molecule could be optimized after rational introduction of proper hydrophilic amino acids for disruption of the large hydrophobic aggregation-prone clusters. In addition to SAP (87–89),

several online programs such as TANGO³ (90–92), PASTA⁴ (93), AGGRESCAN⁵ (94), and Aggrescan3D⁶ (95) are also widely used to predict aggregation-prone regions within proteins. Therefore, it is desired that new Ig variants could be identified in the future.

In many instances, it might be desirable for a therapeutic mAb and Fc-fusion protein to lack/reduce effector functions. According to previous studies, two sets of mutations in CH2 domain including “TM” (triple mutations of L234F/L235E/P331S) and “YTE” (M252Y/S254T/T256E) are effective in abolishing the binding of Fc to FcyRs (96) and C1q and enhancing the pH-dependent binding to FcRn (97, 98), respectively, which can generate an IgG variant (TM-YTE) with extended half-life but without Fc-mediated effector functions *in vivo*. However, these mutations adversely influence the stability and aggregation propensity and result in many difficulties for further applications (99). For example, it has been shown that replacement of the original amino acids M252, S254, and T256 to Y, T, and E significantly reduced the stability and increased the aggregation tendency due to the increased local flexibility of the 244–254 segment in CH2 (100, 101). To compensate the decreased physicochemical properties, several mutants were designed with different combinations of mutations with the strategies including substitution of charged residues (e.g., E) by uncharged residues (e.g., Q). According to a serial of experiments by characterization of designed mutants, one novel mutant (FQQ-YTE) with combinational mutations of L234F/L235Q/K322Q/M252Y/S254T/T256E (**Figure 3B**) was identified, which had significantly improved conformational stability while retaining the same biological activities as TM-YTE mutant (99).

Introduction of Intra- and Intermolecular Non-Covalent Interactions in CH3

Sequence analysis among different Ig classes and subtypes can provide useful clues for Fc optimization. One good example is the mutation on bovine IgG1 CH3 for increased stability deduced from the sequence and structural information (102). According to sequence alignment and frequency analysis among 36 unique IgG Fc sequences originating from 19 different mammalian species, bovine IgG1 demonstrated the closest resemblance to the consensus sequence other than primate IgG sequences, while a few crucial positions could be mutated to make the molecule more stable. Therefore, the residues S174, Y179, G197, S207, and T246 in bovine IgG1 CH3 numbered according to the reference (102) which are partnered with G371, D376, K392, G402, and L441 in human IgG1 CH3 were selected to be substituted by G, D, K/A, G, and L, respectively. Four of these 5 mutant positions are at residue sites of reasonable heterogeneity (i.e., the measured positional entropies are in the top 70% for all residue positions), while mutation at S207 (G402) was the only position that highly conserved because only 4 of the 36 sequences have another residue other than G. In spatial structure, each residue is far away from the four others. After measurement of

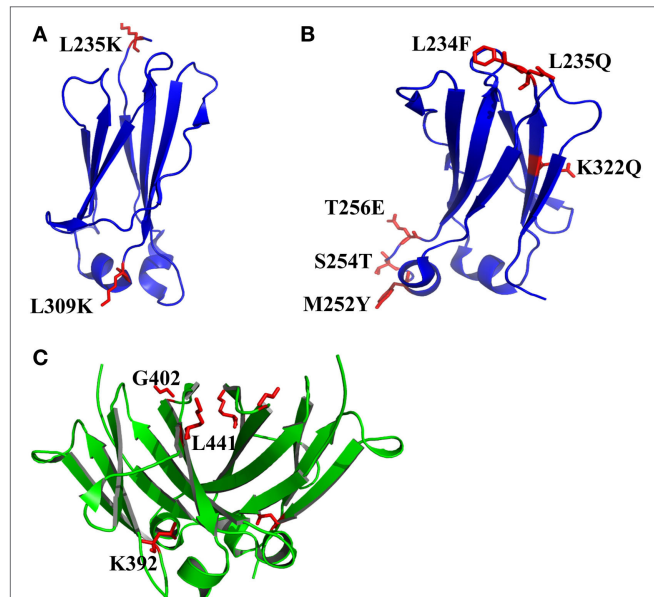


FIGURE 3 | The structures of CH2 and CH3 domains [PDB 3AVE (47)] with optimized non-covalent interactions presented by PyMOL. **(A)** CH2 L235K/L309K mutant. **(B)** CH2 L234F/L235Q/K322Q/M252Y/S254T/T256E mutant (FQQ-YTE). **(C)** The residues K392, G402, and L441 in human IgG1 CH3 domain, which can be used to replace the corresponding residues in the bovine CH3 domain (G197, S207, and T246) for increase of the stability. The mutated residues for additional disulfide bonds are colored by red.

³<http://tango.crg.es>.

⁴<http://protein.bio.unipd.it/pasta2/index.html>.

⁵<http://bioinf.uab.es/aap/>.

⁶<http://biocomp.chem.uw.edu.pl/A3D/>.

heat-induced unfolding, one combination with G197K/S207G/T246L (**Figure 3C**) showed the highest T_m , which increased about 10°C compared with that of wide-type bovine IgG1 CH3. The experimental results could be explained as follows. First, among these mutations, replacement of G197 to K392 inserts a lysine at the interface between the CH3 dimer locating at the hydrophobic portion of the side-chain that packs against a hydrophobic patch created by F210 (F405) and V202 (V397) of the opposite dimer subunit. Although adding a hydrophobic moiety like alanine to this cavity is also better than original G, introduction of positive charged lysine at this position is shown to be best due to the adjacency to D204 (D399), a negative charged amino acid can possibly enhance the favorability of lysine at this position. Second, substitution of S207 by G402 places G in a tight turn between β -strands, which likely releases strain induced by the tight turn since the backbone dihedral angles of this residue in the crystal structure are outside the generally allowed ranges for α -substituted amino acids (all amino acids other than G). Finally, the mutation of T246 to L441 completely buries the isobutyl side chain into the hydrophobic interior of the β -sandwich. Although burial of three groups are expected for more favorable contributions, the actual effect is not as obvious as desired. The reason is that the side chain of T can compensate somewhat for the loss of buried hydrophobic surface area due to steric placement or hydrogen bonding.

This finding indicates that cross-species analysis provides useful information about the relationship between residues and physicochemical properties, and further guides the rational design for a better Fc with more stable, more aggregation-resistant and more soluble characteristics.

Engineering of Loop and Other Regions in CH2 and CH3

Both CH2 and CH3 domains have several flexible loop regions, which could also be the targets for optimization of the physicochemical properties. For example, to stabilize the CH2 domain, an enhanced aromatic sequon (EAS) (Q295F/Y296A) (**Figure 4A**) was engineered into the top of N-glycosylated DE loop, which led to a 4.8°C increase of the T_m of the purified IgG1 Fc fragment (103). This strategy could be used in optimizing a full-length IgG1 molecule for enhancement of its resistance to unfolding and aggregation. The crystal structure of the EAS-stabilized IgG1 Fc fragment reveals the importance of the GlcNAc1-F295 interaction, as well as the participation of the core fucose (Fuc) attached to GlcNAc1 in an interaction with F295. As mentioned earlier, the yeast display technology is also used in high-throughput screening of improved CH3 mutants with replacement of its original loops for optimization on Fc and development of antigen-specific Fc binders [Fc-antigen binding (Fcab)] (104, 105).

It has been shown that natural β -sheet proteins use negative design to avoid edge-to-edge aggregation, which indicates that the residues at N- and C-termini may be involved in aggregation formation (106). A shortened CH2 (CH2s) (**Figure 4B**) was constructed with truncation of seven unstructured N-terminal residues according to a crystal structure of an intact IgG1 (PDB 1HZH) (51), which showed significantly increased aggregation

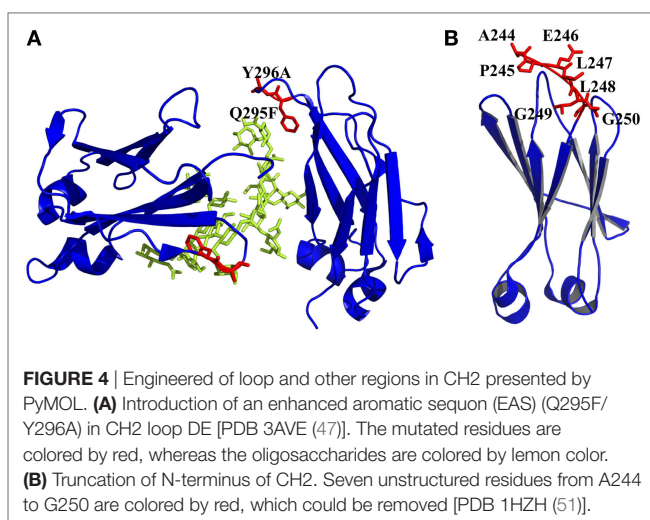


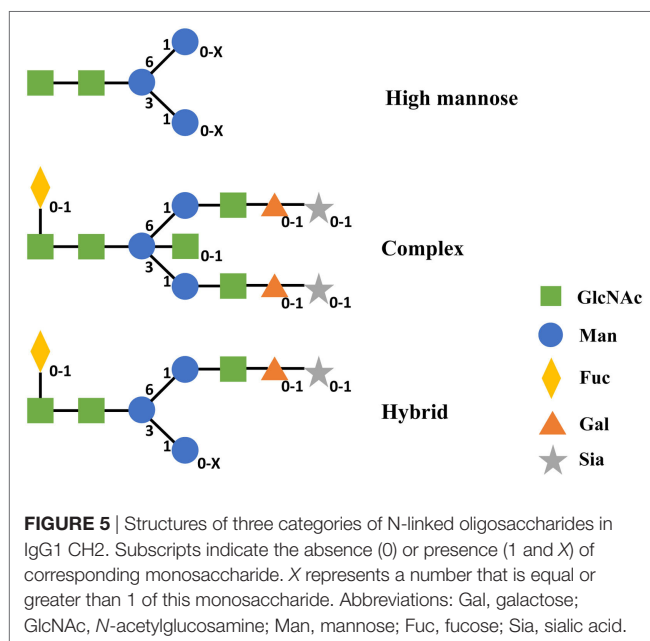
FIGURE 4 | Engineered of loop and other regions in CH2 presented by PyMOL. **(A)** Introduction of an enhanced aromatic sequon (EAS) (Q295F/Y296A) in CH2 loop DE [PDB 3AVE (47)]. The mutated residues are colored by red, whereas the oligosaccharides are colored by lemon color. **(B)** Truncation of N-terminus of CH2. Seven unstructured residues from A244 to G250 are colored by red, which could be removed [PDB 1HZH (51)].

resistance and potential Fc-mediated functions (107). Engineering of C-terminal residues in CH2 might also have the same influence as described earlier. The optimizations on non-covalent interactions in CH2 and CH3 domains are summarized in **Table 1**.

Glycoengineering in Fc

There are only two symmetrical N-glycosylation sites in the Fc fragment, which locate at amino acid position N297 in IgG1 CH2 domain. It has been widely accepted that N-glycan has a critical impact on the structure and effector functions of Fc-based therapeutics (108–111). Absence of the N-glycan can cause dramatic conformational change and decreased stability of the Fc (112–117). Without N-glycan, the binding of Fc to various receptors and their associated biological functions is either reduced or completely lost (112, 116, 118–120). The factors influencing the oligosaccharide profiles of Fc-based therapeutics are very many, such as the use of different cell lines, cell culture conditions, scales, and other factors (121, 122). Therefore, variation of glycoform is one of the main factors that cause heterogeneity of therapeutic antibodies and Fc-fusion proteins. Although aglycosylated Fc-based therapeutics have been explored for clinical use, the majority of these therapeutic proteins are still glycosylated. In most conditions, the function of N-glycan is irreplaceable for the treatment of some diseases.

According to the difference of oligosaccharides on the outer arms, N-glycan can be classified into three categories including high mannose (Man), complex, and hybrid (49). All of these classes share an invariable core structure containing two copies of primary N-acetylglucosamine (GlcNAc), one primary Man and the two secondary Man residues. High Man oligosaccharides are composed of Man only in the outer arms. Complex oligosaccharides are composed of GlcNAc and galactose and potentially sialic acid in the outer arms. Meanwhile, complex oligosaccharides can exist with or without the core Fuc. Hybrid oligosaccharides are made of one arm with complex and the other arm with high Man residues (**Figure 5**) (49). Therefore, different configurations and compositions of N-glycan can lead to >400 different variants concerning the two CH2 domains of IgG Fc (123).



The position of glycosylation on the Fc determines that it has no impact on antigen–antibody binding and FcRn binding, but oligosaccharides are critical for the binding of FcγRs and C1q, which trigger different immune responses (FcγRs for ADCC and C1q for CDC). On the other hand, changes occurring on the composition of N-glycan can influence the conformation of the whole antibody or Fc-fusion protein molecule, causing alteration in the binding affinity for various FcγRs (124). That is one of the reasons for the glycosylation playing such effective role in engineering Fc-based therapeutics.

The process of glycosylation only occurs in eukaryotes, so *Escherichia coli* and Chinese Hamster Ovary cell (CHO) derived IgG1 Fc were usually used to illustrate the impact of N-glycosylation on the stability of Fc, representing aglycosylated and glycosylated Fc proteins, respectively (50). Both of them behave similarly during heat and low pH induced unfolding. First, the tertiary structure and CH2 domain are unfolded, then the secondary structure and CH3 domain are changed. Due to the interaction of oligosaccharides, the glycosylated Fc protein is more compact (smaller hydrodynamic radius) than the aglycosylated Fc protein at neutral pH. In the aspects of thermostability and pH resistance, the Tm of glycosylated CH2 domain is 4–5°C higher than that of aglycosylated domain and the acid resistance of glycosylated Fc is ~0.5 pH lower than aglycosylated Fc (50).

Previous studies have proved that truncation of N-glycosylation is a major method to understand the relationship between the functions, structures and Fc glycoforms. Fc glycoform variants with partial or complete removal of glycan carbohydrates were compared with wtFc by using long molecular dynamics simulations (125). The results indicated that glycan truncation or removal can cause quaternary structural deformation of the Fc due to the disruption or loss of a lot of inter-glycan contacts. Because the existence of the weak binding through two oligosaccharides,

glycan truncation/removal can also cause the tertiary structural deformation of CH2 domains, which results in destabilization of individual CH2 domains. During elevating Tms, glycan truncation is differentially affecting structural deformation in locations of helices 1 and 2 in CH2 that are far from the oligosaccharide attachment point. Deformation of these helices, which form part of the binding surface to FcRn, could affect the binding to FcRn if these regions are unable to refold after Tm normalization. During elevated Tm simulations of the deglycosylated variant, CH2 domains collapse onto CH3 domains. All these studies show that glycosylation plays an important role in the stability of Fc. Besides that, different formations of glycosylation in N297 site were compared, containing three Fc proteins produced from the yeast *Pichia pastoris* with three kinds of glycosylation sites (di-, mono-, and nonglycosylated) and another three different forms of nonglycosylated Fc (mutating N297 to two different amino acids and enzymatic digestion of the Fc glycoforms), to examine the differences of structural stability. Under different pH conditions, the di- and monoglycosylated forms of Fc showed the highest and lowest levels of stability, respectively, while the stability of nonglycosylated form was in the middle and depended on the solution pH (126, 127). Furthermore, hemi-glycosylated (same to monoglycosylation) Fc shows that the binding affinities toward all FcγRs were significantly decreased and a moderate decrease (~20%) in C1q binding, representing change of effector functions (128).

Lots of previous studies have proved that glycosylation also deeply affects the aggregation of antibodies and Fc-fusion proteins (126, 129–131). By comparing the differences between glycosylated and deglycosylated antibodies, it has been found that deglycosylated antibodies had not only less thermostability and resistance to GdnHCl-induced unfolding, but also higher aggregation rates at a accelerated stability study (129). The possible reason for these findings is that disruption of protein–carbohydrate interactions leads to the exposure of aggregation-prone motifs and further results in the aggregation of the whole deglycosylated antibodies (130). The interactions between two monomeric Fc regions of an antibody include protein–protein, carbohydrate–carbohydrate, and protein–carbohydrate, all these forces have contributions to the stability and aggregation resistance. So any change of oligosaccharides (e.g., truncation and variation on glycoforms) might have serious impact on the physicochemical properties of Fc-based therapeutics.

Although the importance of N-glycosylation on Fc is clear, the production of Fc-based proteins with selected glycoforms is still very difficult. For now, the enzymatic modification of recombinant IgGs *in vitro* or engineering the host expression system can be used to modify the glycoforms of Fc-based therapeutics (108).

Due to the complexity and limit of technology for engineering the N-glycoform, lots of work still focuses on the generation of IgG variants with aglycosylation, which only needs to introduce a mutation into N297, for decrease of the effector functions to treat some chronic diseases. However, as described earlier, these mutants may influence the physicochemical properties of Fc-based proteins deeply and cause the loss of efficacy, which will be further discussed in the following paragraph.

RELATIONSHIPS BETWEEN PHYSICOCHEMICAL PROPERTIES AND CLINICAL POTENTIAL

The development of therapeutic antibodies, Fc-fusion proteins, and Fc-based antibody domains faces many challenges from bench to bedside. For example, an mAb may have excellent activities *in vitro* but lose the entire or major function *in vivo* and *vice versa*. Hence, to make a successful Fc-based therapeutics, it may need many modifications before clinical use.

Historically, either IgG2 or IgG4 isotypes have been selected for applications where cytotoxic effector functions are not required due to their limited cytotoxic effector functions (132). However, IgG1 is still the first choice due to its comprehensive advantages in many cases. Therefore, to eliminate undesired effector functions, removal of the glycosylation is an efficient way. A major concern is that deglycosylation will lead to instability and aggregation. Hence, the IgG1 scaffold with stable effector functions missing (81) needs to be further optimized. Based on the computational modeling, two variants mAbW.SEFL2.1 and mAbW.SEFL2.2 with tri-mutations on A287C/N297G/L306C and R292C/N297G/V302C, respectively, as mentioned earlier showed improved stability, decreased clearance rate, and longer half-life (80), which could be used for development of therapeutic mAbs without effector functions.

As mentioned, Etanercept is one of the most successful recombinant Fc-fusion proteins in the market. When administered *in vivo*, the dose of each injection is large (e.g., 25 mg/twice or 50 mg/once per week), which requires high concentration of Etanercept in the formulation. The risk of aggregate formation in this condition is increasing, which may lead to loss of functions and increase of side effects. To improve the solubility and reduce the aggregation, two mutations D239E and L241M were introduced into the Fc portion of Etanercept, which may increase the stability and aggregation resistance of whole recombinant protein (133). Actually, the formation of aggregation should be seriously considered when developing a biosimilar of Etanercept (134).

As a domain from Fc, CH2 has been proposed as a scaffold for development of C-based single domain antibody (C-sdAb), which has been extensively reviewed (10, 28). CH2 could have or partially have Fc effector functions and affinity to FcRn. Therefore, it could have relatively longer serum half-life after engineering due to the containment of FcRn binding sites inherited from Fc (135, 136) compared with other Ig domains (e.g., VH) as binders (29). Based on this scaffold, a panel of C-sdAbs has been selected against different targets (137, 138). However, in general, their activities are modest. Since it has been shown that CH2-based

binders tend to aggregate, a mission for development of clinically potential C-sdAbs is to further modify the scaffold to increase its stability and decrease its aggregation propensity (55, 107, 135, 139, 140), as well as for development of other engineered domains such as Fcab (104, 105, 141), monomeric Fc (142) and monomeric CH3 (82) derived from Fc fragment. Although preliminary results show the proof-of-concept, there is still very long way to achieve the final aim.

SUMMARY AND PROSPECTIVE

The problems caused by instability and aggregation propensity are major restrictions in Fc-based biopharmaceutical industry. Many other reviews have already been focused on these issues (32, 46, 143). In this review, we summarized and discussed current status in the related field in Fc engineering. Although lots of work has been done to increase the stability and aggregation resistance of Fc, it seems that the *in vivo* outcomes are not very clear after optimization. On the other hand, plenty of work has also been done to enhance the Fc-mediated effector functions and extend the half-life. However, the value for clinical application is not well verified. At present the fact is that only a few candidates among many finally enter the market due to various reasons. Therefore, more attentions should be paid toward the relationship between physicochemical optimizations and potential clinical applications, which may accelerate the development of Fc-based therapeutics.

AUTHOR CONTRIBUTIONS

RG designed the review article topic and text structure; CY, XG, and RG wrote the manuscript.

ACKNOWLEDGMENTS

The authors are thankful to The Core Facility and Technical Support, Wuhan Institute of Virology, Wuhan Institute of Biotechnology as well as Wuhan Key Laboratory on Emerging Infectious Diseases and Biosafety for the supports. This work was funded by the “Personalized Medicines—Molecular Signature-based Drug Discovery and Development”, Strategic Priority Research Program of the Chinese Academy of Sciences (Grant No. XDA12020346), the Key Program of Chinese Academy of Sciences (Grant No. ZDRW-ZS-2016-4), the National Key Research and Development Program of China (Grant No. 2016YFC1202902), and the “One-Three-Five” Strategic Programs of Wuhan Institute of Virology, Chinese Academy of Sciences (Grant No. Y605221SA1).

REFERENCES

- Kuhn C, Weiner HL. Therapeutic anti-CD3 monoclonal antibodies: from bench to bedside. *Immunotherapy* (2016) 8(8):889–906. doi:10.2217/imt-2016-0049
- Singh S, Kumar N, Dwivedi P, Charan J, Kaur R, Sidhu P, et al. Monoclonal antibodies: a review. *Curr Clin Pharmacol* (2017). doi:10.2174/157488471266170809124728
- Reichert JM. Antibodies to watch in 2017. *MAbs* (2017) 9(2):167–81. doi:10.1080/19420862.2016.1269580
- Frenzel A, Schirrmann T, Hust M. Phage display-derived human antibodies in clinical development and therapy. *MAbs* (2016) 8(7):1177–94. doi:10.1080/19420862.2016.1212149
- Traunecker A, Schneider J, Kiefer H, Karjalainen K. Highly efficient neutralization of HIV with recombinant CD4-immunoglobulin molecules. *Nature* (1989) 339(6219):68–70. doi:10.1038/339068a0

6. Allaway GP, Davis-Bruno KL, Beaudry GA, Garcia EB, Wong EL, Ryder AM, et al. Expression and characterization of CD4-IgG2, a novel heterotetramer that neutralizes primary HIV type 1 isolates. *AIDS Res Hum Retroviruses* (1995) 11(5):533–9. doi:10.1089/aid.1995.11.533
7. Jacobson JM, Israel RJ, Lowy I, Ostrow NA, Vassilatos LS, Barish M, et al. Treatment of advanced human immunodeficiency virus type 1 disease with the viral entry inhibitor PRO 542. *Antimicrob Agents Chemother* (2004) 48(2):423–9. doi:10.1128/AAC.48.2.423-429.2004
8. Mohler KM, Torrance DS, Smith CA, Goodwin RG, Stremler KE, Fung VP, et al. Soluble tumor necrosis factor (TNF) receptors are effective therapeutic agents in lethal endotoxemia and function simultaneously as both TNF carriers and TNF antagonists. *J Immunol* (1993) 151(3):1548–61.
9. Azevedo VF, Galli N, Kleinfelder A, D’Ippolito J, Urbano PC. Etanercept biosimilars. *Rheumatol Int* (2015) 35(2):197–209. doi:10.1007/s00296-014-3080-5
10. Gong R, Xiao G. Engineered antibody variable and constant domains as therapeutic candidates. *Pharm Pat Anal* (2013) 2(5):637–46. doi:10.4155/ppa.13.44
11. Chatenoud L. CD3-specific antibody-induced active tolerance: from bench to bedside. *Nat Rev Immunol* (2003) 3(2):123–32. doi:10.1038/nri1000
12. Schroeder HW Jr, Cavacini L. Structure and function of immunoglobulins. *J Allergy Clin Immunol* (2010) 125(2 Suppl 2):S41–52. doi:10.1016/j.jaci.2009.09.046
13. Edelman GM, Cunningham BA, Gall WE, Gottlieb PD, Rutishauser U, Waxdal MJ. The covalent structure of an entire gammaG immunoglobulin molecule. *Proc Natl Acad Sci U S A* (1969) 63(1):78–85. doi:10.1073/pnas.63.1.78
14. Ravetch JV, Bolland S. IgG Fc receptors. *Annu Rev Immunol* (2001) 19:275–90. doi:10.1146/annurev.immunol.19.1.275
15. Woof JM, Burton DR. Human antibody-Fc receptor interactions illuminated by crystal structures. *Nat Rev Immunol* (2004) 4(2):89–99. doi:10.1038/nri1266
16. Walport MJ. Complement. First of two parts. *N Engl J Med* (2001) 344(14):1058–66. doi:10.1056/NEJM200104053441406
17. Walport MJ. Complement. Second of two parts. *N Engl J Med* (2001) 344(15):1140–4. doi:10.1056/NEJM200104123441506
18. Roopenian DC, Akilesh S. FcRn: the neonatal Fc receptor comes of age. *Nat Rev Immunol* (2007) 7(9):715–25. doi:10.1038/nri2155
19. Levin D, Golding B, Strome SE, Sauna ZE. Fc fusion as a platform technology: potential for modulating immunogenicity. *Trends Biotechnol* (2015) 33(1):27–34. doi:10.1016/j.tibtech.2014.11.001
20. Scott AM, Wolchok JD, Old LJ. Antibody therapy of cancer. *Nat Rev Cancer* (2012) 12(4):278–87. doi:10.1038/nrc3236
21. Vivar N, Van Vollenhoven RF. Advances in the treatment of rheumatoid arthritis. *F1000Prime Rep* (2014) 6:31. doi:10.12703/P6-31
22. Zhu Z, Prabakaran P, Chen W, Broder CC, Gong R, Dimitrov DS. Human monoclonal antibodies as candidate therapeutics against emerging viruses and HIV-1. *Virol Sin* (2013) 28(2):71–80. doi:10.1007/s12250-013-3313-x
23. Chiu ML, Gilliland GL. Engineering antibody therapeutics. *Curr Opin Struct Biol* (2016) 38:163–73. doi:10.1016/j.sbi.2016.07.012
24. Schmidt SR. Fusion-proteins as biopharmaceuticals – applications and challenges. *Curr Opin Drug Discov Devel* (2009) 12(2):284–95.
25. Huang C. Receptor-Fc fusion therapeutics, traps, and MIMETIBODY technology. *Curr Opin Biotechnol* (2009) 20(6):692–9. doi:10.1016/j.copbio.2009.10.010
26. Czajkowsky DM, Hu J, Shao Z, Pleass RJ. Fc-fusion proteins: new developments and future perspectives. *EMBO Mol Med* (2012) 4(10):1015–28. doi:10.1002/emmm.201201379
27. Wu B, Sun YN. Pharmacokinetics of peptide-Fc fusion proteins. *J Pharm Sci* (2014) 103(1):53–64. doi:10.1002/jps.23783
28. Dimitrov DS. Engineered CH2 domains (nanoantibodies). *MAbs* (2009) 1(1):26–8. doi:10.4161/mabs.1.1.7480
29. Holliger P, Hudson PJ. Engineered antibody fragments and the rise of single domains. *Nat Biotechnol* (2005) 23(9):1126–36. doi:10.1038/nbt1142
30. Ying T, Gong R, Ju TW, Prabakaran P, Dimitrov DS. Engineered Fc based antibody domains and fragments as novel scaffolds. *Biochim Biophys Acta* (2014) 1844(11):1977–82. doi:10.1016/j.bbapap.2014.04.018
31. Knopp GW, Stadlmayr G, Ruker F. IgG Fc fragment as a scaffold for development of targeted therapeutics. *Curr Pharm Biotechnol* (2016) 17(15):1315–23. doi:10.2174/1389201018666161114152527
32. Lowe D, Dudgeon K, Rouet R, Schofield P, Jermutus L, Christ D. Aggregation, stability, and formulation of human antibody therapeutics. *Adv Protein Chem Struct Biol* (2011) 84:41–61. doi:10.1016/B978-0-12-386483-3.00004-5
33. Shieh IC, Patel AR. Predicting the agitation-induced aggregation of monoclonal antibodies using surface tensiometry. *Mol Pharm* (2015) 12(9):3184–93. doi:10.1021/acs.molpharmaceut.5b00089
34. Torigu T, Maruno T, Hamaji Y, Ohkubo T, Uchiyama S. Synergistic effect of cavitation and agitation on protein aggregation. *J Pharm Sci* (2017) 106(2): 521–9. doi:10.1016/j.xphs.2016.10.015
35. Harn N, Allan C, Oliver C, Midgley CR. Highly concentrated monoclonal antibody solutions: direct analysis of physical structure and thermal stability. *J Pharm Sci* (2007) 96(3):532–46. doi:10.1002/jps.20753
36. He F, Hogan S, Latypov RF, Narhi LO, Razinkov VI. High throughput thermostability screening of monoclonal antibody formulations. *J Pharm Sci* (2010) 99(4):1707–20. doi:10.1002/jps.21955
37. Perico N, Purtell J, Dillon TM, Ricci MS. Conformational implications of an inverted pH-dependent antibody aggregation. *J Pharm Sci* (2009) 98(9):3031–42. doi:10.1002/jps.21539
38. Ejima D, Tsumoto K, Fukada H, Yumioka R, Nagase K, Arakawa T, et al. Effects of acid exposure on the conformation, stability, and aggregation of monoclonal antibodies. *Proteins* (2007) 66(4):954–62. doi:10.1002/prot.21243
39. Dani B, Platz R, Tzannis ST. High concentration formulation feasibility of human immunoglobulin G for subcutaneous administration. *J Pharm Sci* (2007) 96(6):1504–17. doi:10.1002/jps.20508
40. Barnard JG, Singh S, Randolph TW, Carpenter JF. Subvisible particle counting provides a sensitive method of detecting and quantifying aggregation of monoclonal antibody caused by freeze-thawing: insights into the roles of particles in the protein aggregation pathway. *J Pharm Sci* (2011) 100(2):492–503. doi:10.1002/jps.22305
41. Zhang A, Singh SK, Shirts MR, Kumar S, Fernandez EJ. Distinct aggregation mechanisms of monoclonal antibody under thermal and freeze-thaw stresses revealed by hydrogen exchange. *Pharm Res* (2012) 29(1):236–50. doi:10.1007/s11095-011-0538-y
42. Fleischman ML, Chung J, Paul EP, Lewus RA. Shipping-induced aggregation in therapeutic antibodies: utilization of a scale-down model to assess degradation in monoclonal antibodies. *J Pharm Sci* (2017) 106(4):994–1000. doi:10.1016/j.xphs.2016.11.021
43. Cleland JL, Lam X, Kendrick B, Yang J, Yang TH, Overcashier D, et al. A specific molar ratio of stabilizer to protein is required for storage stability of a lyophilized monoclonal antibody. *J Pharm Sci* (2001) 90(3):310–21. doi:10.1002/1520-6017(200103)90:3<310::AID-JPS6>3.0.CO;2-R
44. Cromwell ME, Hilario E, Jacobson F. Protein aggregation and bioprocessing. *AAPS J* (2006) 8(3):E572–9. doi:10.1208/aapsj080366
45. Chennamsetty N, Voynov V, Kayser V, Helk B, Trout BL. Design of therapeutic proteins with enhanced stability. *Proc Natl Acad Sci U S A* (2009) 106(29):11937–42. doi:10.1073/pnas.0904191106
46. Perchiacca JM, Tessier PM. Engineering aggregation-resistant antibodies. *Annu Rev Chem Biomol Eng* (2012) 3:263–86. doi:10.1146/annurev-chembioeng-062011-081052
47. Matsumiya S, Yamaguchi Y, Saito J, Nagano M, Sasakawa H, Otaki S, et al. Structural comparison of fucosylated and nonfucosylated Fc fragments of human immunoglobulin G1. *J Mol Biol* (2007) 368(3):767–79. doi:10.1016/j.jmb.2007.02.034
48. Dwek RA, Lelouch AC, Wormald MR. Glycobiology: ‘the function of sugar in the IgG molecule?’ *J Anat* (1995) 187(Pt 2):279–92.
49. Liu H, Nowak C, Andrien B, Shao M, Ponniah G, Neill A. Impact of IgG Fc-oligosaccharides on recombinant monoclonal antibody structure, stability, safety, and efficacy. *Biotechnol Prog* (2017) 33(5):1173–81. doi:10.1002/btpr.2498
50. Li CH, Narhi LO, Wen J, Dimitrova M, Wen ZQ, Li J, et al. Effect of pH, temperature, and salt on the stability of *Escherichia coli*- and Chinese hamster ovary cell-derived IgG1 Fc. *Biochemistry* (2012) 51(50):10056–65. doi:10.1021/bi300702e

51. Saphire EO, Parren PW, Pantophlet R, Zwick MB, Morris GM, Rudd PM, et al. Crystal structure of a neutralizing human IgG against HIV-1: a template for vaccine design. *Science* (2001) 293(5532):1155–9. doi:10.1126/science.1061692
52. Prabakaran P, Vu BK, Gan J, Feng Y, Dimitrov DS, Ji X. Structure of an isolated unglycosylated antibody C(H)2 domain. *Acta Crystallogr D Biol Crystallogr* (2008) 64(Pt 10):1062–7. doi:10.1107/S0907444908025274
53. Feige MJ, Walter S, Buchner J. Folding mechanism of the CH2 antibody domain. *J Mol Biol* (2004) 344(1):107–18. doi:10.1016/j.jmb.2004.09.033
54. Latypov RF, Hogan S, Lau H, Gadgil H, Liu D. Elucidation of acid-induced unfolding and aggregation of human immunoglobulin IgG1 and IgG2. *Fe. J Biol Chem* (2012) 287(2):1381–96. doi:10.1074/jbc.M111.297697
55. Gong R, Vu BK, Feng Y, Prieto DA, Dyba MA, Walsh JD, et al. Engineered human antibody constant domains with increased stability. *J Biol Chem* (2009) 284(21):14203–10. doi:10.1074/jbc.M900769200
56. Garber E, Demarest SJ. A broad range of Fab stabilities within a host of therapeutic IgGs. *Biochem Biophys Res Commun* (2007) 355(3):751–7. doi:10.1016/j.bbrc.2007.02.042
57. Hari SB, Lau H, Razinkov VI, Chen S, Latypov RF. Acid-induced aggregation of human monoclonal IgG1 and IgG2: molecular mechanism and the effect of solution composition. *Biochemistry* (2010) 49(43):9328–38. doi:10.1021/bi100841u
58. Thakkar SV, Sahni N, Joshi SB, Kerwin BA, He F, Volkin DB, et al. Understanding the relevance of local conformational stability and dynamics to the aggregation propensity of an IgG1 and IgG2 monoclonal antibodies. *Protein Sci* (2013) 22(10):1295–305. doi:10.1002/pro.2316
59. Neergaard MS, Nielsen AD, Parshad H, Van De Weert M. Stability of monoclonal antibodies at high-concentration: head-to-head comparison of the IgG1 and IgG4 subclass. *J Pharm Sci* (2014) 103(1):115–27. doi:10.1002/jps.23788
60. Van Buren N, Rehder D, Gadgil H, Matsumura M, Jacob J. Elucidation of two major aggregation pathways in an IgG2 antibody. *J Pharm Sci* (2009) 98(9):3013–30. doi:10.1002/jps.21514
61. Fast JL, Cordes AA, Carpenter JF, Randolph TW. Physical instability of a therapeutic Fc fusion protein: domain contributions to conformational and colloidal stability. *Biochemistry* (2009) 48(49):11724–36. doi:10.1021/bi900853v
62. Thies MJ, Kammermeier R, Richter K, Buchner J. The alternatively folded state of the antibody C(H)3 domain. *J Mol Biol* (2001) 309(5):1077–85. doi:10.1006/jmbi.2001.4707
63. Dall'Acqua W, Simon AL, Mulkerrin MG, Carter P. Contribution of domain interface residues to the stability of antibody CH3 domain homodimers. *Biochemistry* (1998) 37(26):9266–73. doi:10.1021/bi980270i
64. Thies MJ, Talamo F, Mayer M, Bell S, Ruoppolo M, Marino G, et al. Folding and oxidation of the antibody domain C(H)3. *J Mol Biol* (2002) 319(5):1267–77. doi:10.1016/S0022-2836(02)00375-3
65. McAuley A, Jacob J, Kolvenbach CG, Westland K, Lee HJ, Brych SR, et al. Contributions of a disulfide bond to the structure, stability, and dimerization of human IgG1 antibody CH3 domain. *Protein Sci* (2008) 17(1):95–106. doi:10.1110/ps.073134408
66. Sakurai K, Nakahata R, Lee YH, Kardos J, Ikegami T, Goto Y. Effects of a reduced disulfide bond on aggregation properties of the human IgG1 CH3 domain. *Biochim Biophys Acta* (2015) 1854(10 Pt A):1526–35. doi:10.1016/j.bbapap.2015.02.020
67. Traxlmayr MW, Hasenhindl C, Hackl M, Stadlmayr G, Rybka JD, Borth N, et al. Construction of a stability landscape of the CH3 domain of human IgG1 by combining directed evolution with high throughput sequencing. *J Mol Biol* (2012) 423(3):397–412. doi:10.1016/j.jmb.2012.07.017
68. Yageta S, Shibuya R, Imamura H, Honda S. Conformational and colloidal stabilities of human immunoglobulin G Fc and its cyclized variant: independent and compensatory participation of domains in aggregation of multidomain proteins. *Mol Pharm* (2017) 14(3):699–711. doi:10.1021/acs.molpharmaceut.6b00983
69. Yageta S, Lauer TM, Trout BL, Honda S. Conformational and colloidal stabilities of isolated constant domains of human immunoglobulin G and their impact on antibody aggregation under acidic conditions. *Mol Pharm* (2015) 12(5):1443–55. doi:10.1021/mp500759p
70. Hagihara Y, Saerens D. Engineering disulfide bonds within an antibody. *Biochim Biophys Acta* (2014) 1844(11):2016–23. doi:10.1016/j.bbapap.2014.07.005
71. Bai Y. Intracellular neutralization of viral infection in polarized epithelial cells by neonatal Fc receptor (FcRN)-mediated IgG transport. *Proc Natl Acad Sci U S A* (2011) 108(45):18406–11. doi:10.1073/pnas.1115348108
72. Klein F, Halper-Stromberg A, Horwitz JA, Gruell H, Scheid JF, Bournazos S, et al. HIV therapy by a combination of broadly neutralizing antibodies in humanized mice. *Nature* (2012) 492(7427):118–22. doi:10.1038/nature11604
73. Williams WB, Liao HX, Moody MA, Kepler TB, Alam SM, Gao F, et al. HIV-1 vaccines. Diversion of HIV-1 vaccine-induced immunity by gp41-microbiota cross-reactive antibodies. *Science* (2015) 349(6249):aab1253. doi:10.1126/science.aab1253
74. Auffray C, Sikorav JL, Ollo R, Rougeon F. Correlation between D region structure and antigen-binding specificity: evidences from the comparison of closely related immunoglobulin VH sequences. *Ann Immunol (Paris)* (1981) 132D(1):77–88.
75. Frisch C, Kolmar H, Schmidt A, Kleemann G, Reinhardt A, Pohl E, et al. Contribution of the intramolecular disulfide bridge to the folding stability of REIV, the variable domain of a human immunoglobulin kappa light chain. *Fold Des* (1996) 1(6):431–40. doi:10.1016/S1359-0278(96)00059-4
76. Colby DW, Chu Y, Cassady JP, Duenwald M, Zazulak H, Webster JM, et al. Potent inhibition of huntingtin aggregation and cytotoxicity by a disulfide bond-free single-domain intracellular antibody. *Proc Natl Acad Sci U S A* (2004) 101(51):17616–21. doi:10.1073/pnas.0408134101
77. Goncalvez AP, Chien CH, Tubthong K, Gorshkova I, Roll C, Donau O, et al. Humanized monoclonal antibodies derived from chimpanzee Fabs protect against Japanese encephalitis virus in vitro and in vivo. *J Virol* (2008) 82(14):7009–21. doi:10.1128/jvi.00291-08
78. Franey H, Brych SR, Kolvenbach CG, Rajan RS. Increased aggregation propensity of IgG2 subclass over IgG1: role of conformational changes and covalent character in isolated aggregates. *Protein Sci* (2010) 19(9):1601–15. doi:10.1002/pro.434
79. McConnell AD, Spasojevich V, Macomber JL, Krapf IP, Chen A, Sheffer JC, et al. An integrated approach to extreme thermostabilization and affinity maturation of an antibody. *Protein Eng Des Sel* (2013) 26(2):151–64. doi:10.1093/protein/gzs090
80. Jacobsen FW, Stevenson R, Li C, Salimi-Moosavi H, Liu L, Wen J, et al. Engineering an IgG scaffold lacking effector function with optimized developability. *J Biol Chem* (2017) 292(5):1865–75. doi:10.1074/jbc.M116.748525
81. Liu L, Jacobsen FW, Everds N, Zhuang Y, Yu YB, Li N, et al. Biological characterization of a stable effector functionless (SEFL) monoclonal antibody scaffold in vitro. *J Biol Chem* (2017) 292(5):1876–83. doi:10.1074/jbc.M116.748707
82. Ying T, Chen W, Feng Y, Wang Y, Gong R, Dimitrov DS. Engineered soluble monomeric IgG1 CH3 domain: generation, mechanisms of function, and implications for design of biological therapeutics. *J Biol Chem* (2013) 288(35):25154–64. doi:10.1074/jbc.M113.484154
83. Wozniak-Knopp G, Stadlmann J, Ruker F. Stabilisation of the Fc fragment of human IgG1 by engineered intradomain disulfide bonds. *PLoS One* (2012) 7(1):e30083. doi:10.1371/journal.pone.0030083
84. Wozniak-Knopp G, Ruker F. A C-terminal interdomain disulfide bond significantly stabilizes the Fc fragment of IgG. *Arch Biochem Biophys* (2012) 526(2):181–7. doi:10.1016/j.abb.2012.03.024
85. Chennamsetty N, Helk B, Voynov V, Kayser V, Trout BL. Aggregation-prone motifs in human immunoglobulin G. *J Mol Biol* (2009) 391(2):404–13. doi:10.1016/j.jmb.2009.06.028
86. Voynov V, Chennamsetty N, Kayser V, Helk B, Trout BL. Predictive tools for stabilization of therapeutic proteins. *MAbs* (2009) 1(6):580–2. doi:10.4161/mabs.1.6.9773
87. Chennamsetty N, Voynov V, Kayser V, Helk B, Trout BL. Prediction of aggregation-prone regions of therapeutic proteins. *J Phys Chem B* (2010) 114(19):6614–24. doi:10.1021/jp911706q
88. Chennamsetty N, Voynov V, Kayser V, Helk B, Trout BL. Prediction of protein binding regions. *Proteins* (2011) 79(3):888–97. doi:10.1002/prot.22926
89. Lauer TM, Agrawal NJ, Chennamsetty N, Egodage K, Helk B, Trout BL. Developability index: a rapid in silico tool for the screening of antibody

- aggregation propensity. *J Pharm Sci* (2012) 101(1):102–15. doi:10.1002/jps.22758
90. Linding R, Schymkowitz J, Rousseau F, Diella F, Serrano L. A comparative study of the relationship between protein structure and beta-aggregation in globular and intrinsically disordered proteins. *J Mol Biol* (2004) 342(1):345–53. doi:10.1016/j.jmb.2004.06.088
 91. Fernandez-Escamilla AM, Rousseau F, Schymkowitz J, Serrano L. Prediction of sequence-dependent and mutational effects on the aggregation of peptides and proteins. *Nat Biotechnol* (2004) 22(10):1302–6. doi:10.1038/nbt1012
 92. Rousseau F, Schymkowitz J, Serrano L. Protein aggregation and amyloidosis: confusion of the kinds? *Curr Opin Struct Biol* (2006) 16(1):118–26. doi:10.1016/j.sbi.2006.01.011
 93. Walsh I, Seno F, Tosatto SC, Trovato A. PASTA 2.0: an improved server for protein aggregation prediction. *Nucleic Acids Res* (2014) 42(Web Server issue):W301–7. doi:10.1093/nar/gku399
 94. Conchillo-Sole O, de Groot NS, Aviles FX, Vendrell J, Daura X, Ventura S. AGGRESCAN: a server for the prediction and evaluation of “hot spots” of aggregation in polypeptides. *BMC Bioinformatics* (2007) 8:65. doi:10.1186/1471-2105-8-65
 95. Zambrano R, Jamroz M, Szczasiuk A, Pujols J, Kmiecik S, Ventura S. AGGRESCAN3D (A3D): server for prediction of aggregation properties of protein structures. *Nucleic Acids Res* (2015) 43(W1):W306–13. doi:10.1093/nar/gkv359
 96. Organesyan V, Gao C, Shirinian L, Wu H, Dall'Acqua WF. Structural characterization of a human Fc fragment engineered for lack of effector functions. *Acta Crystallogr D Biol Crystallogr* (2008) 64(Pt 6):700–4. doi:10.1107/s0907444908007877
 97. Shields RL, Namenuk AK, Hong K, Meng YG, Rae J, Briggs J, et al. High resolution mapping of the binding site on human IgG1 for Fc gamma RI, Fc gamma RII, Fc gamma RIII, and FcRn and design of IgG1 variants with improved binding to the Fc gamma R. *J Biol Chem* (2001) 276(9):6591–604. doi:10.1074/jbc.M009483200
 98. Dall'Acqua WF, Kiener PA, Wu H. Properties of human IgG1s engineered for enhanced binding to the neonatal Fc receptor (FcRn). *J Biol Chem* (2006) 281(33):23514–24. doi:10.1074/jbc.M604292200
 99. Borrok MJ, Mody N, Lu X, Kuhn ML, Wu H, Dall'Acqua WF, et al. An “Fc-silenced” IgG1 format with extended half-life designed for improved stability. *J Pharm Sci* (2017) 106(4):1008–17. doi:10.1016/j.xphs.2016.12.023
 100. Majumdar R, Esfandiar R, Bishop SM, Samra HS, Middaugh CR, Volkin DB, et al. Correlations between changes in conformational dynamics and physical stability in a mutant IgG1 mAb engineered for extended serum half-life. *Mabs* (2015) 7(1):84–95. doi:10.4161/19420862.2014.985494
 101. Edgeworth MJ, Phillips JJ, Lowe DC, Kippen AD, Higazi DR, Scrivens JH. Global and local conformation of human IgG antibody variants rationalizes loss of thermodynamic stability. *Angew Chem Int Ed Engl* (2015) 54(50):15156–9. doi:10.1002/anie.201507223
 102. Demarest SJ, Rogers J, Hansen G. Optimization of the antibody C(H)3 domain by residue frequency analysis of IgG sequences. *J Mol Biol* (2004) 335(1):41–8. doi:10.1016/j.jmb.2003.10.040
 103. Chen W, Kong L, Connelly S, Dendle JM, Liu Y, Wilson IA, et al. Stabilizing the CH2 domain of an antibody by engineering in an enhanced aromatic sequon. *ACS Chem Biol* (2016) 11(7):1852–61. doi:10.1021/acschembio.5b01035
 104. Traxlmayr MW, Lobner E, Antes B, Kainer M, Wiederkum S, Hasenhindl C, et al. Directed evolution of Her2/neu-binding IgG1-Fc for improved stability and resistance to aggregation by using yeast surface display. *Protein Eng Des Sel* (2013) 26(4):255–65. doi:10.1093/protein/gzs102
 105. Hasenhindl C, Traxlmayr MW, Wozniak-Knopp G, Jones PC, Stadlmayr G, Ruker F, et al. Stability assessment on a library scale: a rapid method for the evaluation of the commutability and insertion of residues in C-terminal loops of the CH3 domains of IgG1-Fc. *Protein Eng Des Sel* (2013) 26(10):675–82. doi:10.1093/protein/gzt041
 106. Richardson JS, Richardson DC. Natural beta-sheet proteins use negative design to avoid edge-to-edge aggregation. *Proc Natl Acad Sci U S A* (2002) 99(5):2754–9. doi:10.1073/pnas.052706099
 107. Gong R, Wang Y, Ying T, Feng Y, Streaker E, Prabakaran P, et al. N-terminal truncation of an isolated human IgG1 CH2 domain significantly increases its stability and aggregation resistance. *Mol Pharm* (2013) 10(7):2642–52. doi:10.1021/mp400075f
 108. Jefferis R. Glycosylation as a strategy to improve antibody-based therapeutics. *Nat Rev Drug Discov* (2009) 8(3):226–34. doi:10.1038/nrd2804
 109. Li T, DiLillo DJ, Bournazos S, Giddens JP, Ravetch JV, Wang LX. Modulating IgG effector function by Fc glycan engineering. *Proc Natl Acad Sci U S A* (2017) 114(13):3485–90. doi:10.1073/pnas.1702173114
 110. Liu L. Antibody glycosylation and its impact on the pharmacokinetics and pharmacodynamics of monoclonal antibodies and Fc-fusion proteins. *J Pharm Sci* (2015) 104(6):1866–84. doi:10.1002/jps.24444
 111. Raju TS. Terminal sugars of Fc glycans influence antibody effector functions of IgGs. *Curr Opin Immunol* (2008) 20(4):471–8. doi:10.1016/j.co.2008.06.007
 112. Tao MH, Morrison SL. Studies of glycosylated chimeric mouse-human IgG. Role of carbohydrate in the structure and effector functions mediated by the human IgG constant region. *J Immunol* (1989) 143(8):2595–601.
 113. Raju TS, Scallon BJ. Glycosylation in the Fc domain of IgG increases resistance to proteolytic cleavage by papain. *Biochem Biophys Res Commun* (2006) 341(3):797–803. doi:10.1016/j.bbrc.2006.01.030
 114. Ghirlando R, Lund J, Goodall M, Jefferis R. Glycosylation of human IgG-Fc: influences on structure revealed by differential scanning micro-calorimetry. *Immunol Lett* (1999) 68(1):47–52. doi:10.1016/S0165-2478(99)00029-2
 115. Hristodorov D, Fischer R, Joerissen H, Muller-Tiemann B, Apeler H, Linden L. Generation and comparative characterization of glycosylated and aglycosylated human IgG1 antibodies. *Mol Biotechnol* (2013) 53(3):326–35. doi:10.1007/s12033-012-9531-x
 116. Kayser V, Chennamsetty N, Voynov V, Forrer K, Helk B, Trout BL. Glycosylation influences on the aggregation propensity of therapeutic monoclonal antibodies. *Biotechnol J* (2011) 6(1):38–44. doi:10.1002/biot.201000091
 117. Mimura Y, Church S, Ghirlando R, Ashton PR, Dong S, Goodall M, et al. The influence of glycosylation on the thermal stability and effector function expression of human IgG1-Fc: properties of a series of truncated glycoforms. *Mol Immunol* (2000) 37(12–13):697–706. doi:10.1016/S0161-5890(00)00105-X
 118. Boyd PN, Lines AC, Patel AK. The effect of the removal of sialic acid, galactose and total carbohydrate on the functional activity of campath-1H. *Mol Immunol* (1995) 32(17–18):1311–8. doi:10.1016/0161-5890(95)00118-2
 119. Houde D, Peng Y, Berkowitz SA, Engen JR. Post-translational modifications differentially affect IgG1 conformation and receptor binding. *Mol Cell Proteomics* (2010) 9(8):1716–28. doi:10.1074/mcp.M900540-MCP200
 120. Nose M, Wigzell H. Biological significance of carbohydrate chains on monoclonal antibodies. *Proc Natl Acad Sci U S A* (1983) 80(21):6632–6. doi:10.1073/pnas.80.21.6632
 121. Liu H, Nowak C, Shao M, Ponniah G, Neill A. Impact of cell culture on recombinant monoclonal antibody product heterogeneity. *Biotechnol Prog* (2016) 32(5):1103–12. doi:10.1002/bptr.2327
 122. Liu L, Stadheim A, Hamuro L, Pittman T, Wang W, Zha D, et al. Pharmacokinetics of IgG1 monoclonal antibodies produced in humanized *Pichia pastoris* with specific glycoforms: a comparative study with CHO produced materials. *Biologicals* (2011) 39(4):205–10. doi:10.1016/j.biologicals.2011.06.002
 123. Jefferis R. Glycosylation of recombinant antibody therapeutics. *Biotechnol Prog* (2005) 21(1):11–6. doi:10.1021/bp040016j
 124. Pincetic A, Bournazos S, DiLillo DJ, Maamary J, Wang TT, Dahan R, et al. Type I and type II Fc receptors regulate innate and adaptive immunity. *Nat Immunol* (2014) 15(8):707–16. doi:10.1038/ni.2939
 125. Buck PM, Kumar S, Singh SK. Consequences of glycan truncation on Fc structural integrity. *Mabs* (2013) 5(6):904–16. doi:10.4161/mabs.26453
 126. Schaefer JV, Pluckthun A. Engineering aggregation resistance in IgG by two independent mechanisms: lessons from comparison of *Pichia pastoris* and mammalian cell expression. *J Mol Biol* (2012) 417(4):309–35. doi:10.1016/j.jmb.2012.01.027
 127. Alsenaidy MA, Okbazghi SZ, Kim JH, Joshi SB, Middaugh CR, Tolbert TJ, et al. Physical stability comparisons of IgG1-Fc variants: effects of N-glycosylation site occupancy and Asp/Gln residues at site Asn 297. *J Pharm Sci* (2014) 103(6):1613–27. doi:10.1002/jps.23975
 128. Ha S, Ou Y, Vlasak J, Li Y, Wang S, Vo K, et al. Isolation and characterization of IgG1 with asymmetrical Fc glycosylation. *Glycobiology* (2011) 21(8):1087–96. doi:10.1093/glycob/cwr047

129. Zheng K, Bantog C, Bayer R. The impact of glycosylation on monoclonal antibody conformation and stability. *MAbs* (2011) 3(6):568–76. doi:10.4161/mabs.3.6.17922
130. Voynov V, Chennamsetty N, Kayser V, Helk B, Forrer K, Zhang H, et al. Dynamic fluctuations of protein-carbohydrate interactions promote protein aggregation. *PLoS One* (2009) 4(12):e8425. doi:10.1371/journal.pone.0008425
131. Onitsuka M, Kawaguchi A, Asano R, Kumagai I, Honda K, Ohtake H, et al. Glycosylation analysis of an aggregated antibody produced by Chinese hamster ovary cells in bioreactor culture. *J Biosci Bioeng* (2014) 117(5):639–44. doi:10.1016/j.jbiosc.2013.11.001
132. Jefferis R. Recombinant antibody therapeutics: the impact of glycosylation on mechanisms of action. *Trends Pharmacol Sci* (2009) 30(7):356–62. doi:10.1016/j.tips.2009.04.007
133. Sun P, Unger JB, Guo Q, Gong J, Ma H, Palmer PH, et al. Comorbidity between depression and smoking moderates the effect of a smoking prevention program among boys in China. *Nicotine Tob Res* (2007) 9(Suppl 4): S599–609. doi:10.1080/1462200701697653
134. Cho IH, Lee N, Song D, Jung SY, Bou-Assaf G, Susic Z, et al. Evaluation of the structural, physicochemical, and biological characteristics of SB4, a biosimilar of etanercept. *MAbs* (2016) 8(6):1136–55. doi:10.1080/19420862.2016.1193659
135. Gong R, Wang Y, Feng Y, Zhao Q, Dimitrov DS. Shortened engineered human antibody CH2 domains: increased stability and binding to the human neonatal Fc receptor. *J Biol Chem* (2011) 286(31):27288–93. doi:10.1074/jbc.M111.254219
136. Gehlsen K, Gong R, Bramhill D, Wiersma D, Kirkpatrick S, Wang Y, et al. Pharmacokinetics of engineered human monomeric and dimeric CH2 domains. *MAbs* (2012) 4(4):466–74. doi:10.4161/mabs.20652
137. Xiao X, Feng Y, Vu BK, Ishima R, Dimitrov DS. A large library based on a novel (CH2) scaffold: identification of HIV-1 inhibitors. *Biochem Biophys Res Commun* (2009) 387(2):387–92. doi:10.1016/j.bbrc.2009.07.044
138. Gong R, Wang Y, Ying T, Dimitrov DS. Bispecific engineered antibody domains (nanoantibodies) that interact noncompetitively with an HIV-1 neutralizing epitope and FcRn. *PLoS One* (2012) 7(8):e42288. doi:10.1371/journal.pone.0042288
139. Ying T, Wang Y, Prabakaran P, Gong R, Wang L, et al. Engineered antibody domains with significantly increased transcytosis and half-life in macaques mediated by FcRn. *MAbs* (2015) 7(5):922–30. doi:10.1080/19420862.2015.1067353
140. Li D, Gong R, Zheng J, Chen X, Dimitrov DS, Zhao Q. Engineered antibody CH2 domains binding to nucleolin: isolation, characterization and improvement of aggregation. *Biochem Biophys Res Commun* (2017) 485(2):446–53. doi:10.1016/j.bbrc.2017.02.058
141. Wozniak-Knopp G, Bartl S, Bauer A, Mostageer M, Woisetschlag M, Antes B, et al. Introducing antigen-binding sites in structural loops of immunoglobulin constant domains: Fc fragments with engineered HER2/neu-binding sites and antibody properties. *Protein Eng Des Sel* (2010) 23(4):289–97. doi:10.1093/protein/gzq005
142. Ying T, Chen W, Gong R, Feng Y, Dimitrov DS. Soluble monomeric IgG1 Fc. *J Biol Chem* (2012) 287(23):19399–408. doi:10.1074/jbc.M112.368647
143. Chen X, Zeng F, Huang T, Cheng L, Liu H, Gong R. Optimization on Fc for improvement of stability and aggregation resistance. *Curr Pharm Biotechnol* (2016) 17(15):1353–9. doi:10.2174/1389201017666161117145312

Conflict of Interest Statement: The authors declare that the research was conducted in the absence of any commercial or financial relationships that could be construed as a potential conflict of interest.

Copyright © 2018 Yang, Gao and Gong. This is an open-access article distributed under the terms of the Creative Commons Attribution License (CC BY). The use, distribution or reproduction in other forums is permitted, provided the original author(s) or licensor are credited and that the original publication in this journal is cited, in accordance with accepted academic practice. No use, distribution or reproduction is permitted which does not comply with these terms.



Immunoglobulin Fc Heterodimer Platform Technology: From Design to Applications in Therapeutic Antibodies and Proteins

Ji-Hee Ha¹, Jung-Eun Kim¹ and Yong-Sung Kim^{1,2*}

¹ Department of Molecular Science and Technology, Ajou University, Suwon, Korea, ² Department of Applied Chemistry and Biological Engineering, College of Engineering, Ajou University, Suwon, Korea

OPEN ACCESS

Edited by:

Tianlei Ying,
Fudan University, China

Reviewed by:

Sang Taek Jung,
Kookmin University, South Korea
Roland E. Kontermann,
University of Stuttgart, Germany

***Correspondence:**

Yong-Sung Kim
kimys@ajou.ac.kr

Specialty section:

This article was submitted to
Immunotherapies and Vaccines,
a section of the journal
Frontiers in Immunology

Received: 14 July 2016

Accepted: 16 September 2016

Published: 06 October 2016

Citation:

Ha J-H, Kim J-E and Kim Y-S (2016)
Immunoglobulin Fc Heterodimer Platform Technology: From Design to Applications in Therapeutic Antibodies and Proteins.
Front. Immunol. 7:394.
doi: 10.3389/fimmu.2016.00394

The monospecific and bivalent characteristics of naturally occurring immunoglobulin G (IgG) antibodies depend on homodimerization of the fragment crystallizable (Fc) regions of two identical heavy chains (HCs) and the subsequent assembly of two identical light chains (LCs) via disulfide linkages between each HC and LC. Immunoglobulin Fc heterodimers have been engineered through modifications to the CH3 domain interface, with different mutations on each domain such that the engineered Fc fragments, carrying the CH3 variant pair, preferentially form heterodimers rather than homodimers. Many research groups have adopted different strategies to generate Fc heterodimers, with the goal of high heterodimerization yield, while retaining biophysical and biological properties of the wild-type Fc. Based on their ability to enforce heterodimerization between the two different HCs, the established Fc heterodimers have been extensively exploited as a scaffold to generate bispecific antibodies (bsAbs) in full-length IgG and IgG-like formats. These have many of the favorable properties of natural IgG antibodies, such as high stability, long serum half-life, low immunogenicity, and immune effector functions. As of July 2016, more than seven heterodimeric Fc-based IgG-format bsAbs are being evaluated in clinical trials. In addition to bsAbs, heterodimeric Fc technology is very promising for the generation of Fc-fused proteins and peptides, as well as cytokines (immunocytokines), which can present the fusion partners in the natural monomeric or heterodimeric form rather than the artificial homodimeric form with wild-type Fc. Here, we present relevant concepts and strategies for the generation of heterodimeric Fc proteins, and their application in the development of bsAbs in diverse formats for optimal biological activity. In addition, we describe wild-type Fc-fused monomeric and heterodimeric proteins, along with the difficulties associated with their preparations, and discuss the use of heterodimeric Fc as an alternative scaffold of wild-type Fc for naturally monomeric or heterodimeric proteins, to create Fc-fusion proteins with novel therapeutic modality.

Keywords: bispecific antibody, Fc engineering, heterodimeric Fc, Fc-fusion proteins, immunocytokines, antibody engineering

INTRODUCTION

Bispecific antibodies (bsAbs) simultaneously bind two different antigens or two distinct epitopes on the same antigen as a single molecule; they differ from naturally occurring immunoglobulin G (IgG) monospecific antibodies (mAbs) (1, 2). Owing to their additional targeting ability, bsAbs often offer improved clinical benefits for the treatment of complicated diseases, such as cancers and immune disorders, wherein multiple cell-surface receptors or ligands are engaged (1–3). Numerous efforts have been made to engineer mAbs into bsAbs, which has resulted in the generation of more than 60 different bsAb formats (3–5). Many bsAbs have been engineered by linking antibody fragments, such as single-chain variable fragments (scFv), antigen-binding fragments (Fab), and heavy (VH) and light chain (VL) variable domains, as well as their appendages to IgG-format mAbs (3–6). However, these novel formats, deviating from the conventional IgG structure, often suffer from poor physicochemical properties, such as low solubility and aggregation, difficulties in large-scale manufacturing, poor pharmacokinetics, and potential immunogenicity (3–6). To improve the developability, bsAbs in the formats of intact IgG or IgG-like (containing an Fc) architectures have been extensively developed (5–7).

Conventional IgG antibodies are bivalent and monospecific, the assembly of which depends upon *in vivo* homodimerization of two identical heavy chains (HCs), which is mediated by homodimeric associations between CH3 domains, and subsequently disulfide linkages between each HC and each light chain (LC), in B cells (8–11). Thus, the development of bsAbs, using intact IgG formats with wild-type HCs and LCs, faces HC–HC and HC_{VH-CH1}–LC mispairing problems (5, 7). Some approaches for IgG-based bsAbs, based on wild-type homodimeric Fc regions, have been utilized, such as a dual-action Fab (DAF, two-in-one antibody) (12), a κλ-body (13), and a rat/mouse chimeric antibody (14). However, DAF and κλ-body technologies require extensive antibody engineering and screening and are not easy to generate with previously established mAbs. The rat/mouse chimeric antibody requires multiple purification stages, suffers from low purification yields, and faces potential immunogenicity.

To address the HC mispairing problem, heterodimeric Fc technology, which enables two different HCs to be preferentially assembled together, rather than with the same HCs, has been developed (5, 7, 15). Heterodimeric, Fc-based, intact IgG-format bsAbs have been developed in combination with a common LC approach (16) or with two distinct LCs, using the CrossMab technology (17) and ortho-Fab IgG technology (18). Additional heterodimeric Fc scaffolds have been extensively exploited for the generation IgG-like bsAbs by appending antigen-binding antibody fragments, such as VH, VL, scFv, Fab, and single-chain Fab (scFab). Depending on the designed architectures, the resulting bsAbs differ in antigen specificity (from monospecific to tetraspecific) and antigen-binding valency (from monovalent to tetravalent). In addition to the heterodimeric IgG scaffolds for bsAbs, heterodimeric Fc fragments are now emerging as excellent scaffolds to create

Fc-fused monomeric or heterodimeric proteins or cytokines, which are challengeable formats to be achieved by wild-type homodimeric Fc.

In this review, we first focus on the design and generation of heterodimeric Fc and their application in the development of therapeutic bsAbs in diverse formats. We then describe the current status of homodimeric Fc-fused monomeric proteins and peptides and propose that heterodimeric Fc fragments, which can present the fusion partner as native-like monomeric or heterodimeric forms, represent a promising scaffold for the next generation of Fc-fused proteins and cytokines.

HETERODIMERIC Fc ENGINEERING

Wild-type Fc homodimerization is initially mediated by a large, tightly packed interface (~2469 Å² buried surface area), between the two identical CH3 domains with sub-nanomolar affinity, and subsequently by disulfide linkages in the hinge region (**Figure 1A**) (8, 9). For this reason, heterodimeric Fc variants have been mainly engineered through the replacement of homodimer-favoring interactions at the CH3 domain interface with heterodimer-favoring interactions. This is achieved by introducing asymmetric mutations in each CH3 domain, which promotes the assembly of HCs from two different antibodies (**Figure 1B**). This heterodimeric Fc engineering, using CH3 variant pairs, has been approached using two strategies: (1) structure-based rational design and (2) directed evolution.

X-ray crystal structures of human IgG1 Fc show that Fc homodimerization is driven by both hydrophobic interactions at the center of the CH3 interface core and symmetric electrostatic interactions surrounding the rim of the hydrophobic core (19, 20), as schematically shown in **Figure 2A**. Thus, structure-based rational design of heterodimeric Fc fragments has been utilized to generate heterodimeric CH3 variant pairs (CH3A:CH3B) with different mutations in each chain at the CH3 interface core such that the variant pair thermodynamically favors the formation of heterodimers over the homodimers. The structure-based rational design of such heterodimeric CH3 variant pairs can be classified into four strategies: (i) symmetric-to-asymmetric steric complementarity design (e.g., KiH, HA-TF, and ZW1) (21–24), (ii) charge-to-charge swap (e.g., DD-KK) (25), (iii) charge-to-steric complementarity swap plus additional long-range electrostatic interactions (e.g., EW-RVT) (26), and (iv) isotype strand swap [e.g., strand-exchange engineered domain (SEED)] (7, 24), as summarized in **Table 1**. Critical parameters in heterodimeric Fc engineering include the yield of heterodimeric Fc formation over unwanted homodimeric Fc contaminants, minimal loss in stability relative to the natural Fc, and maintaining natural Fc-like properties, such as serum half-lives and effector functions. Heterodimeric Fc-directed bsAb formation usually yields greater than 90% of the desired product by co-expressing two heterodimer Fc-based antibodies. This makes it feasible for large-scale production and quality control to meet clinical needs. In contrast to heterodimeric Fc engineering, an approach to generate monomeric Fc fragments was explored by introducing four mutations at the CH3 interface (27).

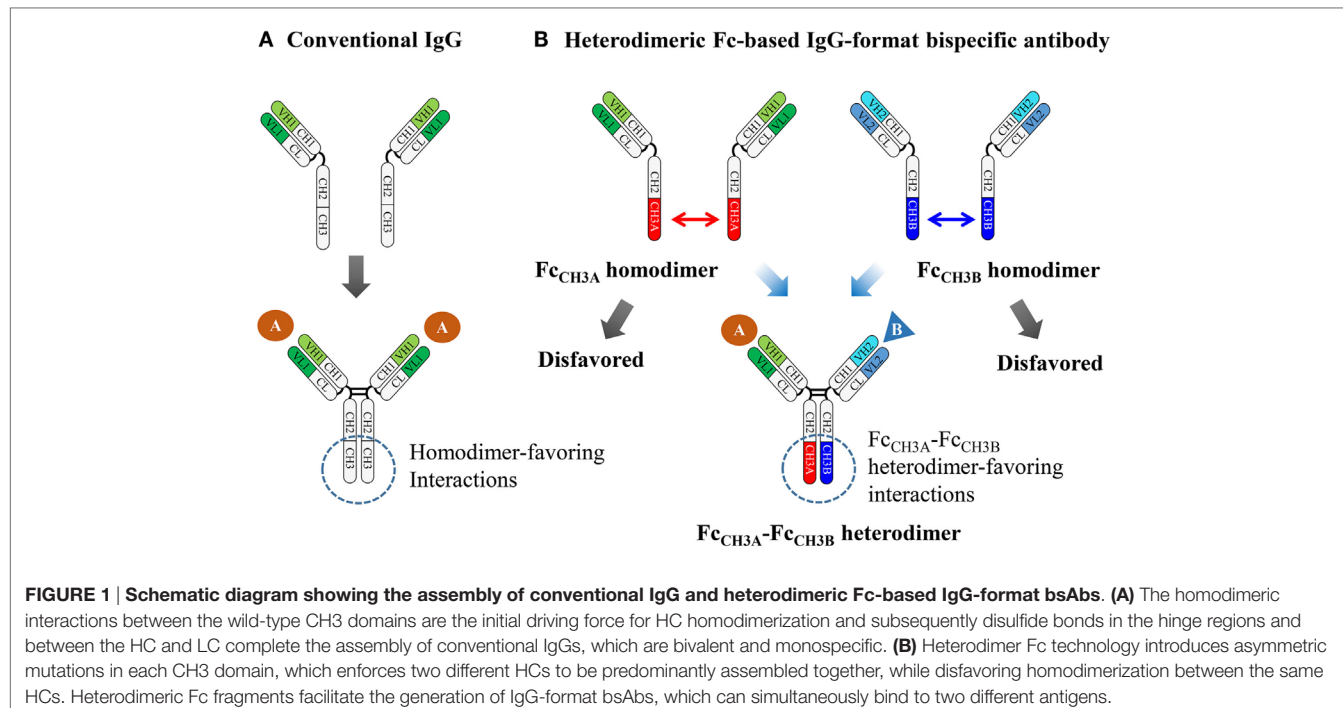


FIGURE 1 | Schematic diagram showing the assembly of conventional IgG and heterodimeric Fc-based IgG-format bsAbs. (A) The homodimeric interactions between the wild-type CH3 domains are the initial driving force for HC homodimerization and subsequently disulfide bonds in the hinge regions and between the HC and LC complete the assembly of conventional IgGs, which are bivalent and monospecific. **(B)** Heterodimer Fc technology introduces asymmetric mutations in each CH3 domain, which enforces two different HCs to be predominantly assembled together, while disfavoring homodimerization between the same HCs. Heterodimeric Fc fragments facilitate the generation of IgG-format bsAbs, which can simultaneously bind to two different antigens.

Symmetric-to-Asymmetric Steric Complementarity Design

In a pioneering approach, Carter and colleagues from Genentech conceived the heterodimeric Fc variant and invented the so-called “Knobs-into-Holes (KiH)” Fc technology (21, 22). The concept was to introduce a “knob” in one CH3 domain (CH3A) by substitution of a small residue with a bulky one (i.e., T366W_{CH3A} in EU numbering). To accommodate the “knob,” a complementary “hole” surface was created on the other CH3 domain (CH3B) by replacing the closest neighboring residues to the knob with smaller ones (i.e., T366S/L368A/Y407V_{CH3B}) (Figure 2B) (15). The “hole” mutation was optimized by structured-guided phage library screening (21). X-ray crystal structures of KiH Fc variants (28, 33) demonstrated that heterodimerization is thermodynamically favored by hydrophobic interactions driven by steric complementarity at the inter-CH3 domain core interface, whereas the knob–knob and the hole–hole interfaces do not favor homodimerization owing to steric hindrance and disruption of the favorable interactions, respectively. The KiH Fc was further engineered to improve purity and stability by introducing an additional inter-CH3 domain disulfide bond pair, S354C_{CH3A}–Y349C_{CH3B}, generating the KiH_{S-S} Fc variant. This exhibited a high yield of heterodimerization (~95%) and improved thermal melting (T_m) of the CH3 domain by 6 to ~78°C (16). Most KiH Fc-based bsAbs currently being evaluated in clinical trials have adopted the KiH_{S-S} Fc as a scaffold (Table 2).

Extensive strategies combining structure-based computational design of many variants and subsequent experimental validation to assess the heterodimerization yield have been adopted to generate other heterodimeric Fc variants with sterically complementary mutations. These include HA-TF Fc from

Xencor (23) and ZW1 Fc from Zymeworks (24). Particularly, ZW1 was generated by a two-stage approach, combining negative design to first destabilize the natural Fc homodimer-favoring interactions at the CH3–CH3 interfaces and then positive design of the previously designed variant to increase biophysical stability (24, 45). Negative design, maximizing unfavorable interactions in potential homodimers while promoting specificity between heterodimeric species, generated an Fc variant with F405A/Y407V_{CH3A}–T366L/T394W_{CH3B}, and resulting in a heterodimerization yield of ~95% (24). However, the T_m of the CH3 domain was ~72°C, similar to that of KiH Fc (22), but ~10°C lower than that of the wild-type CH3 domain (30). The subsequent positive design, which added T350V/L351Y_{CH3A}–T350V/K392L_{CH3B} mutations to the first variant, yielded ZW1 (T350V/L351Y/F405A/Y407V_{CH3A}–T350V/T366L/K392L/T394W_{CH3B}), which retained the high Fc heterodimerization yield of ~95% and exhibited Fc stability similar to that of the wild-type CH3 domain with a T_m value of 81.5°C (24). The high heterodimer purity of ZW1, validated by stable expression in Chinese hamster ovary (CHO) cells, and the favorable biophysical properties could improve the manufacturability of ZW1-based bsAbs (45).

More recently, Leaver-Fay et al. (29) computationally produced heterodimeric Fc variants, using an explicit multistate design (sequence optimization) combined with negative design to destabilize and eliminate homodimer-favoring inter-CH3 interactions. One of the best clones, 7.8.60 Fc, was first designed by introducing mutations of D399M_{CH3A}–K409V_{CH3B} to eliminate the conserved electrostatic interactions of D399-K392/K409 in the wild-type CH3 interface. In the next-round, computational optimization identified the following substitutions sequentially: Y407A_{CH3A}–T366V_{CH3B} to minimize CH3B

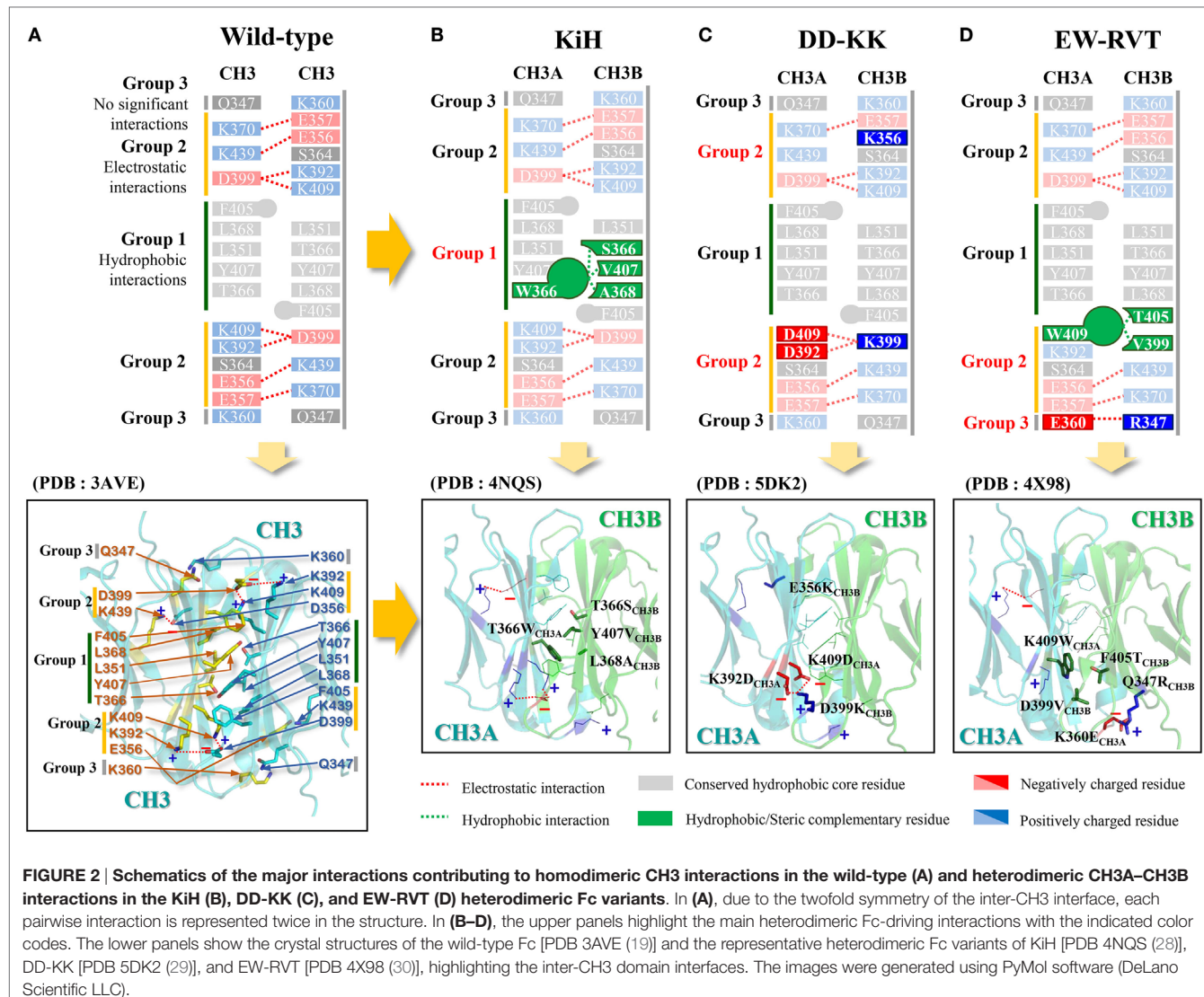


FIGURE 2 | Schematics of the major interactions contributing to homodimeric CH3 interactions in the wild-type (A) and heterodimeric CH3A–CH3B interactions in the KiH (B), DD-KK (C), and EW-RVT (D) heterodimeric Fc variants. In (A), due to the twofold symmetry of the inter-CH3 interface, each pairwise interaction is represented twice in the structure. In (B–D), the upper panels highlight the main heterodimeric Fc-driving interactions with the indicated color codes. The lower panels show the crystal structures of the wild-type Fc [PDB 3AVE (19)] and the representative heterodimeric Fc variants of KiH [PDB 4NQS (28)], DD-KK [PDB 5DK2 (29)], and EW-RVT [PDB 4X98 (30)], highlighting the inter-CH3 domain interfaces. The images were generated using PyMol software (DeLano Scientific LLC).

homodimerization and to improve the heterodimer formation, K360D_{CH3A} – Q347R_{CH3B} to eliminate CH3B homodimers, and finally E345R_{CH3B} to strengthen the K360D_{CH3A}–Q347R_{CH3B} interaction (Table 1). The crystal structure determined clearly resolved the interface and showed that the models were very accurate. The 7.8.60 heterodimeric Fc combined with orthogonal Fab interface mutation technology (18) produced intact IgG-format bsAbs with ~93% purity (29).

Charge-to-Charge Swap Design

As an alternative approach, Gunasekaran et al. from Amgen (25) sought to design a heterodimeric Fc by reversing symmetric charge complementarity at the CH3 domain interface, while retaining hydrophobic core integrity (Figure 2C). Owing to twofold symmetry at the inter-CH3 interface, the targeted electrostatic interaction pairs were symmetrically duplicated on both peripheral sides of the hydrophobic core (Figure 2A). They converted the symmetric charge-pair residues into asymmetric charge

polarity by first designing a K409D_{CH3A}–D399K_{CH3B} pair variant and then further screening for additional charge-pair mutations through experimentally assessing heterodimerization yield. This resulted in DD-KK with K409D/K392D_{CH3A}–D399K/E356K_{CH3B} mutation pairs. The asymmetric charge mutation pairs drove heterodimerization, whereas “positively charged” and “negatively charged” homodimers were suppressed by unfavorable repulsive charge interactions. Particularly, E356K_{CH3B} was introduced in an attempt to suppress the Fc_{CH3B}–Fc_{CH3B} homodimerization to increase the purity of Fc_{CH3A}–Fc_{CH3B} heterodimer. The DD-KK design resulted in greater than 90% heterodimerization depending on the transfection ratio of the two chains.

Charge-to-Steric Complementarity Swap and Long-Range Electrostatic Interaction Design

The concept of KiH and DD-KK Fc design can be summarized as the replacement of the symmetric hydrophobic and electrostatic

TABLE 1 | Design and strategies for heterodimeric Fc variants.

Heterodimeric Fc name	Paired mutations		Heterodimer-favoring interactions	PDB ID	Reference
	CH3A chain	CH3B chain			
KiH	T366W	T366S/L368A/Y407V	Hydrophobic/steric complementarity	4NQS/5DI8/5HY9	(28)
KiH _{S-S}	T366W/S354C	T366S/L368A/Y407V/Y349C	KiH + inter-CH3 domain S-S bond	–	(16, 29)
HA-TF	S364H/F405A	Y349T/T394F	Hydrophobic/steric complementarity	–	(23)
ZW1	T350V/L351Y/F405A/Y407V	T350V/T366L/K392L/T394W	Hydrophobic/steric complementarity	4BSW	(24)
7.8.60	K360D/D399M/Y407A	E345R/Q347R/T366V/K409V	Hydrophobic/steric complementarity + electrostatic complementarity	5DJZ (Partial)	(29)
DD-KK	K409D/K392D	D399K/E356K	Electrostatic complementarity	5DK2	(25)
EW-RVT	K360E/K409W	Q347R/D399V/F405T	Hydrophobic/steric complementarity plus long-range electrostatic interaction	4X98	(26, 30)
EW-RVT _{S-S}	K360E/K409W/Y349C	Q347R/D399V/F405T/S354C	EW-RVT + inter-CH3 domain S-S bond	4X99	(30)
SEED	IgA-derived 45 residues on IgG1 CH3	IgG1-derived 57 residues on IgA CH3	Hydrophobic/steric complementarity (strand exchange between IgG and IgA)	–	(31)
A107	K370E/K409W	E357N/D399V/F405T	Hydrophobic/steric complementarity + hydrogen bonding complementarity (directed evolution using yeast surface display)	–	(32)

TABLE 2 | Heterodimeric Fc-based antibody formats, generated in previous studies, and now being evaluated in clinical trials.

Antibody format	Heterodimeric Fc scaffold	Fusion format (target)		Clinical trials	Reference
		Fc _{CH3A}	Fc _{CH3B}		
Monospecific and monovalent antibodies					
VH-Fc/VL-Fc	EW-RVT	VH (c-Met)	VL (c-Met)	–	(26)
Fc/Fab-Fc	KiH	–	Fab (c-Met)	Phase 3 (failed)	(34)
HC _{VH-CH1} -Fc/LC-Fc	DD-KK	HC _{VH-CH1} (mTNFR1)	LC (mTNFR1)	–	(25)
IgG-like formats with appendages of scFv and scFab					
scFv-Fc/scFv-Fc	EW-RVT	scFv (c-Met)	scFv (VEGFR-2)	–	(26)
scFv-Fc/scFv-Fc	DD-KK	scFv (CD3)	scFv (TARTK)	–	(25)
Fc/scFv ₂ -Fc (Fc/BiTE-Fc)	KiH	–	scFv ₂ (CD3/EpCAM)	–	(35)
Fab-Fc/scFv-Fc	HA-TF	Fab (CD123)	scFv (CD3)	Phase 1	(36)
		Fab (CD20)	scFv (CD3)	Phase 1	
Fab-Fc/scFab-Fc (OAscFab-IgG)	KiH _{S-S}	Fab (EGFR)	scFab (IGF-1R)	–	(37)
scFab-Fc/scFab-Fc-scFv	KiH _{S-S}	scFab-Fc (EGFR)	scFab-Fc-scFv (IGF1R/HER3)	–	(38)
scFab-Fc-scFv /scFab-Fc-scFv	KiH _{S-S}	scFab-Fc-scFv (EGFR/HER3)	scFab-Fc-scFv (IGF1R/HER3)	–	(38)
Fab-CrossMab ^{CH1-CL} IgG	KiH _{S-S}	Fab (CEA)	Fab-CrossFab ^{CH1-CL} (CEA/CD3)	Phase 1	(39, 40)
Fv-/Fv-CrossMab ^{CH1-CL} IgG	KiH _{S-S}	Fv-Fab-Fc (HER2/VEGF)	Fv-CrossFab ^{CH1-CL} -Fc (HER2/EGFR)	–	(41)
Intact IgG formats with correct LC association					
Common LC-IgG	KiH _{S-S}	Fab (FIXa)	Fab (FX)	Phase 3	(42)
CrossMab ^{CH1-CL} IgG	KiH _{S-S}	Fab (Ang-2)	CrossFab ^{CH1-CL} (VEGFA)	Phase 1 (RG7221); Phase 2 (RG7716)	(17, 39)
Four-in-one CrossMab ^{CH1-CL} IgG	KiH _{S-S}	Dual-action Fab (EGFR/HER3)	Dual-action CrossFab ^{CH1-CL} (HER2/VEGF)	–	(41)
Ortho-Fab IgG	DD-KK	Ortho-Fab (EGFR)	Ortho-Fab (c-Met)	Phase 1	(18)
Intact IgG formats with <i>in vitro</i> assembly					
IgG	KiH	Fab (BACE1)	Fab (TfR)	–	(43, 44)

interactions conserved at the CH3 interface with the same, but asymmetric, interactions. In contrast to the sterics-based KiH design and charge-swap DD-KK design, Choi et al. (26) replaced the conserved, symmetric electrostatic interactions at the buried interface of the CH3 domains with asymmetric hydrophobic interactions. This resulted in the generation of a W-VT Fc variant with K409W_{CH3A}-D399V/F405T_{CH3B} mutations, favoring Fc heterodimer formation (~77% purity) due to complementary hydrophobic interactions, while disfavoring homodimers owing to the loss of the K409-D399 electrostatic interactions and the

steric collision of K409W_{CH3A}-F405_{CH3A}. To increase the heterodimerization yield of W-VT, they replaced a K360-Q347 pair with negligible interactions, owing to the long distance (4.61 Å) at the rim of the CH3 interface (19) with the K360E_{CH3A}-Q347R_{CH3B} asymmetric mutation pair, which favors the heterodimer because of the long-range electrostatic interaction at a distance of 3.45 Å (30). The combined heterodimeric Fc, called EW-RVT (Figure 2D), showed a heterodimer yield of ~91% and a CH3 domain T_m value of ~77.5°C, which were comparable to those of KiH and DD-KK Fc variants (26). The X-ray crystal structure

of the EW-RVT Fc heterodimer led to the addition of an inter-CH3 disulfide bond with a Y349C_{CH3A}-S354C_{CH3B} pair, yielding EW-RVT_{S-S} Fc. The asymmetric disulfide bond was confirmed by resolving the crystal structure (30). EW-RVT_{S-S} Fc showed improved heterodimer yield (by ~3%) and higher thermodynamic stability of the CH3 domain (by ~2.8°C) compared to those parameters of the parent EW-RVT Fc (30). The crystal structures of EW-RVT and EW-RVT_{S-S} Fc fragments, obtained to determine the molecular details of the CH3A/CH3B interface, revealed that the mutations did not cause any significant changes in the Fc structure (30). In agreement with the crystal structure, the EW-RVT Fc heterodimer displayed the native IgG1-like, pH-dependent, neonatal Fc receptor (FcRn) binding pattern, and Fcγ receptor (FcγR) interaction, which were equivalent to those of the native IgG1 (previously reported) (46, 47). This suggests that the EW-RVT-based antibody will have similar serum half-lives and effector functions to those of the conventional human IgG1.

Isotype Strand Swap Design

Davis et al. from Merck Serono (31) designed a heterodimeric Fc by mixing human IgG and IgA CH3 domain segments to create a complementary CH3 heterodimer, which was referred to as SEED Fc. Native CH3 domains of human IgA and IgG are structurally similar (10), but cannot dimerize because of lower homology within interface residues. They analyzed the structural dimerization motif in the CH3 domain of each isotype and devised SEED through the exchange of some β-strand segments in the CH3 domain of each isotype to drive heterodimer formation through steric complementary contact surfaces. The SEED-based antibodies (e.g., SEEDbody) were purified with a protein A resin and exhibited long serum half-life and effector functions comparable to those of wild-type human IgG1 Fc-based antibodies (48). However, owing to the artificial sequence of the SEED CH3 heterodimer, the potential immunogenicity has not been determined.

Directed Evolution of Heterodimeric Fc

Aforementioned Fc heterodimers have been generated through structure-based rational design or computational modeling. Recently, Choi et al. (32) generated heterodimeric Fc variants through directed evolution combined with yeast surface display and high-throughput screening (49, 50). A combinatorial heterodimeric Fc library display system was developed by mating two haploid yeast cell lines; one haploid cell line displayed an Fc chain library (displayed Fc_{CH3A}) with mutations in one CH3 domain on the yeast cell surface, and the other cell line secreted an Fc chain library (secreted Fc_{CH3B}) with mutations in the other CH3 domain. In the mated cells, secreted Fc_{CH3B} was displayed on the cell surface through heterodimerization with the displayed Fc_{CH3A}. Fluorescence-based detection of this interaction enabled screening of the library for heterodimeric Fc variants by flow cytometry. For the proof-of-concept, they constructed combinatorial heterodimeric Fc libraries with simultaneous mutations on targeted residues of both CH3A and CH3B based on the template of the W-VT Fc variant, and screened the libraries to isolate numerous heterodimeric Fc variants with heterodimerization yields of ~90%. This directed evolution

approach identified unexpected heterodimer-favoring mutation pairs at the CH3 interface, such as hydrogen bonding or cation–π interactions, as well as homodimer-disfavoring pairs, which have not been tested by structure-guided rational design. The best clone, A107, exhibited a heterodimerization yield of ~93%, which was much higher than that (~77%) of the parent W-VT Fc variant.

HETERODIMERIC Fc-BASED ANTIBODIES IN DIVERSE FORMATS

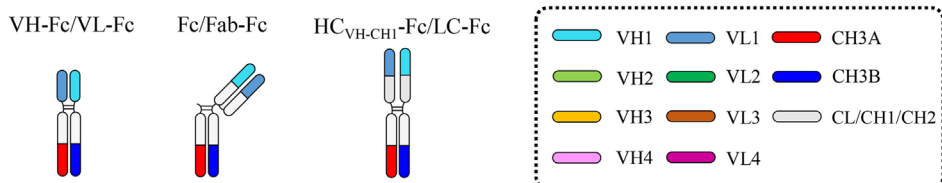
Heterodimeric Fc are compatible with independent fusion of two different antigen-binding units to the N- and/or C-terminus of each Fc chain. This facilitates the creation of diverse heterodimeric Fc-based antibodies with differences in specificity, binding valency, geometry of target-binding sites, among others, as summarized in **Figure 3** and **Table 2**.

Monospecific and Monovalent Antibodies

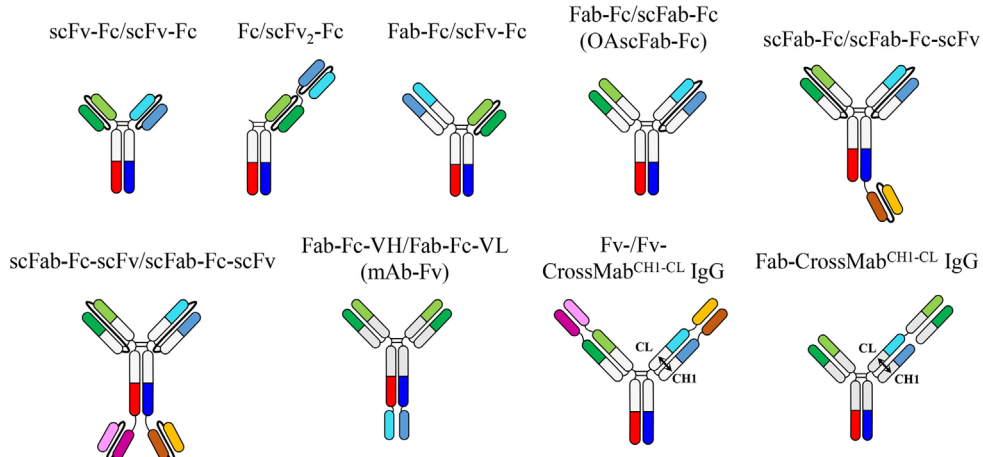
Heterodimeric Fc-based monospecific antibodies (mAbs) with monovalent antigen binding have been generated by fusion of the Fab to the N-terminus of only one Fc chain (Fc/Fab-Fc), the scFv to the N-terminus of only one Fc chain (Fc/scFv-Fc), the VH-CH1 (HC_{VH-CH1}) and VL-CL to the respective N-termini of each heterodimeric Fc chain (HC_{VH-CH1}-Fc/LC-Fc), or the VH and VL to the respective N-termini of each heterodimeric Fc chain (VH-Fc/VL-Fc) (**Figure 3**).

The Y-shape of typical IgG antibodies often limits their utility against some targets, whereby bivalent target-binding dimerizes and agonizes, rather than antagonizes, the intended targets. For example, targeting the c-Met receptor tyrosine kinase with bivalent antibodies can mimic the ligand hepatocyte growth factor (HGF)-mediated agonism via receptor dimerization (51). To address this issue, Genentech developed a KiH Fc-based, one-armed Fc/Fab-Fc format monovalent antibody, onartuzumab (MetMab), through fusion of a humanized anti-c-Met 5D5 Fab to the N-terminus of only the “hole” of the Fc chain (34). Whereas the bivalent anti-c-Met 5D5 IgG antibody acted as an agonist causing c-Met-activated tumor cell growth, rather than growth inhibition, the monovalent MetMab bound the receptor in a one-to-one fashion to inhibit HGF binding and block receptor activation, thus acting as an antagonist. Co-expression of three chains, specifically the Fc, HC_{VH-CH1}-Fc, and LC, from three respective cistrons on a single plasmid, and targeting these chains to the periplasmic space of *Escherichia coli*, efficiently resulted in the production of MetMab. Purification by size-exclusion chromatography yielded ~95% purity (34). A clinical trial of MetMab combined with the epidermal growth factor receptor (EGFR) kinase inhibitor erlotinib to block metastasis in non-small cell lung cancer was recently halted in Phase 3, but other clinical trials with MetMab are expected. The EW-RVT Fc variant was also applied to make a MetMab-like monovalent antibody in the VH-Fc/VL-Fc format, called msMet, wherein the VH and VL of MetMab were fused to the N-terminus of each heterodimeric Fc chain (26). As a single agent, the msMet antibody suppressed the *in vivo* tumor growth of human gastric cancer xenografts in mice.

A Monospecific and monovalent antibodies



B IgG-like formats with appendages of scFv and scFab



C Intact IgG formats with correct LC association

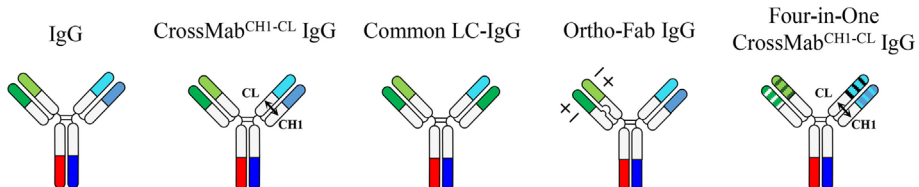


FIGURE 3 | Overview of heterodimeric Fc-based antibodies, which are subdivided into three classes: (A) monospecific and monovalent antibodies, (B) IgG-like formats with appendages of scFv and scFab, and (C) intact IgG formats with correct LC association. Each domain is color coded as indicated in the dotted box. Connecting peptide linkers in scFv and scFab fragments are shown by thin black lines. Details are described in the text.

DD-KK Fc was exploited to generate a monovalent 14D2 antibody, in the $\text{HC}_{\text{VH-CH1}}\text{-Fc}/\text{LC-Fc}$ format, to target tumor necrosis factor receptor 1 (TNFR1) by linking the VH-CH1 and VL-CL of the anti-TNFR1 14D2 antibody to the N-terminus of each heterodimeric Fc chain (25). The parent bivalent 14D2 antibody showed undesirable activity, specifically activation of TNFR1 at low doses via cross-linking of the receptor, similar to that observed for the TNF ligand. However, the monovalent antibody was devoid of agonistic activity, and blocked TNF-mediated chemokine induction in mice. Importantly, the monovalent 14D2 antibody exhibited similar pharmacokinetic profiles as the full-length IgG when injected in mice.

IgG-Like Formats with Appendages of scFv and scFab

Heterodimeric Fc technology can resolve the HC mispairing problem, but still faces the challenge of a LC-pairing problem, specifically, cognate $\text{HC}_{\text{VH-CH1}}\text{-LC}$ pairing in the Fab region,

to generate bsAbs in intact IgG formats (5, 7). To address the $\text{HC}_{\text{VH-CH1}}\text{-LC}$ -pairing problem, single-chain antigen-binding units, such as scFv and scFab, have been, respectively, linked to each heterodimeric Fc chain or tandemly linked to one heterodimeric Fc chain, generating IgG-like bsAbs in formats of scFv-Fc/scFv-Fc, scFab-Fc/scFab-Fc, Fc/scFv₂-Fc, Fab-Fc-VH/Fab-Fc-VL, Fab-Fc/scFv-Fc, Fab-Fc/scFab-Fc, and scFab-Fc-(scFv)/scFab-Fc-scFv (Figure 3).

The EW-RVT Fc was exploited to generate a bsAb, dubbed bsVeMet, simultaneously targeting both c-Met and VEGF receptor 2 (VEGFR-2), with two respective antigen-specific scFvs fused to the N-termini of each heterodimeric Fc in the format of scFv-Fc/scFv-Fc (26). The bsVeMet more potently inhibited HGF and VEGF-stimulated cell proliferation, downstream signaling, and *in vivo* angiogenesis than the two parent mAbs.

Furthermore, bsAbs have been extensively designed to recruit immune effector cells, such as T cells, to tumor cells (52, 53). Bispecific T-cell Engager (BiTE) was constructed by tandem

connection of two scFvs, one of which was specific to CD3 on T cells and the other was specific to a tumor-associated antigen on tumor cell surfaces. The goal of this strategy was to engage cytotoxic T cells for lysis of the targeted antigen-expressing cancer cells, and was first developed by Mack and colleagues (54). Later, the CD19 × CD3 BiTE blinatumomab was developed by Micromet and clinically approved in 2014 for the treatment of relapsed/refractory B-cell acute lymphocytic leukemia (55). However, the serum half-life of tandem scFv-based BiTEs in mice was only 5–6 h (56), which was much shorter than that of Fc-containing antibodies. The fast clearance of blinatumomab requires infusions or repeated injections to maintain a therapeutically effective dose over a prolonged period, specifically, daily infusions for 8 weeks in clinical trials (57). To improve pharmacokinetics of such scFv-based BiTEs, a DD-KK Fc-based bsAb was generated in the scFv-Fc/scFv-Fc format by fusing two scFvs with different binding specificities, one against human CD3 and the other against a tumor-associated receptor tyrosine kinase (TARTK), to each Fc heterodimer chain (25). Due to the presence of the Fc region, the scFv-Fc/scFv-Fc antibody exhibited a much longer *in vivo* half-life in mice and could be administered more infrequently compared to other types of CD3 bispecific scFv fragments (25). The CD3 × TARTK bsAb completely suppressed the growth of the TARTK-positive glioma in a xenograft mouse model.

Xu et al. from Sutro Biopharma (35) produced a KiH Fc-based BiTE bsAbs using the *E. coli*-based cell-free expression system. They designed epithelial cell adhesion molecule (EpCAM) × CD3 bsAbs in the two-armed scFv-Fc/scFv-Fc format or the one-armed Fc/scFv₂-Fc (i.e., Fc/BiTE-Fc) format and further reversed the two formats by exchanging the “knob” Fc and “hole” Fc fusion partner. They found that the expression yield and biological activities, such as dual targeting and tumor cell killing by engaging T cells, was highly variable and depended on the formats. This suggested that a more sophisticated optimization process is necessary to determine the optimal ratio of the two expression plasmids for enhanced cell-free expression of the Fc fusion partner for the two scFvs or the tandem scFv BiTE. Intriguingly, the KiH Fc-based bsAb (100 kDa) showed significantly longer serum half-life ($T_{1/2} \approx 4.9\text{--}5.2$ days) than the BiTE control (50 kDa) ($T_{1/2} \approx 0.2$ days), but were less stable than trastuzumab IgG (150 kDa) ($T_{1/2} \approx 25$ days) and scFv-Fc (100 kDa) ($T_{1/2} \approx 9.1$ days) in mice. This might be attributed to destabilizing mutations in the CH3 domains of the KiH Fc (35).

Using an HA-TF Fc scaffold, Xencor generated Her2 × CD3 or Her2 × CD16 bsAbs in Fab-Fc-VH/Fab-Fc-VL (dubbed mAb-Fv) format through the fusion of VH and VL domains of CD3 or CD16 antibodies to the C-termini of two distinct HCs (23). The advantage of the mAb-Fv format is improved tumor targeting due to bivalent antigen engagement through two intact arms of the IgG mAb, compared to the monovalent target-binding formats, such as scFv-Fc/scFv-Fc and scFab-Fc/scFab-Fc. However, mAb-Fv showed non-native oligomeric species and the C-terminal Fv exhibited inferior affinity to the CD16 or CD3 antigen compared to the parent Fab. This was most likely due to steric hindrance and suggested the need for C-terminal-fused Fv optimization. For these reasons, Xencor adopted an HA-TF Fc-based Fab-Fc/

scFv-Fc bsAb format (dubbed “plug-and-play” platform), which showed native mAb-like stability and non-compromised antigen-binding activity (36). For example, the Fab-Fc/scFv-Fc formatted bsAbs, such as CD123 × CD3 (XmAb14045) and CD20 × CD3 (XmAb13676), are expected to begin clinical Phase 1 trials for acute myeloid leukemia (NCT02730312) and B-cell malignancies, respectively, in 2016.¹ Glenmark Pharm is also developing bsAbs in a heterodimeric Fc-based Fab-Fc/scFv-Fc format (dubbed “BEAT” by Glenmark), in which the heterodimeric Fc was designed by introducing mutations, mimicking the natural association of the heterodimeric T-cell receptor (TCR) α and β chains, into the interface between the two CH3 domains of IgG (58).

Schanzer et al. from Roche (37, 59) generated a KiH Fc-based bsAb XGFR in the format of Fab-Fc/scFab-Fc for targeting EGFR with the Fab format in one arm and the insulin-like growth factor receptor type I (IGF-1R) with scFab format in the other arm. The format of XGFR bsAb, the so-called one arm scFab IgG (OAscFab-IgG) was devised to prevent incorrect pairing of LCs, while maintaining the closest possible format to intact IgG. XGFR was produced with high expression yields comparable to those of the respective parent IgG mAbs. However, other tested bsAb formats of IgG-scFv (IGF-1R IgG with C-terminal attachment of disulfide-stabilized EGFR scFv) and dual-variable domain (DVD)-IgG (IGF-1R IgG with the N-terminal attachment of EGFR VH and VL in the HC and LC, respectively) showed ~2-fold and ~16-fold lower expression yields than that of the OAscFab-IgG format (37, 59). To further increase immune effector functions triggered by XGFR bsAb, the heterodimeric Fc portion was glycoengineered to remove the fucosylation, leading to strong antibody-dependent cell-mediated cytotoxicity. The resulting XGFR demonstrated potent anti-tumor efficacy in multiple mouse xenograft tumor models (37, 59). In addition, Castoldi et al. from Roche (38) constructed a KiH_{s-s} Fc-based trispecific antibody (dubbed TriMAb) in the scFab-Fc-(scFv)/scFab-Fc-scFv format, in which anti-EGFR and anti-IGF-1R scFabs are on the respective arm of IgG with anti-Her3 scFv fused to the C-terminus of both chains or only one chain. The EGFR × IGF-1R × HER3 TriMAb showed growth inhibitory effects comparable to that of a combination of each single parental antibody, in a model cell proliferation assay.

Intact IgG Formats with Correct LC Association

IgG-like bsAbs based on appending scFv and scFab to heterodimeric Fc fragments have overcome HC_{VH-CH1}-LC mispairing issues within the Fab region, but they are limited in their use of linkers, the length and composition of which often needs to be optimized. A sub-optimal linker can cause undesirable problems, such as loss of antigen binding, due to binding site hindrance, poor expression levels, immunogenicity, poor pharmacokinetics, and *in vivo* cleavage. Thus, many attempts have been made to develop bsAbs that deviate minimally from natural IgG antibodies without the use of artificial linkers. Since antigen specificity usually resides in the Fv chain composed of the VH and VL, correct

¹<http://xencor.com/>

pairing between the cognate HC and LC during co-expression and assembly of bsAbs is essential to ensure antigen-binding specificity and affinity. LC mispairing occurs because the Fab heterodimerization interfaces of VH–VL and CH1–CL between two distinct antibodies are almost identical, though the complementarity determining regions (CDRs) of VH and VL are quite different. Thus, to generate bsAbs using a full-length IgG format, cognate $\text{HC}_{\text{VH-CH1}}$ –LC pairing should be ensured, in addition to correct HC pairing by heterodimeric Fc technology. The LC mispairing problem has been addressed by using a common LC (15, 16), a domain crossover (CrossMab) (17), and a designed orthogonal Fab interface (18) (**Figure 3**).

The use of a common LC, compatible with the two distinct $\text{HC}_{\text{VH-CH1}}$ s, is a straightforward way to construct bsAbs with intact IgG formats (15). Two mAbs can be first isolated from a human scFv phage library sharing identical VLs and then assembled into a single IgG format using KiH Fc-based HC heterodimerization (16, 60). However, this approach constrains antibody discovery for two different targets with a single LC or requires novel antibody libraries, and is difficult to adopt when using two different previously established antibodies. A notable example of an IgG-format bsAb using a common LC in combination with a KiH Fc is emicizumab (ACE910) developed by Chugai, which targets factor IXa and factor X (FIXa × FX) (61, 62). They first generated various FIXa- and FX-specific mAbs by immunizing mice with human FIXa and FX antigens and then generated a lead chimeric bsAb based on the retention of biological activity and the feasibility of using only one LC (62). FIXa and FX form a complex with cofactor FVIII but the complex formation is deficient in hemophilia A patients. Standard treatment for this disease includes frequent injection of recombinant or plasma-derived factor VIII (62). Emicizumab mimics FVIII functions by allowing FIXa and FX to be close for the formation of the complex. This is because the distance between the FIXa- and FX-binding sites of FVIIIa is similar to that between the two antigen-binding site arms of the Y-shaped IgG. Emicizumab overcomes the short half-life ($T_{1/2} \approx 0.5$ days) of recombinant FVIII and is expected the lower immunogenicity. Emicizumab is now in a Phase 3 clinical study in patients with hemophilia A (NCT02622321) (42).

To facilitate antibody generation with a common LC, Merus developed a transgenic mouse (MeMo), engineered to generate antibodies with a single human common LC and diverse human HCs (63). The MeMo technology combined with their own CH3-domain engineered heterodimeric Fc technology allows them to generate intact IgG-format bsAb (dubbed Biclonics by Merus).² A Biclonics-based bsAb MCLA-128 targeting Her2 × Her3 is now being evaluated in Phase 1/2 clinical trials for patients with solid tumors (64).

CrossMab technology from Roche (17) is another strategy to solve the $\text{HC}_{\text{VH-CH1}}$ –LC association problem in combination with KiH Fc technology. This technology keeps one Fab untouched, whereas the VH or CH1 domain of the other Fab is switched with partner VL or CL domains. In the early proof-of-concept stage of CrossMabs, they were evaluated in three formats according to

the crossover region: (1) CrossMab^{Fab}, crossover of the complete VH–CH1 and VL–CL domains, (2) CrossMab^{VH–VL}, crossover of only the VH and VL domains, and (3) CrossMab^{CH1–CL}, crossover of only the CH1 and CL domains. Although the three CrossMab variants showed comparable thermal stability to that of the parental IgG mAbs, the CrossMab^{CH1–CL} format showed only minimal unwanted side products; however, the other two formats produced some portion of side products (17). For this reason, the CrossMab^{CH1–CL} format was predominantly used over the other two formats. CrossMab-based bsAbs might be easily derived from pre-existing antibody pairs using domain crossover without the need for identification of common LC and the Fab interface mutations, required for correct LC association (39). Many CrossMAbs have been generated and evaluated and currently four different CrossMab-based bsAbs are now in active Phase 1/2 clinical trials (39) (**Table 1**). For example, two versions of a VEGF × Ang2 CrossMab^{CH1–CL} are currently being evaluated in clinical trials: (1) RG7221 (Vanucizumab), one VEGF × Ang2 CrossMab^{CH1–CL}, in Phase 1 in patients with cancers (NCT01688206) and (2) RG7716, the other tailor-made VEGF × Ang2 CrossMab^{CH1–CL}, in Phase 2 trials for patients with macular degeneration (NCT02484690).

The CrossMab^{CH1–CL} format was further extended by fusion of a Fab to the N-terminus to generate the Fab-CrossMab^{CH1–CL} format for trivalent bsAbs (**Figure 3**). Using this format, IgG-based T-cell bsAbs (TCBs) with bivalent binding to carcinoembryonic antigen (CEA), dubbed CEA-TCB, was developed (40). Currently, a Phase 1 clinical trial of CEA-TCB is ongoing (NCT02324257) for the treatment of CEA-expressing solid tumors (39). Furthermore, the genetic fusion of the two different DAFs (dual-action Fabs, i.e., two-in-one antibody), one EGFR × Her3 DAF and another Her2 × VEGF DAF, to the N-terminus of each arm of a KiH-based four-in-one CrossMab^{CH1–CL} format generated the EGFR × Her3 × Her2 × VEGF targeting tetraspecific IgG-format antibody (41) (**Figure 3**). The same group also generated an EGFR × Her3 × Her2 × VEGF targeting tetraspecific, tetravalent antibody by combining the CrossMab^{CH1–CL} and DVD-IgG technologies (65), resulting in the Fv-/Fv-CrossMab^{CH1–CL} IgG format (41) (**Figure 3**).

An alternative approach for enforcing correct $\text{HC}_{\text{VH-CH1}}$ –LC association includes introduction of a set of mutations at the heterodimeric VL–CL and VH–CH1 interface (18, 66, 67), similar to modification of the CH3 interface for the heterodimeric Fc design. In an ortho-Fab IgG approach (18), structure-based regional design introduced complementary mutations at the LC and $\text{HC}_{\text{VH-CH1}}$ interface in only one Fab, without any changes being made to the other Fab (**Figure 3**). Based on the ortho-Fab IgG format combined with heterodimeric Fc technology, the EGFR × c-Met bsAb (LY3164530) from Eli Lilly was generated, which is currently being evaluated in a Phase 1 clinical study of patients with advanced or metastatic cancer (NCT02221882). Zymeworks is also currently developing intact IgG-format bsAbs generated by the combination of ortho-Fab IgG and ZW1 Fc technologies.³

²<http://www.merus.nl/>

³<http://www.zymeworks.com/>

In Vitro Assembly of Intact IgG Formats

Heterodimeric Fc technology alone, without the combination of HC_{VH-CH1}-LC association technology, can generate intact IgG-format bsAbs by separate expression of two parental half-antibodies [HC-LC (HL) pairs] and subsequent *in vitro* recombination into desirable bsAbs, the assembly of which is driven by heterodimer-favoring Fc interactions under controlled biochemical conditions (60). This approach allows the correct HC_{VH-CH1}-LC association during the expression stage of the parental half-antibody and maintains the cognate HC_{VH-CH1}-LC pairing in the next *in vitro* assembly step. Spiess et al. from Genentech (68) further combined the two separate processes into one step by co-culture of two transformed *E. coli* cell lines, each expressing a half-antibody. They demonstrated the robustness of the technology by producing 28 unique IgG bsAbs. However, this *E. coli* expression system was limited to production of non-glycosylated antibodies. Shatz et al. (69) applied this technology to a mammalian expression system to produce glycosylated antibodies. A notable example of a bsAb prepared using the above manufacturing system is the TfR × BACE1 bsAb that targets TfR (transferrin receptor) and BACE1 (β-site amyloid precursor protein-cleaving enzyme) (43, 44). In a human TfR knock-in mouse, the bsAb could cross the blood-brain barrier and accumulated in the mouse brain where it inhibited BACE1 to reduce brain Aβ production (44). This bsAb was validated in preclinical models, and is now on the path to clinical trials.

Unlike the human IgG1 isotype, IgG4 has been shown to undergo Fab arm exchange (FAE) both *in vivo* and *in vitro*, in which one half-antibody (HL pair) recombines with other half-antibodies from other IgG4 molecules (10, 70, 71). The structural basis of IgG4 for FAE resides in the IgG4 core hinge region (²²⁶Cys-Pro-Ser-Cys-Pro²³⁰), and especially the Ser228 residue and the CH3 domains (critically, the R409 residue) (70, 72). To confer FAE ability to IgG1, two groups engineered FAE-capable IgG1 by introducing the FAE-associated IgG4-specific mutation pairs at the core hinge region and inter-CH3 interface, for example, D221E/P228E/L368E_{CH3A}-D221R/P228R/K409R_{CH3B} (dubbed EEE-RRR) from Rinat-Pfizer (73), or only at the inter-CH3 interface, such as K409R_{CH3A}-K405L_{CH3B} (dubbed Duobody) from Genmab (72). The retention of the stable wild-type IgG1 hinge in the Duobody technology might be beneficial for the generation of bsAbs, which are resistant to reduction under physiological conditions *in vivo* and are much more stable during storage after FAE-mediated manufacturing (74). It should be noted that the above two mutation pairs at the CH3 interface are not enough to predominantly produce heterodimeric Fc fragments when the two HCs are co-expressed, unlike the KiH, DD-KK, and EW-RVT heterodimeric Fc technology. Instead, two mAbs based on the FAE-capable IgG1 are separately expressed and purified and then mixed together under mild redox conditions, resulting in a stable IgG1 bsAb with high yields (greater than 90%) (72–74). The EGFR × c-Met bsAb (JNJ-61186372) generated by Duobody technology was effective against EGFR inhibitor-resistant lung tumors in mice (75).

Fc-FUSED PROTEINS WITH THE NATURAL MONOMERIC OR HETERODIMERIC FORM

The genetic fusion of proteins, such as ligand-binding soluble receptors, cytokines, growth factors, enzymes, and peptides, to the Fc domain of human IgG1 is a well-established strategy to extend the serum half-life and often enhance biological activity through dimerization of the fusion partner (76–78). Conjugation to the Fc may also enhance tissue penetration of the fusion partner by FcRn-mediated transcytosis (79, 80). In addition, the Fc moiety in many cases improves the biophysical properties of its fusion partner, such as the solubility and stability of the protein (81). At the end of 2015, about 11 Fc-fusion proteins had been clinically approved (82). All of the marketed Fc-fusion proteins and many others in clinical trials are based on the wild-type human IgG1 Fc, which presents the fusion partner as a homodimer due to the homodimeric Fc structure. However, some cytokines and hormones naturally occurring in monomeric or heterodimeric forms exhibit markedly improved pharmacokinetics and even biological activities when they are fused to the Fc in natural forms (83). Thus, Fc-fusion, while keeping the original configuration of the fusion partners, is desirable for those proteins. However, as described below, generation of such Fc-fused monomeric or heterodimeric proteins based on the wild-type Fc is not straightforward (Figures 4A–C) due to the homodimeric structure. A promising solution to this limitation is the use of a heterodimeric Fc as an alternative scaffold to wild-type Fc (Figures 4D,E).

Wild-Type Fc-Fused Protein Monomers

Naturally occurring monomeric cytokines and hormones, such as erythropoietin (Epo), interferon α/β (IFNα/β), and Factor IX (FIX), Fc-fused proteins in the native monomer format, dubbed Fc-fused monomers, showed improved pharmacokinetics and even biological activities, compared to Fc-fused dimers (83). Epo is a glycoprotein hormone drug of ~34 kDa that exerts its effects by binding to the Epo receptor to stimulate red blood cell production (84). Bitonti et al. (85, 86) demonstrated that human IgG1 Fc-fused Epo in monomeric format (Epo-Fc monomer), consisting of a single molecule of Epo conjugated to a wild-type Fc dimer (Figure 4A), exhibited enhanced pharmacokinetic and pharmacodynamic properties, compared to the Epo-Fc dimer, in both cynomolgus monkeys and humans. The inferior activity of the Epo-Fc dimer might be attributed to steric hindrance introduced by two molecules of Epo linked to a dimeric Fc; this could adversely affect the binding to respective receptors (83). To prepare an Epo-Fc monomer, two plasmids encoding FLAG-tagged Epo-Fc at the C-terminus (Epo-Fc-FLAG) and untagged Epo-Fc were first co-transfected into CHO cells. Three protein products were produced by the cells: the Epo-Fc/Epo-Fc homodimer (Epo-Fc dimer), the EpoFc/Epo-Fc-FLAG heterodimer (Epo-Fc monomer), and the Epo-Fc-FLAG/Epo-Fc-FLAG homodimer. The Epo-Fc monomer was purified using a combination of protein A chromatography, size-exclusion chromatography, and subsequently FLAG-affinity chromatography (85, 87).

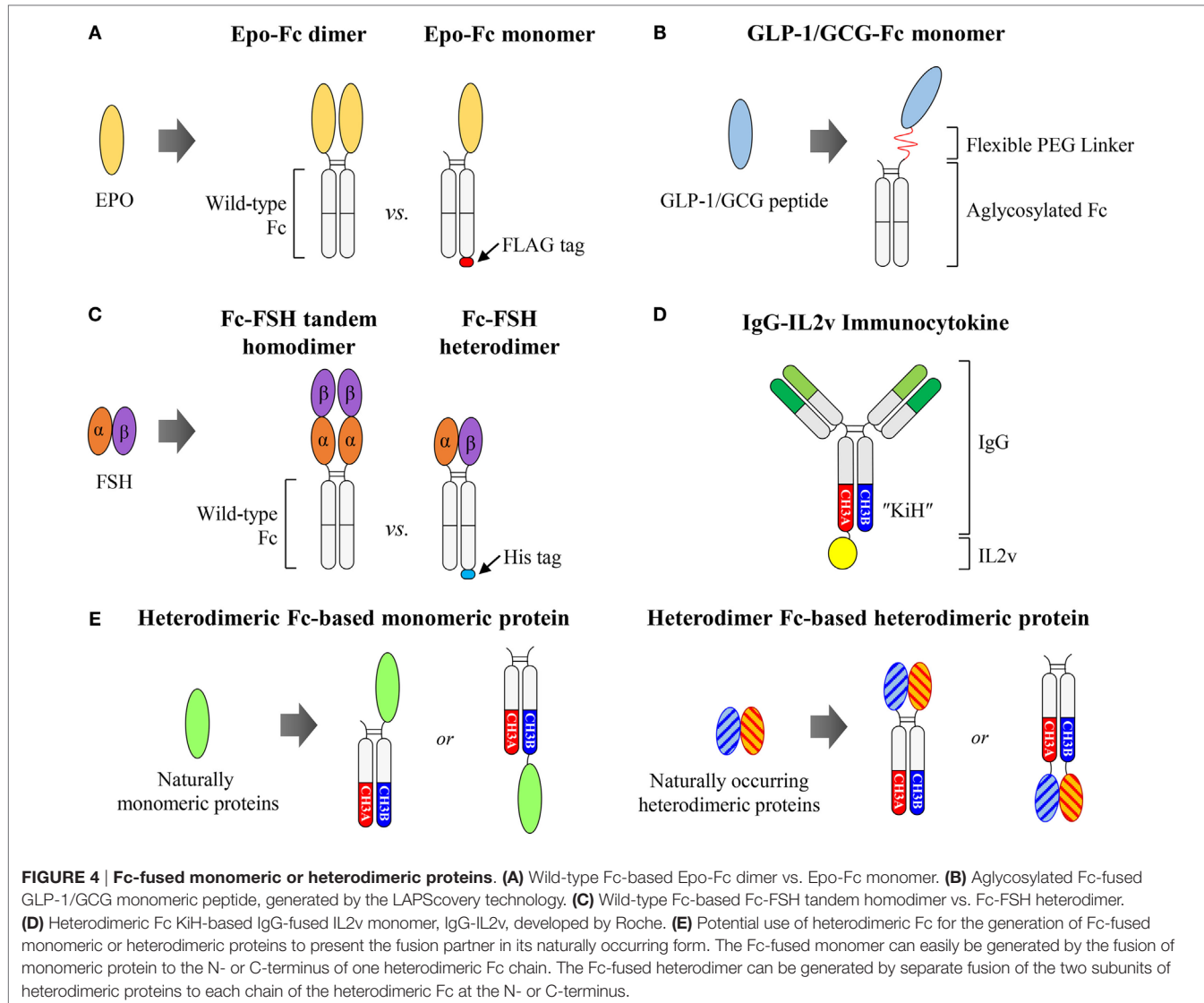


FIGURE 4 | Fc-fused monomeric or heterodimeric proteins. **(A)** Wild-type Fc-based Epo-Fc dimer vs. Epo-Fc monomer. **(B)** Aglycosylated Fc-fused GLP-1/GCG monomeric peptide, generated by the LAPScovery technology. **(C)** Wild-type Fc-based Fc-FSH tandem homodimer vs. Fc-FSH heterodimer. **(D)** Heterodimeric Fc KiH-based IgG-fused IL2v monomer, IgG-IL2v, developed by Roche. **(E)** Potential use of heterodimeric Fc for the generation of Fc-fused monomeric or heterodimeric proteins to present the fusion partner in its naturally occurring form. The Fc-fused monomer can easily be generated by the fusion of monomeric protein to the N- or C-terminus of one heterodimeric Fc chain. The Fc-fused heterodimer can be generated by separate fusion of the two subunits of heterodimeric proteins to each chain of the heterodimeric Fc at the N- or C-terminus.

Similar to the Epo-Fc monomer, Fc-fused monomer formats of IFN β , IFN α , and FIX exhibited much better biological activity in the monkey models compared to corresponding Fc-fused dimers (83). Intriguingly, in the case of IFN α , the IFN α -Fc monomer showed very similar pharmacokinetics to that of the IFN α -Fc dimer; however, the IFN α -Fc monomer displayed much better *in vivo* efficacy compared to the IFN α -Fc dimer (83). This enhanced efficacy of IFN α -Fc monomer was also dependent on the length of the linker between the IFN α and Fc regions. Longer linker length resulted in increased specific activity of the IFN α -Fc monomer, indicating that there might have been some steric hindrance between IFN α and its receptor. The Fc-fused monomer was then prepared as described previously for the Epo-Fc monomer. Thus, the desired Fc-fused monomer could theoretically be prepared up to only 33% of the total expression yield. Despite many desirable properties of Fc-fused monomers, the development of wild-type Fc-based monomers faces difficulties associated with isolating desired Fc-fused monomers from

other format mixtures using robust purification steps, and is also limited by the inherent poor yield of a maximum of 33%.

For Fc-fused monomeric peptides, Kang et al. from Hanmi Pharm (88) developed a glucagon-like peptide-1 (GLP-1)/glucagon (GCG) dual agonist for the potential treatment of obesity and diabetes by activating both GLP-1 and GCG receptors based on LAPScovery™ (Long-Acting Protein/Peptide Discovery) technology. They chemically conjugated GLP-1/GCG peptides to only one arm of human IgG1 aglycosylated Fc fragments, produced from *E. coli* via a flexible polyethylene glycol (PEG) linker (**Figure 4B**). The GLP-1/GCG-Fc monomer exhibited markedly improved pharmacokinetics and greater *in vivo* biological activity compared to the GLP-1/GCG-Fc dimer (89). However, the preparation of the GLP-1/GCG-Fc monomer was complicated, requiring separate Fc preparation, *in vitro* chemical conjugation of the GLP-1/GCG peptide to the Fc via a PEG linker, and, finally, multi-step purification of the desired product from the reaction mixture (89). Based on LAPScovery technology, aglycosylated

Fc-fused monomers for insulin, human growth hormone, and granulocyte-colony stimulating factor were developed, and are now in clinical trials in Europe.⁴

Wild-Type Fc-Fused Protein Heterodimers

For heterodimeric proteins composed of two different subunits, the Fc-fusion format, achieved by fusion of each subunit independently to separate Fc fragments might be desirable to maintain biological activity, in comparison to the homodimeric form by tandem subunit linkage to wild-type Fc. Follicle-stimulating hormone (FSH) is a non-covalently linked heterodimeric protein consisting of α and β subunits, and its recombinant protein is commonly used for therapy in the treatment of both male and female infertility (90). However, it requires daily injections for several days for up to months due to its short half-life (35 h in humans) (90). To prepare long-acting FSH, Low et al. (91) designed a human IgG1 Fc-fused FSH in two different formats. One is a single chain-linked FSH-Fc (Fc-FSH tandem homodimer) with tandemly linked α - β subunits fused to the N-terminus of the Fc fragment. The other is a heterodimeric FSH-Fc (Fc-FSH heterodimer) with α and β subunits fused separately to the N-termini of each arm of the Fc fragment (**Figure 4C**). They found that the Fc-FSH heterodimer was significantly more active than the Fc-FSH tandem homodimer, whereas the two Fc-fusion proteins had similar terminal serum half-lives in both rodents and monkeys. It is likely that the architecture of the Fc-FSH heterodimer might present the α and β subunits in a more favorable conformation for bioactivity than that of the Fc-FSH tandem homodimer. To purify Fc-FSH heterodimers, they inserted a 6 \times His-tag into the C-terminus of the β subunit-fused Fc fragment only. As a result, whereas the Fc-FSH tandem homodimer was ~90% pure following a single protein A chromatography step, the Fc-FSH heterodimer required additional purification by nickel affinity chromatography to achieve similar purity. However, in addition to multi-step purifications, such preparations of Fc-FSH heterodimers gave lower purification yields (33%) compared to the total expression yield.

Antibody-Fused Cytokines, Immunocytokines

Cytokines are key players in controlling immune responses during physiological and pathophysiological processes (92). Various cytokines have been clinically approved for diverse immune-related diseases, including interleukin-2 (IL2) and tumor necrosis factor (TNF) as well as INF α for malignant cancer therapy (92, 93). However, the therapeutic efficacy of cytokines is often hampered by poor pharmacokinetics and significant toxicity associated with their systemic administration. To overcome such limitations, antibody-cytokine fusion proteins, the so-called immunocytokines, have been devised in an attempt to enhance antibody-mediated tumor tissue targeting of cytokines, and to increase serum half-lives (93, 94). However, a recent study in mice using an immunocytokine of IL2-fused to tumor antigen-specific IgG in format of IgG-IL2, showed that the biodistribution

and pharmacokinetics are entirely governed by the cytokine IL2 moiety, rather than the expected antibody-targeting antigen specificity (95). The IgG-IL2 predominantly remained systemic and was associated with innate immune cells expressing IL2 receptors regardless of antigen specificity or Fc γ R interactions, whereas the parent IgG antibody was preferentially accumulated in antigen-targeted tumors (95). Rather than the IgG-IL2 immunocytokine, a combination of an anti-tumor antigen IgG antibody and an untargeted Fc-IL2 monomer was approached for synergistic anti-tumor immunotherapy (96).

Furthermore, the biodistribution of immunocytokines was considerably influenced by the ratio of antibody to cytokine. IL12 is a heterodimer (~70 kDa) consisting of heavy (p40) and light (p35) chain subunits, which are covalently linked by disulfide bonds (97). In an attempt to develop IL12-based immunocytokines combined with an L19 scFv that targets the EDB domain of fibronectin, Gafner et al. (98) constructed three different forms of immunocytokines differing in the ratio of antibody to cytokine. They found that the format with 2:1 antibody to cytokine ratio of p40-L19 scFv/L19 scFv-p35, a heterodimeric fusion protein in which the disulfide-linked p35 and p40 subunits of IL12 are fused to L19 scFv, displayed the highest tumor-targeting performance in biodistribution studies. Thus, enhanced therapeutic activity was observed when compared to the other two formats having 1:1 or 2:2 ratio of antibody to cytokine. Similar results were also obtained with IL12 immunocytokines generated with a different F8 scFv antibody (99). With a monomeric cytokine of IL7 (~20 kDa), the same group evaluated the biodistribution of three different formats of IL7-fused F8 scFv immunocytokines differing in antibody to cytokine ratios (100). They found that, as in the case of IL12, the format with a 2:1 antibody to cytokine ratio showed the highest tumor localization compared to the other two formats with 1:1 and 2:2 ratios.

Heterodimeric Fc-Fused Immunocytokines

The above results suggest that increasing the antibody to cytokine ratio results in improved tumor tissue localization via decreasing cytokine-mediated targeting, which can potentially reduce the dose-related toxicity. IgG-based immunocytokines have been typically generated by fusion of cytokines to the C-terminus of homodimeric Fc fragments of HCs, which present the cytokine as a homodimeric form (31). However, such IgG-based immunocytokines might display poor pharmacokinetics and distribution, as shown with IgG-IL2 formats (95, 101). To generate an IgG-based cytokine monomer format for monomeric (e.g., IL2, IL4, IL7, IL9, IL15, and IL21) and heterodimeric cytokines (e.g., IL12, IL23, IL27, and IL35), a heterodimeric Fc is an attractive scaffold to present cytokines with native structures. Roche (102, 103) generated CEA-targeted IgG-fused IL2 monomeric immunocytokines (CEA-IL2v) by fusion of an engineered IL2 variant (IL2v) to the C-terminus of an antibody with the KIH heterodimeric Fc to obtain a 2:1 antigen-binding valence to cytokine ratio (**Figure 4D**). Similarly, they also developed the fibroblast activation protein (FAP)-directed IgG-IL2v monomeric immunocytokine (FAP-IL2v) (103, 104). Both CEA-IL2v (NCT02004106, NCT02350673) and FAP-IL2v (NCT02627274) are now being evaluated in Phase 1 clinical trials.

⁴<http://www.hanmipharm.com/>

CONCLUSION AND PROSPECTS

In summary, immunoglobulin Fc heterodimer technology is very useful in generation of bsAbs with various antigen specificities and binding valencies in full-length IgG and IgG-like formats, while retaining many favorable properties of natural IgG antibodies. As of July 2016, more than seven heterodimeric Fc-based IgG-format bsAbs are now being evaluated in clinical trials (**Table 2**). Nonetheless, there are some issues to be considered for heterodimeric Fc-based bsAbs. All of the heterodimeric Fc-based bsAbs require assembly with three or four separate chains, which often hampers cell line development for high yield expression. Since each heterodimeric Fc chain has different mutations in each CH3 domain, the expression level and stability are somewhat different from each other, often requiring optimizing processes to identify the best pair between heterodimeric Fc chain and fusion partner (35). Furthermore, since the so far developed Fc heterodimers do not reach a 100% heterodimerization yield, the downstream process to ensure high bsAb purity, to meet clinical needs, should be considered from the initial stage of the heterodimeric Fc-based bsAb design.

In addition to bsAbs, heterodimeric Fc technology is now emerging as a promising scaffold for the generation of Fc-fused proteins and cytokines in monomeric or heterodimeric formats. The generation of Fc-fused monomeric proteins with wild-type Fc fragments is not any more desirable because it requires additional artificial sequences, such as extra tags for selective affinity chromatography and also multiple purification steps with limited purification yields (maximum 33%). Fusion to heterodimeric Fc fragments can present the fusion partner in its natural monomeric form for monomeric proteins and peptides as

well as natural heterodimeric forms for heterodimeric proteins, rather than the artificial homodimeric form for wild-type Fc fragments (**Figure 4E**). This heterodimeric Fc capability will facilitate the development of the next generation of Fc-fused proteins that maintain full function of the fusion partner, while retaining the Fc-mediated extended half-life and immune effector functions. The reduced binding valency might further help to reduce target receptor-mediated clearance. Particularly, in tumor-targeting IgG-based immunocytokines, the heterodimeric Fc-fused cytokines, in their natural forms, improve tumor tissue accumulation by reducing associations with immune cells, and thereby minimizing systemic toxicity. This facilitates their development as therapeutic agents. Some heterodimeric Fc-based IgG-fused immunocytokines are now in clinical trials and many more are expected to be developed.

AUTHOR CONTRIBUTIONS

JHH, JEK, and YSK designed the review article topic, surveyed relevant literatures and patents, and analyzed the data; YSK designed and supervised the review article; and JHH and YSK wrote the manuscript with input from all the other authors.

FUNDING

This work was supported by grants from the Pioneer Research Center Program (2014M3C1A3051470) and the Global Frontier Project (2013M3A6A4043874) from the National Research Foundation(NRF), and the Korea Health Technology R&D Project (HI16C0992) through the Korea Health Industry Development Institute (KHIDI), funded by the Republic of Korea.

REFERENCES

1. Chan AC, Carter PJ. Therapeutic antibodies for autoimmunity and inflammation. *Nat Rev Immunol* (2010) 10(5):301–16. doi:10.1038/nri2761
2. Weiner GJ. Building better monoclonal antibody-based therapeutics. *Nat Rev Cancer* (2015) 15(6):361–70. doi:10.1038/nrc3930
3. Fan G, Wang Z, Hao M, Li J. Bispecific antibodies and their applications. *J Hematol Oncol* (2015) 8:130. doi:10.1186/s13045-015-0227-0
4. Kontermann RE. Dual targeting strategies with bispecific antibodies. *MAbs* (2012) 4(2):182–97. doi:10.4161/mabs.4.2.19000
5. Spiess C, Zhai Q, Carter PJ. Alternative molecular formats and therapeutic applications for bispecific antibodies. *Mol Immunol* (2015) 67(2 Pt A):95–106. doi:10.1016/j.molimm.2015.01.003
6. Kontermann RE, Brinkmann U. Bispecific antibodies. *Drug Discov Today* (2015) 20(7):838–47. doi:10.1016/j.drudis.2015.02.008
7. Klein C, Sustmann C, Thomas M, Stubenrauch K, Croasdale R, Schanzer J, et al. Progress in overcoming the chain association issue in bispecific heterodimeric IgG antibodies. *MAbs* (2012) 4(6):653–63. doi:10.4161/mabs.21379
8. Irani V, Guy AJ, Andrew D, Beeson JG, Ramsland PA, Richards JS. Molecular properties of human IgG subclasses and their implications for designing therapeutic monoclonal antibodies against infectious diseases. *Mol Immunol* (2015) 67(2 Pt A):171–82. doi:10.1016/j.molimm.2015.03.255
9. Schroeder HW Jr, Cavacini L. Structure and function of immunoglobulins. *J Allergy Clin Immunol* (2010) 125(2 Suppl 2):S41–52. doi:10.1016/j.jaci.2009.09.046
10. Vidarsson G, Dekkers G, Rispens T. IgG subclasses and allotypes: from structure to effector functions. *Front Immunol* (2014) 5:520. doi:10.3389/fimmu.2014.00520
11. Sela-Culang I, Kunik V, Ofran Y. The structural basis of antibody-antigen recognition. *Front Immunol* (2013) 4:302. doi:10.3389/fimmu.2013.00302
12. Bostrom J, Yu S-F, Kan D, Appleton BA, Lee CV, Billeci K, et al. Variants of the antibody herceptin that interact with HER2 and VEGF at the antigen binding site. *Science* (2009) 323(5921):1610–4. doi:10.1126/science.1165480
13. Fischer N, Elson G, Magistrelli G, Dheilly E, Fouque N, Laurendon A, et al. Exploiting light chains for the scalable generation and platform purification of native human bispecific IgG. *Nat Commun* (2015) 6:6113. doi:10.1038/ncomms7113
14. Lindhofer H, Mocikat R, Steipe B, Thierfelder S. Preferential species-restricted heavy/light chain pairing in rat/mouse quadromas. Implications for a single-step purification of bispecific antibodies. *J Immunol* (1995) 155(1):219–25.
15. Carter P. Bispecific human IgG by design. *J Immunol Methods* (2001) 248(1–2):7–15. doi:10.1016/S0022-1759(00)00339-2
16. Merchant AM, Zhu Z, Yuan JQ, Goddard A, Adams CW, Presta LG, et al. An efficient route to human bispecific IgG. *Nat Biotechnol* (1998) 16(7):677–81. doi:10.1038/nbt0798-677
17. Schaefer W, Regula JT, Bahner M, Schanzer J, Croasdale R, Durr H, et al. Immunoglobulin domain crossover as a generic approach for the production of bispecific IgG antibodies. *Proc Natl Acad Sci U S A* (2011) 108(27):11187–92. doi:10.1073/pnas.1019002108
18. Lewis SM, Wu X, Pustilnik A, Sereno A, Huang F, Rick HL, et al. Generation of bispecific IgG antibodies by structure-based design of an orthogonal Fab interface. *Nat Biotechnol* (2014) 32(2):191–8. doi:10.1038/nbt.2797
19. Matsumiya S, Yamaguchi Y, Saito J, Nagano M, Sasakawa H, Otaki S, et al. Structural comparison of fucosylated and nonfucosylated Fc fragments of human immunoglobulin G1. *J Mol Biol* (2007) 368(3):767–79. doi:10.1016/j.jmb.2007.02.034
20. Miller S. Protein-protein recognition and the association of immunoglobulin constant domains. *J Mol Biol* (1990) 216(4):965–73. doi:10.1016/S0022-2836(99)80014-X

21. Atwell S, Ridgway JB, Wells JA, Carter P. Stable heterodimers from remodeling the domain interface of a homodimer using a phage display library. *J Mol Biol* (1997) 270(1):26–35. doi:10.1006/jmbi.1997.1116
22. Ridgway JB, Presta LG, Carter P. ‘Knobs-into-holes’ engineering of antibody CH₃ domains for heavy chain heterodimerization. *Protein Eng* (1996) 9(7):617–21. doi:10.1093/protein/9.7.617
23. Moore GL, Bautista C, Pong E, Nguyen DH, Jacinto J, Eivazi A, et al. A novel bispecific antibody format enables simultaneous bivalent and monovalent co-engagement of distinct target antigens. *Mabs* (2011) 3(6):546–57. doi:10.4161/mabs.3.6.18123
24. Von Kreudenstein TS, Escobar-Carbrera E, Lario PI, D’Angelo I, Brault K, Kelly J, et al. Improving biophysical properties of a bispecific antibody scaffold to aid developability: quality by molecular design. *Mabs* (2013) 5(5):646–54. doi:10.4161/mabs.25632
25. Gunasekaran K, Pentony M, Shen M, Garrett L, Forte C, Woodward A, et al. Enhancing antibody Fc heterodimer formation through electrostatic steering effects: applications to bispecific molecules and monovalent IgG. *J Biol Chem* (2010) 285(25):19637–46. doi:10.1074/jbc.M110.117382
26. Choi HJ, Kim YJ, Lee S, Kim YS. A heterodimeric Fc-based bispecific antibody simultaneously targeting VEGFR-2 and Met exhibits potent antitumor activity. *Mol Cancer Ther* (2013) 12(12):2748–59. doi:10.1158/1535-7163.MCT-13-0628
27. Ying T, Chen W, Gong R, Feng Y, Dimitrov DS. Soluble monomeric IgG1 Fc. *J Biol Chem* (2012) 287(23):19399–408. doi:10.1074/jbc.M112.368647
28. Elliott JM, Ultsch M, Lee J, Tong R, Takeda K, Spiess C, et al. Antiparallel conformation of knob and hole glycosylated half-antibody homodimers is mediated by a CH2-CH3 hydrophobic interaction. *J Mol Biol* (2014) 426(9):1947–57. doi:10.1016/j.jmb.2014.02.015
29. Leaver-Fay A, Froning KJ, Atwell S, Aldaz H, Pustilnik A, Lu F, et al. Computationally designed bispecific antibodies using negative state repertoires. *Structure* (2016) 24(4):641–51. doi:10.1016/j.str.2016.02.013
30. Choi HJ, Seok SH, Kim YJ, Seo MD, Kim YS. Crystal structures of immunoglobulin Fc heterodimers reveal the molecular basis for heterodimer formation. *Mol Immunol* (2015) 65(2):377–83. doi:10.1016/j.molimm.2015.02.017
31. Davis JH, Aperlo C, Li Y, Kurosawa E, Lan Y, Lo KM, et al. SEEDbodies: fusion proteins based on strand-exchange engineered domain (SEED) CH₃ heterodimers in an Fc analogue platform for asymmetric binders or immuno-fusions and bispecific antibodies. *Protein Eng Des Sel* (2010) 23(4):195–202. doi:10.1093/protein/gzp094
32. Choi HJ, Kim YJ, Choi DK, Kim YS. Engineering of immunoglobulin Fc heterodimers using yeast surface-displayed combinatorial Fc library screening. *PLoS One* (2015) 10(12):e0145349. doi:10.1371/journal.pone.0145349
33. Mimoto F, Kadono S, Katada H, Igawa T, Kamikawa T, Hattori K. Crystal structure of a novel asymmetrically engineered Fc variant with improved affinity for Fc γ R_{IIA}. *Mol Immunol* (2014) 58(1):132–8. doi:10.1016/j.molimm.2013.11.017
34. Merchant M, Ma X, Maun HR, Zheng Z, Peng J, Romero M, et al. Monovalent antibody design and mechanism of action of onartuzumab, a MET antagonist with anti-tumor activity as a therapeutic agent. *Proc Natl Acad Sci U S A* (2013) 110(32):E2987–96. doi:10.1073/pnas.1302725110
35. Xu Y, Lee J, Tran C, Heibeck TH, Wang WD, Yang J, et al. Production of bispecific antibodies in “knobs-into-holes” using a cell-free expression system. *Mabs* (2015) 7(1):231–42. doi:10.4161/19420862.2015.989013
36. Moore G, Desjarlais J, RASHID R, Bennett MJ. *Heterodimeric proteins*. (2014). WO 2014/145806 A2.
37. Schanzer JM, Wartha K, Croasdale R, Moser S, Kunkele KP, Ries C, et al. A novel glycoengineered bispecific antibody format for targeted inhibition of epidermal growth factor receptor (EGFR) and insulin-like growth factor receptor type I (IGF-1R) demonstrating unique molecular properties. *J Biol Chem* (2014) 289(27):18693–706. doi:10.1074/jbc.M113.528109
38. Castoldi R, Jucknischke U, Pradel LP, Arnold E, Klein C, Scheiblich S, et al. Molecular characterization of novel trispecific ErbB-cMet-IGF1R antibodies and their antigen-binding properties. *Protein Eng Des Sel* (2012) 25(10):551–9. doi:10.1093/protein/gzs048
39. Klein C, Schaefer W, Regula JT. The use of CrossMAb technology for the generation of bi- and multispecific antibodies. *Mabs* (2016) 8(6):1010–20. doi:10.1080/19420862.2016.1197457
40. Bacac M, Fauti T, Sam J, Colombetti S, Weinzierl T, Ouaret D, et al. A novel carcinoembryonic antigen T-cell bispecific antibody (CEA TCB) for the treatment of solid tumors. *Clin Cancer Res* (2016) 22(13):3286–97. doi:10.1158/1078-0432.CCR-15-1696
41. Hu S, Fu W, Xu W, Yang Y, Cruz M, Beregov SD, et al. Four-in-one antibodies have superior cancer inhibitory activity against EGFR, HER2, HER3, and VEGF through disruption of HER/MET crosstalk. *Cancer Res* (2015) 75(1):159–70. doi:10.1158/0008-5472.CAN-14-1670
42. Shima M, Hanabus H, Taki M, Matsushita T, Sato T, Fukutake K, et al. Factor VIII-mimetic function of humanized bispecific antibody in hemophilia A. *N Engl J Med* (2016) 374(21):2044–53. doi:10.1056/NEJMoa1511769
43. Yu YJ, Atwal JK, Zhang Y, Tong RK, Wildsmith KR, Tan C, et al. Therapeutic bispecific antibodies cross the blood-brain barrier in nonhuman primates. *Sci Transl Med* (2014) 6(261):261ra154. doi:10.1126/scitranslmed.3009835
44. Yu YJ, Zhang Y, Kenrick M, Hoyte K, Luk W, Lu Y, et al. Boosting brain uptake of a therapeutic antibody by reducing its affinity for a transcytosis target. *Sci Transl Med* (2011) 3(84):84ra44. doi:10.1126/scitranslmed.3002230
45. Spreiter Von Kreudenstein T, Lario PI, Dixit SB. Protein engineering and the use of molecular modeling and simulation: the case of heterodimeric Fc engineering. *Methods* (2014) 65(1):77–94. doi:10.1016/j.ymeth.2013.10.016
46. Lee CH, Choi DK, Choi HJ, Song MY, Kim YS. Expression of soluble and functional human neonatal Fc receptor in *Pichia pastoris*. *Protein Expr Purif* (2010) 71(1):42–8. doi:10.1016/j.pep.2009.12.004
47. Bruhns P, Iannascoli B, England P, Mancardi DA, Fernandez N, Jorieux S, et al. Specificity and affinity of human Fc γ gamma receptors and their polymorphic variants for human IgG subclases. *Blood* (2009) 113(16):3716–25. doi:10.1182/blood-2008-09-179754
48. Muda M, Gross AW, Dawson JP, He C, Kurosawa E, Schweickhardt R, et al. Therapeutic assessment of SEED: a new engineered antibody platform designed to generate mono- and bispecific antibodies. *Protein Eng Des Sel* (2011) 24(5):447–54. doi:10.1093/protein/gzq123
49. Baek DS, Kim YS. Construction of a large synthetic human Fab antibody library on yeast cell surface by optimized yeast mating. *J Microbiol Biotechnol* (2014) 24(3):408–20. doi:10.4014/jmb.1401.01002
50. Baek DS, Kim YS. Humanization of a phosphothreonine peptide-specific chicken antibody by combinatorial library optimization of the phosphoepitope-binding motif. *Biochem Biophys Res Commun* (2015) 463(3):414–20. doi:10.1016/j.bbrc.2015.05.086
51. Prat M, Crepaldi T, Pennacchietti S, Bussolino F, Comoglio PM. Agonistic monoclonal antibodies against the Met receptor dissect the biological responses to HGF. *J Cell Sci* (1998) 111(Pt 2):237–47.
52. Frankel SR, Baeuerle PA. Targeting T cells to tumor cells using bispecific antibodies. *Curr Opin Chem Biol* (2013) 17(3):385–92. doi:10.1016/j.cbpa.2013.03.029
53. Maher J, Adamo AA. Antitumor immunity: easy as 1, 2, 3 with monoclonal bispecific trifunctional antibodies? *Cancer Res* (2013) 73(18):5613–7. doi:10.1158/0008-5472.CAN-13-1852
54. Mack M, Riethmuller G, Kufer P. A small bispecific antibody construct expressed as a functional single-chain molecule with high tumor cell cytotoxicity. *Proc Natl Acad Sci U S A* (1995) 92(15):7021–5. doi:10.1073/pnas.92.15.7021
55. Goebeler ME, Bargou R. Blinatumomab: a CD19/CD3 bispecific T cell engager (BiTE) with unique anti-tumor efficacy. *Leuk Lymphoma* (2016) 57(5):1021–32. doi:10.3109/10428194.2016.1161185
56. Stork R, Campigna E, Robert B, Muller D, Kontermann RE. Biodistribution of a bispecific single-chain diabody and its half-life extended derivatives. *J Biol Chem* (2009) 284(38):25612–9. doi:10.1074/jbc.M109.027078
57. Bargou R, Leo E, Zugmaier G, Klinger M, Goebeler M, Knop S, et al. Tumor regression in cancer patients by very low doses of a T cell-engaging antibody. *Science* (2008) 321(5891):974–7. doi:10.1126/science.1158545
58. Moretti P, Skegro D, Ollier R, Wassmann P, Aebscher C, Laurent T, et al. BEAT® the bispecific challenge: a novel and efficient platform for the expression of bispecific IgGs. *BMC Proceedings* (2013) 7:O9. doi:10.1186/1753-6561-7-S6-O9
59. Schanzer JM, Wartha K, Moessner E, Hosse RJ, Moser S, Croasdale R, et al. XGFR*, a novel affinity-matured bispecific antibody targeting IGF-1R and EGFR with combined signaling inhibition and enhanced immune

- activation for the treatment of pancreatic cancer. *MAbs* (2016) 8(4):811–27. doi:10.1080/19420862.2016.1160989
60. Jackman J, Chen Y, Huang A, Moffat B, Scheer JM, Leong SR, et al. Development of a two-part strategy to identify a therapeutic human bispecific antibody that inhibits IgE receptor signaling. *J Biol Chem* (2010) 285(27):20850–9. doi:10.1074/jbc.M110.113910
 61. Sampei Z, Igawa T, Soeda T, Okuyama-Nishida Y, Moriyama C, Wakabayashi T, et al. Identification and multidimensional optimization of an asymmetric bispecific IgG antibody mimicking the function of factor VIII cofactor activity. *PLoS One* (2013) 8(2):e57479. doi:10.1371/journal.pone.0057479
 62. Kitazawa T, Igawa T, Sampei Z, Muto A, Kojima T, Soeda T, et al. A bispecific antibody to factors IXa and X restores factor VIII hemostatic activity in a hemophilia A model. *Nat Med* (2012) 18(10):1570–4. doi:10.1038/nm.2942
 63. Klohn PC, Wuellner U, Zizlsperger N, Zhou Y, Tavares D, Berger S, et al. IBC's 23rd annual antibody engineering, 10th annual antibody therapeutics international conferences and the 2012 annual meeting of the antibody society: December 3–6, 2012, San Diego, CA. *MAbs* (2013) 5(2):178–201. doi:10.4161/mabs.23655
 64. Calvo E, Alsina M, Schellens JH, Huiterna AD, Tabernero J, de Vries-Schultink A, et al. A phase I/II study of MCLA-128, a full length IgG1 bispecific antibody targeting HER2 and HER3, in patients with solid tumors. *Cancer Res* (2016) 76(14 Suppl):CT050-CT. doi:10.1158/1538-7445.AM2016-CT050
 65. Wu C, Ying H, Grinnell C, Bryant S, Miller R, Clabbers A, et al. Simultaneous targeting of multiple disease mediators by a dual-variable-domain immunoglobulin. *Nat Biotechnol* (2007) 25(11):1290–7. doi:10.1038/nbt1345
 66. Wu X, Sereno AJ, Huang F, Lewis SM, Lieu RL, Weldon C, et al. Fab-based bispecific antibody formats with robust biophysical properties and biological activity. *MAbs* (2015) 7(3):470–82. doi:10.1080/19420862.2015.1022694
 67. Liu Z, Leng EC, Gunasekaran K, Pentony M, Shen M, Howard M, et al. A novel antibody engineering strategy for making monovalent bispecific heterodimeric IgG antibodies by electrostatic steering mechanism. *J Biol Chem* (2015) 290(12):7535–62. doi:10.1074/jbc.M114.620260
 68. Spiess C, Merchant M, Huang A, Zheng Z, Yang NY, Peng J, et al. Bispecific antibodies with natural architecture produced by co-culture of bacteria expressing two distinct half-antibodies. *Nat Biotechnol* (2013) 31(8):753–8. doi:10.1038/nbt.2621
 69. Shatz W, Chung S, Li B, Marshall B, Tejada M, Phung W, et al. Knobs-into-holes antibody production in mammalian cell lines reveals that asymmetric afucosylation is sufficient for full antibody-dependent cellular cytotoxicity. *MAbs* (2013) 5(6):872–81. doi:10.4161/mabs.26307
 70. Aalberse RC, Schuurman J. IgG4 breaking the rules. *Immunology* (2002) 105(1):9–19. doi:10.1046/j.0019-2805.2001.01341.x
 71. van der Neut Kolfschoten M, Schuurman J, Losen M, Bleeker WK, Martinez-Martinez P, Vermeulen E, et al. Anti-inflammatory activity of human IgG4 antibodies by dynamic Fab arm exchange. *Science* (2007) 317(5844):1554–7. doi:10.1126/science.1144603
 72. Labrijn AF, Meesters JI, de Goeij BE, van den Bremer ET, Neijssen J, van Kampen MD, et al. Efficient generation of stable bispecific IgG1 by controlled Fab-arm exchange. *Proc Natl Acad Sci U S A* (2013) 110(13):5145–50. doi:10.1073/pnas.1220145110
 73. Strop P, Ho WH, Boustany LM, Abdiche YN, Lindquist KC, Farias SE, et al. Generating bispecific human IgG1 and IgG2 antibodies from any antibody pair. *J Mol Biol* (2012) 420(3):204–19. doi:10.1016/j.jmb.2012.04.020
 74. Gramer MJ, van den Bremer ET, van Kampen MD, Kundu A, Kopfmann P, Etter E, et al. Production of stable bispecific IgG1 by controlled Fab-arm exchange: scalability from bench to large-scale manufacturing by application of standard approaches. *MAbs* (2013) 5(6):962–73. doi:10.4161/mabs.26233
 75. Moores SL, Chiu ML, Bushey BS, Chevalier K, Luistro L, Dorn K, et al. A novel bispecific antibody targeting EGFR and cMet is effective against EGFR inhibitor-resistant lung tumors. *Cancer Res* (2016) 76(13):3942–53. doi:10.1158/0008-5472.can-15-2833
 76. Czajkowsky DM, Hu J, Shao Z, Pleass RJ. Fc-fusion proteins: new developments and future perspectives. *EMBO Mol Med* (2012) 4(10):1015–28. doi:10.1002/emmm.201201379
 77. Levin D, Golding B, Strome SE, Sauna ZE. Fc fusion as a platform technology: potential for modulating immunogenicity. *Trends Biotechnol* (2015) 33(1):27–34. doi:10.1016/j.tibtech.2014.11.001
 78. Kim YJ, Bae J, Shin TH, Kang SH, Jeong M, Han Y, et al. Immunoglobulin Fc-fused, neuropilin-1-specific peptide shows efficient tumor tissue penetration and inhibits tumor growth via anti-angiogenesis. *J Control Release* (2015) 216:56–68. doi:10.1016/j.jconrel.2015.08.016
 79. Dickinson BL, Badizadegan K, Wu Z, Ahouse JC, Zhu X, Simister NE, et al. Bidirectional FcRn-dependent IgG transport in a polarized human intestinal epithelial cell line. *J Clin Invest* (1999) 104(7):903–11. doi:10.1172/JCI6968
 80. Jiang X, Hu J, Thirumalai D, Zhang X. Immunoglobulin transporting receptors are potential targets for the immunity enhancement and generation of mammary gland bioreactor. *Front Immunol* (2016) 7:214. doi:10.3389/fimmu.2016.00214
 81. Huang C. Receptor-Fc fusion therapeutics, traps, and MIMETIBODY technology. *Curr Opin Biotechnol* (2009) 20(6):692–9. doi:10.1016/j.copbio.2009.10.010
 82. Strohl WR. Fusion proteins for half-life extension of biologics as a strategy to make biobetters. *BioDrugs* (2015) 29(4):215–39. doi:10.1007/s40259-015-0133-6
 83. Dumont JA, Low SC, Peters RT, Bitonti AJ. Monomeric Fc fusions: impact on pharmacokinetic and biological activity of protein therapeutics. *BioDrugs* (2006) 20(3):151–60. doi:10.2165/00063030-200620030-00002
 84. Livnah O, Johnson DL, Stura EA, Farrell FX, Barbone FP, You Y, et al. An antagonist peptide-EPO receptor complex suggests that receptor dimerization is not sufficient for activation. *Nat Struct Biol* (1998) 5(11):993–1004. doi:10.1038/2965
 85. Bitonti AJ, Dumont JA, Low SC, Peters RT, Kropp KE, Palombella VJ, et al. Pulmonary delivery of an erythropoietin Fc fusion protein in non-human primates through an immunoglobulin transport pathway. *Proc Natl Acad Sci U S A* (2004) 101(26):9763–8. doi:10.1073/pnas.0403235101
 86. Dumont JA, Bitonti AJ, Clark D, Evans S, Pickford M, Newman SP. Delivery of an erythropoietin-Fc fusion protein by inhalation in humans through an immunoglobulin transport pathway. *J Aerosol Med* (2005) 18(3):294–303. doi:10.1089/jam.2005.18.294
 87. Peters RT, Mezo AR, Rivera DS, Bitonti AJ, Low SC. *Immunoglobulin Chimeric Monomer-Dimer Hybrids*. (2008). US7404956 B2.
 88. Kang J, Kim JH, Yi J, Han O, Kim Y, Baek E, et al. The ultra-long acting LAPS GLP/GCG dual agonist, HM12525A, demonstrated safety and prolonged pharmacokinetics in healthy volunteers: a phase 1 first-in-human study. *DIABETOLOGIA*; 2015, Sep Vol. 58, Spring ST, New York, NY: Springer (2015), p. S380–1.
 89. Hwang SY, Kim JY, Kim SS, Choi IY, Jung SY, Kwon SC. *Use of a Long Acting glp-1/Glucagon Receptor Dual Agonist for the Treatment of Non-Alcoholic Fatty Liver Disease*. (2016). WO 2016043533 A1.
 90. le Cotonne JY, Porchet HC, Beltrami V, Khan A, Toon S, Rowland M. Clinical pharmacology of recombinant human follicle-stimulating hormone (FSH). I. Comparative pharmacokinetics with urinary human FSH. *Fertil Steril* (1994) 61(4):669–78.
 91. Low SC, Nunes SL, Bitonti AJ, Dumont JA. Oral and pulmonary delivery of FSH-Fc fusion proteins via neonatal Fc receptor-mediated transcytosis. *Hum Reprod* (2005) 20(7):1805–13. doi:10.1093/humrep/deh896
 92. Kontermann RE. Antibody-cytokine fusion proteins. *Arch Biochem Biophys* (2012) 526(2):194–205. doi:10.1016/j.abb.2012.03.001
 93. Neri D, Sondel PM. Immunocytokines for cancer treatment: past, present and future. *Curr Opin Immunol* (2016) 40:96–102. doi:10.1016/j.co.2016.03.006
 94. Kiefer JD, Neri D. Immunocytokines and bispecific antibodies: two complementary strategies for the selective activation of immune cells at the tumor site. *Immunol Rev* (2016) 270(1):178–92. doi:10.1111/imr.12391
 95. Tzeng A, Kwan BH, Opel CF, Navaratna T, Wittrup KD. Antigen specificity can be irrelevant to immunocytokine efficacy and biodistribution. *Proc Natl Acad Sci U S A* (2015) 112(11):3320–5. doi:10.1073/pnas.1416159112
 96. Zhu EF, Gai SA, Opel CF, Kwan BH, Surana R, Mihm MC, et al. Synergistic innate and adaptive immune response to combination immunotherapy with anti-tumor antigen antibodies and extended serum half-life IL-2. *Cancer Cell* (2015) 27(4):489–501. doi:10.1016/j.ccr.2015.03.004
 97. Vignali DA, Kuchroo VK. IL-12 family cytokines: immunological playmakers. *Nat Immunol* (2012) 13(8):722–8. doi:10.1038/ni.2366

98. Gafner V, Trachsel E, Neri D. An engineered antibody-interleukin-12 fusion protein with enhanced tumor vascular targeting properties. *Int J Cancer* (2006) 119(9):2205–12. doi:10.1002/ijc.22101
99. Pasche N, Wulhfard S, Pretto F, Carugati E, Neri D. The antibody-based delivery of interleukin-12 to the tumor neovasculature eradicates murine models of cancer in combination with paclitaxel. *Clin Cancer Res* (2012) 18(15):4092–103. doi:10.1158/1078-0432.CCR-12-0282
100. Pasche N, Woytschak J, Wulhfard S, Villa A, Frey K, Neri D. Cloning and characterization of novel tumor-targeting immunocytokines based on murine IL7. *J Biotechnol* (2011) 154(1):84–92. doi:10.1016/j.jbiotec.2011.04.003
101. Becker JC, Pancook JD, Gillies SD, Furukawa K, Reisfeld RA. T cell-mediated eradication of murine metastatic melanoma induced by targeted interleukin 2 therapy. *J Exp Med* (1996) 183(5):2361–6. doi:10.1084/jem.183.5.2361
102. Nicolini V, Waldhauer I, Freimoser A, Colombetti S, Cavallo F, Bacac M, et al. Combination with the novel tumor-targeted CEA-IL2v immunocytokine enhances the activity of ADCC-competent and glycoengineered antibodies in vitro and in vivo. *Cancer Res* (2014) 74(19 Suppl):2579. doi:10.1158/1538-7445.AM2014-2579
103. Auer J, Bruenker P, FAUTI T, Jaeger C, Klein C, Schaefer W, et al. *Bispecific Antigen Binding Molecules*. (2013). WO 2013026831 A1.
104. Waldhauer I, Nicolini V, Dunn C, Freimoser-Grundschober A, Danny G, Boerman O, et al. Novel tumor-targeted, engineered IL-2 variant (IL2v)-based immunocytokines for immunotherapy of cancer. *Blood* (2013) 122(21):2278.

Conflict of Interest Statement: The authors declare that the research was conducted in the absence of any commercial or financial relationships that could be construed as a potential conflict of interest.

Copyright © 2016 Ha, Kim and Kim. This is an open-access article distributed under the terms of the Creative Commons Attribution License (CC BY). The use, distribution or reproduction in other forums is permitted, provided the original author(s) or licensor are credited and that the original publication in this journal is cited, in accordance with accepted academic practice. No use, distribution or reproduction is permitted which does not comply with these terms.



Corrigendum: Immunoglobulin Fc Heterodimer Platform Technology: From Design to Applications in Therapeutic Antibodies and Proteins

Ji-Hee Ha¹, Jung-Eun Kim¹ and Yong-Sung Kim^{1,2*}

¹Department of Molecular Science and Technology, Ajou University, Suwon, South Korea, ²Department of Applied Chemistry and Biological Engineering, College of Engineering, Ajou University, Suwon, South Korea

Keywords: bispecific antibody, Fc engineering, heterodimeric Fc, Fc-fusion proteins, immunocytokines, antibody engineering

A corrigendum on

Immunoglobulin Fc Heterodimer Platform Technology: From Design to Applications in Therapeutic Antibodies and Proteins

by Ha J-H, Kim J-E, Kim Y-S. *Front Immunol* (2016) 7:394. doi: 10.3389/fimmu.2016.00394

OPEN ACCESS

Edited and Reviewed by:

Tianlei Ying,
Fudan University, China

*Correspondence:

Yong-Sung Kim
kimys@ajou.ac.kr

Specialty section:

This article was submitted to
Vaccines and Molecular
Therapeutics,
a section of the journal
Frontiers in Immunology

Received: 19 October 2017

Accepted: 02 November 2017

Published: 13 November 2017

Citation:

Ha J-H, Kim J-E and Kim Y-S (2017)
Corrigendum: Immunoglobulin Fc Heterodimer Platform Technology:
From Design to Applications in Therapeutic Antibodies and Proteins.
Front. Immunol. 8:1582.
doi: 10.3389/fimmu.2017.01582

In the original article, there was an error [wrong description on LY3164530 (Eli Lilly) antibody in the last paragraph of page 9 of original article].

A correction has been made to section “HETERODIMERIC Fc-BASED ANTIBODIES IN DIVERSE FORMATS”, subsection “Intact IgG Formats with Correct LC Association”, sixth Paragraph (line 8–12 of the sixth paragraph) (In the last paragraph of page 9 of original article):

An alternative approach for enforcing correct HC_{VH-CH1}-LC association includes introduction of a set of mutations at the heterodimeric VL-CL and VH-CH1 interface (18, 66, 67), similar to modification of the CH3 interface for the heterodimeric Fc design. In an ortho-Fab IgG approach (18), structure-based regional design introduced complementary mutations at the LC and HC_{VH-CH1} interface in only one Fab, without any changes being made to the other Fab (Figure 3). Zymeworks is currently developing intact IgG-format bsAbs generated by the combination of ortho-Fab IgG and ZW1 Fc technologies (<http://www.zymeworks.com/>).

The authors apologize for this error and state that this does not change the scientific conclusions of the article in any way.

Conflict of Interest Statement: The authors declare that the research was conducted in the absence of any commercial or financial relationships that could be construed as a potential conflict of interest.

Copyright © 2017 Ha, Kim and Kim. This is an open-access article distributed under the terms of the Creative Commons Attribution License (CC BY). The use, distribution or reproduction in other forums is permitted, provided the original author(s) or licensor are credited and that the original publication in this journal is cited, in accordance with accepted academic practice. No use, distribution or reproduction is permitted which does not comply with these terms.



Engineered Soluble Monomeric IgG1 Fc with Significantly Decreased Non-Specific Binding

Chunyu Wang¹, Yanling Wu¹, Lili Wang¹, Binbin Hong¹, Yujia Jin¹, Dan Hu¹, Gang Chen¹, Yu Kong¹, Ailing Huang¹, Guoqiang Hua² and Tianlei Ying^{1*}

¹Key Laboratory of Medical Molecular Virology of Ministries of Education and Health, School of Basic Medical Sciences, Fudan University, Shanghai, China, ²Institute of Radiation Medicine, Fudan University, Shanghai, China

OPEN ACCESS

Edited by:

Florian Krammer,
Icahn School of Medicine at
Mount Sinai, United States

Reviewed by:

Wenqian He,
Abvvie Biotherapeutics
Corporation, United States
Johannes S. Gach,
University of California,
Irvine, United States

*Correspondence:

Tianlei Ying
tlying@fudan.edu.cn

Specialty section:

This article was submitted to
Vaccines and Molecular
Therapeutics,
a section of the journal
Frontiers in Immunology

Received: 13 August 2017

Accepted: 30 October 2017

Published: 13 November 2017

Citation:

Wang C, Wu Y, Wang L, Hong B, Jin Y, Hu D, Chen G, Kong Y, Huang A, Hua G and Ying T (2017) Engineered Soluble Monomeric IgG1 Fc with Significantly Decreased Non-Specific Binding. *Front. Immunol.* 8:1545.
doi: 10.3389/fimmu.2017.01545

Due to the long serum half-life provided by the neonatal Fc receptor (FcRn) recycling, the IgG1 Fc has been pursued as the fusion partner to develop therapeutic Fc-fusion proteins, or as the antibody-derived scaffold that could be engineered with antigen-binding capabilities. In previous studies, we engineered the monomeric Fc by mutating critical residues located on the IgG1 Fc dimerization interface. Comparing with the wild-type dimeric Fc, monomeric Fc might possess substantial advantages conferred by its smaller size, but also suffers the disadvantage of non-specific binding to some unrelated antigens, raising considerable concerns over its potential clinical development. Here, we describe a phage display-based strategy to examine the effects of multiple mutations of IgG1 monomeric Fc and, simultaneously, to identify new Fc monomers with desired properties. Consequently, we identified a novel monomeric Fc that displayed significantly decreased non-specificity. In addition, it exhibited higher thermal stability and comparable pH-dependent FcRn binding to the previous reported monomeric Fc. These results provide baseline to understand the mechanism underlying the generation of soluble IgG1 Fc monomers and warrant the further clinical development of monomeric Fc-based fusion proteins as well as antigen binders.

Keywords: monomeric IgG1 Fc, non-specific binding, neonatal Fc receptor, half-life, monoclonal antibody

INTRODUCTION

Monoclonal antibodies (mAbs) have become the fastest growing class of biological therapeutics, with over 50 such molecules approved by the FDA for therapeutic use and hundreds more currently in clinical development (1–5). Most of the mAbs on the market are IgG1 antibodies partially because of the long *in vivo* half-life conferred by their pH-dependent association with the neonatal Fc receptor (FcRn). The Fc region of IgG1 can bind to FcRn in the acidic environment of the endosome after antibody internalization, protecting antibody from degradation until its back to the cell surface for re-release into circulation at neutral pH (6, 7). This mechanism enables a less frequent dosing and/or lower dose than other biologics lacking the IgG1 Fc region (8–10). Therefore, it is promising to develop novel long-acting protein therapeutics based on IgG1 Fc by fusing Fc to otherwise fast-turnover therapeutic proteins. IgG1 Fc is also being pursued as the novel antibody-derived scaffold that could be engineered with antigen-binding capabilities, aiming to overcome the limitations of full-size mAbs, such as poor tissue penetration, high manufacturing cost, and hindered access to sterically restricted epitopes (11–14).

However, until now, only a few Fc-fusion proteins have been approved by FDA, and even fewer Fc-based antigen binders are in pre-clinical and clinical development. The applicability of IgG1 Fc is largely hampered by its homodimeric nature, resulting in the large size of fusion proteins and the inability to generate a monovalent fusion construct. Besides, wild-type IgG1 Fc contains multiple binding sites in order to interact with a variety of distinct cell receptors and complement proteins, e.g., FcRn, Fc γ receptors (Fc γ Rs), complement component 1q (C1q), tripartite motif-containing protein 21 (TRIM21) (15–18), and the introduction of mutant sites in the Fc region are prone to induce non-specific binding to irrelevant proteins. Therefore, a key challenge is to avoid the introduction of non-specific cross-reactivity during the engineering of IgG1 Fc for desired properties (19), e.g., reduced molecular weight, improved stability and solubility, or enhanced *in vivo* half-life and effector functions.

In the previous studies, we generated a large phage library ($\sim 1.3 \times 10^9$ diversity) of IgG1 Fc molecules with extensive mutations in the dimerization interface, and developed a phage display-based multiple panning/screening strategy to search for monomeric Fc constructs (20, 21). One of the identified Fc monomer, designated as mFc, has only four mutations to the wild-type IgG1 Fc, and is half the size (molecular mass 27 vs.

54 kDa). It was used to generate mFc-based fusion proteins due to the comparable pharmacokinetics to dimeric Fc. Recently, we also used mFc as the scaffold for generating antigen binders (Figure 1A). By introducing point mutations in the CH2 domain and CDR3-grafting onto the CH3 domain of the mFc scaffold, we successfully identified panels of high-affinity mFc-based binders against viral and cancer antigens (unpublished data). However, we found that these binders and mFc *per se* exhibited different extents of non-specific binding at high protein concentrations ($>1 \mu\text{M}$) to some unrelated antigens, raising considerable concerns over their potential clinical development. We hypothesized that the non-specificity came from the introduced mutations at the IgG1 Fc dimerization interface. Hence, a current priority is to understand the role each of the four mFc mutations plays in the formation of monomer and introduction of non-specificity, and translate this information into the design of a new generation of monomeric IgG1 Fc constructs with minimal non-specific bindings.

Here, we describe a novel strategy to examine the effects of multiple mutations of IgG1 mFc and, simultaneously, to identify new Fc monomers with desired properties. Based on our knowledge of Fc homo-dimerization, we designed a phage display library that enables a combination of rational and random

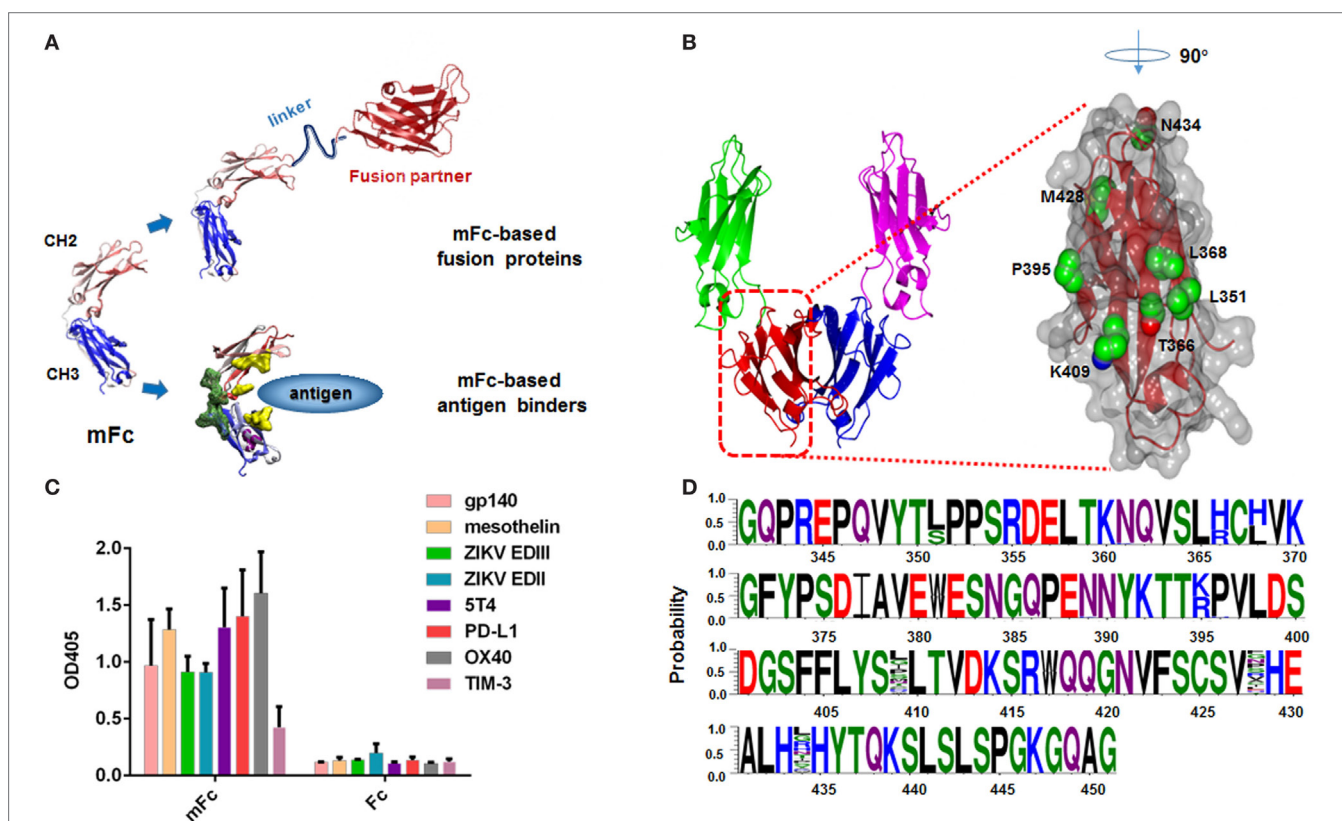


FIGURE 1 | Design and construction of a large Fc mutant library. **(A)** Representative of mFc used to generate mFc-based fusion proteins or mFc-based antigen binders. **(B)** Structure of human IgG1 Fc CH3 domain, showing key residues in its dimerization interface and neonatal Fc receptor-binding region (Protein Data Bank code 2WAH). **(C)** Binding of $2\mu\text{M}$ mFc and Fc to eight recombinant viral proteins and cancer-related antigens (HIV-1 gp140, ZIKV EDII, ZIKV EDIII, mesothelin, 5T4, PD-L1, OX40, TIM-3) measured by ELISA. The recombinant antigens were coated on ELISA plates, and HRP conjugated anti-FLAG antibody was used for detection of Fc and mFc. **(D)** Sequences of 30 randomly selected clones from Fc mutant library, showing its diversity.

scanning mutagenesis of seven mFc residues (positions Leu-351, Thr-366, Leu-368, Pro-395, Lys-409, Met-428, and Asn-434). All these residues have been previously identified to impact the Fc dimerization or FcRn binding (**Figure 1B**) (6, 15, 20–22). The displayed variants were then subjected to five rounds of extensive bio-panning based on their conformation, specific and non-specific FcRn binding. While the non-monomeric mutants have diverse sequences, the identified IgG1 Fc monomers have similar positive-charged amino acids at positions 366 and 368 (T366R, L368H), suggesting a critical role of these mutations in the disruption of Fc dimerization. Importantly, we identified a novel monomeric Fc mutant that still maintained FcRn-binding capability, and exhibited significantly decreased non-specific binding as compared to the previously developed monomeric IgG1 Fc mutants. These results provide baseline to understand the mechanism underlying the generation of soluble IgG1 Fc monomers and warrant the further clinical development of mFc-based fusion proteins as well as antigen binders.

MATERIALS AND METHODS

Library Construction and Selection of Fc Mutant Clones

A large phage display library, with an estimated diversity of 1.28×10^5 , was constructed by site-directed mutation of four residues of human IgG1 Fc (Leu-351, Thr-366, Leu-368, and Pro-395), and randomly mutation of the other three residues, one located at the CH3 dimer interface (Lys-409) and the other two located within the FcRn-binding site of CH3 (Met-428 and Asn-434). The synthesized gene (Genewiz Inc., Suzhou, China) was cloned into the pComb3x phagemid as described previously (20, 21). Amplified libraries with 10^{12} phage-displayed Fc mutants were used in the following bio-panning. After two rounds of protein G panning using protein G magnetic beads (Roche Applied Science), the phages capable of binding to protein G were amplified from the TG1 cells and used in the bio-panning against FcRn. The FcRn, being composed of alpha chain (or heavy chain) and a beta 2 microglobulin noncovalently linked at the 1:1 M ratio, was expressed in mammalian cells and purified as a soluble protein as previously described. Next, 10^{12} phages were mixed with phosphate-buffered saline (PBS, pH 6.0) and incubated with biotin-labeled FcRn conjugated to magnetic beads (Invitrogen, Carlsbad, CA, USA) for 1.5 h at room temperature. After incubation, the beads were washed two times for the first round and increase progressively for the later rounds with PBS (pH 6.0) containing 0.05% Tween 20. The bound phages were eluted with PBS (pH 7.4), amplified by infecting TG1 cells along with helper phage M13KO7 (Thermo Fisher). Positive clones that bound to FcRn at pH 6.0, but did not bind at pH 7.4 were randomly picked from the fifth selection round bio-panning using monoclonal phage ELISA.

Expression and Purification of Fc Mutants

The selected clones were sequenced, and plasmids extracted from these clones were used for transformation of HB2151 cells. A single and freshly transformed colony was added to 3 ml

2YT medium with 100 µg/ml ampicillin and 2% (w/v) glucose, incubated at 37°C with vigorous shaking at 250 rpm for 3–4 h, and then transferred into 200 ml of SB medium with 100 µg/ml ampicillin for continued incubation until optical density of the culture at 600 nm reached 0.6. Next, IPTG (isopropyl-1-thio-β-D-galactopyranoside) was added to a final concentration of 1 mM to induce protein expression, and the culture was further incubated overnight at 30°C, 250 rpm. Bacteria were collected by centrifugation at 8,000 rpm for 10 min and re-suspended in 30 ml PBS buffer. Polymixin B (Sigma-Aldrich) (0.5 µm/ml) was added to the bacteria solution (1:1,000). After 30 min incubation with rotation at 250 rpm at 30°C, the suspension was centrifuged at 8,000 rpm for 10 min at 4°C. Proteins were purified using protein G column (Roche Applied Science) according to the manufacturer's protocol. The degree of protein purity was determined by SDS-PAGE, and protein concentration was measured spectrophotometrically.

Size Exclusion Chromatography (SEC)

Protein samples were prepared at concentrations of 400–500 µg/ml in PBS buffer. Each sample (250 µg) was injected onto an analytical Superdex 75 10/300 GL column (GE Healthcare) connected to an FPLC ÄKTA BASIC pH/C system (GE Healthcare). PBS was used as the running buffer at the flow rate 0.5 ml/min, and the eluted proteins were monitored at 280 nm. Fc (50 kDa) and mFc (25 kDa) were used to define the molecular mass. A minimum of three independent experiments was performed.

Circular Dichroism (CD)

The CD spectra were collected on a Jasco J-815 spectropolarimeter (Jasco International). The protein samples were dissolved in PBS at a final concentration of 0.25 mg/ml. For evaluation of thermal stability, the spectra were analyzed by monitoring the molar ellipticity changes at 216 nm as a function of temperature increase (0.1 cm path length). The instrument was programmed to acquire spectra at 1°C intervals over the range 20–100°C. A minimum of three independent experiments was performed.

Binding ELISA

ELISA was used to determine the binding capability of the selected proteins to various unrelated antigens. All Fc mutants (mFc, 1-B10-9, 1-D1-15) were expressed in *E. coli* HB2151, as described above. Antigens (gp140, mesothelin, ZIKV EDII, ZIKV EDIII, 5T4, PD-L1, OX40, TIM-3) were coated on 96-well ELISA plates (Corning, #3690) overnight with 100 ng/well in PBS at 4°C, and blocked with 100 µl per well of 3% MPBS (PBS with 3% milk) at 37°C for 1 h. The plates were washed with PBS with 0.05% Tween 20 (PBST), then threefold serial diluted proteins were added and incubated at 37°C for 1.5 h. Plates were washed five times with PBST and 50 µl of 1:1,000 HRP conjugated anti-FLAG antibody (Sigma-Aldrich) in PBS were added per well before incubation at 37°C for 45 min. After extensive washes with PBST, the binding was measured by the addition of diammonium 2,2'-azino-bis (3-ethylbenzothiazoline-6-sulfonate) (ABTS) substrate (Roche Applied Science) and signal reading was carried out at 405 nm.

FcRn Binding Measured by Bio-Layer Interferometry (BLI)

The binding of proteins to soluble human FcRn was measured by BLI using an Octet-Red96 system (Pall ForteBio) in 96-well plates (Greiner) at 37°C. Purified human FcRn (biotin labeled) was diluted in PBS with 0.02% Tween 20 (pH 7.4) and loaded onto streptavidin coated Dip-and-Read biosensor tips (Pall ForteBio) until saturation. Next, the tips were washed in the same buffer (60 s) for blocking unoccupied streptavidin-binding sites and were placed for 5 min in wells containing proteins. The proteins were diluted in PBS with 0.02% Tween 20 for the detection of binding at pH 7.4 or 6.0. A twofold dilution of proteins (mFc, 1-B10, 1-D1) was prepared from 10 μM to 0.625 μM. Then the sensor surfaces were regenerated with glycine buffer (pH 1.7) after 5 min of dissociation. The experiments included the following steps at 37°C: (1) equilibration step with assay buffer (PBS with 0.02% Tween 20, pH 7.4) for 10 min, (2) baseline step with assay buffer for 60 s, (3) loading step with 30 μg/ml biotin-FcRn in assay buffer for 5 min, (4) baseline step with assay buffer (pH 6.0/7.4) for 5 min, (5) association step with varying concentrations of proteins in assay buffer (pH 6.0/7.4) for 5 min, (6) dissociation step with assay buffer for 5 min, and (7) regeneration step with glycine buffer (pH 1.7) for 5 s, repeat three times. The curves were fitted based on the 1:1 binding kinetic model using ForteBio Data Analysis software.

Statistics

Statistical analysis was performed using SPSS 19.0 software. The comparison of binding capability of the selected Fc mutants to various unrelated antigens were carried out by Student's *t*-test. All comparisons were two-tailed and *p* < 0.05 was considered statistically significant.

RESULTS

Construction of a Large Fc Mutant Library and Selection of Monomeric Fc

We have previously reported the generation of three mFc proteins using a combination of rational design and multiple panning/screening procedure (20, 21). Previous studies have focused on reducing the molecular weight of Fc. The resulting Fc monomers were found to possess high stability, FcRn-binding capability and similar serum half-life as compared to the wild-type IgG1 Fc *in vivo* (20). Despite this, we recently found that they displayed relatively strong non-specific binding to unrelated antigens at high protein concentration. As shown in **Figure 1C**, at a concentration of 2 μM, mFc evidently bound to all eight tested viral proteins and cancer-related antigens, including HIV-1 gp140, Zika virus (ZIKV) envelope protein domain II (EDII), domain III (EDIII), mesothelin, 5T4, PD-L1, OX40, TIM-3. We hypothesized the non-specificity came from the introduced mutations located at the original CH3 dimerization interface of IgG1 Fc, and could be resolved by the change of mutation sites of mFc. Therefore, based on our knowledge of Fc homodimerization, we designed a phage display library that enables a combination of rational and random scanning mutagenesis of 7

IgG1 Fc residues (positions Leu-351, Thr-366, Leu-368, Pro-395, Lys-409, Met-428, and Asn-434). Among them, five residues (positions Leu-351, Thr-366, Leu-368, Pro-395, Lys-409) were previously found to greatly impact Fc dimerization, since some specific combinations of their mutations were able to result in soluble monomeric Fcs. In light of the experience gained during the development of monomeric Fcs (20, 21), we simultaneously mutated Leu-351 to Ser or unchanged, Thr-366 to Arg or His, Leu-368 to His or unchanged, Pro-395 to Lys or Arg, and Lys-409 to any of the 20 amino acids (random mutation). Meanwhile, two other residues (Met-428, Asn-434), the mutation of which has been reported to enhance FcRn binding, were randomly mutated to compromise the potential decrease of FcRn-binding activity due to the mutagenesis. Combination of these mutations resulted in a large phage display library containing 1.28×10^5 unique IgG1 Fc mutants. The diversity was verified by randomly picked and sequenced 30 clones from this library (**Figure 1D**).

In addition to the library design, we also improved the library panning procedures to generate clones with decreased non-specific binding (**Figure 2A**). In the previous studies, we screened for phage-displayed soluble and well-folded Fc mutants by purifying phages with protein G resin. The aggregated or non-structured mutants were not able to bind protein G and, therefore, were removed from the library. Although this screening was quite potent and effective, we realized that the mutants with high non-specificity can still bind protein G and thus retained in the following FcRn panning rounds. To address this issue, in the current study, instead of protein G resin we used protein G covalently attached to magnetic beads, which enables the harsh and thorough washing of the bound phages in solution. Moreover, we panned against protein G magnetic beads for two rounds, instead of one round of screening in the previous studies (20), enabling the enrichment of strong and specific protein G binders and, importantly, the removal of Fc mutants with non-specific bindings.

After two rounds of protein G panning, the enriched library was further panned against human FcRn for three additional rounds (**Figure 2A**). To isolate binders with pH-dependent FcRn binding, phages were washed using buffer at acidic pH (6.0) and eluted from beads using buffer at neutral pH (7.4). Using this procedure, 45 clones were selected from the final enriched library by monoclonal phage ELISA. Interestingly, the sequences of the Fc mutants were very diverse, suggesting that soluble Fc mutants with potent FcRn binding could be achieved by multiple combinational mutations.

Next, we assessed the oligomeric state of the Fc mutants by SEC. All these Fc mutants were highly expressed in soluble form in *E. coli*, and 10–20 mg purified protein could be obtained from 1 l bacterial culture under optional conditions. One Fc mutant, designated as 1-B10-9, was found to be pure monomeric, with a single monomer peak eluted at 12.0 ml (**Figures 2B** and **3A**). Our previously reported monomeric Fc (molecular masses of 27 kDa) displayed an identical pattern with a single peak also at 12.0 ml (data not shown). All other mutants were found to exist as a mixture of monomer and dimer, as exemplified by 1-D1-15 (**Figures 2B** and **3A**). Surprisingly, 1-B10-9 has Arg, His, and Lys at positions 366, 368, and 395, respectively, which are

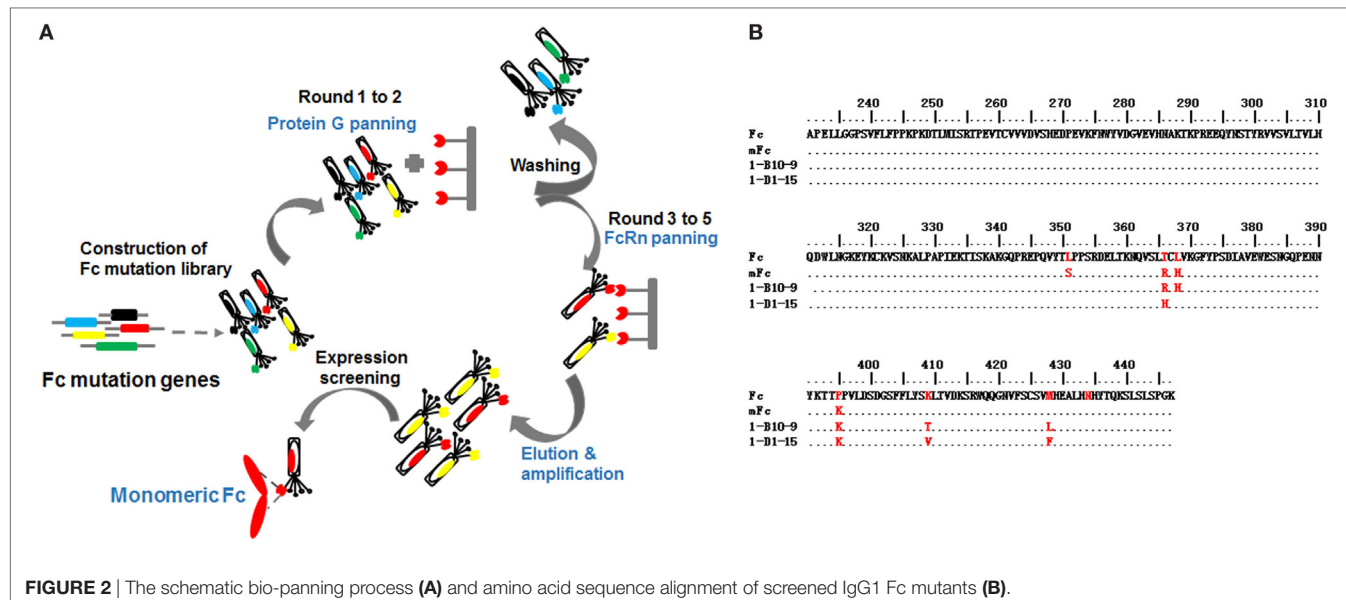


FIGURE 2 | The schematic bio-panning process (**A**) and amino acid sequence alignment of screened IgG1 Fc mutants (**B**).

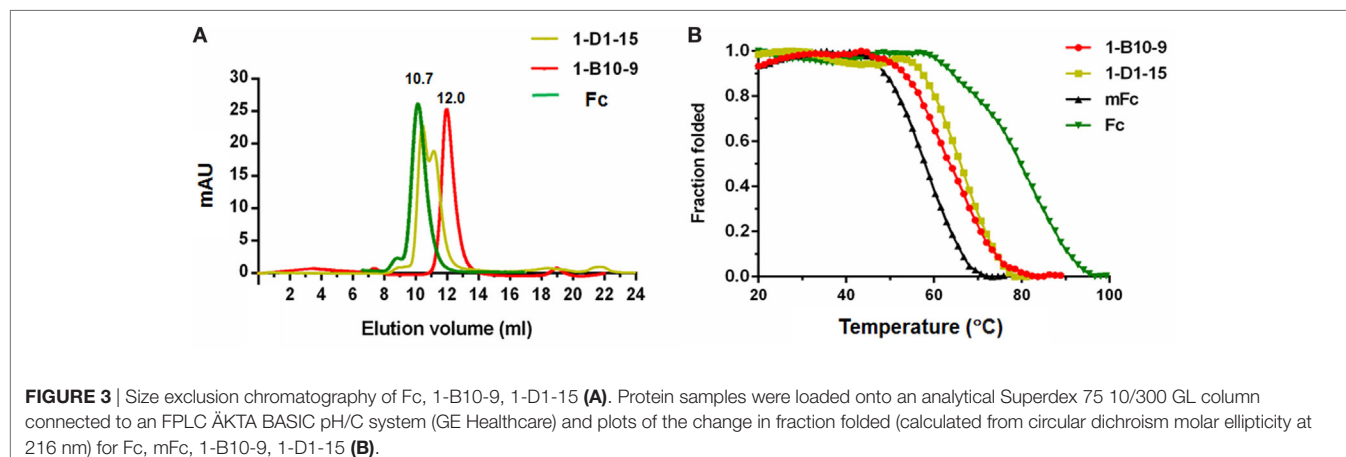


FIGURE 3 | Size exclusion chromatography of Fc, 1-B10-9, 1-D1-15 (**A**). Protein samples were loaded onto an analytical Superdex 75 10/300 GL column connected to an FPLC AKTA BASIC pH/C system (GE Healthcare) and plots of the change in fraction folded (calculated from circular dichroism molar ellipticity at 216 nm) for Fc, mFc, 1-B10-9, 1-D1-15 (**B**).

identical to the previously reported mFc. This result suggests that these mutants are essential to maintain a pure monomeric state. Different from mFc, 1-B10-9 has no mutation at position 351 as compared to the wild-type Fc, but has two additional mutations, K409T and M428L as compared to mFc (Figure 2B).

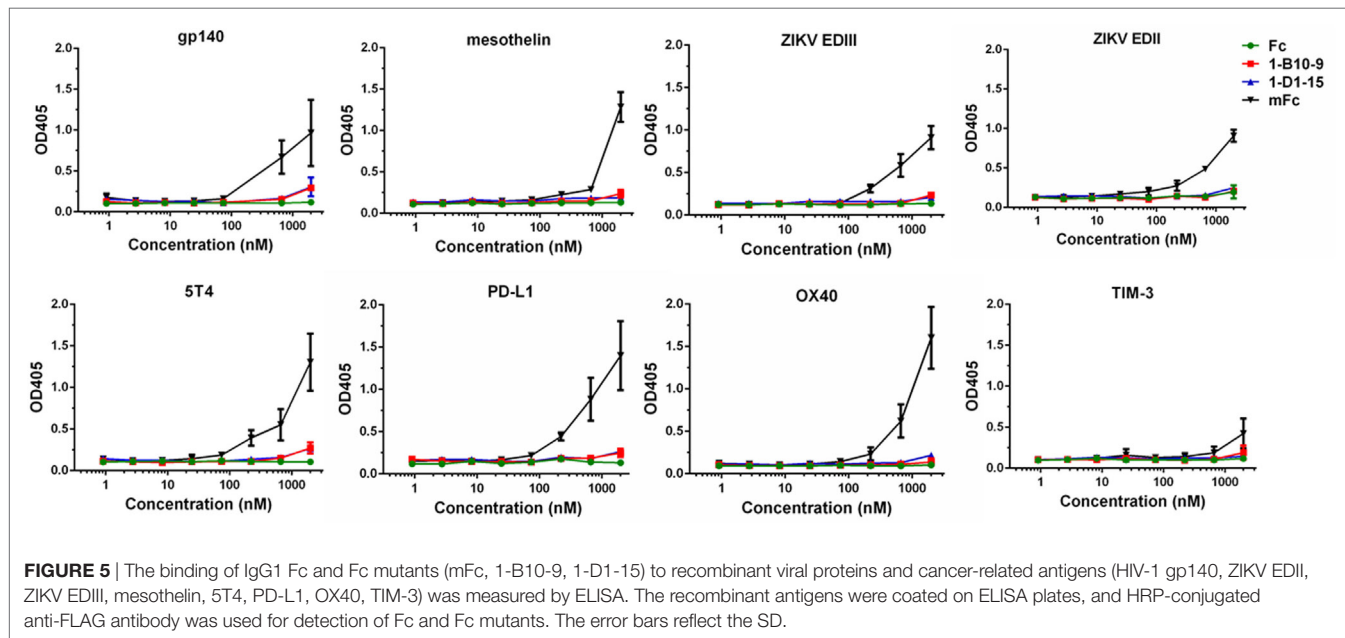
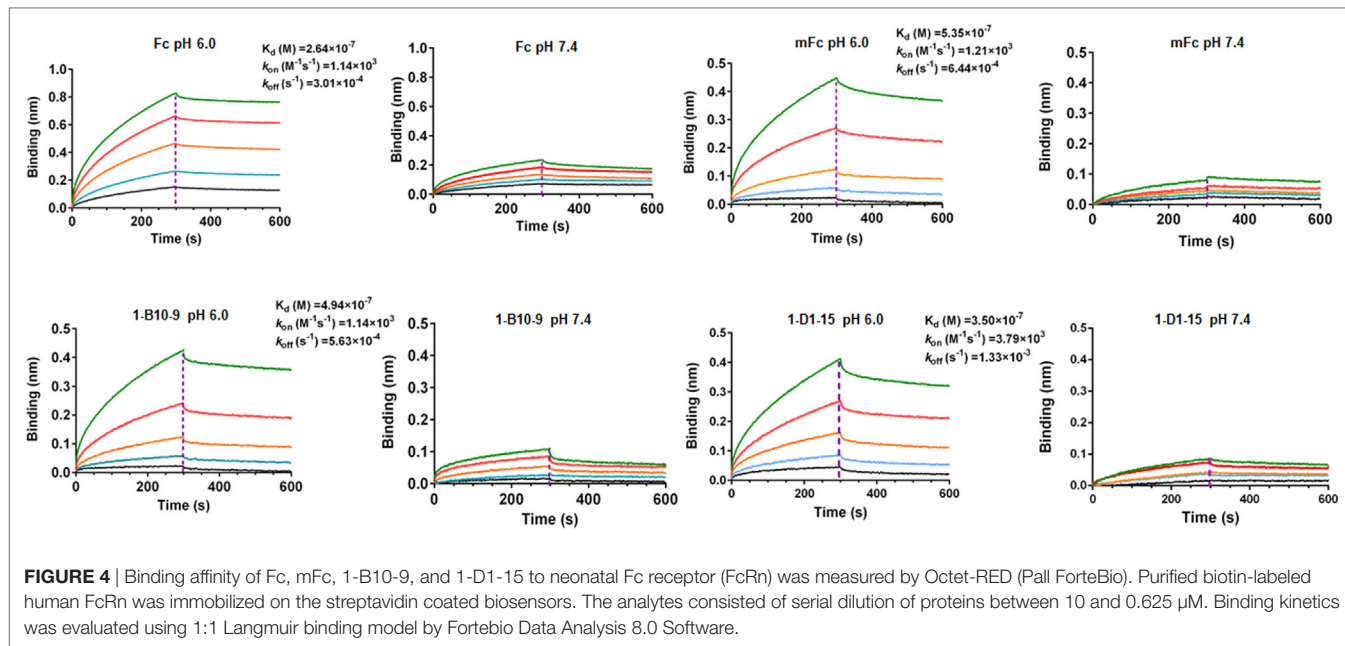
Stability of Monomeric Fc

To detect the thermal stability of the Fc mutants, their CD ellipticity at 216 nm was measured as a function of temperature. The previously reported mFc and the wild-type dimeric IgG1 Fc were used as controls. Interestingly, we found that 1-B10-9 and 1-D1-15 were more stable than the previously identified mFc. The midpoint transition (melting) temperature (Tm) for mFc was $58.4 \pm 0.2^\circ\text{C}$, which is in consistent with the previous report ($54.3 \pm 0.1^\circ\text{C}$) (21). The Tm for 1-B10-9, 1-D1-15, and Fc were 64.0 ± 0.1 , 66.6 ± 0.2 , and $80.6 \pm 0.3^\circ\text{C}$, respectively (Figure 3B). These results suggest that different mutation sites

affect the stability of IgG1 Fc mutants, and that the additional mutations identified on 1-B10-9 and 1-D1-15 may stabilize the constructs.

The New Monomeric Fc Binds to Human FcRn

We next examined whether 1-B10-9 could bind to human FcRn in a pH-dependent manner as the wild-type Fc or mFc using BLI by Octet-RED (Pall ForteBio). Streptavidin coated biosensors immobilized with biotinylated human FcRn were exposed to different concentrations of 1-B10-9, 1-D1-15, mFc, and the wild-type Fc. The assay was carried out under pH 6.0 and pH 7.4, respectively, and the biosensors were regenerated with pH 1.7 buffer. As shown in Figure 4, the wild-type Fc and Fc mutants (mFc, 1-B10-9, 1-D1-15) displayed potent binding to FcRn at pH 6.0. The equilibrium dissociation constant (K_D) of the wild-type Fc for FcRn was $0.26 \mu\text{M}$ with on-rate (k_{on}) of $1.1 \times 10^3 \text{ M}^{-1}\text{s}^{-1}$ and off-rate



(k_{off}) of $3.0 \times 10^{-4} \text{ s}^{-1}$, which is comparable to that in the previous report (K_D of $0.11 \mu\text{M}$) (20). The 1-B10-9 displayed very similar binding kinetics (k_{on} of $1.1 \times 10^3 \text{ M}^{-1}\text{s}^{-1}$, k_{off} of $5.6 \times 10^{-4} \text{ s}^{-1}$) to mFc (k_{on} of $1.2 \times 10^3 \text{ M}^{-1}\text{s}^{-1}$, k_{off} of $6.4 \times 10^{-4} \text{ s}^{-1}$), while the 1-D1-15 displayed slightly faster on-rate ($3.8 \times 10^3 \text{ M}^{-1}\text{s}^{-1}$) and faster off-rate ($1.3 \times 10^{-4} \text{ s}^{-1}$). All these three Fc mutants (mFc, 1-B10-9, 1-D1-15) exhibited very similar binding affinities to FcRn (K_D of 0.54 , 0.49 , and $0.35 \mu\text{M}$, respectively). On the contrary, the wild-type Fc and the Fc mutants showed drastically reduced binding to FcRn when the assay was performed at pH 7.4 (Figure 4). Taken together, these results demonstrated that 1-B10-9 maintained the characteristic pH-dependent FcRn binding of IgG1 Fc.

The New Monomeric Fc Has Significantly Decreased Non-Specific Binding

To evaluate the effectiveness of our strategy in reducing non-specific binding, we randomly selected a panel of viral or cancer-related antigens available in our laboratory, and measured the binding of IgG1 Fc and Fc mutants to these recombinant proteins. Such antigens include HIV-1 gp140, ZIKV glycoprotein EDII, EDIII, mesothelin, 5T4, PD-L1, OX40, and TIM-3. The ELISA plates were coated with these antigens and incubated with serial dilutions of Fc or Fc mutants. As shown in Figure 5, the previously developed mFc displayed relatively strong non-specific binding to all these proteins especially at the highest concentration tested

(2 μ M). Strikingly, 1-B10-9, as well as 1-D1-15 and IgG1 Fc, showed significantly lower ($p < 0.05$) binding to these antigens at high concentrations (Figure 5). These results confirmed that the Fc mutants with significantly decreased non-specificity could be successfully identified using the present library-based panning approach.

DISCUSSION

In previous studies, we have described the generation of several monomeric Fcs (mFc.1, mFc.23, mFc.67, and mFc) by mutating four to seven critical residues located on the IgG1 Fc dimerization interface (20, 21). The monomeric Fcs bound FcRn comparably with the wild-type dimeric Fc, providing direct evidence that Fc dimerization is not required for effective binding to FcRn. This property is critical for the developability of monomeric Fc-based therapeutics, as various studies have demonstrated that half-life of an IgG depends on its pH-dependent binding to FcRn, and that Fc engineering to enhance FcRn binding is effective for elongating half-life or increasing cellular uptake of IgG (6, 14, 23, 24). Based on this finding, we have furthered our studies and developed a number of mFc-based or mFc-derived constructs (monomeric CH3, CH2-CH3 hybrids, etc.) and used them as fusion partners to generate monomeric fusion proteins (25–27). Some of these fusion proteins showed the improved transport across FcRn-expressing cells and did not induce Fc-mediated cytotoxicity *in vitro* (ADCC and CDC) (21). Meanwhile, we introduced point mutations in the CH2 domain and grafted CDR3 regions onto the CH3 domain of mFc, we successfully identified panels of high-affinity binders by panning mFc-based libraries against viral and cancer antigens (unpublished data). The size of mFc is largely reduced compared with the wild-type Fc, and therefore, the mFc-based fusion proteins or antigen binders could achieve enhanced tissue penetration and wider range of possible targets, as well as lower production costs.

In spite of these advantages, in the follow-up study, we found that the binding to unrelated proteins was generally observed for such monomeric Fcs, raising potential risks for their clinical application due to the immunogenicity and pharmacokinetics-related issues. For instance, the unwanted formation of antigen–antibody immune complexes can elicit a variety of downstream effects and further immunogenic responses (28). Their levels, kinetics of interaction, size, polyclonal diversity, distribution, elimination, and antibody-mediated physiological effects can be potentially translated to clinically observable adverse effects (29, 30). Besides, unrelated proteins could bind to the FcRn-binding site of the monomeric Fcs, thereby inhibiting FcRn-mediated recycling of fusion proteins or mFc-based binders. We reasoned that the non-specificity came from the introduced mutations during the generation of monomeric Fc. Therefore, in the present study, we re-designed a phage-displayed Fc mutant library that enables a combination of rational and random scanning mutagenesis of seven mFc residues, and largely improved our

panning and screening procedure with a focus to remove non-specific binding. Using these strategies, we identified a new monomeric Fc, 1-B10-9, that displayed significantly decreased non-specificity. In addition, it exhibited higher thermal stability than mFc, and comparable pH-dependent FcRn-binding capability.

Several conclusions can be drawn from these results. First, the successful generation of new monomeric Fc with minimal non-specificity demonstrates the robust performance of the present approach in reducing non-specific protein binding. One major difference to the previous strategies probably comes from the introduction of Protein G magnetic beads to enrich for the strongest Protein G binders. In contrast to the previous studies using Protein G resin only to remove unstructured mutants (20), the application of Protein G beads enabled harsh and adjustable washing conditions to remove non-specific binders and to result in focused enrichment of Fc mutants with the most potent Protein G binding. Only neglectable binding to unrelated antigens was detected not only for the dimeric Fc and the monomeric 1-B10-9 but also for 1-D1-15, the Fc mutant existing as a mixture of monomer and oligomer as suggested by SEC analysis (Figures 3A,5). This result suggests that the non-specificity was from the introduced mutation amino acids, rather than the monomeric nature of Fc mutants. Interestingly, we found that the non-specificity was probably not due to the hydrophobicity of these residues, as all the Fc mutants possess comparable calculated hydrophobicity index (mFc, -0.654; 1-B10-9, -0.610; 1-D1-15, -0.553). Second, the current display-based strategy allows for the examination of each mutation residues related to the functionality of IgG1 Fc mutants. This can be achieved by rationally or randomly mutating the residue of interest in a displayed mutation library and subsequently analyzing the sequences enriched from bio-panning for those with particular properties. For instance, whereas the non-monomeric Fc mutants have diverse sequences, the identified new IgG1 monomeric Fc, 1-B10-9, has the identical T366R and L368H mutations to the previous reported mFc, suggesting the essential roles of these two mutations in maintaining monomeric status. It is possible that a positively charged surface formed by these two mutations plays a role in the disruption of dimerization. The 1-D1-15, in contrast, has a histidine at residue 366 but a leucine at residue 368, and exists in a non-monomeric form. Besides, the other two residues that located at the CH3 dimerization interface (residues 351 and 409) may play a crucial role in the non-specific binding of Fc mutants. Of note, only the previous-developed mFc has a L351S mutation, suggesting that the Ser-351 residue *per se* or the local conformational change introduced by this mFc mutation may contribute to its relative strong non-specific binding to unrelated targets.

In summary, this study suggests that the new monomeric IgG1 Fc, 1-B10-9, could be potentially applicable in the engineering and development of novel biopharmaceuticals due to its high stability, pH-dependent FcRn binding, and significantly decreased non-specificity compared with the previous reported monomeric Fc mutants.

AUTHOR CONTRIBUTIONS

TY and CW conceived and designed the project. CW, YW, LW, YJ, and GC carried out the experiments. CW, BH, DH, YK, AH, and GH analyzed the data. TY and CW wrote the paper with input from all co-authors.

REFERENCES

- Schrama D, Reisfeld RA, Becker JC. Antibody targeted drugs as cancer therapeutics. *Nat Rev Drug Discov* (2006) 5(2):147–59. doi:10.1038/nrd1957
- Nelson AL, Dhimolea E, Reichert JM. Development trends for human monoclonal antibody therapeutics. *Nat Rev Drug Discov* (2010) 9(10):767–74. doi:10.1038/nrd3229
- Reichert JM, Valge-Archer VE. Development trends for monoclonal antibody cancer therapeutics. *Nat Rev Drug Discov* (2007) 6(5):349–56. doi:10.1038/nrd2241
- Carter PJ. Potent antibody therapeutics by design. *Nat Rev Immunol* (2006) 6(5):343–57. doi:10.1038/nri1837
- Dimitrov DS. Therapeutic antibodies, vaccines and antibodyomes. *mAbs* (2010) 2(3):347–56. doi:10.4161/mabs.2.3.11779
- Roopenian DC, Akilesh S. FcRn: the neonatal Fc receptor comes of age. *Nat Rev Immunol* (2007) 7(9):715–25. doi:10.1038/nri2155
- Kuo TT, Baker K, Yoshida M, Qiao SW, Aveson VG, Lencer WI, et al. Neonatal Fc receptor: from immunity to therapeutics. *J Clin Immunol* (2010) 30(6):777–89. doi:10.1007/s10875-010-9468-4
- Nelson AL, Reichert JM. Development trends for therapeutic antibody fragments. *Nat Biotechnol* (2009) 27(4):331–7. doi:10.1038/nbt0409-331
- Leader B, Baca QJ, Golan DE. Protein therapeutics: a summary and pharmacological classification. *Nat Rev Drug Discov* (2008) 7(1):21–39. doi:10.1038/nrd2399
- Wang L, Ying T. New directions for half-life extension of protein therapeutics: the rise of antibody Fc domains and fragments. *Curr Pharm Biotechnol* (2016) 17:1348–52. doi:10.2174/138920101766160823144032
- Woźniak-Knopp G, Bartl S, Bauer A, Mostageer M, Woisetschlager M, Antes B, et al. Introducing antigen-binding sites in structural loops of immunoglobulin constant domains: Fc fragments with engineered HER2/neu-binding sites and antibody properties. *Protein Eng Des Sel* (2010) 23(4):289–97. doi:10.1093/protein/gzp005
- Woisetschlager M, Antes B, Borrowdale R, Wiederkum S, Kainer M, Steinkellner H, et al. In vivo and in vitro activity of an immunoglobulin Fc fragment (Fcab) with engineered Her-2/neu binding sites. *Biotechnol J* (2014) 9(6):844–51. doi:10.1002/biot.201300387
- Leung KM, Batey S, Rowlands R, Isaac SJ, Jones P, Drewett V, et al. A HER2-specific modified Fc fragment (Fcab) induces antitumor effects through degradation of HER2 and apoptosis. *Mol Ther* (2015) 23(11):1722–33. doi:10.1038/mt.2015.127
- Ying T, Gong R, Ju TW, Prabakaran P, Dimitrov DS. Engineered Fc based antibody domains and fragments as novel scaffolds. *Biochim Biophys Acta* (2014) 1844(11):1977–82. doi:10.1016/j.bbapap.2014.04.018
- Vaccaro C, Zhou J, Ober RJ, Ward ES. Engineering the Fc region of immunoglobulin G to modulate in vivo antibody levels. *Nat Biotechnol* (2005) 23(10):1283–8. doi:10.1038/nbt1143
- Hargreaves CE, Rose-Zerilli MJ, Machado LR, Iriyama C, Hollox EJ, Cragg MS, et al. Fc gamma receptors: genetic variation, function, and disease. *Immunol Rev* (2015) 268(1):6–24. doi:10.1111/imr.12341
- Kouser L, Madhukaran SP, Shastri A, Saraon A, Ferluga J, Al-Mozaini M, et al. Emerging and novel functions of complement protein C1q. *Front Immunol* (2015) 6:317. doi:10.3389/fimmu.2015.00317
- Foss S, Watkinson R, Sandlie I, James LC, Andersen JT. TRIM21: a cytosolic Fc receptor with broad antibody isotype specificity. *Immunol Rev* (2015) 268(1):328–39. doi:10.1111/imr.12363
- Vendel MC, Favis M, Snyder WB, Huang F, Capili AD, Dong J, et al. Secretion from bacterial versus mammalian cells yields a recombinant scFv with variable folding properties. *Arch Biochem Biophys* (2012) 526:188–93. doi:10.1016/j.abb.2011.12.018
- Ying T, Chen W, Gong R, Feng Y, Dimitrov DS. Soluble monomeric IgG1 Fc. *J Biol Chem* (2012) 287(23):19399–408. doi:10.1074/jbc.M112.368647
- Ying T, Feng Y, Wang Y, Chen W, Dimitrov DS. Monomeric IgG1 Fc molecules displaying unique Fc receptor interactions that are exploitable to treat inflammation-mediated diseases. *mAbs* (2014) 6(5):1201–10. doi:10.4161/mabs.29835
- Martin WL, West AJ, Gan L, Bjorkman PJ. Crystal structure at 2.8 Å of an FcRn/heterodimeric Fc complex: mechanism of pH-dependent binding. *Mol Cell* (2001) 7(4):867–77. doi:10.1016/S1097-2765(01)00230-1
- Simister NE, Mostov KE. An Fc receptor structurally related to MHC class I antigens. *Nature* (1989) 337(6203):184–7. doi:10.1038/337184a0
- Zalevsky J, Chamberlain AK, Horton HM, Karki S, Leung IW, Sproule TJ, et al. Enhanced antibody half-life improves in vivo activity. *Nat Biotechnol* (2010) 28(2):157–9. doi:10.1038/nbt.1601
- Ying T, Ju TW, Wang Y, Prabakaran P, Dimitrov DS. Interactions of IgG1 CH2 and CH3 domains with FcRn. *Front Immunol* (2014) 5:146. doi:10.3389/fimmu.2014.00146
- Ying T, Chen W, Feng Y, Wang Y, Gong R, Dimitrov DS. Engineered soluble monomeric IgG1 CH3 domain: generation, mechanisms of function, and implications for design of biological therapeutics. *J Biol Chem* (2013) 288(35):25154–64. doi:10.1074/jbc.m113.484154
- Ying T, Wang Y, Feng Y, Prabakaran P, Gong R, Wang L, et al. Engineered antibody domains with significantly increased transcytosis and half-life in macaques mediated by FcRn. *mAbs* (2015) 7(5):922–30. doi:10.1080/19420862.2015.1067353
- Bosques CJ, Manning AM. Fc-gamma receptors: attractive targets for autoimmune drug discovery searching for intelligent therapeutic designs. *Autoimmun Rev* (2016) 15(11):1081–8. doi:10.1016/j.autrev.2016.07.035
- Maeda A, Iwayanagi Y, Haraya K, Tachibana T, Nakamura G, Nambu T, et al. Identification of human IgG1 variant with enhanced FcRn binding and without increased binding to rheumatoid factor autoantibody. *mAbs* (2017) 9(5):844–53. doi:10.1080/19420862.2017.1314873
- Krishna M, Nadler SG. Immunogenicity to biotherapeutics – the role of anti-drug immune complexes. *Front Immunol* (2016) 7:21. doi:10.3389/fimmu.2016.00021

FUNDING

This work was supported by the National Natural Science Foundation of China (31570936, 81630090, 81561128006), the Shanghai Pujiang Talent Program (15PJ1400800), and the 1000 Young Talents Program of China.

Conflict of Interest Statement: The authors declare that the research was conducted in the absence of any commercial or financial relationships that could be construed as a potential conflict of interest.

Copyright © 2017 Wang, Wu, Wang, Hong, Jin, Hu, Chen, Kong, Huang, Hua and Ying. This is an open-access article distributed under the terms of the Creative Commons Attribution License (CC BY). The use, distribution or reproduction in other forums is permitted, provided the original author(s) or licensor are credited and that the original publication in this journal is cited, in accordance with accepted academic practice. No use, distribution or reproduction is permitted which does not comply with these terms.



OPEN ACCESS

Edited by:

Tianlei Ying,
Fudan University, China

Reviewed by:

Dimitar S. Dimitrov,
National Institutes of Health, USA
Lisa F. P. Ng,
Singapore Immunology Network
(A*STAR), Singapore

***Correspondence:**

Hin Chu
hinchu@hku.hk;
Kwok-Yung Yuen
kyyuen@hku.hk

[†]These authors contributed equally to
the study as co-first authors.

[‡]These authors contributed
equally to the study as
co-corresponding authors.

Specialty section:

This article was submitted to
Vaccines and Molecular
Therapeutics,
a section of the journal
Frontiers in Immunology

Received: 14 January 2017

Accepted: 06 March 2017

Published: 21 March 2017

Citation:

Ye Z-W, Yuan S, Poon K-M,
Wen L, Yang D, Sun Z, Li C, Hu M,
Shuai H, Zhou J, Zhang M-Y,
Zheng B-J, Chu H and Yuen K-Y
(2017) Antibody-Dependent
Cell-Mediated Cytotoxicity
Epitopes on the Hemagglutinin
Head Region of Pandemic H1N1
Influenza Virus Play Detrimental
Roles in H1N1-Infected Mice.
Front. Immunol. 8:317.
doi: 10.3389/fimmu.2017.00317

Antibody-Dependent Cell-Mediated Cytotoxicity Epitopes on the Hemagglutinin Head Region of Pandemic H1N1 Influenza Virus Play Detrimental Roles in H1N1-Infected Mice

Zi-Wei Ye^{1†}, Shuofeng Yuan^{1†}, Kwok-Man Poon¹, Lei Wen¹, Dong Yang¹, Zehua Sun¹, Cun Li¹, Meng Hu¹, Huiping Shuai¹, Jie Zhou^{1,2}, Mei-Yun Zhang¹, Bo-Jian Zheng¹, Hin Chu^{1,2‡} and Kwok-Yung Yuen^{1,2,3,4‡}

¹Department of Microbiology, The University of Hong Kong, Hong Kong, ²State Key Laboratory of Emerging Infectious Diseases, The University of Hong Kong, Hong Kong, ³Research Centre of Infection and Immunology, The University of Hong Kong, Hong Kong, ⁴Carol Yu Centre for Infection, The University of Hong Kong, Hong Kong

Engaging the antibody-dependent cell-mediated cytotoxicity (ADCC) for killing of virus-infected cells and secretion of antiviral cytokines and chemokines was incorporated as one of the important features in the design of universal influenza vaccines. However, investigation of the ADCC epitopes on the highly immunogenic influenza hemagglutinin (HA) head region has been rarely reported. In this study, we determined the ADCC and antiviral activities of two putative ADCC epitopes, designated E1 and E2, on the HA head of a pandemic H1N1 influenza virus *in vitro* and in a lethal mouse model. Our data demonstrated that sera from the E1-vaccinated mice could induce high ADCC activities. Importantly, the induction of ADCC response modestly decreased viral load in the lungs of H1N1-infected mice. However, the elevated ADCC significantly increased mouse alveolar damage and mortality than that of the PBS-vaccinated group ($P < 0.0001$). The phenotype was potentially due to an exaggerated inflammatory cell infiltration triggered by ADCC, as an upregulated release of cytotoxic granules (perforin) was observed in the lung tissue of E1-vaccinated mice after H1N1 influenza virus challenge. Overall, our data suggested that ADCC elicited by certain domains of HA head region might have a detrimental rather than protective effect during influenza virus infection. Thus, future design of universal influenza vaccine shall strike a balance between the induction of protective immunity and potential side effects of ADCC.

Keywords: antibody-dependent cell-mediated cytotoxicity, H1N1 influenza virus, hemagglutinin, lung damage, mice

INTRODUCTION

Influenza viruses, as one of the major zoonotic pathogens, have continuously caused global health concerns due to their high propensity for unpredictable genetic mutation in major surface antigens, hemagglutinin (HA), and neuramindase. Antivirals and vaccines are vital in combating the threat of influenza epidemics and pandemics. However, the increasing usage of licensed antivirals has resulted in the global emergence of amantadine- and/or oseltamivir-resistant strains of influenza virus. Typical examples include the worldwide spread of adamantine resistant A(H3N2) viruses since 2003, oseltamivir-resistant seasonal A(H1N1) viruses since 2007, adamantine-resistant pandemic A(H1N1) viruses in 2009, and peramivir-resistant A(H7N9) viruses in 2013 (1). On the other hand, seasonal influenza vaccines have to be updated annually due to the continuous antigenic drift and shift (2). Otherwise, the mismatch between vaccinated formulations and that of natural selection would considerably limit the effectiveness of influenza vaccines.

Neutralizing antibodies have traditionally been thought to provide protection against influenza viruses. Nevertheless, the effectiveness induced by such vaccines is limited by the emergence of mutant viruses that are resistant to antibody-mediated neutralization (3). In this regard, the quest for universal influenza vaccines has fueled the interest in broadly reactive antibodies in addition to direct virus neutralizations. Antibody-dependent cell-mediated cytotoxicity (ADCC) uses effector arms of both innate and adaptive immune responses to eliminate target cells. Natural killer (NK) cells, upon triggered by specific ADCC antibodies, mediate the clearance of virus-infected cells (4). The NK cell CD16 receptor recognizes the Fc portion of IgG1 antibodies that in turn bind to antigens on virus-infected cells (5). This interaction induces degranulation of NK cells to release perforin/granzymes as well as secretion of antiviral cytokines such as interferon- γ (IFN- γ) and tumor necrosis factor- α (TNF- α) (5).

Since ADCC could invoke protective immune response against infections from a broad array of viruses, the ADCC antibody response was incorporated as one of the most important features of potential universal vaccine candidates by the World Health Organization. Notably, multiple components of influenza viruses are known to induce ADCC, including the viral surface proteins such as HA (6) and M2 ectodomain (7, 8), as well as the internal proteins including NP and M1 (9). The glycoprotein HA consists of two functional domains, the immunodominant globular head domain and the more conserved stalk domain (10). Conventionally, neutralizing antibody response to influenza virus is dominated by antibodies that target the head region, which block the virus receptor-binding site. Compared with the bulky globular HA head, the HA stem region is far less immunogenic, and antibodies directed to this domain occur at a relatively low frequency. However, a rare class of neutralizing antibodies that target a conserved site in the HA stem was reported recently, which might shed new light for the development of universal influenza vaccines (6).

We have previously identified two putative ADCC epitopes that mapped to the HA head of a pandemic H1N1 influenza virus

(11). Both epitopes, designated E1 and E2, revealed by epitope mapping of convalescent-phase plasma IgG antibodies from six H1N1-infected human subjects, are dominant and highly conserved (11). In this study, we further dissected the function of the two ADCC epitopes *in vitro* and in a lethal mouse model. Surprisingly, our results demonstrated that the ADCC response elicited by the E1 epitope triggered a detrimental rather than protective effect against influenza virus infection. While the anti-viral efficacy provided by the stalk-specific ADCC antibodies has been confirmed (12), our data raised concerns on the side effect of certain HA head epitopes in devising a universal influenza vaccine. In this regard, our study suggested that a delicate balance between protective immunity and over induction of ADCC should be maintained, which should be an important consideration in evaluating vaccine safety.

MATERIALS AND METHODS

Cells and Viruses

The LA4 cell line, which was derived from mouse lung adenoma, was maintained in DMEM/F-12 medium (Gibco) supplemented with 20% heat-inactivated fetal bovine serum (FBS), 50 U/ml penicillin, and 50 μ g/ml streptomycin (P/S). Peripheral blood mononuclear cells (PBMCs) were prepared by Ficoll-Paque separation (13) of heparinized whole blood obtained from healthy BALB/c mice (6–8 weeks old). To prepare the ADCC target cells, LA4 cells were transfected with an HA expression plasmid that based on the cDNA fragment of influenza virus strain A/Hong Kong/415742/2009(H1N1)pdm09. Specifically, the full-length HA fragment was cloned into a mammalian expression vector pEAK10 plasmid containing a mouse IgG1 Fc gene (CH2 + CH3) (14). The pandemic H1N1 influenza virus strain A/Hong Kong/415742/2009(H1N1)pdm09 was used for *in vitro* virus infection; while its mouse-adapted version, A/Hong Kong/415742Md/2009 (H1N1)pdm09 was propagated in embryonated hens' eggs and utilized for *in vivo* experiment (15). The viruses were stored in –80°C in aliquot and titrated by standard plaque assay. All experiments with live viruses were conducted using biosafety level 2 facilities as described previously (16).

Mouse Study

BALB/c female mice, 6–8 weeks old, were kept in biosafety level 2 housing and given access to standard pellet feed and water *ad libitum*. All experimental protocols followed the standard operating procedures of the biosafety level 2 animal facilities and were approved by the Animal Ethics Committee in the University of Hong Kong (17).

Vaccination

Vaccinations were carried out to immunize the mice with E1 or E2 or HA epitopes by DNA priming and protein boost. PBS was used as a negative control. The specified vaccination scheme was listed in Table 1. To prepare the DNA plasmids, either of the E1 or E2 fragment (11) was cloned into the mammalian expression vector pEAK10 as described for the HA plasmid construction. The resultant plasmid DNA (100 μ g per mice) was used for DNA

TABLE 1 | Mouse vaccinations scheme.

Inoculation and bleed	Day	PBS group (n = 15)	E1 group (n = 15)	E2 group (n = 15)	Hemagglutinin (HA) group (n = 15)
Bleed 0	0				6- to 8-week female mice
Primary inoculate (DNA)	1	PBS (100 µl)	E1 plasmid (100 µg/100 µl)	E2 plasmid (100 µg/100 µl)	HA plasmid (100 µg/100 µl)
Bleed 1	28				
Boost 1 (DNA)	29	PBS (100 µl)	E1 plasmid (100 µg/100 µl)	E2 plasmid (100 µg/100 µl)	HA plasmid (100 µg/100 µl)
Boost 2 (protein) ^a	43	PBS (100 µl)	E1 protein (25 µg/100 µl)	E2 protein (25 µg/100 µl)	HA protein (25 µg/100 µl)
Boost 3 (protein) ^a	57	PBS (100 µl)	E1 protein (25 µg/100 µl)	E2 protein (25 µg/100 µl)	HA protein (25 µg/100 µl)
Bleed 2	68				
Virus challenge	69		(1,000 FPU/mouse for all groups, record the mouse body weight, and survival every day, until day 83)		

^aSigma adjuvant system was added as adjuvant.

priming of the mice by electroporation. To prepare protein for vaccination, recombinant HA, E1, and E2 fusion proteins were expressed in FreeStyle 293FT™ transient expression system (Invitrogen) and purified by protein A affinity (GE Healthcare). Subsequently, proteins were dialyzed and concentrated with Vivaspin 20 centrifugal concentrator (GE Healthcare), followed by protein boosting through intramuscular route. Each mouse received 25 µg protein at each protein boosting. Sera were obtained at day 68 postimmunization before virus challenge. Antibody titers raised against E1, E2, and HA in mouse sera were evaluated by ELISA as previously described with some modifications (18). Mouse sera collected from the PBS-treated group were taken as a background control.

Virus Challenge Study

Immunized mice (15 mice/group) were inoculated with five 50% lethal dose (LD_{50}) of mouse-adapted pandemic H1N1 influenza virus by intranasal route, i.e., 1,000 PFU/mouse. Animal survival and body weight were monitored daily for 14 days after virus challenge. A body weight loss of 30% was set as the humane endpoint. Three mice per group were randomly selected and euthanized on day 3 and 5 post-challenge, respectively. Mouse lungs were collected from the euthanized mice. Half of the lung tissues were harvested for virus titration by RT-qPCR methods (19), while the other half were immediately fixed in 10% of PBS buffered formaldehyde for histopathological analyses as described previously (20).

Histopathological Assessment

Slides were examined in a blinded manner and scored with a semiquantitative system according to the relative degree of inflammation and tissue damage (21–24). Inflammation was scored as follows: 0, no inflammation; 1, perivascular cuff of inflammatory cells; 2, mild inflammation (extending throughout 25% of the lung); 3, moderate inflammation (25–50% of the lung); 4, severe inflammation involving over one half of the lung.

ADCC Assay

Antibody-dependent cell-mediated cytotoxicity activity, reflected by the rate of cell death, was measured by a flow cytometry-based assay that described previously with some modifications (11).

Generally, the PKH-67 dye (Sigma) was utilized to label the target cells, i.e., HA-transfected LA-4 cells; while 7-Aminoactinomycin D (7-AAD; Invitrogen) was used to stain the dead cells that mediated by ADCC activity. Experimentally, PKH-67-labeled target cells and unlabeled effector cells (i.e., PBMCs) were prepared in RPMI 1640 medium (Gibco) containing 10% FBS and 1% P/S with a cell density of 10^6 and 10^8 cells/ml, respectively. Subsequently, 50 µl of target cells were dispensed into a round-bottom 96-well plate, followed by addition of 1 µl of mouse serum. Mouse serum concentration in each group was normalized before addition according to their titers determined by ELISA. One hour after incubation, 50 µl of effector cells were added to incubate with the target cells. Three hours later, another 1 µl of 7-AAD was added to each well before performing the flow cytometry. Cell death was determined with a FACSAria III flow cytometer using the BD FACS software (BD Biosciences). Percent cell death was calculated by software analysis of four identifiable cell populations: live effector cells (no dye), dead effector cells (7-AAD positive), live target cells (PKH-67 positive), and dead target cells (PKH-67 and 7-AAD double positive). Assay controls used to define cell populations included target cells alone (background cell death) and target cells with 1 µl Triton X-100 added (maximum cell death). Percent ADCC was calculated as $\frac{[(\text{percent experimental lysis} - \text{percent spontaneous lysis}) / (\text{percent maximum lysis} - \text{percent spontaneous lysis})]}{100\%}$, in which percent spontaneous lysis refers to the percent lysis of infected cells with effectors but in the absence of serum, while percent maximum lysis refers to the percent lysis of infected cells with effectors in the presence of 1% Triton X-100. Experiments were performed in triplicate and repeated twice for confirmation.

Confocal Imaging

Immunostaining was performed as previously described to visualize perforin expression in mouse lung tissues (25). Rat anti-mouse perforin (abcam Ab16074) and goat anti-rat Alexa 594 were used as primary and secondary antibodies, respectively. Images were acquired with a Carl Zeiss LSM 780 system.

Quantitative Real-time RT-PCR

RNA extraction, reverse transcription, and qPCR were performed as previously described (26, 27). In brief, total RNA was extracted

from mouse lung with RNeasy Mini Kit (Qiagen) and reverse transcribed with Transcripter First Strand cDNA Synthesis Kit (Roche). Real time PCR was performed using LightCycler® 96 (Roche) machine according to the manufacturer's instructions. Relative gene expression was normalized to the corresponding β -actin values. The sequences of the primers for RT-qPCR are listed in Table S1 in Supplementary Material.

Statistical Analysis

Statistical comparison was performed by Student's *t*-test using GraphPad Prism 6. Differences were considered statistically significant when $P < 0.05$.

RESULTS

ADCC Responses Are Enhanced by the Sera of E1-Vaccinated Mice

In our previous study, we mapped two putative ADCC epitopes, E1 and E2, on the HA head region. By depleting E1 and/or E2 from clinical plasma IgG antibodies, the ADCC activity dropped significantly, which suggested that the two epitopes played potential roles in eliciting ADCC (11). In this study, we sought to confirm the function of these putative epitopes in the induction of ADCC activity using a mouse model. Immunization of mice gave raise to IgG titers against the E1, E2, or HA protein, as quantified by ELISA (Figure 1). A prime/boost immunization strategy was adopted, and mice that immunized with PBS or HA were included as a negative or a positive control, respectively

(Table 1). Our results indicated that serum samples from mice vaccinated with E1 (Figure 1A) or E2 (Figure 1B) both exhibited strong dilution-dependent antibody responses, reaching a titer of more than 1:5000. Additionally, using HA as the coating antigen for ELISA, we demonstrated that E1 and E2 sera could bind full-length HA at a comparable efficiency (Figure S1 in Supplementary Material). Taken together, our data suggested that the vaccination was successful and the resultant serum samples could be utilized for further investigations.

Next, ADCC activities in serum samples from E1-, E2-, or HA-immunized mice were evaluated by flow cytometry-based ADCC assays. To this end, the HA-transfected LA4 cells were labeled with the cell-membrane marker PKH67 and utilized as target cells for ADCC-specific antibody binding. Subsequently, the vaccinated mouse serum was added to bridge the interaction between target cells and PBMC effector cells (Figure 2). The presence of ADCC-mediated antibody was determined by analyzing the cytotoxicity rate within the cell mixture that contained the target cells, serum, and effector cells, in which the dead target cell population was revealed by the cell death marker, 7AAD (Figure 3). As shown in Figures 3A–G, sera from the E1-vaccinated mice consistently triggered the highest 7AAD + rate among all evaluated groups, suggesting that a higher percentage of cell lysis was induced in the E1 group in comparison to the other groups. The percentage of cytotoxicity was normalized using the formula reported by Srivastava et al., with spontaneous and maximum cell cytotoxicity rate taken into consideration (11). Quantitatively, sera from the E1-vaccinated mice elicited a significantly increased ($P < 0.05$) ADCC activity in comparison with the PBS-vaccinated group (Figure 3H). Of note, though sera from the E2-Vaccinated mice triggered a subtle increase in ADCC activity, the difference was not statistically significant (Figure 3H). Intriguingly, albeit HA contained the E1 epitope, sera from the HA-vaccinated group did not induce a significantly elevated cytotoxicity response in comparison to that of the PBS control group (Figure 3H).

E1-Vaccinated Mice Are Adversely Affected by ADCC

Since E1 was capable of inducing ADCC activities, we hypothesized that E1-vaccinated mice could potentially be protected by the elicited ADCC activity after influenza virus challenge. To this end, we inoculated the vaccinated mice with pandemic H1N1 influenza virus in a lethal mouse model (Figure 4A). As shown in Figure 4B, mice in the HA-vaccinated group, as a positive control, demonstrated a substantial reduction of viral load on both day 3 and day 5 post-inoculation in comparison to the PBS-vaccinated group. Importantly, we detected an approximately one log decrease of viral load in the mouse lungs of the E1-vaccinated group in comparison to that of the PBS-vaccinated group on day 5 post-inoculation, while no significant difference could be observed between the two groups on day 3 post-virus challenge (Figure 4B). In addition, the viral load in the lungs of the E1-vaccinated mice was notably lower on day 5 when compared with that of day 3, suggesting that the ADCC effect was triggered between day 3 and 5 post-inoculation (Figure 4B).

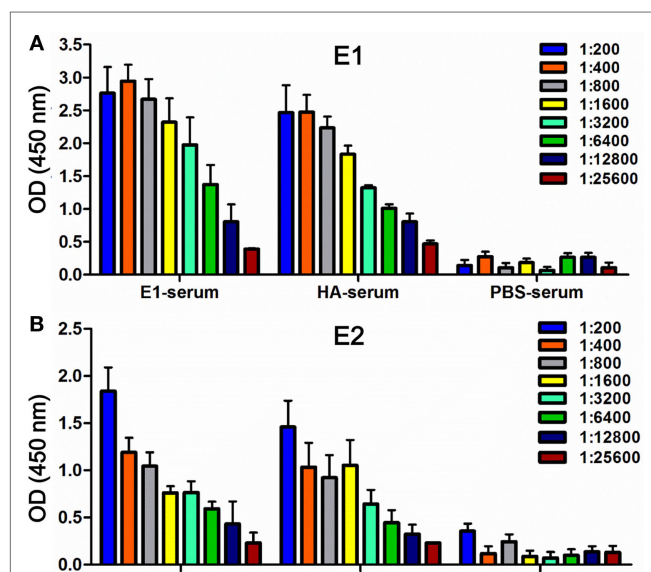


FIGURE 1 | Detection of binding activities in mouse serum samples. ELISA was used to measure antibody titers in serum samples collected from the mice vaccinated with E1 (E1-serum), E2 (E2-serum), HA (HA-serum), or PBS (PBS-serum) on day 68. Binding was tested against either the antigen E1-Fc (A) or E2-Fc (B), respectively. Binding intensities were measured at an absorbance of 450 nm. The experiments were conducted in triplicate. Data shown represents the mean values \pm SD ($n = 6$).

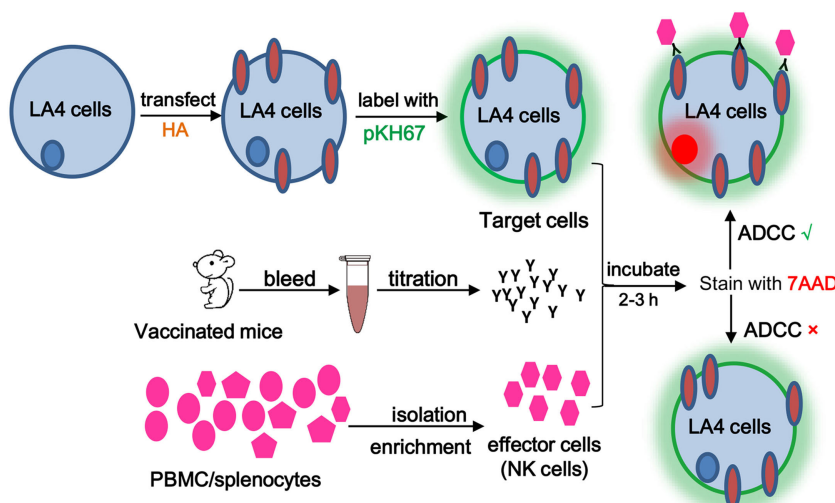


FIGURE 2 | Schematic diagram of the antibody-dependent cell-mediated cytotoxicity (ADCC) assay. ADCC activity was determined by a flow cytometry-based assay using two fluorescent dyes. PKH-67, a membrane-labeling dye, was used to specifically identify the HA-transfected target cells. 7AAD was excluded by viable cells but could penetrate the cell membrane of dead or dying cells and intercalate into double-stranded DNA. Briefly, 50 μ l of PKH-67-labeled target cells (10^6 cells/ml) was dispensed into a round-bottom 96-well plate, followed by addition of E1/E2/HA/PBS sera and effector/PBMC cells. Following a 3-h incubation, 7-AAD was added. Cell death was determined on a FACSaria III flow cytometer using BD FACS Diva software (BD Biosciences). Percent cell death was analyzed by the Flowjo software.

In parallel, we measured the survival rate and body weight changes of the mice. As shown in **Figure 4C**, all mice from the HA-vaccinated group survived the course of infection while all mice received PBS-treatment died, indicating that the virus challenge was successful. Unexpectedly, our results demonstrated that the mice in the E1-vaccinated group succumbed to influenza virus infection at a significantly earlier time ($P < 0.0001$) post-inoculation when compared with that of the PBS-vaccinated control group (**Figure 4C**). In line with the survival rate, mice from the E1-vaccinated group suffered from an apparently accelerated weight loss starting on day 3 post-inoculation in comparison to mice from the PBS- and E2-vaccinated groups, although the difference did not reach statistical significance (**Figure 4D**).

Next, we carried out histopathological examinations on the lung sections of the virus-infected mice. Using uninfected mouse lung tissues as a control (**Figures 5I,J**), our observation showed that on both day 3 and day 5, mice from the HA-vaccinated group (**Figures 5G,H**) exhibited ameliorated alveolar morphology changes when compared with those from the E1 (**Figures 5C,D**), E2 (**Figures 5E,F**), and PBS (**Figures 5A,B**) groups. Importantly, the lung pathological scores of mice from the HA-vaccinated group on both day 3 and day 5 were significantly lower than those of the PBS-treated mice (**Figures 5K,L**); while mice from the E1-vaccinated group suffered from a significantly more dramatic interstitial inflammatory infiltration than that of the PBS-treated mice on day 5 (**Figure 5L**). This result indicated that the detrimental lung damage of E1-vaccinated mice, possibly triggered by ADCC, might account for the reduced viral load in lungs as well as the earlier drop in survival.

To address whether the severe lung damage in the E1-vaccinated group could be attributed to the ADCC effect, we

performed immunofluorescence staining to visualize the expression level of perforin among different mouse groups. Perforin is released by activated NK cells and is known as a marker of ADCC activation (28). As quantitated in **Figure 6M**, the E1-vaccinated mice (**Figures 6D–F**) demonstrated the highest perforin expression level in the lung sections amongst the other three groups on day 5 post infection (**Figures 6A–C,G–L**). However, the mRNA expression level of perforin was not significantly different across all evaluated groups (**Figure 6N**).

Binding of Fc receptor (FcR) on effector cells triggers the secretion of cytotoxic granules as well as antiviral cytokines and chemokines, such as IFN- γ and TNF- α (4). To investigate if elevated expression of proinflammatory cytokines might contribute to the lung damage, we measured the mRNA expression level of representative cytokines including TNF- α (**Figure 7A**), IL-1 β (**Figure 7B**), and IFN- γ (**Figure 7C**) in the mouse lungs samples. Our results showed that the gene expression of all three proinflammatory cytokines were significantly enhanced in the E1-vaccinated group when compared with those of the PBS-treated group (**Figure 7**), which were in line with the perforin protein expression pattern in **Figure 6**. Together, our data suggested that the E1 epitope from the HA head domain mediated unfavorable ADCC that resulted in a more severe lung damage and exacerbated mouse mortality despite a successful control of the H1N1 influenza viral load.

DISCUSSION

Antibody-dependent cell-mediated cytotoxicity, as a bridge of the innate and adaptive immunity, plays important roles in humoral and cellular immune response (4, 9). Since ADCC antibodies are

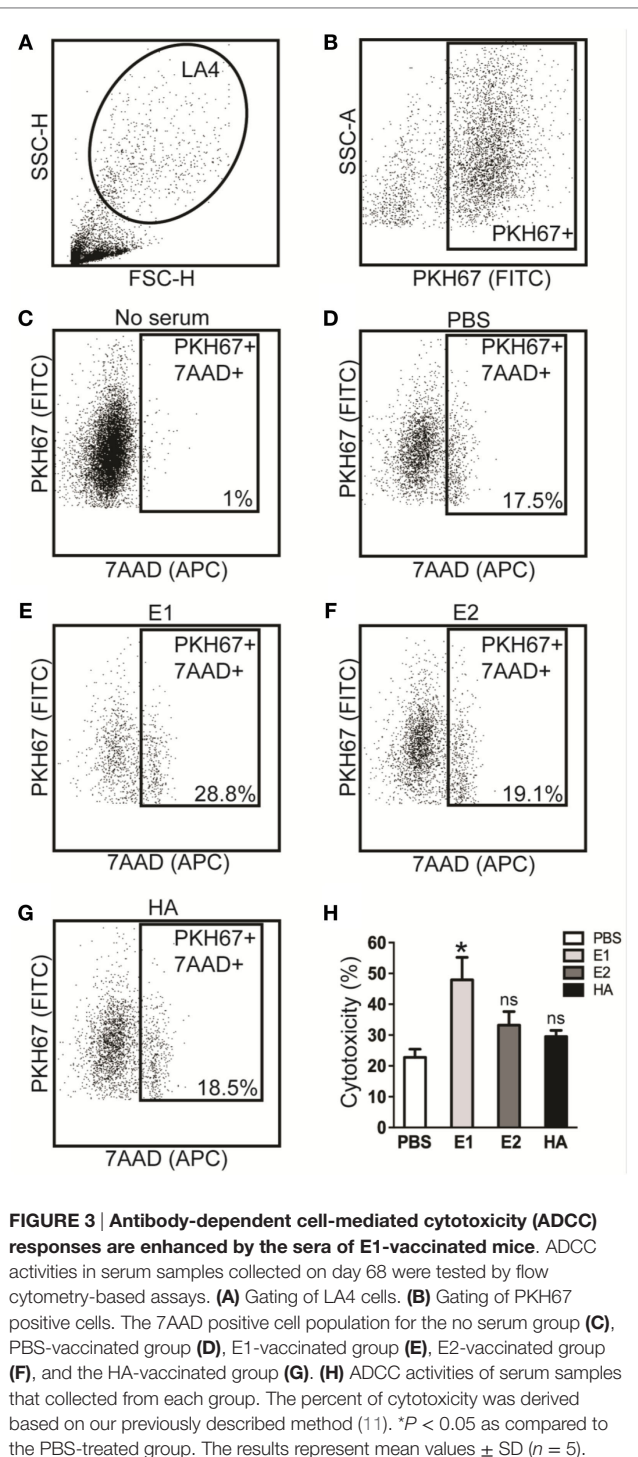


FIGURE 3 | Antibody-dependent cell-mediated cytotoxicity (ADCC) responses are enhanced by the sera of E1-vaccinated mice. ADCC activities in serum samples collected on day 68 were tested by flow cytometry-based assays. **(A)** Gating of LA4 cells. **(B)** Gating of PKH67 positive cells. The 7AAD positive cell population for the no serum group **(C)**, PBS-vaccinated group **(D)**, E1-vaccinated group **(E)**, E2-vaccinated group **(F)**, and the HA-vaccinated group **(G)**. **(H)** ADCC activities of serum samples that collected from each group. The percent of cytotoxicity was derived based on our previously described method (11). *P < 0.05 as compared to the PBS-treated group. The results represent mean values \pm SD ($n = 5$).

known to recognize a wide range of viral proteins that lead to the lysis of virus-infected cells, a better understanding on the ADCC mechanism during influenza virus infections will facilitate the development of universal influenza vaccines with broader protections (4, 9, 29). The conserved viral proteins or domains, such as M2 extracellular domain and HA stem domain, have been widely studied as potential targets of domain-based universal influenza

vaccines. Jegerlehner and colleagues have demonstrated that the protective role of M2 ADCC-mediating antibodies was dependent on FcR (7, 8). DiLillo et al. provided further support that the influenza-specific ADCC antibody, though elicited by the HA stem, also required FcRs interaction for protection against lethal influenza infection (6). Collectively, both studies highlighted the functional importance of FcR during ADCC-mediated virus clearance. On the other side, unexpected cases have been reported that young adults without prior exposure to the 1968 H3N2 virus produced robust ADCC-mediating antibody response upon infection of this virus strain. Some individuals even possessed cross-reactive ADCC-mediating antibodies toward avian H5N1 and H7N7 strains in the absence of prior exposure (30). However, the mechanism of such antibody responses remains unclear to date.

In this study, we investigated the ADCC effect of the two putative HA head epitopes *in vitro* and *in vivo*. Our data demonstrated that E1-induced ADCC activity against H1N1 influenza virus infection *in vitro* (Figure 3). Unexpectedly, although E1 vaccination decreased the viral load in H1N1-infected mice (Figure 4B), it induced exacerbated lung damage (Figure 5) and a higher level of NK activity (Figure 6) that accelerated mouse death (Figure 4C). NK cells, which offer the first line of defense against virus infection, have been widely considered to be beneficial to the host during viral infections. However, a recent report by Zhou et al. revealed that adoptive transfer of NK cells from influenza virus-infected lungs, but not uninfected lung, resulted in a more rapid weight loss and increased mortality of virus-infected mice (31). This finding was in line with our observation that E1-induced ADCC exhibited deleterious impact to promote mortality during influenza virus infection.

Most healthy donors have a persistently low level of cross-reactive ADCC-mediating antibodies, while these cross-reactive antibodies are found in individuals in the absence of detectable neutralization (4, 9). In our previous study, both E1 and E2 epitopes were identified as putative regions that could induce ADCC activity. The depletion of such antibodies in human plasma significantly decreased the ADCC effect. However, for certain samples, it appeared that more diluted plasma exhibited higher ADCC activity than less diluted plasma, and the use of IgG antibodies at a low concentration led to a higher ADCC activity than the use of IgG antibodies at a high concentration (11). To date, there is no conclusive study on the correlation between antibody concentration and ADCC activity, neither was the optimal concentration of ADCC antibodies that could protect against virus infection elucidated. In this context, we demonstrated here that an overwhelming production of ADCC antibodies in the absence of neutralization might not play a protective role against influenza virus infection. Indeed, multiple factors such as saturation of antibodies or interference from non-ADCC antibodies may contribute to the induction of ADCC (4, 11). In this case, the threshold level of protective ADCC-mediating antibodies should be investigated in further studies.

Various ADCC assays that mainly differ in the choice of effector cells and measurement of ADCC activity have been reported (4, 9). For example, some studies used HA-transfected or virus-infected A549 cells as target cells, which were susceptible

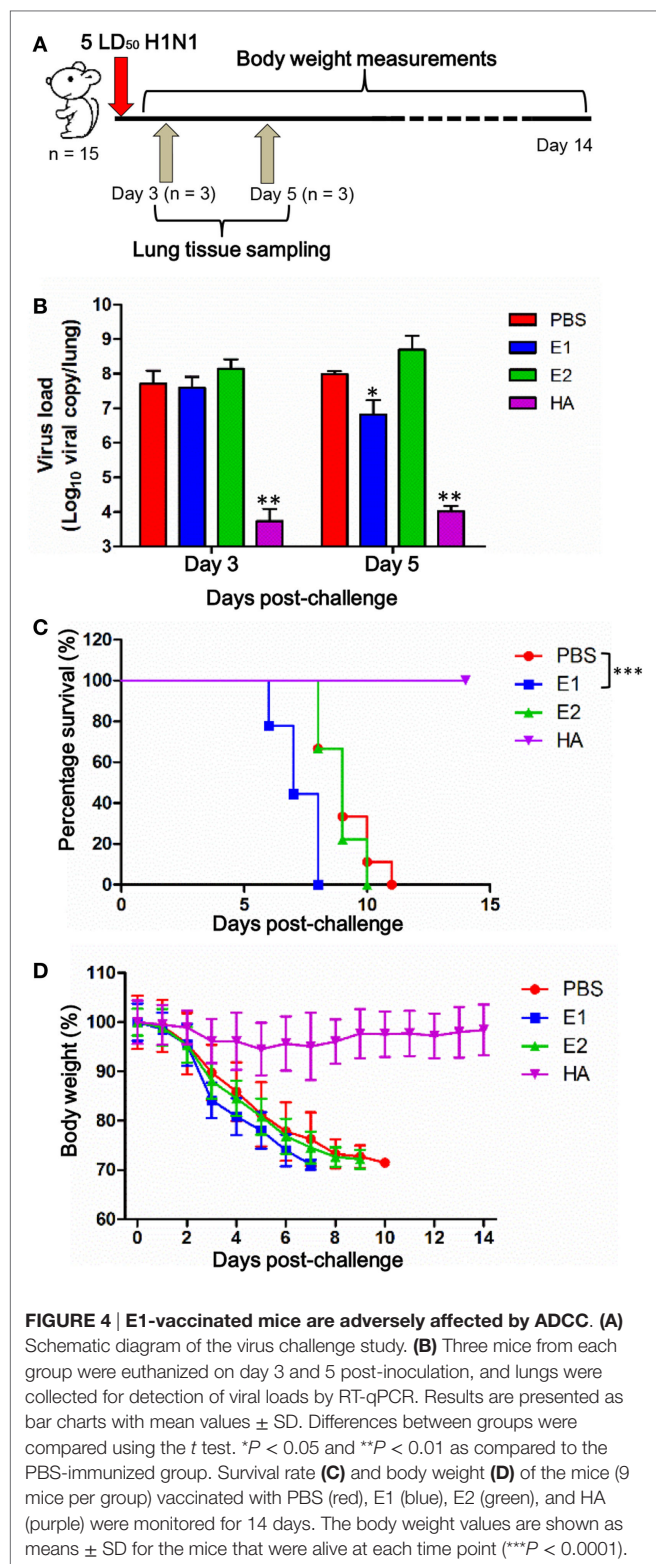


FIGURE 4 | E1-vaccinated mice are adversely affected by ADCC. (A) Schematic diagram of the virus challenge study. (B) Three mice from each group were euthanized on day 3 and 5 post-inoculation, and lungs were collected for detection of viral loads by RT-qPCR. Results are presented as bar charts with mean values \pm SD. Differences between groups were compared using the *t* test. **P* < 0.05 and ***P* < 0.01 as compared to the PBS-immunized group. Survival rate (C) and body weight (D) of the mice (9 mice per group) vaccinated with PBS (red), E1 (blue), E2 (green), and HA (purple) were monitored for 14 days. The body weight values are shown as means \pm SD for the mice that were alive at each time point (***P* < 0.0001).

to NK cell-mediated ADCC after incubating with the sera from healthy donors or clinical blood samples (6, 32, 33). In our case, we isolated PBMCs from healthy mice as effector cells and measured the death rate of target cells in the presence of vaccinated mouse sera (Figure 2). At the same time, utilization of flow cytometry for

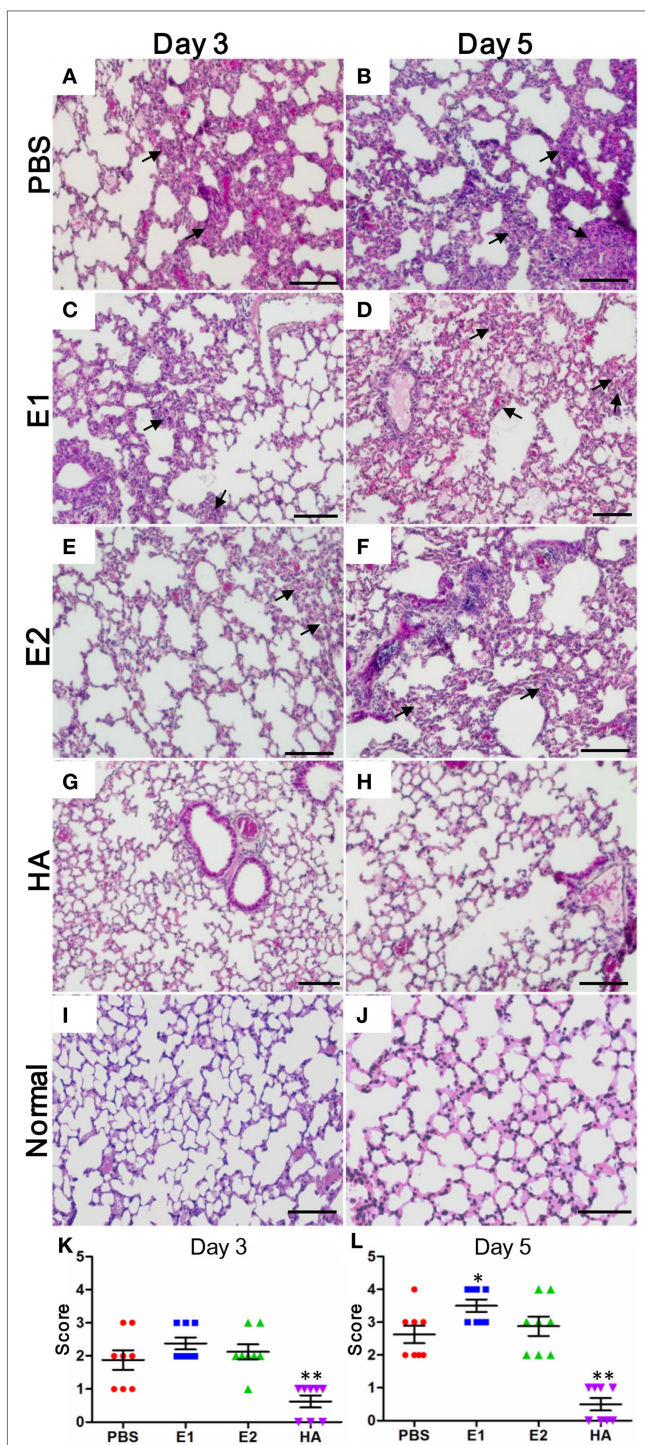


FIGURE 5 | Lungs of E1-vaccinated mice exhibit more severe histopathological changes upon influenza virus infection. Representative histologic sections of the lung tissues from the mice harvested on day 3 and 5 post-inoculation were stained with H&E. The level of inflammatory infiltrate and thickening of the alveolar septum (as alveolar damage) was detected in samples from mice vaccinated with PBS (A,B), E1 (C,D), E2 (E,F), and HA (G,H). Lung tissues from the uninfected normal mice were included for comparisons (I,J). The black arrows indicate inflammatory cell infiltration. Scale bars represent 20 μ m. (K,L) Pathological changes were scored as the criteria indicated in Section “Materials and Methods” (**P* < 0.05; ***P* < 0.01).

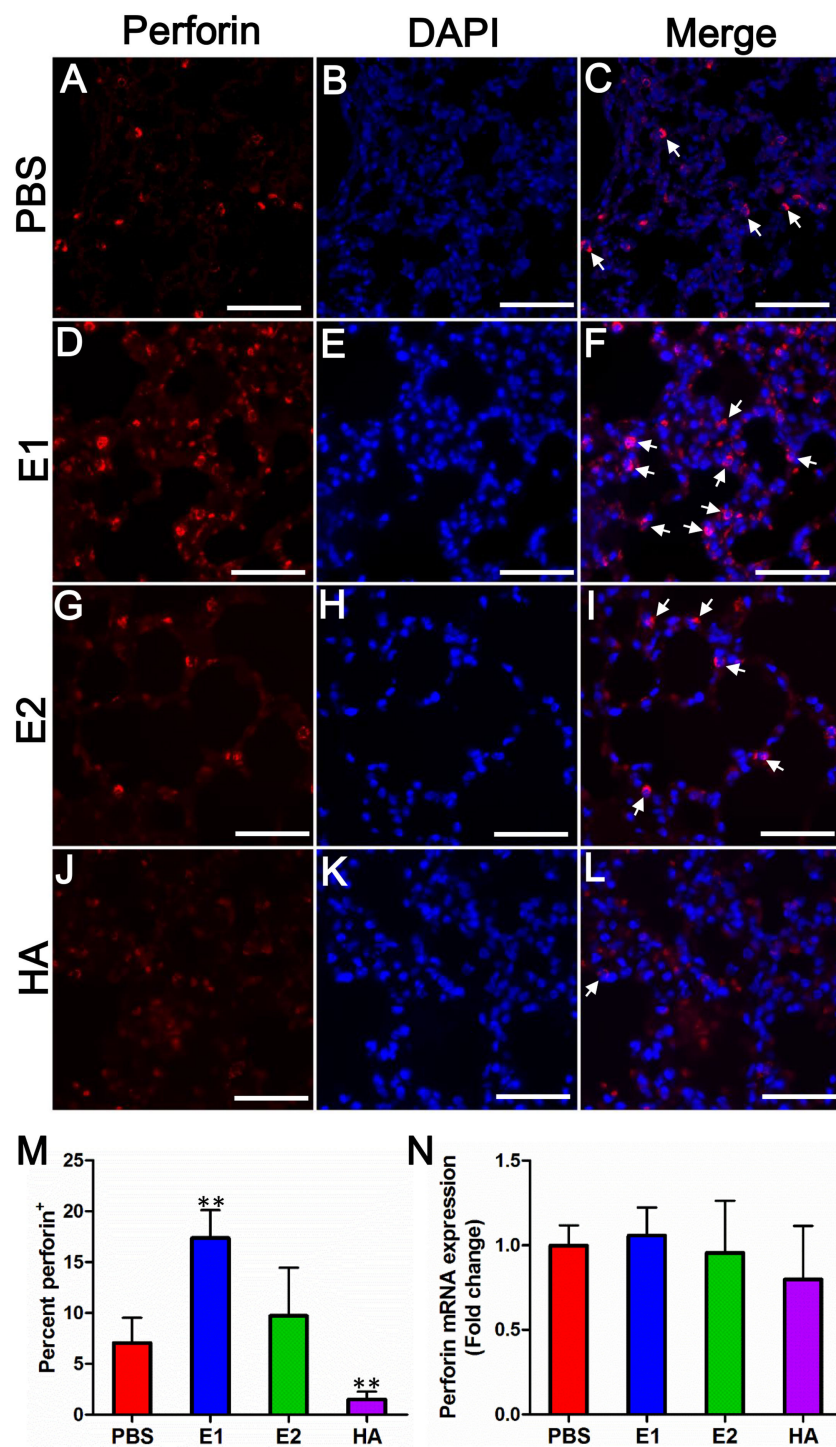


FIGURE 6 | E1-vaccinated mice express perforin at a higher level than that of PBS-, E2-, or HA-vaccinated mice upon influenza virus infection.

Perforin expression (red) from mouse lung tissues on day 5 post-inoculation was immunolabeled with rat anti-mouse perforin followed by goat anti-rat Alexa 594 (A–L). Nuclei were labeled by DAPI (blue). The white arrows indicate site of perforin expressing. Scale bars represent 20 μ m. (M) Quantification of the percentage of perforin protein expression of each group. % = (perforin positive cell/total cells) \times 100 (** P < 0.01). (N) Quantitative real time RT-PCR comparing perforin mRNA expression levels from mouse lung tissues on day 5 post-inoculation. Data are shown as fold change compared to the perforin mRNA expression level of the PBS group. The results represent mean values \pm SD (n = 5).

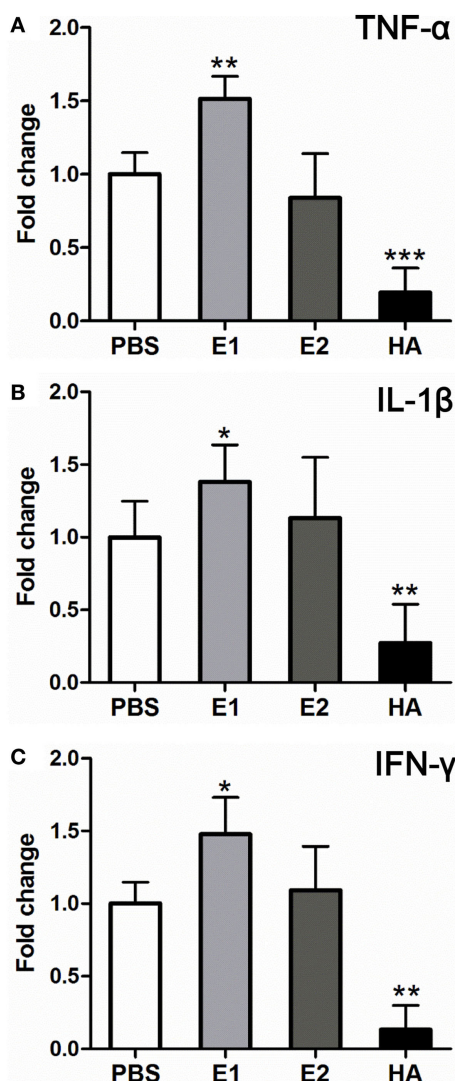


FIGURE 7 | Proinflammatory cytokines are further upregulated in the E1-vaccinated mice upon influenza virus infection in comparison with those in the PBS-vaccinated mice. Quantitative real time RT-PCR comparing gene expression levels of TNF- α (A), IL-1 β (B), and IFN- γ (C) from mouse lung tissues on day 5 post-virus challenge. Data are shown as fold change compared to the expression level of individual gene in the PBS group (* $P < 0.05$; ** $P < 0.01$; *** $P < 0.001$). The results represent mean values \pm SD ($n = 5$).

quantitation of cell cytotoxicity provided an efficient and precise way to assess the ADCC responses (Figure 3). Importantly, the H1N1-infected LA4 cells showed a low background of cell death in the absence of antibodies (Figure 3C), which suggested LA4 as an ideal cell line for the mouse-specific ADCC assay. Collectively, the established *in vitro* ADCC assay, together with the BALC/c mouse model, might be applied for the evaluation of other influenza-specific ADCC epitopes.

Experimental mouse models are an invaluable scientific resource that allow comprehensive investigation of key biological

questions *in vivo* and provide an essential platform in the study of many human diseases. It has been widely acknowledged that the mouse and human antibody repertoire share a general similarity (34–36). However, differences in germline antibody repertoire exist between species, and the number of mature naïve B cells from mice is smaller than that from humans (37). Both variations may contribute to the dissimilarities in the antibodies elicited by the E1-containing fragments in humans compared to those in mice. Due to the diversity of the B cell antigen receptor repertoire between the mouse and human model, the antibodies bind to the same fragments in distinct host models might potentially have slightly different epitopes. Alternatively, there may be fundamental differences between murine and human in terms of the regulation in NK cell cytotoxic granule secretion (38).

Surprisingly, distinct expression patterns of perforin were detected between protein (Figure 6M) and mRNA (Figure 6N) levels. The discrepancy might be explained by a previous finding that resting murine NK cells are “pre-armed” with high amounts of perforin mRNA, which can be rapidly translated into protein upon activation *in vitro* and *in vivo* (38). This mechanism of murine NK cells facilitates a better control of perforin expression, allowing a rapid production of effector proteins without the need of *de novo* gene transcription (38). Upon activation, ADCC effector cells produce various cytokines such as TNF- α , IL-1 β , and IFN- γ . Further, cytokines may represent one of the arming pathways that stimulate the translation of perforin (38). Notably, human NK cell is minimally cytotoxic at rest, expresses little perforin protein, and becomes potently cytotoxic only after cytokine activation (39, 40). Our result showed that TNF- α , IL-1 β , and IFN- γ were significantly elevated in E1-vaccinated group when compared with those of the PBS-treated group (Figure 7). In this regard, the upregulation of these cytokines may activate the cytotoxic perforin to cause the detrimental damage in mouse lungs.

In our previous study, E1 and E2 epitopes were located on the HA head (Figure S2 in Supplementary Material), both of which are conserved in H1N1 strains from 2009 (2009_H1N1) (11). To date, however, the role of HA head during influenza virus infection and ADCC activation has not been fully delineated. In a recent study, DiLillo and colleagues reported that neutralizing antibodies targeting the HA stem but not the HA head were capable of conferring influenza-specific ADCC (6). They proposed that only the anti-stem antibodies could bind in a correct conformation to ligate FcRs, which was based on the observation that a strain-specific anti-HA head antibody (PY102) was unable to mediate Fc γ R binding and to protect mice. On the other hand, HA head-induced ADCC activities were reported by a number of other groups (41–43), which was in agreement with our findings. The discrepancy between these observations might be due to the sequential and structural variations among subtypes/strains of influenza virus used. Interestingly, although both E1 and E2 epitopes are located on the HA head, serum from the HA-vaccinated group did not trigger a significantly elevated cytotoxicity response (Figure 3H), implying that additional regulators exist to control the ADCC activity.

In summary, we provided *in vitro* and *in vivo* evidence to verify the effect of the HA head epitope E1-mediated ADCC. Importantly, our data suggested that E1-mediated ADCC alone caused detrimental effect during influenza virus infection, which raised concerns on using this conserved non-neutralizing region of the HA head in future designs of a universal influenza vaccine. In fact, the “headless HA” has been recommended in several vaccine designs that aimed to make use of ADCC antibodies (44–47). Our data provided further evidence in support of this “headless HA” vaccine design strategy.

AUTHOR CONTRIBUTIONS

Z-WY and SY designed and performed the experiments. K-YY and HC conceived the study. LW performed the molecular modeling. ZS, MH, DY, M-YZ, and B-JZ gave conceptual advice and technical support. K-MP, CL, JZ, and HS conducted the histopathological observation and immunostaining. Z-WY, SY, HC, and K-YY wrote the manuscript.

REFERENCES

1. Hayden FG, de Jong MD. Emerging influenza antiviral resistance threats. *J Infect Dis* (2011) 203(1):6–10. doi:10.1093/infdis/jiq012
2. Treanor J. Influenza vaccine – outmaneuvering antigenic shift and drift. *N Engl J Med* (2004) 350(3):218–20. doi:10.1056/NEJMmp038238
3. Belongia EA, Simpson MD, King JP, Sundaram ME, Kelley NS, Osterholm MT, et al. Variable influenza vaccine effectiveness by subtype: a systematic review and meta-analysis of test-negative design studies. *Lancet Infect Dis* (2016) 16(8):942–51. doi:10.1016/S1473-3099(16)00129-8
4. Jegaskanda S, Reading PC, Kent SJ. Influenza-specific antibody-dependent cellular cytotoxicity: toward a universal influenza vaccine. *J Immunol* (2014) 193(2):469–75. doi:10.4049/jimmunol.1400432
5. Chung AW, Navis M, Isitman G, Centre R, Finlayson R, Bloch M, et al. Activation of NK cells by ADCC responses during early HIV infection. *Viral Immunol* (2011) 24(2):171–5. doi:10.1089/vim.2010.0108
6. DiLillo DJ, Tan GS, Palese P, Ravetch JV. Broadly neutralizing hemagglutinin stalk-specific antibodies require FcγR interactions for protection against influenza virus *in vivo*. *Nat Med* (2014) 20(2):143–51. doi:10.1038/nm.3443
7. Jegerlehner A, Schmitz N, Storni T, Bachmann MF. Influenza A vaccine based on the extracellular domain of M2: weak protection mediated via antibody-dependent NK cell activity. *J Immunol* (2004) 172(9):5598–605. doi:10.4049/jimmunol.172.9.5598
8. Simhadri VR, Dimitrova M, Mariano JL, Zenarruzabeitia O, Zhong W, Ozawa T, et al. A human anti-M2 antibody mediates antibody-dependent cell-mediated cytotoxicity (ADCC) and cytokine secretion by resting and cytokine-preactivated natural killer (NK) cells. *PLoS One* (2015) 10(4):e0124677. doi:10.1371/journal.pone.0124677
9. Vanderven HA, Ana-Sosa-Batiz F, Jegaskanda S, Rockman S, Laurie K, Barr I, et al. What lies beneath: antibody dependent natural killer cell activation by antibodies to internal influenza virus proteins. *EBioMedicine* (2016) 8:277–90. doi:10.1016/j.ebiom.2016.04.029
10. Shi Y, Wu Y, Zhang W, Qi J, Gao GF. Enabling the ‘host jump’: structural determinants of receptor-binding specificity in influenza A viruses. *Nat Rev Microbiol* (2014) 12(12):822–31. doi:10.1038/nrmicro3362
11. Srivastava V, Yang Z, Hung IF, Xu J, Zheng B, Zhang MY. Identification of dominant antibody-dependent cell-mediated cytotoxicity epitopes on the hemagglutinin antigen of pandemic H1N1 influenza virus. *J Virol* (2013) 87(10):5831–40. doi:10.1128/JVI.00273-13
12. He W, Tan GS, Mullarkey CE, Lee AJ, Lam MM, Krammer F, et al. Epitope specificity plays a critical role in regulating antibody-dependent cell-mediated cytotoxicity against influenza A virus. *Proc Natl Acad Sci U S A* (2016) 113(42):11931–6. doi:10.1073/pnas.1609316113
13. Chu H, Zhou J, Wong BH, Li C, Chan JE, Cheng ZS, et al. Middle east respiratory syndrome coronavirus efficiently infects human primary T lymphocytes and activates the extrinsic and intrinsic apoptosis pathways. *J Infect Dis* (2016) 213(6):904–14. doi:10.1093/infdis/jiv380
14. Zhang MY, Vu BK, Choudhary A, Lu H, Humbert M, Ong H, et al. Cross-reactive human immunodeficiency virus type 1-neutralizing human monoclonal antibody that recognizes a novel conformational epitope on gp41 and lacks reactivity against self-antigens. *J Virol* (2008) 82(14):6869–79. doi:10.1128/JVI.00033-08
15. Zheng B, Chan KH, Zhang AJ, Zhou J, Chan CC, Poon VK, et al. D225G mutation in hemagglutinin of pandemic influenza H1N1 (2009) virus enhances virulence in mice. *Exp Biol Med (Maywood)* (2010) 235(8):981–8. doi:10.1258/ebm.2010.010071
16. Zheng BJ, Chan KW, Lin YP, Zhao GY, Chan C, Zhang HJ, et al. Delayed antiviral plus immunomodulator treatment still reduces mortality in mice infected by high inoculum of influenza A/H5N1 virus. *Proc Natl Acad Sci U S A* (2008) 105(23):8091–6. doi:10.1073/pnas.0711942105
17. Yuan S, Chu H, Zhang K, Ye J, Singh K, Kao RY, et al. A novel small-molecule compound disrupts influenza A virus PB2 cap-binding and inhibits viral replication. *J Antimicrob Chemother* (2016) 71(9):2489–97. doi:10.1093/jac/dkw194
18. Yuan S, Chu H, Ye J, Singh K, Ye Z, Zhao H, et al. Identification of a novel small-molecule compound targeting the influenza A virus polymerase PB1-PB2 interface. *Antiviral Res* (2017) 137:58–66. doi:10.1016/j.antiviral.2016.11.005
19. Yuan S, Zhang N, Singh K, Shuai H, Chu H, Zhou J, et al. Cross-protection of influenza A virus infection by a DNA aptamer targeting the PA endonuclease domain. *Antimicrob Agents Chemother* (2015) 59(7):4082–93. doi:10.1128/AAC.00306-15
20. Yuan S, Chu H, Ye J, Hu M, Singh K, Chow BK, et al. Peptide-mediated interference of PB2-eIF4G1 interaction inhibits influenza A viruses’ replication *in vitro* and *in vivo*. *ACS Infect Dis* (2016) 2(7):471–7. doi:10.1021/acsinfecdis.6b00064
21. van den Brand JM, Stittelaar KJ, van Amerongen G, Rimmelzwaan GF, Simon J, de Wit E, et al. Severity of pneumonia due to new H1N1 influenza virus in ferrets is intermediate between that due to seasonal H1N1 virus and highly pathogenic avian influenza H5N1 virus. *J Infect Dis* (2010) 201(7):993–9. doi:10.1086/651132
22. Sun S, Zhao G, Xiao W, Hu J, Guo Y, Yu H, et al. Age-related sensitivity and pathological differences in infections by 2009 pandemic influenza A (H1N1) virus. *Virol J* (2011) 8:52. doi:10.1186/1743-422X-8-52
23. Crowe CR, Chen K, Pociask DA, Alcorn JF, Krivich C, Enelow RI, et al. Critical role of IL-17RA in immunopathology of influenza infection. *J Immunol* (2009) 183(8):5301–10. doi:10.4049/jimmunol.0900995

ACKNOWLEDGMENTS

We thank Professor Zhi-Wei Chen (AIDS institution, the University of Hong Kong) for facility sharing, and the staff at the Core Facility, Li Ka Shing Faculty of Medicine, the University of Hong Kong, for facilitation of the study.

FUNDING

This work was supported by the Providence Foundation Limited in memory of the late Dr. Lui Hac Minh and the Hong Kong Health and Medical Research Fund (14131352).

SUPPLEMENTARY MATERIAL

The Supplementary Material for this article can be found online at <http://journal.frontiersin.org/article/10.3389/fimmu.2017.00317/full#supplementary-material>.

24. Wang X, Chan CC, Yang M, Deng J, Poon VK, Leung VH, et al. A critical role of IL-17 in modulating the B-cell response during H5N1 influenza virus infection. *Cell Mol Immunol* (2011) 8(6):462–8. doi:10.1038/cmi.2011.38
25. Chan CM, Chu H, Wang Y, Wong BH, Zhao X, Zhou J, et al. Carcinoembryonic antigen-related cell adhesion molecule 5 is an important surface attachment factor that facilitates entry of middle east respiratory syndrome coronavirus. *J Virol* (2016) 90(20):9114–27. doi:10.1128/JVI.01133-16
26. Zhou J, Chu H, Li C, Wong BH, Cheng ZS, Poon VK, et al. Active replication of Middle East respiratory syndrome coronavirus and aberrant induction of inflammatory cytokines and chemokines in human macrophages: implications for pathogenesis. *J Infect Dis* (2014) 209(9):1331–42. doi:10.1093/infdis/jit504
27. Chu H, Zhou J, Wong BH, Li C, Cheng ZS, Lin X, et al. Productive replication of Middle East respiratory syndrome coronavirus in monocyte-derived dendritic cells modulates innate immune response. *Virology* (2014) 45(4–455):197–205. doi:10.1016/j.virol.2014.02.018
28. Wang W, Erbe AK, Hank JA, Morris ZS, Sondel PM. NK cell-mediated antibody-dependent cellular cytotoxicity in cancer immunotherapy. *Front Immunol* (2015) 6:368. doi:10.3389/fimmu.2015.00368
29. Hassane M, Paget C. “Universal flu vaccine”: can NK cell-mediated ADCC tip the scales? *EBioMedicine* (2016) 8:18–9. doi:10.1016/j.ebiom.2016.05.042
30. Jegaskanda S, Vandenberg K, Laurie KL, Loh L, Kramski M, Winnall WR, et al. Cross-reactive influenza-specific antibody-dependent cellular cytotoxicity in intravenous immunoglobulin as a potential therapeutic against emerging influenza viruses. *J Infect Dis* (2014) 210(11):1811–22. doi:10.1093/infdis/jiu334
31. Zhou G, Juang SW, Kane KP. NK cells exacerbate the pathology of influenza virus infection in mice. *Eur J Immunol* (2013) 43(4):929–38. doi:10.1002/eji.201242620
32. Cox F, Baart M, Huizingh J, Tolboom J, Dekking L, Goudsmit J, et al. Protection against H5N1 influenza virus induced by matrix-M adjuvanted seasonal virosomal vaccine in mice requires both antibodies and T cells. *PLoS One* (2015) 10(12):e0145243. doi:10.1371/journal.pone.0145243
33. Jegaskanda S, Co MD, Cruz J, Subbarao K, Ennis FA, Terajima M. Human seasonal influenza A viruses induce H7N9-cross-reactive antibody-dependent cellular cytotoxicity (ADCC) antibodies that are directed towards the nucleoprotein. *J Infect Dis* (2017) 1–6. doi:10.1093/infdis/jiw629
34. Schroeder HW Jr. Similarity and divergence in the development and expression of the mouse and human antibody repertoires. *Dev Comp Immunol* (2006) 30(1–2):119–35. doi:10.1016/j.dci.2005.06.006
35. Mestas J, Hughes CC. Of mice and not men: differences between mouse and human immunology. *J Immunol* (2004) 172(5):2731–8. doi:10.4049/jimmunol.172.5.2731
36. Vossenkamper A, Spencer J. Transitional B cells: how well are the checkpoints for specificity understood? *Arch Immunol Ther Exp (Warsz)* (2011) 59(5):379–84. doi:10.1007/s00005-011-0135-0
37. Benitez A, Weldon AJ, Tatosyan L, Velkuru V, Lee S, Milford TA, et al. Differences in mouse and human nonmemory B cell pools. *J Immunol* (2014) 192(10):4610–9. doi:10.4049/jimmunol.1300692
38. Fehniger TA, Cai SF, Cao X, Bredemeyer AJ, Presti RM, French AR, et al. Acquisition of murine NK cell cytotoxicity requires the translation of a pre-existing pool of granzyme B and perforin mRNAs. *Immunity* (2007) 26(6):798–811. doi:10.1016/j.immuni.2007.04.010
39. Cooper MA, Fehniger TA, Caligiuri MA. The biology of human natural killer-cell subsets. *Trends Immunol* (2001) 22(11):633–40. doi:10.1016/S1471-4906(01)02060-9
40. Bratke K, Kuepper M, Bade B, Virchow JC Jr, Luttmann W. Differential expression of human granzymes A, B, and K in natural killer cells and during CD8+ T cell differentiation in peripheral blood. *Eur J Immunol* (2005) 35(9):2608–16. doi:10.1002/eji.200526122
41. Mesman AW, Westerhuis BM, Ten Hulscher HI, Jacobi RH, de Bruin E, van Beek J, et al. Influenza virus A(H1N1)2009 antibody-dependent cellular cytotoxicity in young children prior to the H1N1 pandemic. *J Gen Virol* (2016) 97(9):2157–65. doi:10.1099/jgv.0.000552
42. Zhong W, Liu F, Wilson JR, Holiday C, Li ZN, Bai Y, et al. Antibody-dependent cell-mediated cytotoxicity to hemagglutinin of influenza A viruses after influenza vaccination in humans. *Open Forum Infect Dis* (2016) 3(2):ofw102. doi:10.1093/ofid/ofw102
43. Jegaskanda S, Job ER, Kramski M, Laurie K, Isitman G, de Rose R, et al. Cross-reactive influenza-specific antibody-dependent cellular cytotoxicity antibodies in the absence of neutralizing antibodies. *J Immunol* (2013) 190(4):1837–48. doi:10.4049/jimmunol.1201574
44. Krammer F. The quest for a universal flu vaccine: headless HA 2.0. *Cell Host Microbe* (2015) 18(4):395–7. doi:10.1016/j.chom.2015.10.003
45. Graves PN, Schulman JL, Young JF, Palese P. Preparation of influenza virus subviral particles lacking the HA1 subunit of hemagglutinin: unmasking of cross-reactive HA2 determinants. *Virology* (1983) 126(1):106–16. doi:10.1016/0042-6822(83)90465-8
46. Wohlbold TJ, Nachbagauer R, Margine I, Tan GS, Hirsh A, Krammer F. Vaccination with soluble headless hemagglutinin protects mice from challenge with divergent influenza viruses. *Vaccine* (2015) 33(29):3314–21. doi:10.1016/j.vaccine.2015.05.038
47. Valkenburg SA, Mallajosyula VV, Li OT, Chin AW, Carnell G, Temperton N, et al. Stalking influenza by vaccination with pre-fusion headless HA mini-stem. *Sci Rep* (2016) 6:22666. doi:10.1038/srep22666

Conflict of Interest Statement: The authors declare that the research was conducted in the absence of any commercial or financial relationships that could be construed as a potential conflict of interest.

Copyright © 2017 Ye, Yuan, Poon, Wen, Yang, Sun, Li, Hu, Shuai, Zhou, Zhang, Zheng, Chu and Yuen. This is an open-access article distributed under the terms of the Creative Commons Attribution License (CC BY). The use, distribution or reproduction in other forums is permitted, provided the original author(s) or licensor are credited and that the original publication in this journal is cited, in accordance with accepted academic practice. No use, distribution or reproduction is permitted which does not comply with these terms.



Immunoglobulin Transporting Receptors Are Potential Targets for the Immunity Enhancement and Generation of Mammary Gland Bioreactor

Xuemei Jiang^{1,2}, Jianjun Hu², Diraviyam Thirumalai¹ and Xiaoying Zhang^{1,2*}

¹ College of Veterinary Medicine, Northwest A&F University, Xianyang, Shaanxi, China, ² Key Laboratory of Tarim Animal Husbandry Science and Technology, College of Animal Science and Technology, Tarim University, Alar, Xinjiang, China

OPEN ACCESS

Edited by:

Tianlei Ying,
Fudan University, China

Reviewed by:

Ronald B. Corley,
Boston University School of
Medicine, USA
Kang Chen,
Wayne State University, USA
National Institutes of Health, USA
Zili Li,
Huazhong Agricultural University,
China

*Correspondence:

Xiaoying Zhang
zhang.xy@nwsuaf.edu.cn

Specialty section:

This article was submitted to
Immunotherapies and Vaccines,
a section of the journal
Frontiers in Immunology

Received: 22 February 2016

Accepted: 17 May 2016

Published: 10 June 2016

Citation:

Jiang X, Hu J, Thirumalai D and
Zhang X (2016) Immunoglobulin
Transporting Receptors Are Potential
Targets for the Immunity
Enhancement and Generation of
Mammary Gland Bioreactor.
Front. Immunol. 7:214.
doi: 10.3389/fimmu.2016.00214

The functions of immunoglobulin transporting receptors (Ig transporting receptors) in immune system encompass from passive immunity to adaptive immunity by transporting immunoglobulins (Igs) and prolonging their half-life as well as enhancing immunosurveillance. Prior to the weaning, Ig transportations from mother to offspring confer the immediate passive immunity for neonates. After the weaning, FcRn and polymeric immunoglobulin receptor on infant intestinal epithelial cells retrieve Ig in intestinal lamina propria into the gut lumen for preventing pathogen invasion. This is not only improving the pathological consequences of infection but also helping the neonates for developing their own immune response; besides it would be the guidance for designing novel vaccines. Moreover, the investigations on Ig transporting receptors over-expressed transgenic animals have been carried out to improve Ig concentrations in serum and milk; thus, it would be a sustainable method to produce antibody-enriched milk-derived colostrum replacer for neonates. In order to generate mammary gland bioreactor, a series of methods have been developed for enhanced regulation of Ig transporting receptors expression and Ig transportation.

Keywords: immunoglobulin transporting receptors, immunoglobulins, immunity, bioreactor

INTRODUCTION

The continuous supply of maternal IgG1 (ruminants) and IgA (monogastric) confers the passive immunity to neonatal mammals until weaning. Neonatal Fc receptor (FcRn) and the polymeric immunoglobulin receptor (pIgR) are responsible for the transportation of these maternal immunoglobulins (Igs). FcRn has been considered as a saturable receptor that mediates the passive transfer of IgG from mother to offspring and protects IgG from catabolism (1). pIgR is responsible for the transport of pentameric IgM and/or dimeric IgA by binding with their joining peptide chain (J-chain) (2). The binding affinity of pIgR toward IgM and IgA is differing among the species; high affinity could be found in human and bovine compared to mice and rats (thereby less IgM and IgA secretion in the milk) (3, 4). The expressions of FcRn and pIgR in mammary gland vary among different animal species and influence the level of Igs in milk. For instance, IgA constitutes 90% of total milk Igs in monogastric species, but it is only 9% in case of bovine (5).

The Igs transport from mother to offspring occurs through placenta and small intestine; these two sites exhibit different significance in different animals (1, 6, 7). Passive immunity relies on prenatal

IgG transfer mediated by FcRn on placental syncytiotrophoblasts in monogastric animals, whereas in ruminants, it relies on Ig absorption from colostrums after birth (1, 8). It has been reported that the FcRn expressed on antigen-presenting cells (APCs) could bind with antigens; then, the immune complexes are delivered to dendritic cells (DCs) for primary immune response (9, 10). In addition, the pIgR on the mucosal surfaces could translocate the secretory IgA (SIgA) from the lamina propria into intestine and maternal precursors of IgA-containing cells would home to the mammary gland where they secrete IgA into milk (11–13). Thus, the FcRn and pIgR could protect animals from the pathogen invasion in intestinal, respiratory and reproductive systems, and/or dietary antigens (1, 12). Hence, both FcRn and pIgR play

important roles for not only strengthening passive immunity but also promoting active immunity. It has also been observed that significant increase in humoral responses and mAbs production without any sign of autoimmunity in the transgenic (tg) mice (14–16).

Numerous studies have reported that multi-copies of FcRn and pIgR in animals could exhibit an increased ability in strengthening immunity. Besides, the strategies of genetic engineering and molecular regulations have been applied to regulate the expression of FcRn and pIgR. Factors involved in the regulation of passive immunity transfer and immunosurveillance are summarized in **Figure 1**. This review aims to summarize the vital roles of FcRn and pIgR for the improvement of passive immunity and adaptive

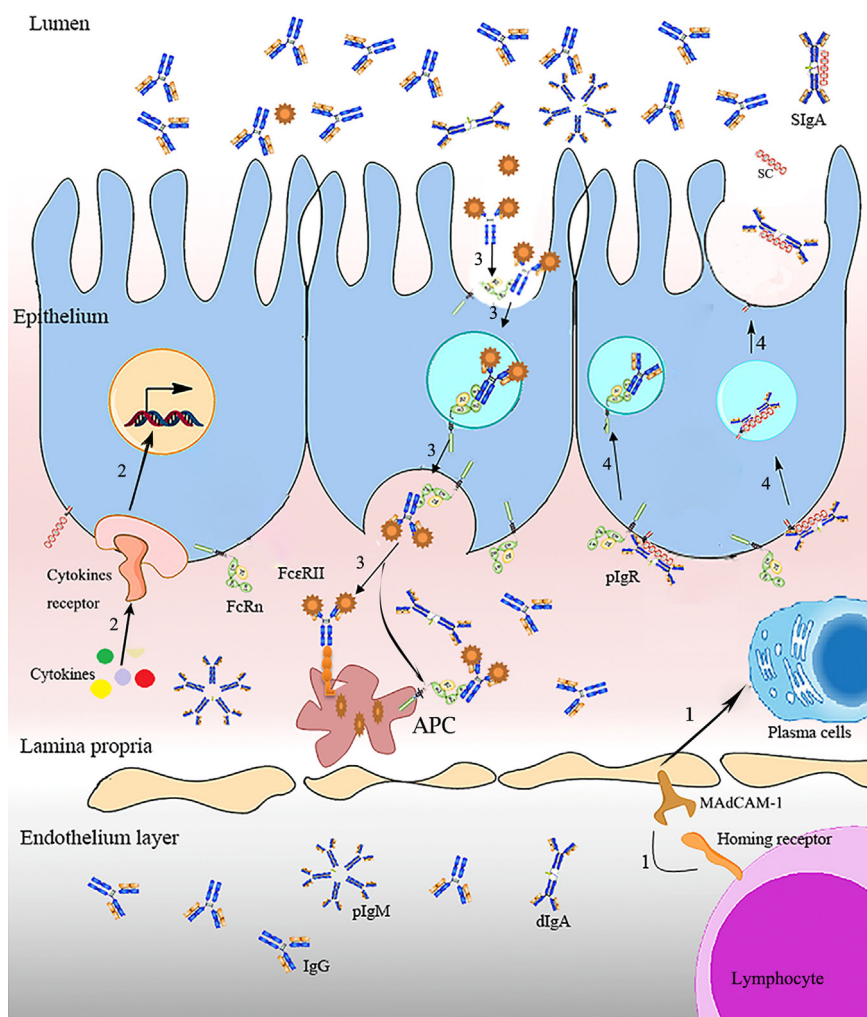


FIGURE 1 | Regulation and surveillance of FcR on immunity. IgA antibody-secreting cells homing receptor (LHR) on lymphocyte homing to diverse mucosal surfaces, binding with vascular addressin MAdCAM-1 (mucosal addressin cell adhesion molecule-1), VCAM-1 (vascular cell adhesion molecule-1), and the mucosal epithelial chemokine CCL28, mediates lymphocytes homing when there is pathogen invasion, a process that enables the passive transfer of maternal IgA antibody from the mother to the gut of the immunologically naive newborn (17). The interactions of signaling proteins activate *FcR* transcription. Molecular containing IgG-Fc (e.g., antigen-antibody/Fc complex) is internalized into acidified endosome (endocytosis) by binding with FcRn on the mucosal surfaces, and presented to APC. Ig transporting receptors mediate Ig transcytosis from the basolateral into the lumen (1, 11).

immunity; as well as the strategies coupled with the regulations of FcRn and pIgR.

PASSIVE IMMUNITY IMPROVEMENT MEDIATED BY FcRn OR pIgR

Ruminants are born hypogammaglobulinemic (reduction in all types of gamma globulins). The young ungulates are depending on mammary secretion of colostrum and intestinal absorption of IgG prior to the development of their own humoral defense system for enhancing intestinal and systemic protection (18). In general, a minimum of 150–200 g of IgG is required for achieving adequate passive transfer within 2 h after birth (19). A failure of passive immunity delivery will occur when a threshold concentration of IgG is not reached before closure occurs (20). Moreover, in a mice study, lacking of maternal antibodies led to delayed generation of their own IgG compared to the normal littermates (21). As such, the intake of antibody-enriched milk (for the neonates) is necessary for the establishment of animals' adaptive immune defense in early life. Since milk is a convenient source of antibody collection, bovine is the superexcellent choice used for polyclonal and monoclonal antibody production. In FcRn over-expressed tg rabbits immunized with ovalbumin, a long serum persistence of IgG (7.1 ± 0.46 days when 5.3 ± 0.3 days in control group) and the highest IgG level [31.61 ± 2.7 mg/ml while 14.8 ± 2.6 mg/ml in wild type (wt) ($p < 0.01$)] were observed (22). In addition, it has been observed that more IgG were transported into milk after upregulated the expression of FcRn receptors in the mammary glands of possum, rabbit, and bovine (23–25). On the other hand, continuous milking is defined as a management system without a planned dry period; it has been described to reduce health problems common in periparturient cattle, but resulting in reduction on colostrum Ig and subsequently calf health (26–28). In FcRn over-expressed tg bovine, the increased IgG protection and transportation could be achieved with adequate IgG along with continuous milking; thus, it reduces the health problems associated with the high yielding transition cow. FcRn or pIgR over-expression in bovine could also be useful for the treatment of mastitis. In general, the control of mastitis during lactation relies on administration of antibiotics or non-steroidal anti-inflammatory drugs; nonetheless, the antibiotic treatment is inefficient and the antibiotic residues would pass on to milk (29). The tg bovine over-expression of pIgR could increase the SIgA in the mammary gland; it would provide stronger and longer protection against the mastitis pathogens from the environment. The free secretory component (SC), the extracellular ligand-binding region of pIgR, is an important component of innate anti-microbial defense (11). In addition, IgA-containing cells would home to the mammary gland when there is inflammation, increased pIgR in mammary gland of tg bovine could transport more SIgA to resist environmental pathogens as well as continuous supply of IgG into milk. Ig-enriched milk from tg animal is an effective alternative to antibiotics, the widespread use of antibiotics alternatives would reduce antibiotic resistance, accordingly, to better maintain the intestinal homeostasis, especially to the newborn (30, 31).

ADAPTIVE IMMUNITY IMPROVEMENT MEDIATED BY FcRn AND pIgR

The presence of FcRn on APCs suggests that FcRn may influence the antigen presentation (32, 33). Generally, vaccines exhibit a shorter half-life (several hours) but immunogen containing IgG-Fc exhibits longer half-life (20 days) with the confirmed involvement of FcRn on enterocytes and APCs; further it could reach up to 30 days in FcRn over-expressed animals (34). The immunization of FcRn over-expressed tg mice led to 3- to 10-fold increases of antigen-specific IgM and IgG in serum, as well as higher number of antigen-specific B cells and DCs in spleen (16). The elevated antigen-specific IgM and IgG levels were proposed to be the result of the increased diversification of the antigen-specific Ab repertoire (35). bFcRn tg mice immunized with a conserved hemagglutinin subunit 2-based synthetic peptide mounted a robust immunoreaction on day 28 that continued to rise through day 50 while wt mice showed a weak immune response (14). The strength humoral immune response was owing to a higher level of ICs and their increased phagocytosis by the tg neutrophils (NE) and greater influx of these cells into the regional secondary lymphoid organs (35, 36). In another study, tg mice expression of bovine FcRn (bFcRn) in secondary lymphoid organs can boost a threefold of antigen-specific activated T helper (Th) cells compared with wt immunized with T-dependent antigens (9). Hence, tg DC can phagocytose and present antigens to Th cells more efficiently when loaded with Antigen–IgG ICs (35, 37). Meanwhile, ligation of FcRn to ICs can also induces the production of IL-12 from DCs, thereby activating CD4+ T(II) cells in the induction of Th1 polarization and priming CD8+ T(I) cells in the promotion of cytotoxicity activation (37).

In general, the antibodies must be active at the portals of viral entry in the gastrointestinal tract to prevent intestinal infection. SIgA, produced by selective transport of pIgA across mucosal epithelial barrier by pIgR, is the first line of specific immunological defense against environmental pathogens. During the adaptive immune response, the immune system could prime pIgR for the transportation of IgA produced in the laminar propria into intestinal tract as SIgA (6, 12). It has been proved that pIgR is involved in lymphocyte homing in addition to transporting mucosal pIgA (11). pIgR knockout mice lack mucosal IgA and accumulate 100-fold of serum IgA than wt, meanwhile, 14-fold IgA-secreting plasma cells was detected in the intestinal lamina propria compared to wt (38). Increased lymphocyte and SIgA in mucosa help to maintain mucosal homeostasis in the intestine of the neonate. FcRn also behave an important factor on bacterial colonization and pathological consequences of infection in addition to antigen presentation. Tg mice with human FcRn exhibited that antigen within the lumen can be retrieved by administering specific IgG intravenously. These formed Antigen–IgG ICs are retrieved by the epithelial cell and transported into the lamina propria, being internalized by APCs (39, 40). In a *Helicobacter heilmannii* infection model, the specific IgG were exclusively presented in gastric juice of wt mice, while lymphoid follicles and bacterial loads have increased along with deeper gastric epithelium invasion in FcRn-deficient mice (41). FcRn over-expressed tg mice fed with *Francisella tularensis* led to more efficient antigen

recognition in the gastrointestinal tract and mucosal localization enhancement that confers immune protection (42). Similarly, the FcRn-mediated transport of IgG across the gastric, genitourinary, and lung epithelium is associated with protection from viral infections and *H. heilmannii* at these sites (39). Likewise, the FcRn is the vehicle that transports luminal antigens across the luminal epithelial barrier and presents the cargo to related immune cells. The application of mucosal vaccination targeted to FcRn can effectively promote the internalization of immunogen, resulting in substantial and enabling immune efficiencies. The non-immunized 7- to 8-month-old bFcRn tg mice did not show detectable antinuclear antibodies with the same general antibody profile compared to wt littermates (43). Hence, tg animal with bFcRn over-expression could be proposed as an ideal choice for monoclonal antibody production; because it enhances immune responsiveness without eliciting autoimmunity (14). However, the vaccinated wt and pIgR knockout mice behaved equally resistant despite dramatic differences in the titer of SIgA in intestinal secretions in a *Salmonella typhimurium* challenge experiment without any differences in terms of CD8+ T cells and T-cell responses (44). In another *S. typhimurium* challenge experiment, pIgR knockout mice were profoundly sensitive to infection with *S. typhimurium* and shed more bacteria that can readily infect other animals (45). These findings suggest that the major role of pIgR probably to resist the invasion of mucosal antigens based on SIgA, rather than protection of local mucosal surfaces by prompting an immune response.

CURRENT UNDERSTANDING ABOUT THE REGULATIONS OF FcRn AND pIgR

In order to increase the host immunity and antibody production, a series of methods have been developed for enhanced regulation of FcRn and pIgR expression. It will bring substantial advantages for the production of antibody-enriched milk, which would replace colostrums and serve as functional food.

Genetic Modulations

Gene polymorphisms and haplotypes of receptor genes are the crucial factor to the antibody production and livability of the neonates (41, 46–48). In order to harvest antibody-enriched colostrum or milks, Ig bioreactors could be bred by genetic engineering with respect to FcRn and pIgR on the basis of their polymorphisms and haplotype research. This would also be useful in the intervention to some immunosuppressed periparturient cows. Besides, the development of nuclear transplantation technique and the CRISPR/Cas9 system (clustered regularly interspaced short palindromic repeats/CRISPR-associated system) realize the possibility for using cattle as an attractive candidate of bioreactor.

Allelic variation in *FCGRT* (which encodes the α -chain of FcRn) is associated with variation of IgG concentration in neonatal calves. Among five different variable number tandem repeat (VNTR1–VNTR5) in *FCGRT* promoter, the monocytes from VNTR3 homozygous individuals express 1.66-fold more FcRn transcript and show an increased binding to polyvalent human IgG when compared with monocytes from VNTR2/VNTR3 heterozygous individuals; VNTR3 allele supports the

transcription of a reporter gene twice as effectively as the VNTR2 allele; moreover, monocytes from VNTR3 homozygous individuals were reported to bind IgG at acidic pH more efficiently than heterozygous individuals (47). β_2 -microglobulin (β_2 M) exons II and IV are identified with 12 single-nucleotide polymorphisms (SNPs) and were assorted into 8 haplotypes. One of the haplotypes (the β_2 M 2, 2) showed an increased risk of failure for IgG transfer (47). Researchers have also identified three divergent haplotypes of pIgR and explained the variation in the concentration of SIgA and the pIgR level (46). Genome-wide analysis identified a significant association between SIgA and six SNPs located in the PIGR, PIGR-2, PIGR-5, PIGR-9, PIGR-13, PIGR-17, and PIGR-19. Pair-wise analysis demonstrated that all six SNPs were in almost complete linkage disequilibrium. PIGR-17 transformed to alanine from valine at codon 580, and PIGR-2 located in the promoter region is likely to influence the quality or quantity of the gene product (49). IgG clearance is more rapid in β_2 M-deficient mice than in α -chain-deficient mice (23, 50, 51). However, the homologous molecules of β_2 M, such as MHC-I, are not known to extend the half-life of IgG. There must be another β_2 M-related molecule that plays a supporting role during the recycling of IgG. These results suggest that supplemental copies of the gene may prolong half-life of IgG as well as maintain a high IgG concentration. A study using FcRn tg mice in mammary glands results in an increase of IgG levels both in milk and serum (23). Another study reported that, tg mouse over expressing bovine *FCGRT* led to a higher transcription and expression of FcRn and an extended IgG half-life (52). Furthermore, the tg mice over-expression of pIgR from 60- to 270-fold above normal pIgR showed total IgA levels in milk to be 1.5- to 2-fold higher compared with IgA levels of wt mice (53). An overview of the genetic modulations on Ig transporting receptors studies associated with transcytosis is shown in **Table 1**.

Genome engineering techniques are targeting Ig transporting receptors for improving the Ig concentrations in milk and maintain immune homeostasis, thereby enhancing the chance to generate Ig bioreactor by combining natural genetic variation selection.

Molecular Modulations

Numerous pieces of evidence suggest that microbial-associated molecular patterns (MAMPs) stimulate expression of pIgR on IECs, as part of a homeostatic loop in which the microbiota enhances the production of SIgA, which in turn regulates the composition and function of the microbiota (57, 58). Ultraviolet-inactivated reovirus induced a stronger increase in pIgR expression than live virus in HT-29 cells, suggesting that the induction of pIgR expression required viral components but not viral replication (59). It has been reported that MAMPs stimulate the expression of pIgR, more specifically, the immune response was initiated by microbial component, the toll-like receptor ligands, and then induced *de novo* synthesis of RelB and activation of *PIGR* transcription through the TLR3 pathway (11). The regulation pathways are presented in **Figure 2**. Additionally, in PRM/Alf mice with a huge extended intestine, a twofold increase of IgA-containing cells and pIgR expression in mammary gland as well as two- to fourfold increase of IgA in milk have been described

TABLE 1 | Genetic modulation on FcRn or plgR.

Receptor	Target gene	Genetic modulation	Species	Experimental outcomes	Reference
FcRn	<i>FCGRT/β2M</i>	<i>FCGRT/β2M</i> over-expression <i>β2M</i> disruption	Murine	Twofold serum IgG increase in milk and two- to fourfold increase in serum	(23)
	<i>FCGRT or β2M</i>	<i>β2M knockout or FCGRT knockout</i>	Murine	10 ⁴ -fold IgG reduction in serum	(21)
	<i>β2M</i>	<i>FCGRT knockout</i>	Murine	Decreased IgG half-lives in β2M-deficient mice (21.8 h) and FcRn FCGRT-deficient mice (26.6 h)	(50)
	<i>β2M</i>	<i>β2M over-expression</i>	Brushtail possum	Increased FcRn transcription and IgG concentration in milk	(24)
	<i>FCGRT</i>	<i>FCGRT</i> over-expression	Murine	Three- to ten-fold increases of antigen-specific IgM and IgG, which lead to twofold increase of specific titers in the hemagglutination inhibition assay	(16)
plgR	<i>PIGR</i>	<i>PIGR</i> over-expression	Murine	1.5- to 2-fold IgA increase in milk	(53)
	<i>PIGR</i>	<i>PIGR</i> over-expression	Murine	10- to 270-fold (0.1–2.7 mg/ml) SC protein increase in milk	(54)
	<i>J chain</i>	<i>J chain</i> disruption	Murine	Stable binding of plgA and SC decreased	(55)
	<i>PIGR</i>	<i>PIGR knockout</i>	Murine	Lack of active external IgA and IgM transcytosis completely	(54)
	<i>rab3b</i>	<i>rab3b</i> over-expression	Epithelial cells	Ten percent reduction of dlgA transcytosis	(56)

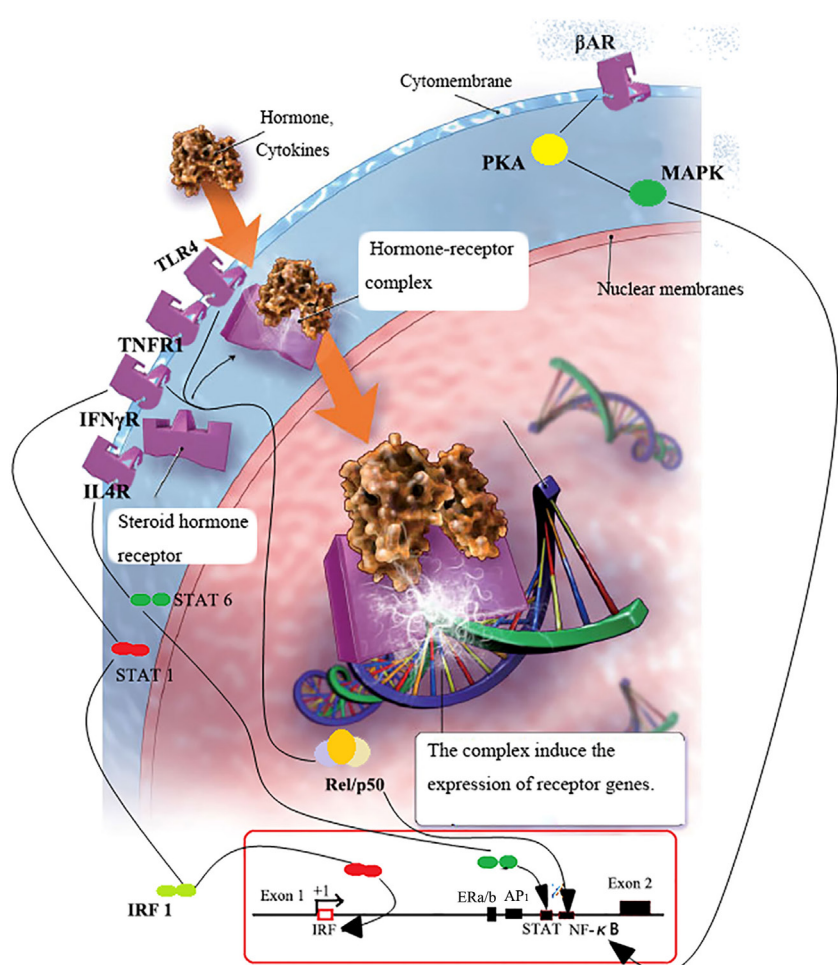


FIGURE 2 | FcRn or plgR transcription regulation. Serum NE binds with β2AR on B cells and activates PKA-p38 MAPK pathways, which subsequently leads to the release of bound p-p38 MAPK to bind with enhancer in the promoter region of *plgR*, and *plgR* increase followed (62). When inflammation occurs, lymphocyte homing induced antibodies production in lamina propria; subsequently, microbes bind with epithelial TLRs with MAMPs and activate NFκB; cytokines released in the vicinity of lymphocytes bind to cytokine receptors and activate IRF-1/NFκB-dependent pathways (58); IRF-1/NFκB proteins get into nucleus and trigger the transcription of Ig transporting receptors (63). As a consequence, concentrations of Ig transporting receptors increase.

compared with C57BL/6J mice (29). This result indicated that the intestine can export IgA-containing cells to the mammary gland; and MAMPs could be a stimulation of pIgR expression and SIgA accumulation in mammary gland and milk. As such, MAMPs can be applied on the Ig transport receptor tg cattle to acquire immune milk with enriched antibody. Additionally, the signals (released by antibody and microbiota in neonate gut) have a modulation effect on the maturation of intestinal barrier function and activation of endogenous Ig transportation, as well as the development of adaptive immunity (60, 61).

Host cytokines, such as IFN- γ , IL-4 and TNF- α can regulate the gene transcriptions of Ig transporting receptor by activating and nuclear of STAT1 dimers, resulting in de novo transcription of AP-1, NF- κ B, and IRF-1 (58, 64) (Figure 2). For instance, ISRE presents at the first outer exon in promoter region of FcRn (the binding site of IRF-1). It has been reported that the stimulation of bovine endothelial cells with the IFN- γ could lead to the appearance of activated STAT1 in the nucleus and increased transcription of the IRF1 gene. This has resulted in rapid upregulation of the bFcRn expression in endothelial cells (65). Interactions among these cytokine-inducible elements in exon 1 and intron 1 of the PIGR gene may be responsible for the observed synergy between IFN- γ , IL-4, and TNF in upregulation of pIgR expression (58, 66). One putative NF κ B transcription binding sites was identified in the 5'-flanking region of the mouse FCGRT promoter and was the close proximity to the transcription start site (63). A fourfold increase of bFcRn gene in spleen, and twofold increase of bFcRn protein in macrophages were observed in the bFcRn tg mice stimulated by intraperitoneal LPS injection (63). The activation of NF- κ B by inflammatory cytokines could enhance the gene transcription of FcRn indirectly by synergizing with STAT1 to activate IRF1 gene transcription, or by binding to a cognate element in the 5'-flanking region of the FcRn genes directly (63, 65, 66). Pro-inflammatory agents can induce the rapid and temporary upregulation of bFcRn; it could be the immunologic adjuvants and optimize the expression and function of Ig transporting receptor in the professional APCs, this contributes to the much augmented humoral immune response.

The concentrations of FcRn are significantly upregulated in late pregnancy and reach their peaks during colostrogenesis; then downregulated in the lactation period and coincident with the Ig concentrations in milk and colostrum that differs at various stages of lactation with the highest concentrations appearing in early colostrum secretions (5). In an *in vitro* study, the stimulation

of bovine mammary epithelial cells with estrogen (E2) and progesterone (P4) induced an increase of FCGRT mRNA, coincident with FcRn expression during late pregnancy and the colostrogenesis period; meanwhile, a similar increase was observed on bRab25 and bRhoB mRNAs (members of GTPases) and assist recycling or transcytosis (67). This reveals the regulatory mechanism of E2/P4 for colostrogenesis extended temporarily by increasing the expression of FcRn and transcytosis-related motor proteins. However, the binding sites of E2/P4 have not yet identified in FcRn gene.

CONCLUSION

The clear understanding of the mechanisms behind the expression and mediation of Ig transporting receptor in the mammary gland and intestinal mucosa would contribute for the better intervention of Ig transfer from mother to fetus. This could also aid for the development of mammary gland bioreactor. Ig transporting receptors could mediate the immunity transfer and immune surveillance, thereby the high survival rate and improved immune system can be achieved. In Ig transporting receptors over-expressed tg animals, the increased Ig concentrations in serum and mucosa can supply adequate Ig through continuous milking as well as safe and effective protection against mastitis pathogens. Moreover, the presence of Ig transporting receptors in mucosal epithelium is capable of transporting antibody or antigen–antibody complex bidirectionally, and further present to APCs. This would help to design immunization strategies for mucosal protection from infections.

AUTHOR CONTRIBUTIONS

XZ, XJ, and JH contributed to conception and design; XJ contributed to acquisition of data and manuscript writing. XJ and JH made equal contribution to this paper.

ACKNOWLEDGMENTS

This work was supported by the Open Foundation of the Provincial Department of the state Key Laboratory of Tarim Animal Husbandry Science and Technology (HS201305), the National Natural Science Foundation (31572556), Ph.D. Programs Foundation of Ministry of Education (20130204110023), the Key Construction Program (2015SD0018) of International Cooperation Base in S&T, Shaanxi Province, China.

REFERENCES

- Roopenian DC, Akilesh S. FcRn: the neonatal Fc receptor comes of age. *Nat Rev Immunol* (2007) 7:715–25. doi:10.1038/nri2155
- Bourges D, Meurens F, Berri M, Chevaleyre C, Zanello G, Levast B, et al. New insights into the dual recruitment of IgA+B cells in the developing mammary gland. *Mol Immunol* (2008) 45:3354–62. doi:10.1016/j.molimm.2008.04.017
- Norderhaug IN, Johansen FE, Schjerven H, Brandtzaeg P. Regulation of the formation and external transport of secretory immunoglobulins. *Crit Rev Immunol* (1999) 19:481–508.
- Norderhaug IN, Johansen FE, Krajci P, Brandtzaeg P. Domain deletions in the human polymeric Ig receptor disclose differences between its dimeric IgA and pentameric IgM interaction. *Eur J Immunol* (1999) 29:3401–9. doi:10.1002/(SICI)1521-4141(199910)29:10<3401::AID-IMMU3401>3.0.CO;2-G
- Hine B, Hunt P, Beasley A, Windon R, Glover S, Colditz I. Selective transport of IgE into ovine mammary secretions. *Res Vet Sci* (2010) 89:184–90. doi:10.1016/j.rvsc.2010.02.010
- Qiao S-W, Kobayashi K, Johansen F-E, Sollid LM, Andersen JT, Milford E, et al. Dependence of antibody-mediated presentation of antigen on FcRn. *Proc Natl Acad Sci U S A* (2008) 105:9337–42. doi:10.1073/pnas.0801717105

7. Baker K, Rath T, Pyzik M, Blumberg RS. The role of FcRn in antigen presentation. *Front Immunol* (2014) 5:408. doi:10.3389/fimmu.2014.00408
8. Cui D, Zhang L, Li J, Zhao Y, Hu X, Dai Y, et al. Bovine FcRn-mediated human immunoglobulin G transfer across the milk-blood barrier in transgenic mice. *PLoS One* (2014) 9:e115972. doi:10.1371/journal.pone.0115972
9. Schneider Z, Jani PK, Szikora B, Vegh A, Kovacs D, Ilias A, et al. Overexpression of bovine FcRn in mice enhances T-dependent immune responses by amplifying T helper cell frequency and Germinal Center Enlargement in the Spleen. *Front Immunol* (2015) 6:357. doi:10.3389/fimmu.2015.00357
10. Weflen AW, Baier N, Tang QJ, Van den Hof M, Blumberg RS, Lencer WI, et al. Multivalent immune complexes divert FcRn to lysosomes by exclusion from recycling sorting tubules. *Mol Biol Cell* (2013) 24:2398–405. doi:10.1091/mbc.E13-04-0174
11. Kaetzel CS. The polymeric immunoglobulin receptor: bridging innate and adaptive immune responses at mucosal surfaces. *Immunol Rev* (2005) 206:83–99. doi:10.1111/j.0105-2896.2005.00278.x
12. Asano M, Komiyama K. Polymeric immunoglobulin receptor. *J Oral Sci* (2011) 53:147–56. doi:10.2334/josnusd.53.147
13. Underdown BJ, Schiff JM. Immunoglobulin A: strategic defense initiative at the mucosal surface. *Annu Rev Immunol* (1986) 4:389–417. doi:10.1146/annurev.iy.04.040186.002133
14. Vegh A, Cervenak J, Jankovics I, Kacskovics I. FcRn overexpression in mice results in potent humoral response against weakly immunogenic antigen. *MAbs* (2011) 3:173–80. doi:10.4161/mabs.3.2.14462
15. Schneider Z, Cervenak J, Baranyi M, Papp K, Prechl J, Laszlo G, et al. Transgenic expression of bovine neonatal Fc receptor in mice boosts immune response and improves hybridoma production efficiency without any sign of autoimmunity. *Immunol Lett* (2011) 137:62–9. doi:10.1016/j.imlet.2011.02.018
16. Cervenak J, Bender B, Schneider Z, Magna M, Carstea BV, Liliom K, et al. Neonatal FcR overexpression boosts humoral immune response in transgenic mice. *J Immunol* (2011) 186:959–68. doi:10.4049/jimmunol.1000353
17. Wilson E, Butcher EC. CCL28 controls immunoglobulin (Ig)A plasma cell accumulation in the lactating mammary gland and IgA antibody transfer to the neonate. *J Exp Med* (2004) 200:805–9. doi:10.1084/jem.20041069
18. Yoshida M, Kobayashi K, Kuo TT, Bry L, Glickman JN, Claypool SM, et al. Neonatal Fc receptor for IgG regulates mucosal immune responses to luminal bacteria. *J Clin Invest* (2006) 116:2142–51. doi:10.1172/JCI27821
19. Osaka I, Matsui Y, Terada F. Effect of the mass of immunoglobulin (Ig) G intake and age at first colostrum feeding on serum IgG concentration in Holstein calves. *J Dairy Sci* (2014) 97(10):6608–12. doi:10.3168/jds.2013-7571
20. Hurley WL, Theil PK. Perspectives on immunoglobulins in colostrum and milk. *Nutrients* (2011) 3:442–74. doi:10.3390/nu3040442
21. Israel EJ, Patel VK, Taylor SF, Marshak-Rothstein A, Simister NE. Requirement for a beta 2-microglobulin-associated Fc receptor for acquisition of maternal IgG by fetal and neonatal mice. *J Immunol* (1995) 154:6246–51.
22. Catunda Lemos AP, Cervenak J, Bender B, Hoffmann OI, Baranyi M, Kerekes A, et al. Characterization of the rabbit neonatal Fc receptor (FcRn) and analyzing the immunophenotype of the transgenic rabbits that overexpresses FcRn. *PLoS One* (2012) 7:e28869. doi:10.1371/journal.pone.0028869
23. Lu W, Zhao Z, Zhao Y, Yu S, Zhao Y, Fan B, et al. Over-expression of the bovine FcRn in the mammary gland results in increased IgG levels in both milk and serum of transgenic mice. *Immunology* (2007) 122:401–8. doi:10.1111/j.1365-2567.2007.02654.x
24. Adamski FM, King AT, Demmer J. Expression of the Fc receptor in the mammary gland during lactation in the marsupial *Trichosurus vulpecula* (brushtail possum). *Mol Immunol* (2000) 37:435–44. doi:10.1016/S0161-5890(00)00065-1
25. Lemos AC, Cervenak J, Bender B, Hoffmann OI, Baranyi M, Kerekes A, et al. Characterization of the rabbit neonatal Fc receptor (FcRn) and analyzing the immunophenotype of the transgenic rabbits that overexpresses FcRn. *PLoS One* (2012) 7:e28869. doi:10.1371/journal.pone.0028869
26. Verweij JJ, Koets AP, Eisenberg SW. Effect of continuous milking on immunoglobulin concentrations in bovine colostrum. *Vet Immunol Immunopathol* (2014) 160:225–9. doi:10.1016/j.vetimm.2014.05.008
27. Suthar VS, Canelas-Raposo J, Deniz A, Heuwieser W. Prevalence of subclinical ketosis and relationships with postpartum diseases in European dairy cows. *J Dairy Sci* (2013) 96:2925–38. doi:10.3168/jds.2012-6035
28. Beam AL, Lombard JE, Kopral CA, Garber LP, Winter AL, Hicks JA, et al. Prevalence of failure of passive transfer of immunity in newborn heifer calves and associated management practices on US dairy operations. *J Dairy Sci* (2009) 92:3973–80. doi:10.3168/jds.2009-2225
29. Boumahrou N, Chevaleyre C, Berri M, Martin P, Bellier S, Salmon H. An increase in milk IgA correlates with both pIgR expression and IgA plasma cell accumulation in the lactating mammary gland of PRM/Alf mice. *J Reprod Immunol* (2012) 96:25–33. doi:10.1016/j.jri.2012.08.001
30. Macpherson AJ, Geuking MB, Slack E, Hapfelmeier S, McCoy KD. The habitat, double life, citizenship, and forgetfulness of IgA. *Immunol Rev* (2012) 245:132–46. doi:10.1111/j.1600-065X.2011.01072.x
31. Janoff EN, Gustafson C, Frank DN. The world within: living with our microbial guests and guides. *Transl Res* (2012) 160:239–45. doi:10.1016/j.trsl.2012.05.005
32. Qiao S-W, Solid LM, Blumberg RS. Antigen presentation in celiac disease. *Curr Opin Immunol* (2009) 21:111–7. doi:10.1016/j.co.2009.03.004
33. Baker K, Qiao S-W, Kuo TT, Aveson VG, Platzer B, Andersen J-T, et al. Neonatal Fc receptor for IgG (FcRn) regulates cross-presentation of IgG immune complexes by CD8–CD11b+ dendritic cells. *Proc Natl Acad Sci USA* (2011) 108:9927–32. doi:10.1073/pnas.1019037108
34. Ye L, Zeng R, Bai Y, Roopenian DC, Zhu X. Efficient mucosal vaccination mediated by the neonatal Fc receptor. *Nat Biotechnol* (2011) 29:158–63. doi:10.1038/nbt.1742
35. Kacskovics I, Cervenak J, Erdei A, Goldsby RA, Butler JE. Recent advances using FcRn overexpression in transgenic animals to overcome impediments of standard antibody technologies to improve the generation of specific antibodies. *MAbs* (2011) 3:431–9. doi:10.4161/mabs.3.5.17023
36. Cervenak J, Kurrle R, Kacskovics I. Accelerating antibody discovery using transgenic animals overexpressing the neonatal Fc receptor as a result of augmented humoral immunity. *Immunol Rev* (2015) 268:269–87. doi:10.1111/imr.12364
37. Baker K, Rath T, Flak MB, Arthur JC, Chen Z, Glickman JN, et al. Neonatal Fc receptor expression in dendritic cells mediates protective immunity against colorectal cancer. *Immunity* (2013) 39:1095–107. doi:10.1016/j.immuni.2013.11.003
38. Uren TK, Johansen FE, Wijburg OL, Koentgen F, Brandtzaeg P, Strugnell RA. Role of the polymeric Ig receptor in mucosal B cell homeostasis. *J Immunol* (2003) 170:2531–9. doi:10.4049/jimmunol.170.5.2531
39. Rath T, Kuo TT, Baker K, Qiao S-W, Kobayashi K, Yoshida M, et al. The immunologic functions of the neonatal Fc receptor for IgG. *J Clin Immunol* (2013) 33:9–17. doi:10.1007/s10875-012-9768-y
40. Yoshida M, Claypool SM, Wagner JS, Mizoguchi E, Mizoguchi A, Roopenian DC, et al. Human neonatal Fc receptor mediates transport of IgG into luminal secretions for delivery of antigens to mucosal dendritic cells. *Immunity* (2004) 20:769–83. doi:10.1016/j.immuni.2004.05.007
41. Suleiman YB, Yoshida M, Nishiumi S, Tanaka H, Mimura T, Nobutani K, et al. Neonatal Fc receptor for IgG (FcRn) expressed in the gastric epithelium regulates bacterial infection in mice. *Mucosal Immunol* (2011) 5:87–98. doi:10.1038/mi.2011.53
42. Végh A, Farkas A, Kovacs D, Papp K, Cervenak J, Schneider Z, et al. FcRn overexpression in transgenic mice results in augmented APC activity and robust immune response with increased diversity of induced antibodies. *PLoS One* (2012) 7:e36286. doi:10.1371/journal.pone.0036286
43. Schneider Z, Cervenak J, Baranyi M, Papp K, Prechl J, László G, et al. Transgenic expression of bovine neonatal Fc receptor in mice boosts immune response and improves hybridoma production efficiency without any sign of autoimmunity. *Immunol Lett* (2011) 137:62–9. doi:10.1016/j.imlet.2011.02.018
44. Sait L, Galic M, Strugnell RA, Janssen PH. Secretory antibodies do not affect the composition of the bacterial microbiota in the terminal ileum of 10-week-old mice. *Appl Environ Microbiol* (2003) 69:2100–9. doi:10.1128/AEM.69.4.2100-2109.2003
45. Wijburg OL, Uren TK, Simpfendorfer K, Johansen FE, Brandtzaeg P, Strugnell RA. Innate secretory antibodies protect against natural *Salmonella typhimurium* infection. *J Exp Med* (2006) 203:21–6. doi:10.1084/jem.20052093
46. Berry S, Coppeters W, Davis S, Burrett A, Thomas N, Palmer D, et al. A triad of highly divergent polymeric immunoglobulin receptor (PIGR) haplotypes with major effect on IgA concentration in bovine milk. *PLoS One* (2013) 8:e57219. doi:10.1371/journal.pone.0057219

47. Sachs UJ, Socher I, Braeunlich CG, Kroll H, Bein G, Santoso S. A variable number of tandem repeats polymorphism influences the transcriptional activity of the neonatal Fc receptor α -chain promoter. *Immunology* (2006) 119:83–9. doi:10.1111/j.1365-2567.2006.02408.x
48. Zhang R, Zhao Z, Zhao Y, Kacskovics I, Eijk MVD, Groot ND, et al. Association of FcRn heavy chain encoding gene (FCGRT) polymorphisms with IgG content in bovine colostrum. *Anim Biotechnol* (2009) 20:242–6. doi:10.1080/10495390903196448
49. Obara W, Iida A, Suzuki Y, Tanaka T, Akiyama F, Maeda S, et al. Association of single-nucleotide polymorphisms in the polymeric immunoglobulin receptor gene with immunoglobulin A nephropathy (IgAN) in Japanese patients. *J Hum Genet* (2003) 48:293–9. doi:10.1007/s10038-003-0027-1
50. Kim J, Bronson C, Wani MA, Oberyszyn TM, Mohanty S, Chaudhury C, et al. β 2-Microglobulin deficient mice catabolize IgG more rapidly than FcRn- α -chain deficient mice. *Exp Biol Med* (2008) 233:603–9. doi:10.3181/0710-RM-270
51. Bender B, Bodrogi I, Mayer B, Schneider Z, Zhao Y, Hammarstrom L, et al. Position independent and copy-number-related expression of the bovine neonatal Fc receptor alpha-chain in transgenic mice carrying a 102 kb BAC genomic fragment. *Transgenic Res* (2007) 16:613–27. doi:10.1007/s11248-007-9108-9
52. Robert-Guroff M. IgG surfaces as an important component in mucosal protection. *Nat Med* (2000) 6:129–30. doi:10.1038/72206
53. De Groot N, Van Kuik-Romeijn P, Lee SH, De Boer HA. Increased immunoglobulin A levels in milk by over-expressing the murine polymeric immunoglobulin receptor gene in the mammary gland epithelial cells of transgenic mice. *Immunology* (2000) 101:218–24. doi:10.1046/j.1365-2567.2000.00094.x
54. Johansen F-E, Pekna M, Norderhaug IN, Haneberg B, Hietala MA, Krajci P, et al. Absence of epithelial immunoglobulin a transport, with increased mucosal leakiness, in polymeric immunoglobulin receptor/secretory component-deficient mice. *J Exp Med* (1999) 190:915–22. doi:10.1084/jem.190.7.915
55. Hendrickson BA, Rindisbacher L, Corthesy B, Kendall D, Waltz DA, Neutra MR, et al. Lack of association of secretory component with IgA in J chain-deficient mice. *J Immunol* (1996) 157:750–4.
56. van IJzendoorn SC, Tuvim MJ, Weimbs T, Dickey BF, Mostov KE. Direct interaction between Rab3b and the polymeric immunoglobulin receptor controls ligand-stimulated transcytosis in epithelial cells. *Dev Cell* (2002) 2:219–28. doi:10.1016/S1534-5807(02)00115-6
57. Macpherson AJ, McCoy KD, Johansen FE, Brandtzaeg P. The immune geography of IgA induction and function. *Mucosal Immunol* (2008) 1:11–22. doi:10.1038/mi.2007.6
58. Johansen FE, Kaetzel CS. Regulation of the polymeric immunoglobulin receptor and IgA transport: new advances in environmental factors that stimulate pIgR expression and its role in mucosal immunity. *Mucosal Immunol* (2011) 4:598–602. doi:10.1038/mi.2011.37
59. Pal K, Kaetzel CS, Brundage K, Cunningham CA, Cuff CF. Regulation of polymeric immunoglobulin receptor expression by reovirus. *J Gen Virol* (2005) 86:2347–57. doi:10.1099/vir.0.80690-0
60. Priestley D, Bittar J, Ibarbia L, Risco C, Galvao K. Effect of feeding maternal colostrum or plasma-derived or colostrum-derived colostrum replacer on passive transfer of immunity, health, and performance of preweaning heifer calves. *J Dairy Sci* (2013) 96:3247–56. doi:10.3168/jds.2012-6339
61. Rogier EW, Frantz AL, Bruno MEC, Leia W, Cohen DA, Stromberg AJ, et al. Secretory antibodies in breast milk promote long-term intestinal homeostasis by regulating the gut microbiota and host gene expression. *Proc Natl Acad Sci USA* (2014) 111:3074–9. doi:10.1073/pnas.1315792111
62. Lara-Padilla E, Campos-Rodriguez R, Jarillo-Luna A, Reyna-Garfias H, Rivera-Aguilar V, Miliar A, et al. Caloric restriction reduces IgA levels and modifies cytokine mRNA expression in mouse small intestine. *J Nutr Biochem* (2011) 22:560–6. doi:10.1016/j.jnutbio.2010.04.012
63. Cervenak J, Doleschall M, Bender B, Mayer B, Schneider Z, Doleschall Z, et al. NF κ B induces overexpression of bovine FcRn: a novel mechanism that further contributes to the enhanced immune response in genetically modified animals carrying extra copies of FcRn. *MAbs* (2013) 5(6):860–71. doi:10.4161/mabs.26507
64. Cox S, Ebersole L, Carpenter G, Proctor G. Effects of autonomic agonists and immunomodulatory cytokines on polymeric immunoglobulin receptor expression by cultured rat and human salivary and colonic cell lines. *Arch Oral Biol* (2007) 52:411–6. doi:10.1016/j.archoralbio.2006.10.006
65. Brandtzaeg P. Role of secretory antibodies in the defence against infections. *Int J Med Microbiol* (2003) 293:3–15. doi:10.1078/1438-4221-00241
66. Pine R. Convergence of TNF alpha and IFN gamma signalling pathways through synergistic induction of IRF-1/ISGF-2 is mediated by a composite GAS/kappa B promoter element. *Nucleic Acids Res* (1997) 25:4346–54. doi:10.1093/nar/25.21.4346
67. Stark A, Vachkova E, Wellnitz O, Bruckmaier R, Baumrucker C. Colostrogenesis: candidate genes for IgG1 transcytosis mechanisms in primary bovine mammary epithelial cells. *J Anim Physiol Anim Nutr* (2013) 97:1114–24. doi:10.1111/jpn.12021

Conflict of Interest Statement: The authors declare that the research was conducted in the absence of any commercial or financial relationships that could be construed as a potential conflict of interest.

Copyright © 2016 Jiang, Hu, Thirumalai and Zhang. This is an open-access article distributed under the terms of the Creative Commons Attribution License (CC BY). The use, distribution or reproduction in other forums is permitted, provided the original author(s) or licensor are credited and that the original publication in this journal is cited, in accordance with accepted academic practice. No use, distribution or reproduction is permitted which does not comply with these terms.



Anti-Bovine Programmed Death-1 Rat–Bovine Chimeric Antibody for Immunotherapy of Bovine Leukemia Virus Infection in Cattle

OPEN ACCESS

Edited by:

Tianlei Ying,
Fudan University, China

Reviewed by:

Daniel Olive,
Institut national de la santé et de la
recherche médicale (INSERM),
France

William Davis,
Washington State University,
United States

*Correspondence:

Satoru Konnai
konnai@vetmed.hokudai.ac.jp

†Present address:

Ryoyo Ikebuchi,
Laboratory of Immunology, Faculty of
Pharmacy, Osaka Ohtani University,
Tondabayashi, Japan

Specialty section:

This article was submitted to
Vaccines and Molecular
Therapeutics,
a section of the journal
Frontiers in Immunology

Received: 22 March 2017

Accepted: 17 May 2017

Published: 07 June 2017

Citation:

Okagawa T, Konnai S, Nishimori A,
Maekawa N, Ikebuchi R, Goto S,
Nakajima C, Kohara J, Ogasawara S,
Kato Y, Suzuki Y, Murata S and
Ohashi K (2017) Anti-Bovine
Programmed Death-1 Rat–Bovine
Chimeric Antibody for
Immunotherapy of Bovine Leukemia
Virus Infection in Cattle.
Front. Immunol. 8:650.
doi: 10.3389/fimmu.2017.00650

Tomohiro Okagawa¹, Satoru Konnai^{1*}, Asami Nishimori¹, Naoya Maekawa¹,
Ryoyo Ikebuchi^{1†}, Shinya Goto¹, Chie Nakajima^{2,3}, Junko Kohara⁴, Satoshi Ogasawara⁵,
Yukinari Kato^{6,7}, Yasuhiko Suzuki^{2,3}, Shiro Murata¹ and Kazuhiko Ohashi¹

¹Department of Disease Control, Graduate School of Veterinary Medicine, Hokkaido University, Sapporo, Japan, ²Division of Bioresources, Research Center for Zoonosis Control, Hokkaido University, Sapporo, Japan, ³Global Station for Zoonosis Control, Global Institution for Collaborative Research and Education (GI-CoRE), Hokkaido University, Sapporo, Japan,

⁴Animal Research Center, Agriculture Research Department, Hokkaido Research Organization, Shintoku, Japan,

⁵Department of Regional Innovation, Tohoku University Graduate School of Medicine, Sendai, Japan, ⁶Department of Antibody Drug Development, Tohoku University Graduate School of Medicine, Sendai, Japan, ⁷New Industry Creation Hatchery Center, Tohoku University, Sendai, Japan

Blockade of immunoinhibitory molecules, such as programmed death-1 (PD-1)/PD-ligand 1 (PD-L1), is a promising strategy for reinvigorating exhausted T cells and preventing disease progression in a variety of chronic infections. Application of this therapeutic strategy to cattle requires bovinized chimeric antibody targeting immunoinhibitory molecules. In this study, anti-bovine PD-1 rat–bovine chimeric monoclonal antibody 5D2 (Boch5D2) was constructed with mammalian expression systems, and its biochemical function and antiviral effect were characterized *in vitro* and *in vivo* using cattle infected with bovine leukemia virus (BLV). Purified Boch5D2 was capable of detecting bovine PD-1 molecules expressed on cell membranes in flow cytometric analysis. In particular, Biacore analysis determined that the binding affinity of Boch5D2 to bovine PD-1 protein was similar to that of the original anti-bovine PD-1 rat monoclonal antibody 5D2. Boch5D2 was also capable of blocking PD-1/PD-L1 binding at the same level as 5D2. The immunomodulatory and therapeutic effects of Boch5D2 were evaluated by *in vivo* administration of the antibody to a BLV-infected calf. Inoculated Boch5D2 was sustained in the serum for a longer period. Boch5D2 inoculation resulted in activation of the proliferation of BLV-specific CD4⁺ T cells and decrease in the proviral load of BLV in the peripheral blood. This study demonstrates that Boch5D2 retains an equivalent biochemical function to that of the original antibody 5D2 and is a candidate therapeutic agent for regulating antiviral immune response *in vivo*. Clinical efficacy of PD-1/PD-L1 blockade awaits further experimentation with a large number of animals.

Keywords: immunoinhibitory molecules, programmed death-1, PD-ligand 1, T-cell exhaustion, immunotherapy, chimeric antibody, bovine leukemia virus, cattle

INTRODUCTION

For decades, a variety of studies have attempted to enhance the T-cell response in chronic infections. However, immunoinhibitory pathways such as programmed death-1 (PD-1)/PD-ligand 1 (PD-L1) downregulate T-cell functions, likely causing the failure of previous attempts to develop vaccines and immunotherapies (1–3). Antibodies that block PD-1/PD-L1 can restore T-cell function and reduce viral load *in vivo* in mouse and non-human primate models (4–6). These antibodies are clearly potential novel therapeutic agents for the control of chronic infections. Recently, anti-human PD-1 antibodies have been approved and launched for the treatment of melanoma, non-small cell lung cancer, renal cell carcinoma, and Hodgkin's lymphoma in humans (7–10). In addition, PD-1/PD-L1 blockade is under consideration for immunotherapy against chronic infections with human immunodeficiency virus, Epstein–Barr virus, hepatitis B virus, hepatitis C virus, and *Mycobacterium tuberculosis* (11–15) in human medicine. To date, however, blockers of PD-1/PD-L1 have not been approved for clinical use in veterinary medicine, including cattle.

Functional exhaustion of T-cell response has also been reported in cattle infected with bovine leukemia virus (BLV) (16–20), *Mycobacterium avium* subsp. *paratuberculosis* (21, 22), *Anaplasma marginale* (23), and *Mycobacterium bovis* (24). T-cell exhaustion may play a role in the immunopathogenesis of these diseases where pathogens evade immune elimination and establish persistent infection. To reveal the mechanism responsible for T-cell exhaustion in cattle, our previous studies investigated the expression and function of the bovine PD-1/PD-L1 pathway in BLV infection (25, 26), paratuberculosis (27), bovine anaplasmosis (28), and bovine mycoplasmosis (29). PD-1 is upregulated in CD4⁺ and/or CD8⁺ T cells during B-cell lymphoma caused by BLV infection (25), subclinical stage of paratuberculosis (27), acute anaplasmosis (28), and clinical mycoplasmosis (29). In contrast, the expression level of PD-L1 increases on infected cells and antigen-presenting cells, including BLV-infected B cells (25, 26), *M. avium* subsp. *paratuberculosis*-infected macrophages (27), and peripheral monocytes in anaplasmosis (28) and mycoplasmosis (29). Thus, the PD-1/PD-L1 axis is involved in the inhibition of T-cell function during disease progression in several chronic infections in cattle. Additionally, we established several clones of anti-bovine PD-1 rat monoclonal antibodies (mAbs) that are capable of blocking the interaction of PD-1 and PD-L1 and activating the functions of bovine T cells (25). More remarkably, PD-1/PD-L1 blockade using one of these blocking mAbs, clone 5D2, inhibits the expression of BLV gp51 protein and B-cell activation *in vitro* (25). Therefore, the PD-1/PD-L1 pathway is a candidate therapeutic target for chronic infections in cattle.

However, blocking antibodies derived from rat are considered to be not suitable for administration to cattle. Previous studies have shown that the administration of mouse antibody to cattle induces the bovine anti-mouse antibody response within 10–14 days in *in vivo* depletion experiments, as the mouse antibody is recognized as a heterologous protein in cattle (30–32). The immunogenicity of heterologous antibody is known to depend mainly (90%) on the constant regions (33). For this

reason, replacing constant regions of heterologous antibody with those of bovine immunoglobulins is expected to reduce the bovine anti-antibody response and remain stable and effective for a longer period *in vivo* (31, 34).

In this study, we established anti-bovine PD-1 rat-bovine chimeric antibody (chAb), named as Boch5D2. Boch5D2 consists of variable regions from anti-bovine PD-1 rat mAb and constant regions from bovine IgG₁ and Ig lambda. Additionally, amino acid residues of the constant domain of Boch5D2 IgG₁ were mutated to reduce effector functions mediated via Fcγ receptors (FcγRs). We examine mammalian expression systems for the production of Boch5D2. The stable expression system was successful in producing sufficient amounts of Boch5D2 for further experiments. The purified Boch5D2 was tested for biochemical properties compared with the original anti-bovine PD-1 rat mAb 5D2. Accordingly, *in vivo* administration of anti-PD-1 antibodies 5D2 and Boch5D2 was conducted to clarify the *in vivo* stability and antiviral effects of these blocking antibodies in BLV-infected cattle.

MATERIALS AND METHODS

Cloning of cDNA Encoding the Variable Regions of Anti-Bovine PD-1 Rat mAb

Total RNA was isolated from cultivated clones of hybridomas producing anti-bovine PD-1 rat mAb (5D2) (25) with the use of the TRIzol reagent (Thermo Fisher Scientific, Waltham, MA, USA) according to the manufacturer's instructions. cDNAs encoding the variable regions of rat immunoglobulin, IgG_{2a}, and Igk were amplified with a 5'-Rapid Amplification of cDNA Ends (5'-RACE) System (Thermo Fisher Scientific). Briefly, first strand cDNAs were synthesized from the obtained total RNA with a rat IgG_{2a}-specific primer (RACE RAG2a-1) and a rat Igk-specific primer (RACE RACK-1) (35). Primer sequences are presented in Table S1 in Supplementary Material. After removal of the RNA template by RNase and purification of the first strand product by S.N.A.P. column (Thermo Fisher Scientific), the obtained cDNAs were tailed with poly(C) on their 3'-ends and further amplified using poly(G) primer and the other gene-specific primers, RACE RAG2a-2 (rat IgG_{2a}) and RACE RACK-2 (rat Igk) (35). The polymerase chain reaction (PCR) amplicons were purified with a FastGene Gel/PCR Extraction Kit (Nippon Genetics, Tokyo, Japan) and cloned into the TA cloning site of pGEM-T Easy Vector (Promega, Madison, WI, USA). The plasmid clones were purified with a Plasmid DNA Purification Kit (Qiagen, Hilden, Germany) and sequenced with a CEQ 2000 DNA Analysis System (Beckman Coulter, Fullerton, CA, USA).

Expression of Boch5D2 in CHO DG44 Cells

The nucleotide sequences of the variable regions of the heavy and light chains of 5D2 were combined with the constant regions of bovine IgG₁ (GenBank accession number X62916) and bovine Ig lambda (GenBank accession number X62917), respectively. For the preparation of Boch5D2 with IgG₁ triggering reduced Fc-mediated effector functions (Boch5D2 IgG₁ ADCC-), amino acid mutations were introduced into the binding sites for FcγRs of bovine IgG₁ CH2 domain (Figure S3A in Supplementary Material)

(36–38). The designed sequences were modified according to the optimal codon usage of Chinese hamster, synthesized (Integrated DNA Technologies, Coralville, IA, USA), and cloned into a pDN112 expression vector (pDN11 with a modified multicloning site) (**Figure 1A**) (38, 39).

Stable high-producer cell lines expressing Boch5D2 were established with the use of the dihydrofolate reductase (dhfr)/methotrexate gene amplification system in dhfr-deficient (dhfr^{-/-}) Chinese hamster ovary (CHO) DG44 cells. CHO DG44 cells were transfected with pDN112-Boch5D2 IgG₁ ADCC– and selected in CD OptiCHO medium (Thermo Fisher Scientific) supplemented with 2 mM GlutaMAX-I (Thermo Fisher Scientific) and 800 µg/ml G418 sulfate (Enzo Life Sciences, Farmingdale, NY, USA). After 3 weeks, the cells were screened for the ability to produce Boch5D2 by dot blotting and enzyme-linked immunosorbent assay (ELISA) with horseradish peroxidase (HRP)-conjugated anti-bovine IgG Fc rabbit polyclonal antibody (Rockland Immunochemicals, Pottstown, PA, USA), as previously described (38). Single-cell cloning of the polyclonal cell lines obtained above was performed by limiting dilution and screened again as described above. Gene amplification of the single-cell clones was subsequently performed in CD OptiCHO medium (Thermo Fisher Scientific) containing 60 nM methotrexate (Enzo Life Sciences). Boch5D2 was produced by shaking cultivation of the established cell lines producing the highest amount of antibody in G418- and methotrexate-free CD OptiCHO medium (Thermo Fisher Scientific) at 37°C and 125 rpm with 5% CO₂ for 14 days. Live and dead cells were counted with a Countess Automated Cell Counter (Thermo Fisher Scientific) on days 3, 7, 10, and 14. At the same time points, the concentration of Boch5D2 in the culture supernatant was determined by bovine IgG ELISA, as described above.

Purification of Boch5D2

Purification of Boch5D2 from the culture supernatant was performed by affinity chromatography with an Ab-Capcher ExTra

(ProteNova, Kagawa, Japan), and the buffer was exchanged with phosphate-buffered saline (PBS) by size exclusion chromatography using PD-10 Desalting Column (GE Healthcare, Buckinghamshire, England, UK). The concentration of Boch5D2 was measured by ultraviolet (UV) absorbance at 280 nm with a NanoDrop 8000 Spectrophotometer (Thermo Fisher Scientific). The purity of Boch5D2 was confirmed by sodium dodecyl sulfate-polyacrylamide gel electrophoresis (SDS-PAGE) in reducing or non-reducing condition using 10% polyacrylamide gel and 2× Laemmli Sample Buffer (Bio-Rad, Hercules, CA, USA). Precision Plus Protein All Blue Standard (Bio-Rad) was used as a molecular-weight size marker, and the proteins were visualized with Quick-CBB (Wako Pure Chemical Industries, Osaka, Japan). The purity of Boch5D2 was evaluated by densitometry with CS Analyzer Software version 3.0 (Atto, Tokyo, Japan) and was routinely >90%.

Binding Assay of Boch5D2 to Membrane-Bound Bovine PD-1

To confirm the binding activity of Boch5D2 to membrane-bound bovine PD-1, flow cytometric analyses were performed using myc-tagged bovine PD-1-expressing CHO DG44 cells (BoPD-1-myc cells) (25). Briefly, BoPD-1-myc cells were incubated with 5D2 (25) or Boch5D2 at room temperature for 30 min. Rat IgG_{2a} (R35-95, BD Biosciences, San Jose, CA, USA) and bovine IgG antibodies (Bethyl Laboratories, Montgomery, TX, USA) were used as isotype controls. The cells were then washed with PBS and labeled with APC-conjugated anti-rat immunoglobulin antibody (Southern Biotech, Birmingham, AL, USA) or APC-conjugated anti-bovine IgG Fc goat antibody (Jackson ImmunoResearch, West Grove, PA, USA) at room temperature for 30 min. Finally, the cells were washed and analyzed immediately using FACS Verse (BD Biosciences) and FCS Express 4 (De Novo Software, Glendale, CA, USA). The primary antibodies used in this experiment are also shown in **Table 1**.

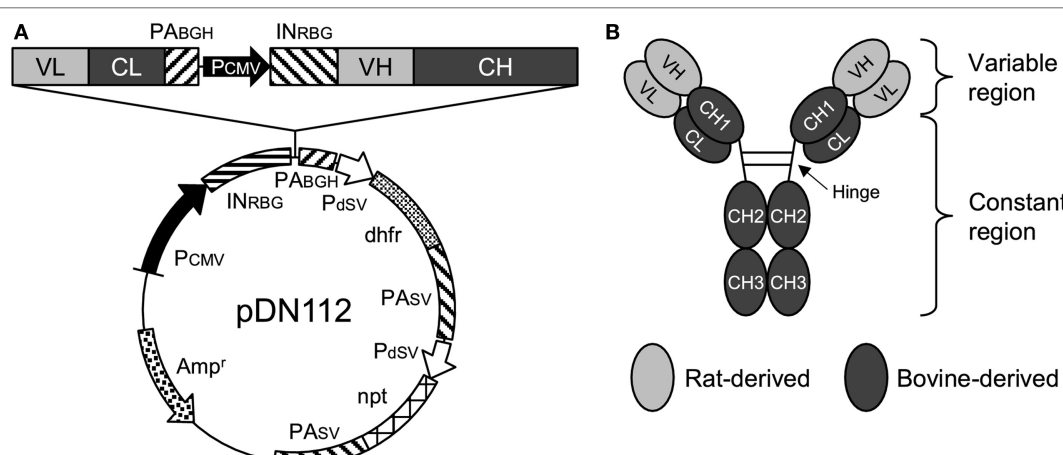


FIGURE 1 | Anti-programmed death-1 chimeric antibody, Boch5D2. **(A)** Schematic structure of a plasmid vector encoding Boch5D2 (pDN112-Boch5D2 IgG₁ ADCC–). A light chain consists of a variable region (VL) and a constant region (CL). A heavy chain consists of a variable region (VH) and a constant region (CH: CH1, hinge, CH2, and CH3). The pDN112 vector includes a neomycin-resistant gene (npt), and a dihydrofolate reductase gene (dhfr). **(B)** Schematic structure of Boch5D2. Boch5D2 is composed of two identical heavy chains and light chains, as with the normal IgG antibody.

TABLE 1 | Primary antibodies used in flow cytometric analyses of this study.

Target	Isotype	Clone	Source	Fluorochrome	Conjugation or labeling
Binding assay of anti-programmed death-1 (PD-1) antibodies					
PD-1	Bovine IgG ₁	Boch5D2	This study	Alexa Fluor 647	Alexa Fluor 647-conjugated anti-bovine IgG Fc antibody (Jackson ImmunoResearch)
Bovine IgG ₁ isotype control	Bovine IgG ₁	Poly	Bethyl	Alexa Fluor 647	Alexa Fluor 647-conjugated anti-bovine IgG Fc antibody (Jackson ImmunoResearch)
PD-1	Rat IgG _{2a}	5D2	In house (25)	APC	APC-conjugated anti-rat Ig antibody (Southern Biotech)
Rat IgG _{2a} isotype control	Rat IgG _{2a}	R35-95	BD Biosciences	APC	APC-conjugated anti-rat Ig antibody (Southern Biotech)
Flow cytometric analysis of T-cell proliferation					
CFSE	–	–	Sigma-Aldrich	CFSE	–
CD3	Mouse IgG ₁	MM1A	WSU Monoclonal Antibody Center	PE	Zenon R-PE Mouse IgG ₁ Labeling Kit (Thermo Fisher Scientific)
CD4	Mouse IgG ₁	CC30	Bio-Rad	Alexa Fluor 647	Zenon Alexa Fluor 647 Mouse IgG ₁ Labeling Kit (Thermo Fisher Scientific)
CD8	Mouse IgG _{2a}	CC63	Bio-Rad	PerCp/Cy5.5	Lightning-Link PerCp/Cy5.5 Conjugation Kit (Innova Biosciences)
TCR1-N24 (δ chain)	Mouse IgG _{2b}	GB21A	WSU Monoclonal Antibody Center	APC/Cy7	Lightning-Link APC/Cy7 Conjugation Kit (Innova Biosciences)
IgM	Mouse IgG ₁	IL-A30	Bio-Rad	PE/Cy7	Lightning-Link PE/Cy7 Conjugation Kit (Innova Biosciences)

CFSE, carboxyfluorescein diacetate succinimidyl ester; PE, phycoerythrin; PerCp, peridinin-chlorophyll-protein complex; APC, allophycocyanin; Cy, cyanin.

Surface Plasmon Resonance (SPR) Analysis

To assess the binding affinity of 5D2 and Boch5D2 to bovine PD-1, SPR analysis was performed using the Biacore system (GE Healthcare) with polyhistidine-tagged bovine PD-1 protein (BoPD-1-His). For the preparation of BoPD-1-His, cDNA encoding the extracellular domain fragment of bovine PD-1 (GenBank accession number AB510901) with a signal sequence was amplified by PCR with gene-specific primers with a Kozak sequence, a C-terminal 6× histidine tag-encoding sequence, and restriction enzyme cleavage sites (Table S1 in Supplementary Material). The amplicon was then cloned into the multicloning site of pCXN2.1(+) (kindly provided by Dr. T. Yokomizo, Juntendo University, Japan) (40). A transient cell line expressing BoPD-1-His was established with the use of Expi293 Expression System (Thermo Fisher Scientific). Briefly, Expi293F cells were transfected with pCXN2.1(+)·BoPD-1-His with the use of ExpiFectamine (Thermo Fisher Scientific) and cultivated with shaking in Expi293 medium (Thermo Fisher Scientific) at 37°C and 125 rpm with 8% CO₂ for 7 days. BoPD-1-His was purified from the culture supernatant with TALON Metal Affinity Resin (Clontech, Palo Alto, CA, USA), and the buffer was exchanged with PBS as described above. The purity of BoPD-1-His was confirmed by SDS-PAGE, and the concentration of BoPD-1-His was determined with a NanoDrop 8000 Spectrophotometer (Thermo Fisher Scientific) as described above.

Surface plasmon resonance measurement was performed on a Biacore X100 instrument (GE Healthcare) at 25°C. Purified BoPD-1-His was immobilized on a CM5 sensor chip (GE Healthcare) by an Amine Coupling Kit (GE Healthcare) following the manufacturer's instructions to analyze 5D2 or Boch5D2 binding. HBS-EP+ (GE Healthcare) was used for both the running and the dilution buffers. Control run responses containing buffer only were subtracted to obtain specific binding responses.

The kinetic constants of 5D2 and Boch5D2 were determined by fitting with the 1:1 kinetic binding model.

Blockade Assay of PD-1/PD-L1 Binding

Bovine PD-1-bovine IgG Fc fusion protein (BoPD-1-Ig) was expressed in a previously established stable expression cell line, purified, and quantified as described previously (38). To confirm the ability of 5D2 and Boch5D2 to block PD-1/PD-L1 binding, biotinylated BoPD-1-Ig (5 µg/ml) was incubated with various concentrations (0.39–50 µg/ml) of 5D2 and Boch5D2 at 37°C for 30 min. The incubated BoPD-1-Ig proteins were then reacted with bovine PD-L1-EGFP-expressing CHO DG44 cells (BoPD-L1-EGFP cells) (38) at 37°C for 30 min. BoPD-1-Ig bound to BoPD-L1-EGFP cells was labeled with APC-conjugated streptavidin (BioLegend, San Diego, CA, USA) at room temperature for 30 min, washed with PBS, and analyzed immediately by FACS Verse (BD Biosciences). Rat IgG_{2a} (R35-95, BD Biosciences) and bovine IgG₁ antibodies (Bethyl Laboratories) were used as isotype controls.

Administration of Boch5D2 to Cattle

To confirm the effects of Boch5D2 in cattle (*in vivo*), a BLV-infected calf (animal number 15-6; Holstein, male, 173 kg, 4 months old) was administered 14 mg (0.08 mg/kg) of purified Boch5D2 intravenously. Peripheral blood was collected before inoculation and more than once a week after inoculation. This animal was inoculated with 1.4×10^8 leukocytes infected with BLV (1.4×10^7 copies of provirus) 8 weeks before antibody inoculation and developed the aleukemic stage of BLV infection. Infected leukocytes were isolated from the blood of a BLV-infected cow in the persistent lymphocytosis stage. These animals were kept in a biosafety level I animal facility at the Animal Research Center, Agricultural Research Department, Hokkaido Research Organization (Shintoku, Hokkaido, Japan). This animal experiment was approved by the Ethics Committee of the Animal

Research Center, Agricultural Research Department, Hokkaido Research Organization.

Detection of Boch5D2 in Serum of the Inoculated Cattle

To determine the kinetics of Boch5D2 in the serum of animal 15-6, anti-PD-1 antibody was detected by ELISA with BoPD-1-His protein. BoPD-1-His was diluted to 10 µg/ml in 0.05 M carbonate-bicarbonate buffer (Sigma-Aldrich, St. Louis, MO, USA) and coated onto Nunc MaxiSorp ELISA plates (Nunc, Roskilde, Denmark) at 4°C overnight. The plates were washed with Tris-buffered saline supplemented with 0.05% Tween20 (TBS-T) and incubated with TBS-T containing 1% skim milk at room temperature for 1 h. After washing with TBS-T, the serum samples of animal 15-6 were incubated in triplicate at room temperature for 1 h. The plates were washed again with TBS-T, and antibody binding to PD-1 was detected by HRP-conjugated anti-bovine IgG Fc rabbit polyclonal antibody (Rockland Immunochemicals) and TMB One Component Substrate (Bethyl Laboratories). The reported values are the means of triplicate samples.

Cell Proliferation Assay

To investigate the effect of PD-1 blockade on the BLV-specific T-cell response, cell proliferation assays were performed. Peripheral blood mononuclear cells (PBMCs) were purified from the blood samples by density gradient centrifugation on Percoll (GE Healthcare), washed three times with PBS, and suspended in PBS. Isolated PBMCs were then labeled with carboxyfluorescein diacetate succinimidyl ester (CFSE) (Sigma-Aldrich) and cultured in triplicate with 2% heat-inactivated culture supernatant of BLV-infected fetal lamb kidney (FLK) cells (41) or BLV gp51 peptide mix [0.1 and 1 µg/ml of each peptide (25)] for 6 days. The heat-inactivated culture supernatant of BLV-uninfected FLK cells was used as a negative control antigen. All cell cultures were grown in 96-well round-bottomed plates (BD Biosciences) containing 1×10^6 PBMCs in 250 µl RPMI 1640 medium (Sigma-Aldrich) supplemented with 10% heat-inactivated fetal bovine serum (Cansera International, Etobicoke, ON, Canada), 200 IU/ml of penicillin, 200 µg/ml of streptomycin, and 0.01% L-glutamine (Thermo Fisher Scientific) at 37°C with 5% CO₂. After 6 days, the PBMCs were harvested and incubated in PBS containing 10% goat serum (Sigma-Aldrich) at room temperature for 15 min to prevent non-specific reactions. The cells were then stained with anti-CD3-PE (MM1A; Washington State University Monoclonal Antibody Center, Pullman, WA, USA), anti-CD4-Alexa Fluor 647 (CC30; Bio-Rad), anti-CD8-PerCp/Cy5.5 (CC63, Bio-Rad), anti-TCR1-N24-APC/Cy7 (anti-TCR δ chain; GB21A; Washington State University Monoclonal Antibody Center), and anti-IgM-PE/Cy7 antibodies (IL-A30; Bio-Rad) at 4°C for 30 min. MM1A and CC30 were pre-labeled with R-PE and Alexa Fluor 647 with Zenon Mouse IgG₁ Labeling Kits (Thermo Fisher Scientific). CC63, GB21A, and IL-A30 were conjugated with PerCp/Cy5.5, APC/Cy7, and PE/Cy7, respectively, with Lightning-Link Conjugation Kits (Innova Biosciences, Cambridge, England, UK). The cells were then washed with PBS containing 1% bovine serum albumin (Sigma-Aldrich) and analyzed immediately by FACS Verse (BD Biosciences) and FCS Express 4 (De Novo Software).

Quantification of BLV Proviral Load

To determine proviral loads in the Boch5D2-inoculated animal, BLV *tax* gene was measured by quantitative real-time PCR. Briefly, genomic DNA was extracted from 2×10^6 PBMCs with a Wizard Genomic DNA Purification Kit (Promega). Amplification of the BLV *tax* gene was performed in a reaction mixture containing 5 µl of Cycleave PCR Reaction Mix (Takara Bio, Otsu, Japan), 0.5 µl of Probe/Primer Mix for BLV (Takara Bio), 1 µl of a DNA template, and 3.5 µl of RNase-Free Distilled Water (Takara Bio) with a LightCycler 480 system II (Roche Diagnostics, Mannheim, Germany). Serial dilution of BLV Positive Control (Takara Bio) was used to generate calibration curves to determine the copy number of the BLV *tax* gene. Each DNA sample was tested in triplicate, and the reported values are the mean numbers of copies per 50 ng of DNA. The concentration of DNA was measured by UV absorbance at 260 nm with a NanoDrop 8000 Spectrophotometer (Thermo Fisher Scientific).

Statistical Analysis

Significant differences were identified by Welch's *t*-test and repeated one-way analysis of variance, followed by Dunnett's test. All statistical tests were performed with GraphPad Prism 6 (GraphPad Software, San Diego, CA, USA). Differences were considered statistically significant when *P* < 0.05.

RESULTS

Treatment of Anti-PD-1 Rat mAb in BLV-Infected Cattle

To evaluate the therapeutic effects of PD-1 blockade *in vivo*, a BLV-infected cow was inoculated with anti-PD-1 rat mAb (5D2). The serum concentration of the inoculated 5D2 was high during the first week postinoculation and decreased from 11 days postinoculation (dpi) (Figure S1 in Supplementary Material). At 18 dpi, 5D2 was not detected in the serum (Figure S1 in Supplementary Material). Before inoculation, *ex vivo* culture of PBMCs resulted in low or no production of interferon-γ (IFN-γ) in response to BLV gp51 peptides (Figure S2A in Supplementary Material), indicating the functional exhaustion of gp51-specific T cells in this animal. After inoculation, however, gp51-specific IFN-γ production was slightly activated until 25 dpi (Figure S2A in Supplementary Material), suggesting that PD-1 blockade partially restores the effector function of BLV-specific T cells *in vivo*. Despite enhancement of the BLV-specific T-cell response, the proviral load of BLV did not change in the animal throughout the experiment (Figure S2B in Supplementary Material).

Establishment of the Anti-Bovine PD-1 Rat-Bovine chAb, Boch5D2

We hypothesized that treatment with anti-PD-1 rat mAb 5D2 could not induce antiviral effects because 5D2 was rapidly eliminated as a heterologous protein in cattle. To obtain a blocking antibody that was more stable *in vivo*, 5D2 was then engineered into an anti-bovine PD-1 rat-bovine chimeric monoclonal antibody, Boch5D2 (Figure 1B). Additionally, Boch5D2 is

desired to induce no Fc-mediated effector functions, such as antibody-dependent cell-mediated cytotoxicity (ADCC). Thus, we introduced amino acid mutations into possible binding sites for Fc γ Rs of a CH2 domain of bovine IgG₁ (Figure S3A in Supplementary Material) according to the confirmed mutations on human IgG₁ (34, 35). Homology modeling predicted the structure of the constant region of bovine IgG₁ and revealed that the target residues for mutation were located in the upper CH2 domain near the hinge region (Figure S3B in Supplementary Material). These residues were estimated to form the binding sites for Fc γ Rs like human IgG₁ (37). We then developed Boch5D2 IgG₁ variants with wild type (IgG₁ WT) and mutated constant regions (IgG₁ ADCC $-$) in Expi293 Expression System (Figure S4A in Supplementary Material). Soluble bovine Fc γ R proteins were also prepared in Expi293 Expression System (Figure S4B in Supplementary Material) and tested for the bindings of Boch5D2 IgG₁ WT and ADCC $-$ (Figure S5 in Supplementary Material). Boch5D2 IgG₁ WT bound strongly to bovine Fc γ RI, weakly to bovine Fc γ RII, but not to bovine Fc γ RIII and Fc γ 2R (Figure S5 in Supplementary Material). The mutations introduced into the CH2 domain of Boch5D2 IgG₁ ADCC $-$ were effective to diminish the interactions with bovine Fc γ RI and Fc γ RII (Figures S5A,B in Supplementary Material). Thus, Boch5D2 IgG₁ ADCC $-$ is expected to induce no effector functions *via* Fc γ Rs and is a suitable form as a blocking antibody targeting PD-1.

Establishment of Stable High-Producer Cell Lines Expressing Boch5D2

To obtain large amount of Boch5D2 (IgG₁ ADCC $-$) for further characterization *in vitro* and *in vivo*, Boch5D2 (IgG₁ ADCC $-$) was stably expressed and produced with the use of the CHO DG44 cell expression system. The highest-producing cell line

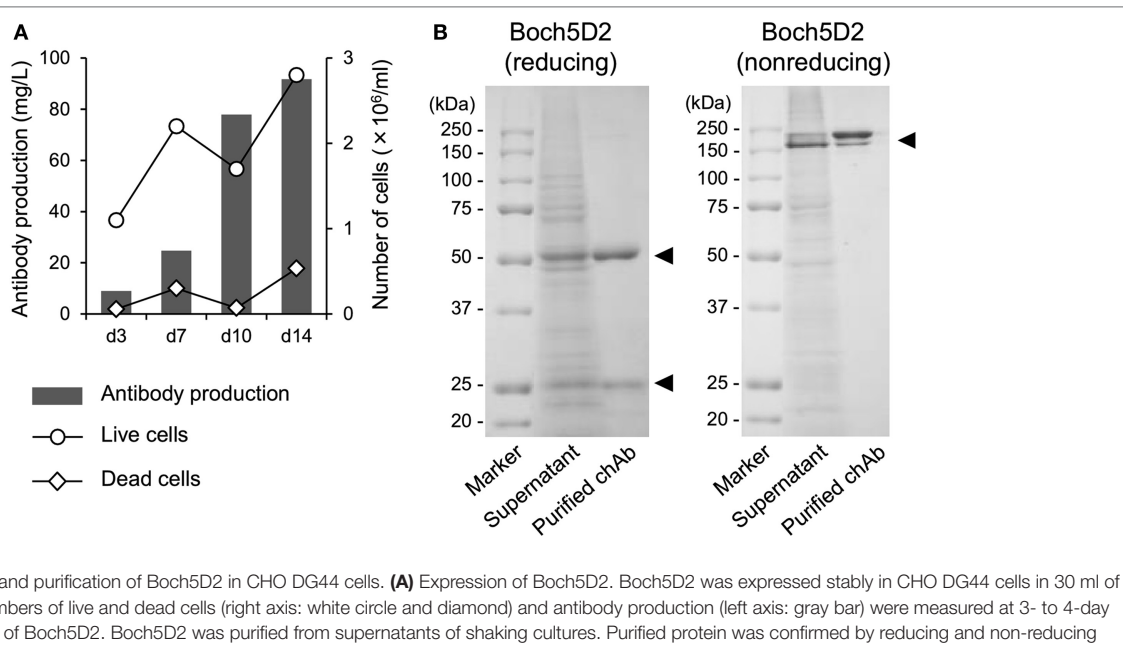
in CHO DG44 cells stably produced 91.7 mg/l of Boch5D2 after 14 days of shaking culture (Figure 2A). Boch5D2 was successfully purified from supernatants with the use of Protein A resin (Figure 2B). As expected, the heavy and light chains of Boch5D2 were detected at approximately 50 and 25 kDa, respectively (Figure 2B). Thus, Boch5D2 has been successfully established and produced with the use of mammalian expression system.

Reactivities of Boch5D2 to Membrane-Bound Bovine PD-1

The binding ability of anti-PD-1 chAb was determined by flow cytometric analysis with membrane-bound PD-1-expressing cells. Flow cytometric analysis showed that Boch5D2 bound to more than 95% of PD-1-expressing cells at 1–100 µg/ml and to 62% at 0.1 µg/ml (Figure 3), representing a binding ability similar to that of 5D2. The Boch5D2 produced in this study is capable of detecting its target with reactivity similar to that of the original rat mAb.

Binding Affinity of Boch5D2 to Bovine PD-1 Protein

To confirm the binding affinity of Boch5D2 to PD-1 protein, BoPD-1-His was prepared in Expi293 Expression System (Figure S6 in Supplementary Material), and SPR analysis was performed with the use of a Biacore instrument. 5D2 and Boch5D2 bound to BoPD-1-His protein successfully. As shown in Table 2, 5D2 and Boch5D2 showed significantly similar affinities for PD-1, with K_D values of 0.12 ± 0.04 and 0.10 ± 0.06 nM, respectively. Therefore, the chimerization of anti-PD-1 antibody does not change its binding affinity to bovine PD-1 protein.



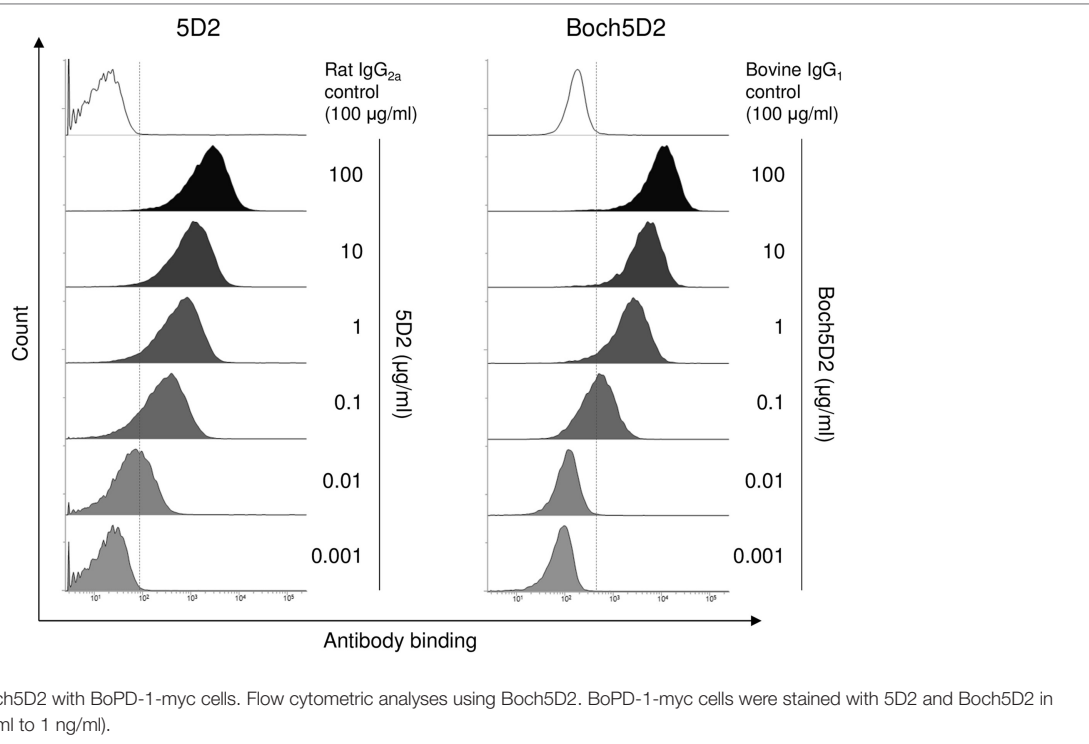


FIGURE 3 | Reactivity of Boch5D2 with BoPD-1-myc cells. Flow cytometric analyses using Boch5D2. BoPD-1-myc cells were stained with 5D2 and Boch5D2 in serial dilutions (from 100 µg/ml to 1 ng/ml).

TABLE 2 | Binding affinity of 5D2 and Boch5D2 to BoPD-1-His protein.

Antibody	k_a (1/Ms)	k_d (1/s)	K_D (M) ^a
5D2	$1.84 \times 10^4 \pm 0.27$	$2.15 \times 10^{-4} \pm 0.44$	$1.22 \times 10^{-8} \pm 0.39$
Boch5D2	$2.07 \times 10^4 \pm 0.06$	$2.16 \times 10^{-4} \pm 1.12$	$1.05 \times 10^{-8} \pm 0.58$

^aThe K_D values of 5D2 and Boch5D2 are not significantly different ($P > 0.05$).

Blockade of PD-1/PD-L1 Binding by Boch5D2

To analyze the blocking activity of Boch5D2, the inhibitory efficacy of chAb in PD-1-Ig binding to PD-L1-expressing cells was evaluated in cell-based experiments using flow cytometry. Preincubation of PD-1-Ig with either 5D2 or Boch5D2 inhibited PD-1/PD-L1 binding in a dose-dependent manner (Figure 4). In preincubations using 50 µg/ml of the antibodies, such as Boch5D2 and 5D2, inhibited 42.4 and 35.2% of PD-1/PD-L1 binding, respectively (Figure 4). Thus, the blocking activity of Boch5D2 is similar to that of the original rat mAb 5D2.

Reactivation of T-Cell Functions by Treatment with Boch5D2 in BLV-Infected Cattle

To evaluate the therapeutic effects of Boch5D2 *in vivo*, a BLV-infected calf was inoculated with anti-PD-1 chAb (Boch5D2). The serum concentration of the inoculated Boch5D2 was relatively high during the first week postinoculation (Figure 5), showing a trend similar to that in a 5D2-inoculated animal (Figure S1 in Supplementary Material). Unlike the concentration of inoculated 5D2, the concentration of Boch5D2 decreased slowly, and it was

still detectable in the serum at 70 dpi when this animal experiment was terminated (Figure 5). The BLV-specific proliferation of PBMCs was analyzed at 1- or 2-day intervals during the first week after inoculation. Activation of CD4⁺ T-cell proliferation stimulated by FLK-BLV antigen was significantly higher from 1 dpi than at 0 dpi (Figure 6A). In contrast, CD8⁺ T-cell proliferation was activated in response not only to FLK-BLV antigen but also to controls (FLK control antigen and medium) after Boch5D2 inoculation (Figure 6A). Furthermore, a proliferation assay with BLV gp51 peptides showed that CD4⁺ T-cell proliferation in response to the peptide antigens was significantly enhanced after inoculation, but that of CD8⁺ T cells was not (Figure 6B). Surprisingly, the enhanced proliferation of BLV-specific CD4⁺ T cells was not impaired at 70 dpi (Figures 6A,B). A single treatment with Boch5D2 activated the effector function of T cells, including BLV-specific CD4⁺ T cells, in a BLV-infected animal in the long term.

Reduction of Proviral Load by the Treatment with Boch5D2 in BLV-Infected Cattle

In this tested animal, the BLV proviral load in PBMCs was 15.4 copies/50 ng DNA before inoculation (at 0 dpi) (Figure 7). This animal remained in the aleukemic stage of BLV infection throughout the experimental period, such that the proviral load was low but detectable. After inoculation with Boch5D2, the proviral load decreased significantly after 1 dpi (5.0 copies/50 ng DNA) (Figure 7), consistent with the enhancement of the BLV-specific T-cell response (Figure 6). The proviral load did not increase after 3 dpi; at 70 dpi, it was 1.4 copies/50 ng DNA, which was 10.7-fold

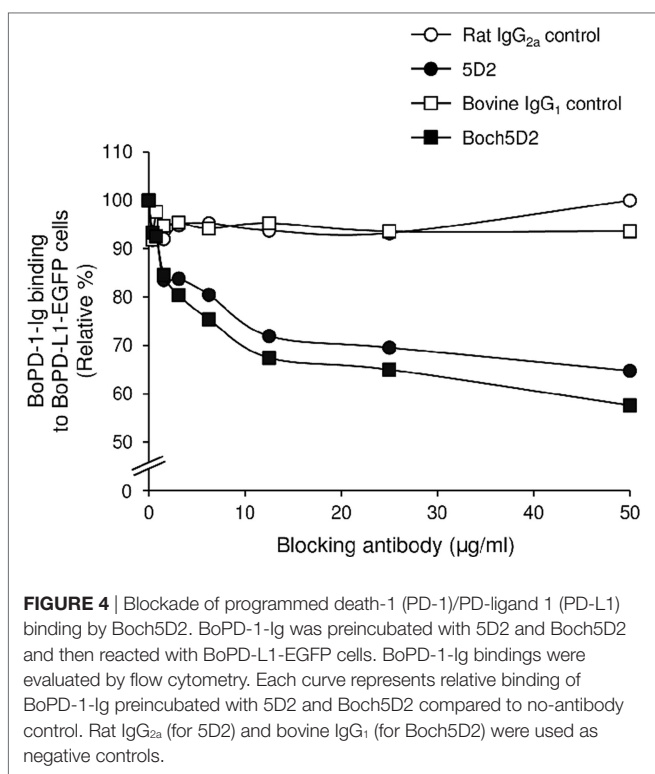


FIGURE 4 | Blockade of programmed death-1 (PD-1)/PD-ligand 1 (PD-L1) binding by Boch5D2. BoPD-1-Ig was preincubated with 5D2 and Boch5D2 and then reacted with BoPD-L1-EGFP cells. BoPD-1-Ig bindings were evaluated by flow cytometry. Each curve represents relative binding of BoPD-1-Ig preincubated with 5D2 and Boch5D2 compared to no-antibody control. Rat IgG_{2a} (for 5D2) and bovine IgG₁ (for Boch5D2) were used as negative controls.

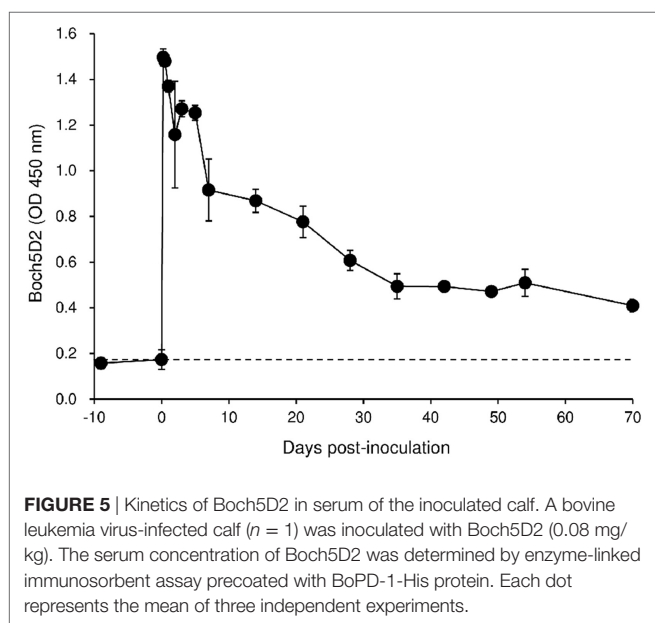


FIGURE 5 | Kinetics of Boch5D2 in serum of the inoculated calf. A bovine leukemia virus-infected calf ($n = 1$) was inoculated with Boch5D2 (0.08 mg/kg). The serum concentration of Boch5D2 was determined by enzyme-linked immunosorbent assay precoated with BoPD-1-His protein. Each dot represents the mean of three independent experiments.

lower than at 0 dpi (Figure 7). Consequently, *in vivo* blockade of PD-1/PD-L1 resulted in a prolonged decrease in BLV-infected lymphocytes in the BLV-infected animal.

DISCUSSION

In this study, anti-bovine PD-1 chAb Boch5D2 was established in mammalian expression systems and exhibited equivalent *in vitro*

activities to the original mAb 5D2 in terms of the binding affinity to bovine PD-1 protein and the blocking activity on bovine PD-1/PD-L1 interaction. Furthermore, the bovinized chimerization of anti-PD-1 mAb improved its *in vivo* stability presumably due to reduced immune response against constant regions of the inoculated antibodies, which is a strong advantage of this strategy. The chimerization technology will be useful to the development of therapeutic antibodies as well as cell type-specific antibodies for *in vivo* depletion experiments.

We administered Boch5D2 to a small calf (173 kg) at a low dose (0.08 mg/kg) as a pilot trial, but administration of the chAb to adult cattle at higher dose requires gram-scale quantities of the chAb. For example, 0.5 g of chAb is required for administration to a 500-kg adult cow at a dose of 1 mg/kg. The current capacity of chAb production in CHO DG44 cell lines is still poor (about 0.1 g/l) and could be improved by further gene amplification using methotrexate at higher concentrations. In addition, large-scale culture using larger culture flasks and bioreactors is helpful for producing large amounts of chAbs (42). In recent studies, higher peak cell concentrations and product titers of up to 5 g/l have been routinely achieved in CHO DG44 cells, as production processes have steadily improved through advances in optimization of selection processes, basal media, and feed supplements (42–44). Thus, optimization of basal media and feed supplements will be among the next strategies for improving the established high-producing cell lines.

Although binding specificity and affinity to antigen are central for functional activity of antibody drug, the adequate choice of the constant region of the heavy chain is also essential to obtain expected effects of antibody treatment. IgG subclass inducing no Fc-mediated effector functions, such as ADCC, complement-dependent cytotoxicity (CDC), and antibody-dependent cell-mediated phagocytosis (ADCP), is considered to be suitable for the blocking antibody targeting PD-1 in human medicine (45, 46). Anti-human PD-1 antibodies launched for cancer therapy (nivolumab and pembrolizumab) are composed of human IgG₄ heavy chain (46), which does not trigger ADCC and CDC functions via its Fc region (45).

Three IgG subclasses, IgG₁, IgG₂, and IgG₃, have been described in cattle (47–49), and cattle do not produce functional IgG₄ because bovine *IGHC4* gene encoding bovine IgG₄ heavy chain exists as a pseudogene on the genome (50). In earlier studies, bovine IgG₁ and IgG₂ are clarified to mediate ADCC and ADCP (51, 52). Bovine IgG₃ is characterized by a longer hinge sequence, which is presumably effective in the cross-linking with Fc_YRs and complement, and triggers active Fc-mediated effector functions like human IgG₃ (45, 49). Thus, intact constant regions of bovine IgG subclasses may not be applied for effective blocking antibody. This study indicates that Boch5D2 IgG₁ ADCC—does not interact with Fc_YRI and Fc_YRII, but Boch5D2 IgG₁ WT does. The mutated bovine IgG₁ may not trigger ADCC and ADCP and is a suitable form for blocking antibody. Further studies are needed to investigate ADCC, ADCP, and CDC functions of the Boch5D2 IgG₁ variants and confirm the efficacy of the amino acid mutations in detail.

In the calf-administered Boch5D2, PD-1 blockade remarkably activated BLV-specific CD4⁺ T-cell proliferation. In contrast, the

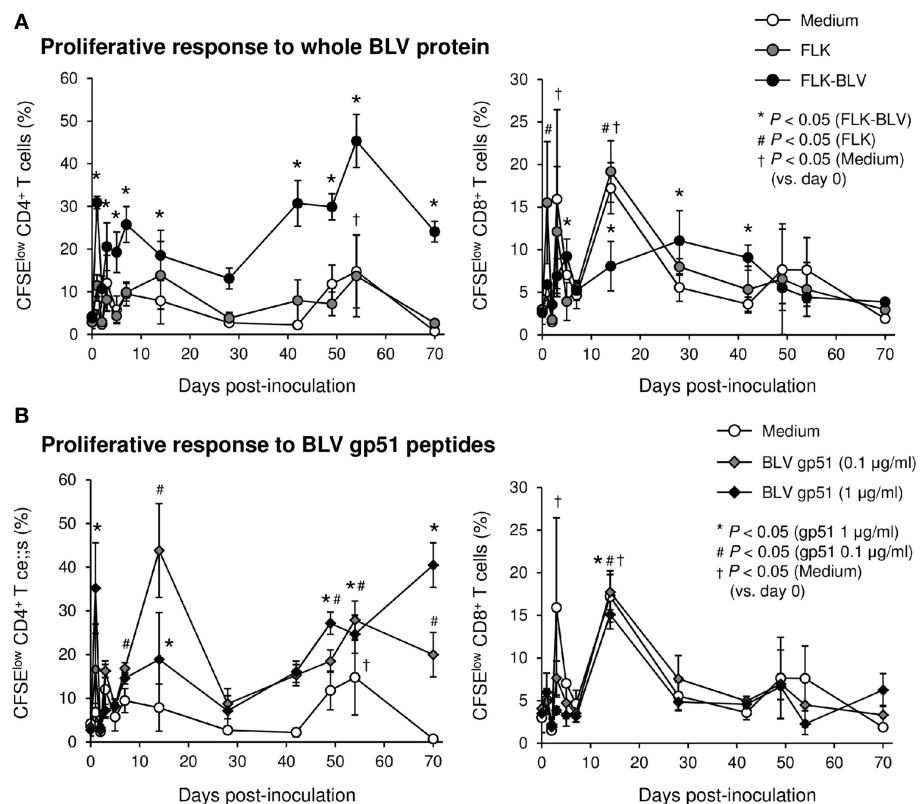


FIGURE 6 | Effect on proliferation of bovine leukemia virus (BLV)-specific T cells of the administration of Boch5D2. T-cell proliferation specific for BLV antigen stimulation. Carboxyfluorescein diacetate succinimidyl ester (CFSE)-labeled peripheral blood mononuclear cells were cultured in triplicate with fetal lamb kidney (FLK)-BLV antigen, control FLK antigen (**A**), or gp51 peptides (0.1 and 1 µg/ml) (**B**) for 6 days. The percentage of CFSE^{low} cells in CD4⁺ and CD8⁺γδTCR⁻ T cells was measured by flow cytometry. CFSE^{low} cells represent cells proliferated during cultivation. Each dot represents the mean of three independent experiments. Significant differences were determined by Dunnett's multiple-comparison test across the time points. *#†P < 0.05 versus 0 dpi in each stimulation.

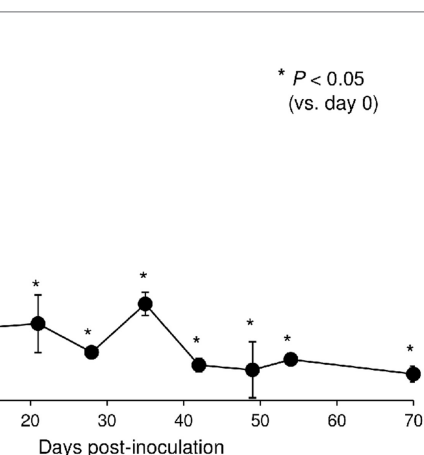


FIGURE 7 | Effect on proviral loads of bovine leukemia virus (BLV) in a calf-administered Boch5D2. Provirus copy number per 50 ng DNA of peripheral blood mononuclear cells (PBMCs) from an inoculated calf. Proviral loads of BLV were quantified in PBMCs at each time point by real-time genomic polymerase chain reaction targeting the BLV tax gene. Each dot represents the mean of three independent experiments. Significant differences were determined by Dunnett's multiple-comparison test across the time points. *P < 0.05 versus 0 dpi.

proliferation of BLV-specific CD8⁺ T-cells was limited before and after the inoculation. This result is consistent with the previous observation that CD4⁺ T cells express more PD-1 than do CD8⁺ T cells in BLV-infected cattle (25). Certainly, most of the PD-1⁺ cells were found among CD4⁺ T cells, with PD-1⁺CD8⁺ T cells representing a minority of the PD-1⁺ cells in this animal before Boch5D2 inoculation (data not shown). In addition, exogenous antigen is mainly recognized by CD4⁺ T cells *via* the MHC II pathways in proliferation assays. CD8⁺ T cells are also stimulated by exogenous antigens by cross-presentation *via* MHC I, but this stimulation is usually insufficient. Thus, BLV antigen-bearing antigen-presenting cells are required for detecting BLV-specific CD8⁺ T-cell responses in the assays. Most importantly, Boch5D2 treatment significantly decreased the BLV proviral load in the calf. This effect was presumably caused by the activation of BLV-specific CD4⁺ T cells. These data suggest that Boch5D2 may prevent disease progression in BLV infection through reduction of the viral load.

A hypothesis arises from the administration of anti-PD-1 rat mAb 5D2. In the BLV-infected cow inoculated with 5D2, PD-1 blockade unexpectedly restored the IFN-γ response specific for BLV gp51 antigens up to 25 dpi. Nevertheless, the BLV proviral load was not decreased in this animal. These results indicate that not only IFN-γ response but also other T-cell functions, such as

proliferative activity, cytotoxic activity, and production of other T-cell cytokines (such as tumor necrosis factor- α and interleukin-2) and effector molecules (such as perforin and granzyme) may be involved in the control of BLV-infected cells *in vivo*.

The PD-1/PD-L1 pathway is expected to be a potential target for reinvigorating the function of exhausted T cells. A number of researchers and pharmaceutical companies have investigated antibody treatments that block the PD-1/PD-L1 pathway in humans, and anti-PD-1 and anti-PD-L1 antibodies have been approved for various human cancers or evaluated in clinical trials (7–11, 46). In the field of veterinary medicine, the PD-1/PD-L1 pathway has also attracted much attention for its potential as a novel target for cancer immunotherapy in companion animals (53–55). We recently established anti-bovine PD-L1 rat-bovine chAb as another candidate agent for blocking the PD-1/PD-L1 pathway (56). Administration of anti-PD-L1 chAb to a BLV-infected calf enhanced BLV-specific CD4 $^{+}$ T-cell proliferation and reduced BLV proviral load *in vivo*, which is consistent with the results in the current study. Thus, targeting the PD-1/PD-L1 pathway is a significant strategy for the regulation of T-cell response to pathogens in cattle.

The current work is a pilot study with a primary aim to determine the effects of Boch5D2 treatment. Although Boch5D2 treatment induced the immunomodulatory and antiviral effects in the initial trial, this result requires confirmation in a clinical trial with a large number of BLV-infected cattle from different herds or farms. Furthermore, we have revealed that T-cell exhaustion mediated by PD-1/PD-L1 presumably facilitates persistent infection and disease progression in BLV infection as well as bovine paratuberculosis, anaplasmosis, and mycoplasmosis (25–29). Clinical trials in cattle with paratuberculosis and anaplasmosis would determine whether Boch5D2 can be applied for a broad-spectrum immunotherapy against chronic infections of cattle. Additionally, expression and functional analyses are required in other infectious diseases of cattle, such as tuberculosis, chronic mastitis, theileriosis, and babesiosis, to expand the potential applications targeting the PD-1/PD-L1 pathway.

ETHICS STATEMENT

This study was carried out in accordance with the recommendations of Guide for the Care and Use of Agricultural Animals in Research and Teaching, Federation of Animal Science Societies. The protocol was approved by the Ethics Committee of the Animal Research Center, Agricultural Research Department, Hokkaido Research Organization (Shintoku, Hokkaido, Japan) and by the

Ethics Committee of Graduate School of Veterinary Medicine, Hokkaido University (Sapporo, Hokkaido, Japan).

AUTHOR CONTRIBUTIONS

SK, YS, SM, and KO were responsible for the conception and design of the study. TO, SK, AN, NM, RI, SG, JK, and SO performed the experiments. TO, SK, CN, JK, YK, YS, SM, and KO analyzed the data. CN, JK, SO, YK, and YS provided intellectual input, laboratory materials, reagents, and/or analytic tools. TO wrote the manuscript. SK, YK, YS, SM, and KO contributed to the revision of the manuscript. All the authors reviewed and approved the final manuscript.

ACKNOWLEDGMENTS

The authors are grateful to Dr. Hideyuki Takahashi, Dr. Yasuyuki Mori, and Dr. Tomio Ibayashi for their valuable advice and discussions, and Susumu Ogawa and the staffs of the Animal Research Center, Agricultural Research Department, Hokkaido Research Organization for the excellent care and handling of animals. We thank Enago (<http://www.enago.jp>) for the English language review.

FUNDING

This work was supported by grants from the Science and Technology Research Promotion Program for Agriculture, Forestry, Fisheries, and Food Industry, Japan (number 26058B to SK), the NARO, Bio-oriented Technology Research Advancement Institution (the special scheme project on regional developing strategy; grant 16817557 to SK), and grants-in-aid for Scientific Research and for Japan Society for the Promotion of Science (JSPS) Fellows from JSPS. This research was partially supported by the Platform for Drug Discovery, Informatics, and Structural Life Science (proposal number 2142) from the Japan Agency for Medical Research and Development, AMED. The funders had no role in study design, data collection and interpretation, or the decision to submit the work for publication.

SUPPLEMENTARY MATERIAL

The Supplementary Material for this article can be found online at <http://journal.frontiersin.org/article/10.3389/fimmu.2017.00650/full#supplementary-material>.

REFERENCES

1. Wherry EJ. T cell exhaustion. *Nat Immunol* (2011) 12:492–9. doi:10.1038/ni.2035
2. Wherry EJ, Kurachi M. Molecular and cellular insights into T cell exhaustion. *Nat Rev Immunol* (2015) 15:486–99. doi:10.1038/nri3862
3. Kahan SM, Wherry EJ, Zajac AJ. T cell exhaustion during persistent viral infections. *Virology* (2015) 479–480:180–93. doi:10.1016/j.virol.2014.12.033
4. Ha S-J, Mueller SN, Wherry EJ, Barber DL, Aubert RD, Sharpe AH, et al. Enhancing therapeutic vaccination by blocking PD-1-mediated inhibitory signals during chronic infection. *J Exp Med* (2008) 205:543–55. doi:10.1084/jem.20071949
5. Velu V, Titanji K, Zhu B, Husain S, Pladevuga A, Lai L, et al. Enhancing SIV-specific immunity *in vivo* by PD-1 blockade. *Nature* (2009) 458:206–10. doi:10.1038/nature07662
6. Shetty RD, Velu V, Titanji K, Bosinger SE, Freeman GJ, Silvestri G, et al. PD-1 blockade during chronic SIV infection reduces hyperimmune activation and

- microbial translocation in rhesus macaques. *J Clin Invest* (2012) 122:1712–6. doi:10.1172/JCI60612DS1
7. Mahoney KM, Freeman GJ, McDermott DF. The next immune-checkpoint inhibitors: PD-1/PD-L1 blockade in melanoma. *Clin Ther* (2015) 37:764–82. doi:10.1016/j.clinthera.2015.02.018
 8. Bagley SJ, Baum JM, Langer CJ. PD-1/PD-L1 immune checkpoint blockade in non-small cell lung cancer. *Clin Adv Hematol Oncol* (2015) 13:676–83.
 9. Massari F, Santoni M, Ciccarese C, Santini D, Alfieri S, Martignoni G, et al. PD-1 blockade therapy in renal cell carcinoma: current studies and future promises. *Cancer Treat Rev* (2015) 41:114–21. doi:10.1016/j.ctrv.2014.12.013
 10. Ok CY, Young KH. Targeting the programmed death-1 pathway in lymphoid neoplasms. *Cancer Treat Rev* (2017) 54:99–109. doi:10.1016/j.ctrv.2017.01.009
 11. Porichis F, Kaufmann DE. Role of PD-1 in HIV pathogenesis and as target for therapy. *Curr HIV/AIDS Rep* (2012) 9:81–90. doi:10.1007/s11904-011-0106-4
 12. Quan L, Chen X, Liu A, Zhang Y, Guo X, Yan S, et al. PD-1 blockade can restore functions of T-cells in Epstein-Barr virus-positive diffuse large B-cell lymphoma *in vitro*. *PLoS One* (2015) 10:e0136476. doi:10.1371/journal.pone.0136476
 13. Ye B, Liu X, Li X, Kong H, Tian L, Chen Y. T-cell exhaustion in chronic hepatitis B infection: current knowledge and clinical significance. *Cell Death Dis* (2015) 6:e1694. doi:10.1038/cddis.2015.42
 14. Urbani S, Amadei B, Tola D, Pedraza G, Sacchelli L, Cavallo MC, et al. Restoration of HCV-specific T cell functions by PD-1/PD-L1 blockade in HCV infection: effect of viremia levels and antiviral treatment. *J Hepatol* (2008) 48:548–58. doi:10.1016/j.jhep.2007.12.014
 15. Singh A, Mohan A, Dey AB, Mitra DK. Inhibiting the programmed death 1 pathway rescues *Mycobacterium tuberculosis*-specific interferon γ -producing T cells from apoptosis in patients with pulmonary tuberculosis. *J Infect Dis* (2013) 208:603–15. doi:10.1093/infdis/jit206
 16. Kabeya H, Ohashi K, Onuma M. Host immune responses in the course of bovine leukemia virus infection. *J Vet Med Sci* (2001) 63:703. doi:10.1292/jvms.63.703
 17. Frie MC, Coussens PM. Bovine leukemia virus: a major silent threat to proper immune responses in cattle. *Vet Immunol Immunopathol* (2015) 163:103–14. doi:10.1016/j.vetimm.2014.11.014
 18. Ohira K, Nakahara A, Konnai S, Okagawa T, Nishimori A, Maekawa N, et al. Bovine leukemia virus reduces anti-viral cytokine activities and NK cytotoxicity by inducing TGF- β secretion from regulatory T cells. *Immun Inflamm Dis* (2016) 4:52–63. doi:10.1002/iid3.93
 19. Orlik O, Splitter GA. Progression to persistent lymphocytosis and tumor development in bovine leukemia virus (BLV)-infected cattle correlates with impaired proliferation of CD4 $^{+}$ T cells in response to gag- and env-encoded BLV proteins. *J Virol* (1996) 70:7584–93.
 20. Lundberg P, Splitter GA. $\gamma\delta^{+}$ T-lymphocyte cytotoxicity against envelope-expressing target cells is unique to the alymphocytic state of bovine leukemia virus infection in the natural host. *J Virol* (2000) 74:8299–306. doi:10.1128/JVI.74.18.8299-8306.2000
 21. Stabel JR. Host responses to *Mycobacterium avium* subsp. *paratuberculosis*: a complex arsenal. *Anim Health Res Rev* (2006) 7:61–70. doi:10.1017/S146625307001168
 22. Sohal JS, Singh SV, Tyagi P, Subhodh S, Singh PK, Singh AV, et al. Immunology of mycobacterial infections: with special reference to *Mycobacterium avium* subspecies *paratuberculosis*. *Immunobiology* (2008) 213:585–98. doi:10.1016/j.imbio.2007.11.002
 23. Brown WC. Adaptive immunity to *Anaplasma* pathogens and immune dysregulation: implications for bacterial persistence. *Comp Immunol Microbiol Infect Dis* (2012) 35:241–52. doi:10.1016/j.cimid.2011.12.002
 24. Welsh MD, Cunningham RT, Corbett DM, Girvin RM, McNair J, Skuce RA, et al. Influence of pathological progression on the balance between cellular and humoral immune responses in bovine tuberculosis. *Immunology* (2005) 114:101–11. doi:10.1111/j.1365-2567.2004.02003.x
 25. Ikebuchi R, Konnai S, Okagawa T, Yokoyama K, Nakajima C, Suzuki Y, et al. Blockade of bovine PD-1 increases T cell function and inhibits bovine leukemia virus expression in B cells *in vitro*. *Vet Res* (2013) 44:59. doi:10.1186/1297-9716-44-59
 26. Ikebuchi R, Konnai S, Shirai T, Sunden Y, Murata S, Onuma M, et al. Increase of cells expressing PD-L1 in bovine leukemia virus infection and enhancement of anti-viral immune responses *in vitro* via PD-L1 blockade. *Vet Res* (2011) 42:103. doi:10.1186/1297-9716-42-103
 27. Okagawa T, Konnai S, Nishimori A, Ikebuchi R, Mizorogi S, Nagata R, et al. Bovine immunoinhibitory receptors contribute to the suppression of *Mycobacterium avium* subsp. *paratuberculosis*-specific T-cell responses. *Infect Immun* (2016) 84:77–89. doi:10.1128/IAI.01014-15
 28. Okagawa T, Konnai S, Deringer JR, Ueti MW, Scoles GA, Murata S, et al. Cooperation of PD-1 and LAG-3 contributes to T-cell exhaustion in *Anaplasma marginale*-infected cattle. *Infect Immun* (2016) 84:2779–90. doi:10.1128/IAI.00278-16
 29. Goto S, Konnai S, Okagawa T, Nishimori A, Maekawa N, Gondaira S, et al. Increase of cells expressing PD-1 and PD-L1 and enhancement of IFN- γ production via PD-1/PD-L1 blockade in bovine mycoplasmosis. *Immun Inflamm Dis* (Forthcoming).
 30. Howard CJ, Sopp P, Parsons KR, Finch J. *In vivo* depletion of BoT4 (CD4) and of non-T4/T8 lymphocyte subsets in cattle with monoclonal antibodies. *Eur J Immunol* (1989) 19:757–64. doi:10.1002/eji.1830190428
 31. Bruce CJ, Howard CJ, Thomas LH, Tempest PR, Taylor G. Depletion of bovine CD8 $^{+}$ T cells with chCC63, a chimaeric mouse-bovine antibody. *Vet Immunol Immunopathol* (1999) 71:215–31. doi:10.1016/S0165-2427(99)00098-7
 32. Valdez RA, McGuire TC, Brown WC, Davis WC, Knowles DP. Long-term *in vivo* depletion of functional CD4 $^{+}$ T lymphocytes from calves requires both thymectomy and anti-CD4 monoclonal antibody treatment. *Immunology* (2001) 102:426–33. doi:10.1046/j.1365-2567.2001.01211.x
 33. Brüggemann M, Winter G, Waldmann H, Neuberger MS. The immunogenicity of chimeric antibodies. *J Exp Med* (1989) 170:2153–7. doi:10.1084/jem.170.6.2153
 34. Chames P, Van Regenmortel M, Weiss E, Baty D. Therapeutic antibodies: successes, limitations and hopes for the future. *Br J Pharmacol* (2009) 157:220–33. doi:10.1111/j.1476-5381.2009.00190.x
 35. Kontermann R, Dübel S. *Antibody Engineering*. 2nd ed. (Vol. 1). Berlin: Springer (2010). 17 p.
 36. Armour KL, Clark MR, Hadley AG, Williamson LM. Recombinant human IgG molecules lacking Fcγ receptor I binding and monocyte triggering activities. *Eur J Immunol* (1999) 29:2613–24. doi:10.1002/(SICI)1521-4141(199908)29:08<2613::AID-IMMU2613>3.0.CO;2-J
 37. Shields RL, Namenuk AK, Hong K, Meng YG, Rae J, Briggs J, et al. High resolution mapping of the binding site on human IgG₁ for Fc γ RI, Fc γ RII, Fc γ RIII, and FcR η and design of IgG₁ variants with improved binding to the Fc γ R. *J Biol Chem* (2001) 276:6591–604. doi:10.1074/jbc.M009483200
 38. Ikebuchi R, Konnai S, Okagawa T, Yokoyama K, Nakajima C, Suzuki Y, et al. Influence of PD-L1 cross-linking on cell death in PD-L1-expressing cell lines and bovine lymphocytes. *Immunology* (2014) 142:551–61. doi:10.1111/imm.12243
 39. Marzi A, Yoshida R, Miyamoto H, Ishijima M, Suzuki Y, Higuchi M, et al. Protective efficacy of neutralizing monoclonal antibodies in a nonhuman primate model of Ebola hemorrhagic fever. *PLoS One* (2012) 7:e36192. doi:10.1371/journal.pone.0036192
 40. Niwa H, Yamamura K, Miyazaki J. Efficient selection for high-expression transfectants with a novel eukaryotic vector. *Gene* (1991) 108:193–9. doi:10.1016/0378-1119(91)90434-D
 41. Mager A, Masengo R, Mammerickx M, Letesson JJ. T cell proliferative response to bovine leukaemia virus (BLV): identification of T cell epitopes on the major core protein (p24) in BLV-infected cattle with normal haematological values. *J Gen Virol* (1994) 75:2223–31. doi:10.1099/0022-1317-75-9-2223
 42. Yu M, Hu Z, Pacis E, Vijayasanakaran N, Shen A, Li F. Understanding the intracellular effect of enhanced nutrient feeding toward high titer antibody production process. *Biotechnol Bioeng* (2011) 108:1078–88. doi:10.1002/bit.23031
 43. Jayapal KP, Wlaschin KF, Hu W-S, Yap MGS. Recombinant protein therapeutics from CHO cells-20 years and counting. *Chem Eng Prog* (2007) 103:40–7.
 44. Reinhart D, Kaisermayer C, Damjanovic L, Kunert R. Benchmarking of commercially available CHO cell culture media for antibody production. *Appl Microbiol Biotechnol* (2015) 99:4645–57. doi:10.1186/1753-6561-7-S6-P13
 45. Vidarsson G, Dekkers G, Rispens T. IgG subclasses and allotypes: from structure to effector functions. *Front Immunol* (2014) 5:520. doi:10.3389/fimmu.2014.00520
 46. Lipson EJ, Forde PM, Hammers HJ, Emens LA, Taube JM, Topalian SL. Antagonists of PD-1 and PD-L1 in cancer treatment. *Semin Oncol* (2015) 42:587–600. doi:10.1053/j.seminoncol.2015.05.013

47. Butler JE. Bovine immunoglobulins: an augmented review. *Vet Immunol Immunopathol* (1983) 4:43–152. doi:10.1016/0165-2427(83)90056-9
48. Kacskovics I, Butler JE. The heterogeneity of bovine IgG2–VIII. The complete cDNA sequence of bovine IgG2a (A2) and an IgG1. *Mol Immunol* (1996) 33:189–95. doi:10.1016/0161-5890(95)00107-7
49. Rabbani H, Brown WR, Butler JE, Hammarstro L. Polymorphism of the IGHG3 gene in cattle. *Immunogenetics* (1997) 46:326–31. doi:10.1007/s002510050279
50. Symons DBA, Clarkson CA, Milstein CP, Brown NR, Beale D. DNA sequence analysis of two bovine immunoglobulin CH gamma pseudogenes. *Int J Immunogenet* (1987) 14:273–83. doi:10.1111/j.1744-313X.1987.tb00392.x
51. McGuire TC, Musoke AJ, Kurtti T. Functional properties of bovine IgG1 and IgG2: interaction with complement, macrophages, neutrophils and skin. *Immunology* (1979) 38:249–56.
52. Howard C. Comparison of bovine IgG₁, IgG₂ and IgM for ability to promote killing of *Mycoplasma bovis* by bovine alveolar macrophages and neutrophils. *Vet Immunol Immunopathol* (1984) 6:321–6. doi:10.1016/0165-2427(84)90057-6
53. Maekawa N, Konnai S, Ikebuchi R, Okagawa T, Adachi M, Takagi S, et al. Expression of PD-L1 on canine tumor cells and enhancement of IFN-γ production from tumor-infiltrating cells by PD-L1 blockade. *PLoS One* (2014) 9:e98415. doi:10.1371/journal.pone.0098415
54. Maekawa N, Konnai S, Okagawa T, Nishimori A, Ikebuchi R, Izumi Y, et al. Immunohistochemical analysis of PD-L1 expression in canine malignant cancers and PD-1 expression on lymphocytes in canine oral melanoma. *PLoS One* (2016) 11:e0157176. doi:10.1371/journal.pone.0157176
55. Regan D, Guth A, Coy J, Dow S. Cancer immunotherapy in veterinary medicine: current options and new developments. *Vet J* (2016) 207:20–8. doi:10.1016/j.tvjl.2015.10.008
56. Nishimori A, Konnai S, Okagawa T, Maekawa N, Ikebuchi R, Goto S, et al. *In vitro* and *in vivo* antivirus activity of an anti-programmed death-ligand 1 (PD-L1) rat-bovine chimeric antibody against bovine leukemia virus infection. *PLoS One* (2017) 12:e0174916. doi:10.1371/journal.pone.0174916

Conflict of Interest Statement: SK, KO, SM, TO, AN, NM, YS, and CN have a patent pending for materials and techniques described in this paper (Japanese patent, application number 2016-159090).

Copyright © 2017 Okagawa, Konnai, Nishimori, Maekawa, Ikebuchi, Goto, Nakajima, Kohara, Ogasawara, Kato, Suzuki, Murata and Ohashi. This is an open-access article distributed under the terms of the Creative Commons Attribution License (CC BY). The use, distribution or reproduction in other forums is permitted, provided the original author(s) or licensor are credited and that the original publication in this journal is cited, in accordance with accepted academic practice. No use, distribution or reproduction is permitted which does not comply with these terms.

Advantages of publishing in Frontiers



OPEN ACCESS

Articles are free to read for greatest visibility and readership



FAST PUBLICATION

Around 90 days from submission to decision



HIGH QUALITY PEER-REVIEW

Rigorous, collaborative, and constructive peer-review



TRANSPARENT PEER-REVIEW

Editors and reviewers acknowledged by name on published articles



REPRODUCIBILITY OF RESEARCH

Support open data and methods to enhance research reproducibility



DIGITAL PUBLISHING

Articles designed for optimal readership across devices



FOLLOW US
@frontiersin



IMPACT METRICS
Advanced article metrics track visibility across digital media



EXTENSIVE PROMOTION
Marketing and promotion of impactful research



LOOP RESEARCH NETWORK
Our network increases your article's readership